Synthesis of Insecticidal Mono- and Diacylhydrazines for Disruption of K^+ Voltage-Gated Channels, Elucidation of Regiochemistry, and Description of Conformational Isomerism by NMR Spectroscopy and Computation

Joseph Shelby Clements II

Dissertation submitted to the faculty of the Virginia Polytechnic Institute and State University in partial fulfillment of the requirements for the degree of

Doctor of Philosophy
In
Chemistry

Paul R. Carlier, Chair
David G. I. Kingston
James M. Tanko
Gordon T. Yee

May 2, 2017
Blacksburg, VA

Keywords: Hydrazine, acylation, α-effect, regioselectivity, hydrazide, voltage-gated, (*E*)-/(*Z*)-, ^{19}F NMR, single electron transfer (SET), rotational barrier, N-N bond rotation, rotational isomerism, helicity, transition state, dihedral angle

Synthesis of Insecticidal Mono- and Diacylhydrazines for Disruption of K^+ Voltage-Gated Channels, Elucidation of Regiochemistry, and Description of Conformational Isomerism by NMR Spectroscopy and Computation

Joseph Shelby Clements II

ABSTRACT

Based on the success of diacyl-*tert*-butylhydrazines RH-5849 and RH-1266 in controlling agricultural crop pests, we endeavored to synthesize our own diacylbenzyl- and arylhydrazine derivatives for use against the malaria vector *Anopheles gambiae*. In the process of producing a library of compounds for assay against *An. gambiae*, it became clear that employing regioselective acylation techniques (in molecules that feature two nucleophilic, acyclic nitrogen atoms α to one another) would be imperative. Synthesis of the library derivatives proceeded rapidly and after topical assay, we found three compounds that were more toxic than the RH-series leads. One of the three displayed an LD_{50} value of half that of RH-1266, though patch clamp assay concluded that toxicity was not necessarily linked to inhibition of mosquito K^+ channel Kv2.1.

The acylation of monoarylhydrazines appears simple, but its regioselectivity is poorly understood when assumed as a function of basicity correlating to nucleophilic strength. We determined the ratio of the rate constants for distal to proximal *N*-acylation using ^{19}F NMR spectroscopic analysis of reactions of 4-fluorophenylhydrazine with limiting (0.2 equiv) acylating agent in the presence of various bases. Acid anhydrides gave consistent preference for distal acylation. The selectivity of acylation by acyl chlorides when using pyridine gives strong distal preference, whereas use of triethylamine or aqueous base in conjunction with aroyl

chlorides showed a moderate preference for proximal acylation. This observation yielded a convenient one-step method to synthesize proximal aroylarylhydrazines in yields comparable or superior to that provided by the standard three-step literature approach. Combined with NMR evidence of the distal nitrogen as the unambigiously stronger base of the two nitrogens, we propose a single electron transfer mechanism that predicts the regiochemistry of arylhydrazines toward acylating agents better than the nucleophilicity model based on pK_a values.

While synthesizing the acylhydrazine library for assay against *An*. *gambiae*, NMR spectroscopy revealed rotational isomerisms of two types: chiral helicity (*M*)/(*P*) and acyl (*E*)/(*Z*)-isomerism due to hindered rotation. Variable temperature NMR allowed the measurement of N-N bond rotational barriers, as well as estimate the barrier of (*E*)/(*Z*) interconversion. We obtained the X-ray crystal structures of four diacylhydrazines to test this hypothesis and revealed both the twist conformation around the N-N bond axis and (*E*)/(*Z*)-isomerism around the proximal acyl group. Computation (which agreed with the crystal structures) allowed us to estimate which (*E*)/(*Z*)-isomers were most likely being observed in solution at room temperature by NMR spectroscopy. In addition, we were able to calculate transition structures corresponding to N-N bond rotational barriers of (*E*,*Z*)- and (*Z*,*Z*)-isomers of model molecules and rationalize the difference in coalescence temperatures between (*E*,*Z*)- and (*Z*,*Z*)-isomers.

GENERAL AUDIENCE ABSTRACT

Herein we present the work of both synthesizing and characterizing the mosquitocidal and chemical properties of acylhydrazines. Part of the challenge of working with hydrazines comes in part from deceptive comparisons to amines and ammonia; hydrazine is as different from ammonia as hydrogen peroxide is from water. We were successful in identifying effective synthetic techniques to obtain our desired acylhydrazines reliably and managed to discover compounds that were better at eliminating *Anopheles gambiae* (the african malaria mosquito vector) than lead compounds from previous researchers. In the process of making the library of compounds for mosquito testing, we explored hydrazine reactivity toward acylating agents in a direct and deeper way than previous work, as well as their dynamic structural features. We employed a battery of techniques, including NMR, X-ray crystallography, and computational molecular modeling to understand these molecules and possibly contribute insight into their biochemical efficacy.

Acknowledgements

Firstly, I would like to extend my gratitude to my PhD advisor Dr. Paul R. Carlier. More than once, we would sit down for a 30 minute meeting about some results from the past week and 2 hours later we would have come up with a new idea to test. My work with Paul Carlier has always been mutual collaboration with emphasis on discovery and clarity. He has shown receptiveness to my ideas and independent thinking; all the while, not being afraid to tell me when I'm wrong...and sometimes vice versa. As we transition from the relationship of the student and the teacher to becoming colleagues, I will still look toward Dr. Carlier for his professional advice and counsel. It has been a pleasure to work with him over these past several years. I would also like to thank my advisory committee Drs. Kingston, Tanko, and Yee for their suggestions, patience, and interest in my work and my professional success.

Secondly, I would like to thank my fellow graduate students, post-doctoral colleagues, collaborators, and analytical staff for their willingness to work with me to achieve success in my research work. I'd like to thank Drs. Qiao-Hong Chen and Ming Ma for their indispensable and practical guidance at the very beginning of my graduate career in organic synthesis. I'd like to thank Drs. Dinesh Nath and Zhong-Ke Yao for working alongside me on acylhydrazine syntheses at the beginning of that project, as well as my former pupil Michael Black. I thank Dr. Eric Nybo for our long friendship and conversations on our research which has proved inspiring time after time. I extend my gratitude to Dr. Gary Richoux, Dr. Astha Verma, Dr. Eugene Camerino, Dr. Neeraj Patwardhan, Sha Ding, and Lixuan Liu for your time and inclination to discuss my work and offer your thoughts. Maryam Ghavami deserves special thanks for contributing her synthetic prowess to my project on regioselective proximal acylation of aryl hydrazines. I am grateful to Dr. Carla Slebodnick for her expertise and advice toward obtaining

the vital X-ray crystal structures for my research. My sincere gratitude goes to Dr. Narasimhamurthy Shanaiah and Ken Knott for their guidance and hours of time in front of the 600 MHz NMR, helping me learn how to do variable temperature measurements properly. I'd like to thank Bill Bebout and Dr. Mehdi Ashraf-Khorassani for their hard work, troubleshooting, and patience with me and my compounds. I'd like to thank our collaborators Drs. Jeff Bloomquist, Fan Tong, Rafique Islam, and Baonan Sun at the University of Florida Department of Entomology and Nematology for their diligent work in biological assay of my compound library for mosquito toxicity as well as K^+ channel inhibition.

Finally, those outside of academia have contributed greatly to my success and they too deserve recognition for their part this accomplishment. My parents, Markus and Sharon Clements deserve thanks for their love, their moral and material support, and allowing me to pursue science and encouraging it at a young age. I thank my sister Kristi Wilkinson for her support and protectiveness of her little brother in his vulnerable young years. My Mother and Father in-law, David and Peggy Heimerdinger supported me when I needed it and I will remember it always. Lastly, I would like to thank my wife Rachel Kathryn Heimerdinger most of all. You were there for me when I was at my weakest in mind and body; it was your love, work, patience, courage, and fortitude that have seen me through to this moment and I am forever grateful.

Dedication

I dedicate this work to Rachel Kathryn Heimerdinger and all those who would pursue and facilitate scientific endeavor for the furtherance of our human civilization.

Chapter 1. Introduction to Hydrazine Chemistry: Nucleophilicity, Synthesis, Conformational Chirality and Isomerism

1.1 Introduction

Hydrazine has been used as a reagent in organic chemistry for over a century, and is used in multiple areas of study and industry. It serves as a blowing agent for polymer foams[1] and has served as hypergolic rocket fuel since the 1940s.[2] It is well known by undergraduate organic students as a reducing agent in the Wolff-Kishner reaction.[3] Beyond simple industrial applications, hydrazine's acyl derivatives are starting materials for synthesizing heterocycles such as indoles,[4] pyrazoles,[5] triazoles,[6-7] and oxadiazoles.[6, 8-9] Acylhydrazines are valuable to medicinal chemistry as peptide mimetics,[10-11] significant to medical history through the famous drug isoniazid,[12-13] and useful as tools for molecular biology as probes.[14]

Acylhydrazines feature prominently in organic chemistry as candidates for pharmaceuticals[12-13] and insecticides[15]. The Carlier Group's interest in the chemistry of acylhydrazines arises from practical concerns: the potential to control the malaria vector *Anopheles gambiae*.[16] Malaria has plagued humankind since the dawn of our evolution and began to proliferate after the advent of agriculture;[17] the word malaria comes to us from medieval Italian, *mala aria*[18] or "bad air". According to the World Health Organization report of 2015, 3.2 billion people are at risk of infection from malaria, with 214 million cases in 2015.[19] The result of these cases of infection were approximately 438,000 deaths, of which 70% were children under the age of 5 years old.[19] Classical pesticide classes, such as organophosphates (which deactivate acetylcholine esterase),[20] and pyrethroids (disrupt Na^+-channels in nerve cells)[21] are losing their potency due to resistant mosquito evolution.[19] The acylhydrazines that

inspired our work were diacyl-*tert*-butylhydrazines (Figure 1), which have been used as agricultural insecticides. They are ecdysone receptor agonists,[22-23] and they cause insect larvae to undergo a premature and fatal molt. Interestingly this class of compounds was observed to exhibit neurotoxic[24] symptoms in adult insects during field testing of RH-5849,[25] a 1,2-diacyl-1-*tert*-butylhydrazine. In a series of papers,[23-24] Salgado demonstrated that these compounds block voltage-dependent potassium channels, and attributed the observed neurotoxicity to this mechanism. Since potassium channels have not been extensively explored as insecticidal targets[16, 26] we thought to investigate the ability of diacylhydrazines to control *Anopheles gambiae*. As I will describe in Chapter 2, we began synthesizing a library of RH series (Figure 1) analogues, in particular those derived from benzyl- and phenylhydrazines.

Figure 1.1. RH diacylhydrazine insecticides.[22]

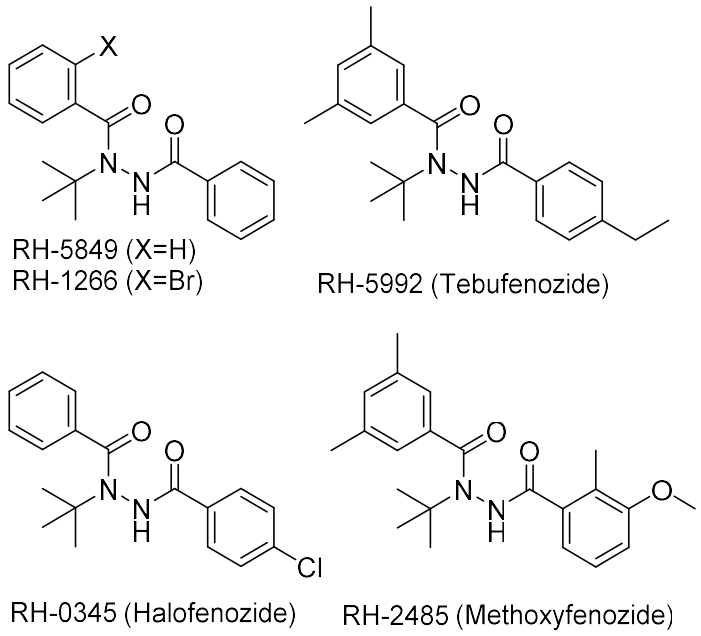

Before describing our work on acylhydrazines, it is appropriate to address some of the unique features of hydrazines that influence synthetic strategy. The topics introduced here will be

expanded upon with their own sections in this Chapter, with references to other Chapters to show where my own research contributes to understanding these areas.

The α-effect that arises from hydrazine's lone pairs provide it with chemical properties that are not fully appreciated until experiments are undertaken. In particular, the assumption that hydrazines will act analogously to diamines is one that quickly proves erroneous. Hydrazine and organohydrazines distinguish themselves from ammonia and amines by a breakdown in correlation between nucleophilicity[27] and basicity[28], as well as the effect of solvent.[27, 29] I will discuss this further in Section 1.3.

Reported difficulties with direct acylation of hydrazines manifest in regards to regioselectivity and polyacylation.[30-31] Regioselectivity in acylation has been shown to depend upon the acylating agent[32] itself and suggests influence of steric hindrance,[33] but without more in-depth study (Chapter 3 will cover my work in this area).[34] In Section 1.5.1, I will review methods for regioselective synthesis acylhydrazines. As will become apparent, no general method yet exists for all hydrazines and all acylating agents, which presents both challenges and opportunities for research.

Figure 1.2. Axially chiral molecules and assignment of helical chirality (*M*/*P*).

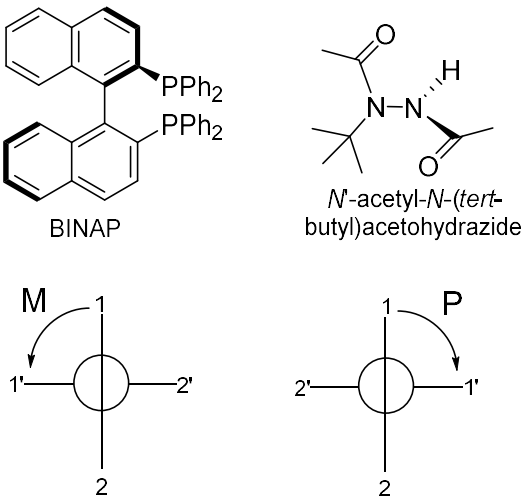

N,N'-disubstituted hydrazines derivatives possess a chiral axis in the same way BINAP does.[35-37] If diastereotopic groups are present, this chiral axis can impart complexity to NMR spectra[38] due to hindered rotation about the N-N bond[39] (Figure 1.2). In addition, acylhydrazines can possess yet another form of stereoisomerism in the form of s-(*E*) and s-(*Z*) rotational isomers of acyl groups (Figure 1.3).[40] The (*E*)/(*Z*) preference of diacylhydrazines can affect the pharmacology of these compounds.[41] These structural features further reinforce the distinction between hydrazines and diamines, and highlight the need for further study of these compounds. My own studies into acylhydrazine rotational isomerisms will appear in Chapter 4.

Figure 1.3. E/Z acylhydrazine rotational isomerism.[40]

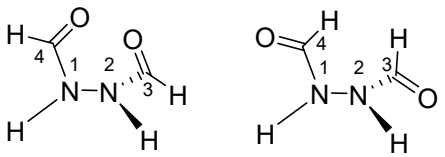

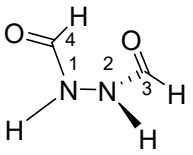

The focus of this review is to provide a starting point of knowledge as it concerns the synthesis, characterization, and physical/chemical study of acylhydrazines and the hydrazines from which they were derived. The aforementioned topics of consideration provide context for certain methods used in later chapters, or why specific reaction conditions were needed. Finally, this chapter will highlight the gaps in the literature about acylhydrazines that my research seeks to address.

1.2 Insecticidal action of diacylhydrazines

As mentioned earlier (Figure 1.1) the inspiration for working on acylhydrazines derives from the work of Vincent Salgado on 1,2-diacyl-1-*tert*-butylhydrazines. Working for Rohm and Haas, Adam Hsu sought to create a different kind of pesticide to control insects through growth regulator molecules, but with simpler structures than the juvenile molting steroid, ecdysone, they wished to mimic.[42] Serendipity led to the discovery of 1,2-diacyl-1-*tert*-butylhydrazines and their capability to mimic ecdysone. RH-5849 (Figure 1) was not only able to produce the molting effects, but also proved to be much less vulnerable to hormone clearance mechanisms that had stymied steroid-based attempts at the same outcomes.[42-43] Common agricultural pests, such as

Spodoptera eridania (southern armyworm) and *Leptinotarsa decemlineata* (Colorado potato beetle) were killed effectively by RH-5849.[42] More notable was the vulnerability of mosquito nymphs, including those of *Anopheles gambiae* to the RH-series, particularly RH-2485 (Figure 1.1), again functioning as ecdysone agonists.[44]

Field observations of RH-series diacylhydrazine testing showed the ability of 1,2-diacyl-1-*tert*-butylhydrazines to be ecdysone agonists in juvenile insects, but this was not the only observation.[45] Adult insects (and some larva, like *Popillia japonica*), that were exposed to RH-5849 and RH-1266 (Figure 1) exhibited symptoms of neurotoxicity, such as self-harm by biting, cessation of feeding, ataxia, and paralysis, followed by death.[23, 25, 45] Salgado was able to demonstrate the source of this neurotoxicity through electrophysiological investigation: the blockage of voltage-dependent K^+-channels (Figure 1.3 shows an example of this channel).[23-24] He showed that this action was present for a variety of tested arthropods: *Manduca sexta* (tobacco hornworm), *Epilachna varivestis* (Mexican bean beetle), *Periplaneta americana* (American cockroach), and *Procambarus clarkii* (Louisiana crawfish).[23] In addition, RH-1266 paired with the pyrethroid fenvalerate showed synergistic toxicity exceeding the calculated LD_{50} of two compounds acting independently.[46] Fenvalerate acting on the Na^+-channel side of the action potential to induce depolarization, combined with RH-1266 operating on the K^+-channel on the other to stop repolarization would explain this result.[46]

Figure 1.4. KvAP, a voltage-dependent K+ channel from *Aeropyrum pernix* (Archea), PDB ID: 1ORQ.[47]

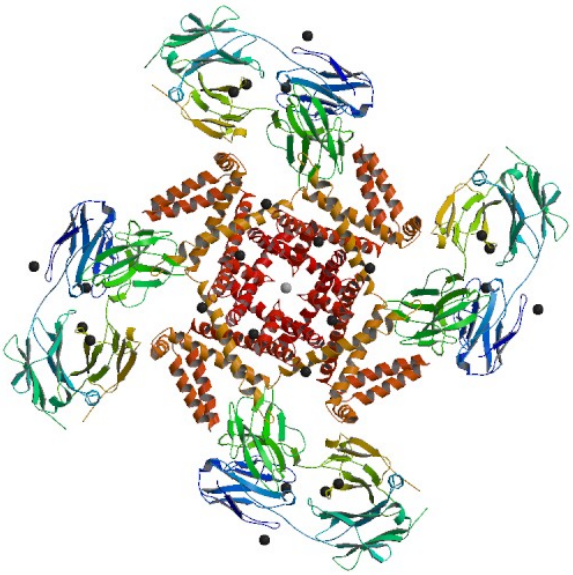

Voltage-gated K^+-channels are common in the muscle and nerve tissue of animals and microorganisms. They are membrane-spanning tetrameric proteins that serve to repolarize a cell after a stimulus activates the coupled Na^+-channel, which depolarized the cell.[48] Figure 1.5 shows an example of an action potential, along with whole-cell current of Na^+ and K^+.[49]

Figure 1.5. Action potential overview.

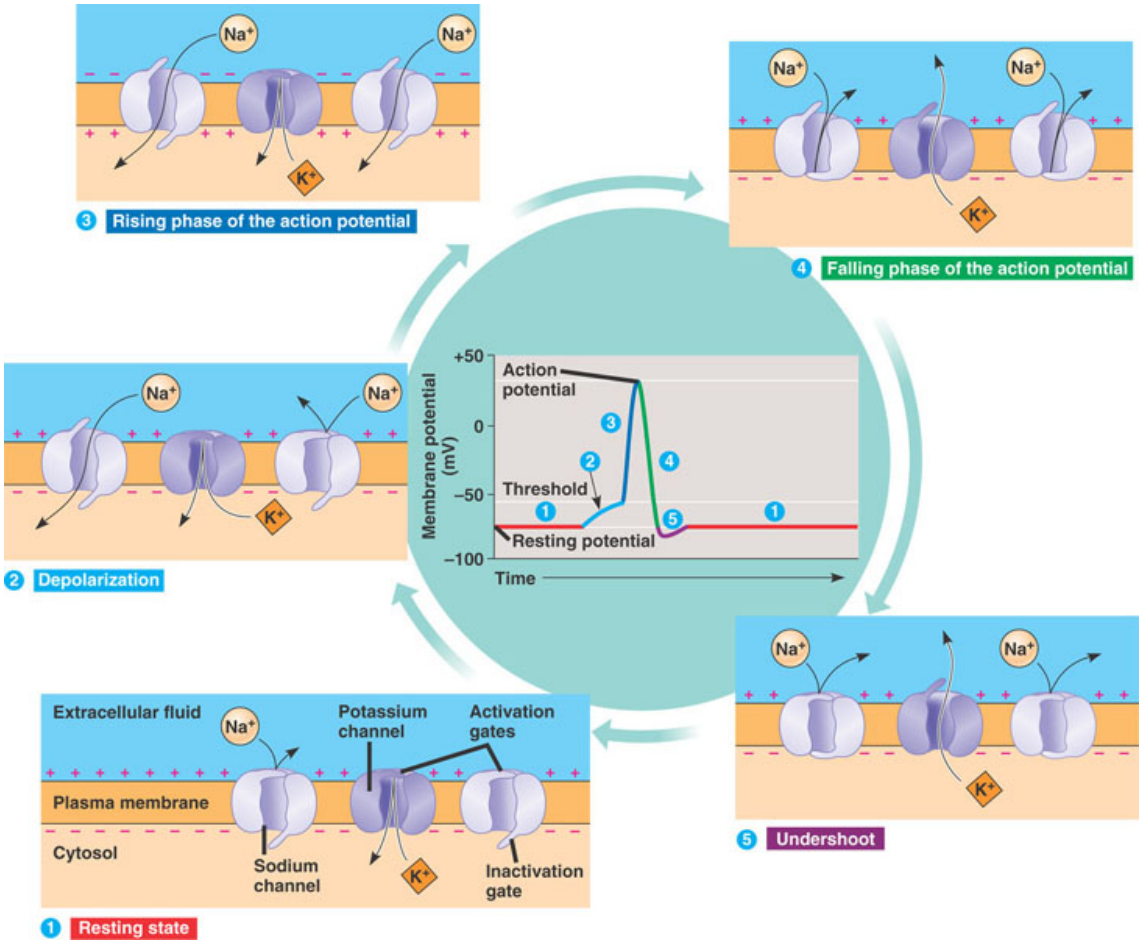

Source: http://cognitiveconsonance.info/wp-content/uploads/2015/08/miscbox2.jpg (accessed Oct 18, 2016).

Classically, pyrethroids have been used to control insect populations in agricultural and public health settings. Pyrethroids work much like their natural counterparts, pyrethrins, in that they block the normal operation of Na^+-channels by preventing the channels from closing, thereby preventing membrane repolarization.[21] As such, most research centered on action potential as a means to kill insects focuses on well-characterized voltage-gated Na^+-channels.[16] As pyrethroid resistant mosquito populations continue to grow ever larger,[19] the proposition of our group and collaborators was another strategy: target the repolarization mechanism of cells through their voltage-gated K^+-channels and thereby circumvent pyrethroid resistance.[16]

Combined with the follow-up studies of the RH series that suggest that they are more environmentally benign than previous insecticides, in collaboration with Dr. Jeffrey Bloomquist (Entomology and Nematology, University of Florida) we began to pursue synthesis of our own acylhydrazine derivatives.[16, 50]

1.3 The α-effect

An overview of the literature of hydrazines would be remiss without mentioning one of the features that sets hydrazines apart from diamines: the α-effect. Edwards and Pearson coined the term in 1962 and described it as such, "If basicity is used as a criterion, a certain group of nucleophiles is found to react more rapidly than expected with a number of substrates…distinguished by the presence of an electronegative atom containing one or more pairs of unshared electrons adjacent to the nucleophilic atom…excess reactivity shown by this class of reagents is called the 'alpha effect'," (examples in Figure 1.6).[51] Despite being known since at least 1947, there is disagreement in the literature about the mechanistic cause of the α-effect. Fina lists the proposed explanations as follows: 1. ground state destabilization via electron-electron repulsion from the adjacent lone pair, 2. transition state stabilization via hydrogen bonding that allows α-nucleophiles to react more quickly, and 3. solvent effects.[52] Regardless of the cause, a lack of correlation between basicity and nucleophilicity is the primary hallmark of the alpha effect.

Figure 1.6. Examples of α-nucleophiles.[52]

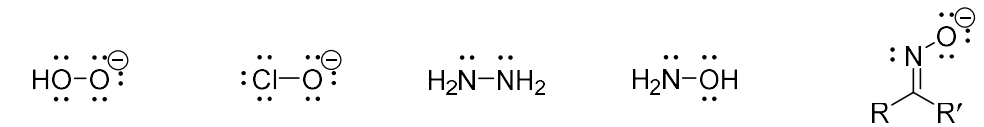

Observations of nucleophilic reaction with selected electrophiles highlight the degree to which the α-effect manifests itself. Table 1.1 will serve to demonstrate the breakdown of correlation between basicity and nucleophilicity in α-nucleophiles. In reaction with p-nitrophenylacetate, (Entry 1, Table 1.1) the rate constant for hydrazine is nearly the same value as ethylenediamine, despite being nearly 100-fold less basic than ethylenediamine (Entry 2). Table 1.1 also shows that the α-effect is even more pronounced with ionic α-nucleophiles, given that weak bases such as potassium hypochlorite (Entry 3) and sodium methyl hydroperoxide (Entry 4) possess rate constants 2- and 140-fold larger than sodium hydroxide (Entry 5) respectively. Despite a basicity >100 million-fold higher, the hydroxide ion reacts with p-nitrophenyl acetate at half the rate of the hypochlorite ion.

Table 1.1. pK_a values and 2nd order rate constants for reaction of neutral and ionic nucleophiles with p-nitrophenyl acetate at 25 °C.[52-53]

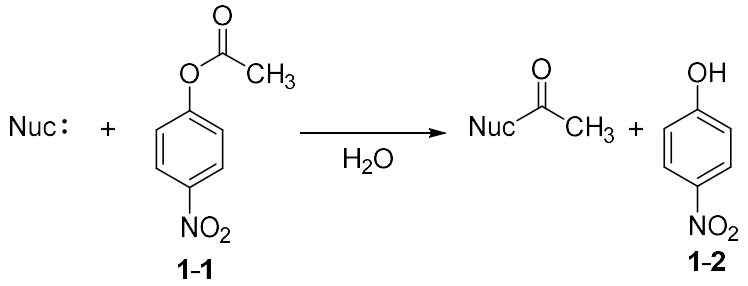

1-1 **1-2**

Entry	Nucleophile	pK_{HA}	rate constant (M^{-1} min^{-1})
1	hydrazine	8.1	403
2	ethylenediamine	10.0	420
3	potassium hypochlorite	7.1	1670
4	sodium methyl hydroperoxide	11.5	125000
5	sodium hydroxide	15.7	890

Fina states that across electrophiles, anionic α-nucleophiles tend to show the α-effect more consistently and strongly, versus the neutral α-nucleophiles.[52] In reactions with fluoridates such as sarin (**1**-**3**), HOO^- reacted at least 50-fold faster than HO^- (Table 1.2, Entries 1 and 2).[52] Oximes (Fina refers to them as hydroxamates)[54] have been measured to reactivate acetylcholinesterase after sarin poisoning at a level much higher than their basicity or polarizability would predict.[52] This observation has practical implications in medicine, as the famous 2-PAM antidote has been in use for decades to counteract organophosphate toxicity and is an α-nucleophile itself as an oxime.[55]

Table 1.2. pK_a values and 2nd order rate constants for reaction of neutral and ionic nucleophiles with sarin at 25 °C.[52-53]

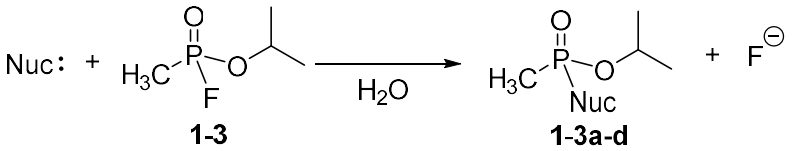

1-3 **1-3a-d**

Entry	Nucleophile	pK_{HA}	rate constant (M^{-1} min^{-1})
1	sodium hydroxide	15.7	25.8
2	sodium hydrogen peroxide	11.5	1340.0
3	salicylaldoxime	9.2	24.9
4	pyridine-2-aldoxime	10.1	28.2

Trends in α-effect manifestation in reaction with electrophilic carbon suggest that higher s-character increases the rate of reaction with α-nucleophiles relative to their normal counterparts, thus $sp > sp^2 > sp^3$ (see Table 1.3).[52]

Table 1.3. 2nd order rate constant ratio variation with carbon electrophile hybridization.[52]

Electrophile	k_{OH^-} (M^{-1} s^{-1})	k_{OOH^-} (M^{-1} s^{-1})	k_{OOH^-}/k_{OH^-}
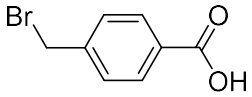	0.16	2.1	13
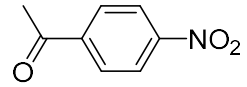	890	68500	77
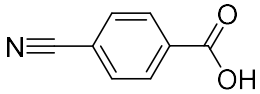	0.0055	6.5	1182

The ratio of rates between the hydroperoxide ion and hydroxide ion increases with the greater s-character of the electrophilic carbon center that is attacked, with a nearly 100-fold increase from sp^3 to sp hybridization. This demonstrates that the α-effect is not static, but can increase or decrease in magnitude depending on the electrophilic substrate. To our knowledge, a definitive explanation for this phenomenon has not yet been presented. There are, however, a few hypotheses that seek to explain the α-effect, and if true, may help predict experimental behavior of α-nucleophiles.

Scheme 1.1. S_N2 Thought Experiment Model.[51]

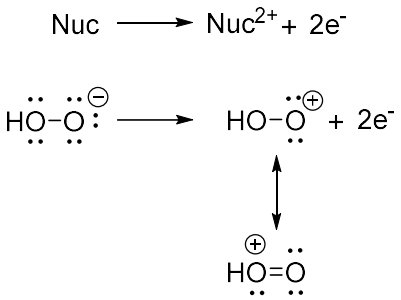

When Edwards and Pearson[51] attempted to explain the α-effect they observed, they utilized a thought experiment: suppose that in the course of an S_N2 reaction, a nucleophile and electrophile are an arbitrarily large distance away from each other. The lone pair of the

nucleophile is donated to the electrophile, but they cannot combine due to distance (see Scheme 1.1).[51] This loss of electrons to something else far away in space is somewhat analogous to the breaking of a C-X bond in an alkyl halide, and anything that would stabilize R^+ should also stabilize Nuc^{2+}.[51] Thus, the lone pair on the α-atom provides stabilization in the transition state to the α-nucleophile as a whole through resonance.[51]

A related explanation for the origin of the α-effect in terms of transition state stabilization was provided by Hoz.[56] Hoz asserted that the alpha effect is a result of a propensity to undergo single electron transfer (SET).[56] SET in nucleophilic reactions is well known in the reactions of Grignard reagents with benzophenone,[57] coupling of the cyclopropenyl anion and cation,[58] and nitration of aromatic systems.[59-60] SET from a nucleophile to a given electrophile results in a transition state characterized as a diradical zwitterion that then collapses to form the product (see Figure 1.7).[56] Interestingly, this model implicates the substrate as a participant in the α-effect, as the ability to form the diradical transition state is dependent on the substrate's propensity to accept a single electron via a low LUMO. Cations, aromatic systems, and unsaturated electrophiles like acyl groups and ketones should have low LUMOs[56] and would participate in this much better than high LUMO substrates like alkyl halides,[52, 61] fitting the trend of higher s-character in carbon electrophilic centers coinciding with observations of the α-effect. Echoing Edwards and Pearson, the argument that α-nucleophiles are well-placed to stabilize this radical nature via the adjacent lone pair is a familiar idea to organic chemists, whether viewing from Valence Bond theory, or from a molecular orbital perspective (an example of stabilization of a 3-electron system is given in Figure 1.7).

Figure 1.7. Single electron transfer between nucleophiles and electrophiles.[56]

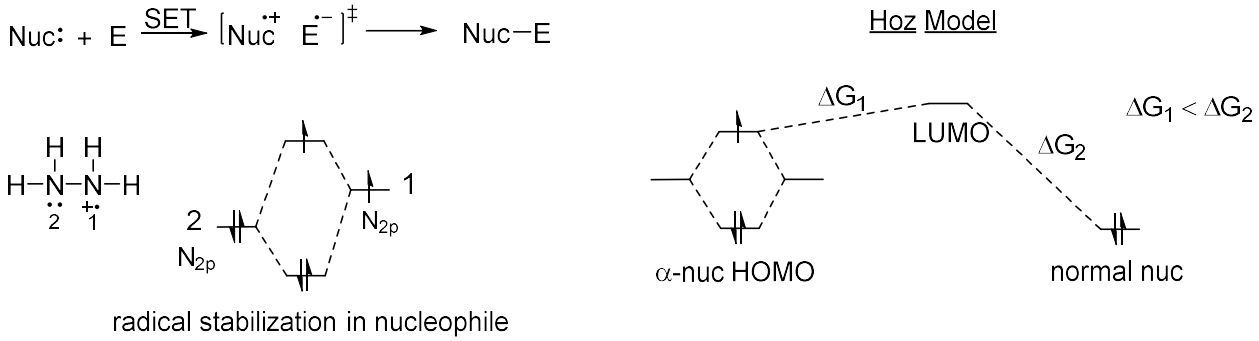

In the Hoz model, to compare reaction rates of α-nucleophiles and normal nucleophiles by their basicity is to ignore the mechanistic underpinnings of what makes the α-effect significant. The strength of an α-nucleophile comes not from its basicity alone, but rather from its ability to create high spin in the transition state.[56] This behavior is more akin to redox chemistry, with α-effect being better predicted by the ionization energy of the nucleophile.[62-63]

Solvent influence on the α-effect has also been studied. Studies on gas-phase reactions[64-65] have shown that the α-effect still exists for α-nucleophiles like the peroxide anion without the aid of solvent in both computation[64] and experiment[65].

Table 1.4. Gas Phase computation of transition state barriers of ionic nucleophiles in reaction with methyl chloride.

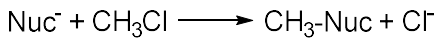

Entry	Nucleophile	Basicity (kJ/mol)[a]	$\Delta E^{\ddagger}_{rel}$ (kJ/mol)
1	hydroxide	1631.0	1.1[b]
2	hydroperoxide	1573.1	0[b]
3	amide	1692.0	3.3[c]
4	hydrazine	1671.6	0[c]

[a] $\Delta H = H(\text{Nu-H}) - H(\text{Nu}^-) - H(\text{H}^+)$. [b] $\Delta E^{\ddagger}_{rel} = \Delta E^{\ddagger}_{nuc} - \Delta E^{\ddagger}_{OH^-}$. [c] $\Delta E^{\ddagger}_{rel} = \Delta E^{\ddagger}_{nuc} - \Delta E^{\ddagger}_{amide}$.

In a computational study by Ren (Table 1.4), the peroxide anion had a reaction barrier that was 1.1 kJ/mol lower than hydroxide (Entries 2 and 1 respectively).[64] For the hydrazine anion (Entry 4) versus amide anion (Entry 3), the barrier was 3.3 kJ/mol lower in favor of hydrazine.[64] In each case, the α-nucleophile had a lower transition state barrier than its more basic and close antecedent. Solvent effects alone cannot account for the α-effect, as the existence of the α-effect in gas phase shows.

The α-effect has been observed in such diverse solvents as acetonitrile, toluene, and water, in addition to gas-phase experiments, so it cannot be a simple consequence of differential solvation.[66] This is not to mean that solvent has insignificant influence, as systematic changes in solvent composition can lead to changes in α-effect magnitude, defined as the ratio k_α/k_n, where the k_α is the rate of reaction of an α-nucleophile with a given electrophile, and k_n is the rate of reaction with the same substrate and reaction conditions but with a reference nucleophile with similar features.[66]

Figure 1.8. Plot of data from Table 1.5.[67]

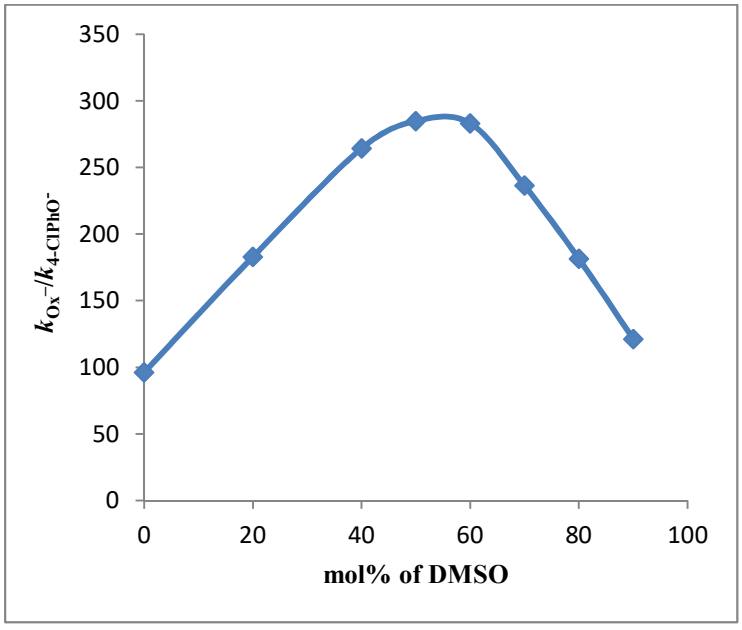

Table 1.5. Effect of DMSO in water on the rate of 1-5 and 1-6 in the reaction with 1-1 at 25.0 °C (I = 0.5 M $Me_4N^+Cl^-$).[67]

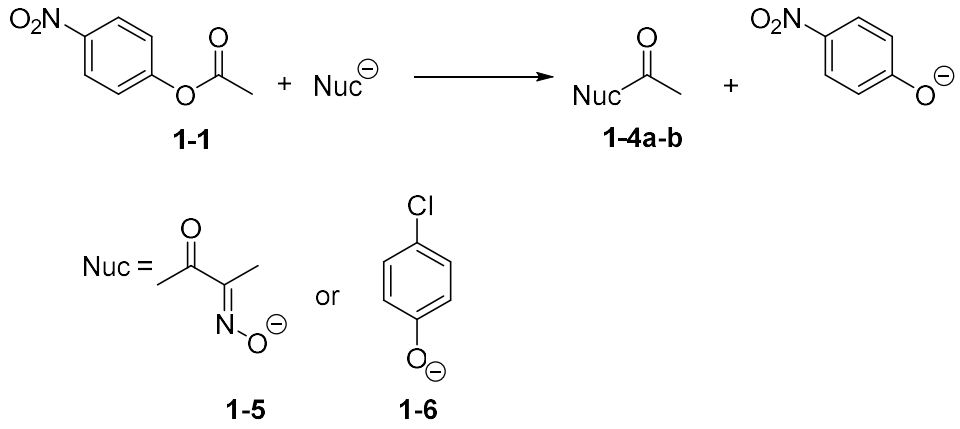

DMSO (mol %)	k_α (M^{-1} s^{-1})	k_n (M^{-1} s^{-1})	k_α/k_n
0	65.8	0.685	96
20	139	0.760	183
40	740	2.80	264
50	1680	5.90	285
60	3850	13.6	283
70	8200	34.7	236
80	17200	94.8	181
90	40500	334	121

The rate constants k_α and k_n are not equally affected by solvent, as it has been shown that they can have different solvation shells. Often, the α-nucleophiles have been shown to be less solvated than their normal counterparts, such as the case with HOO^- vs OH^-, where OH^- is more heavily solvated ($\Delta G_{solv\ OH^-}$ is +12.0 kcal/mol higher than $\Delta G_{solv\ HOO^-}$).[68] In Table 1.5, the value of rates k_α (rate of reaction of **1-5** with p-nitrophenyl acetate) and k_n (rate of reaction of **1-6** with **1-1**) vary with solvent composition starting with water, and steadily increasing the amount of

DMSO. In addition, solvent mixture compositions are not linear in their relationship to k_α/k_n, but can be curved and have maxima outside of the boundary values (Figure 1.8).[67] In the context of the Hoz model, solvent concerns the α-effect insofar as its ability to affect the HOMO-LUMO gap and solvation energies, and thus, can be considered part of the ground-state destabilization or transition-state stabilization hypotheses.

1.4 Direct alkylation of phenylhydrazine by alkylhalides.

Techniques with regards to synthesis of hydrazine derivatives will be illustrative of the importance of recognizing the α-effect's influence. Although alkylation reactions are not the focus of my body of work, a brief example can illustrate the need to understand the true nature nucleophilicity as it concerns hydrazines. Scheme 1.2 shows what may be the best example of this, where alkylation of phenylhydrazine by methyl iodide lead to the quaternization of the proximal nitrogen producing **1-7**, as did further alkylation of **1-8**.[27] Synthesis of **1-7** from phenylhydrazine produced a mixture of products, including **1-8** (1.5%), *N*′,*N*′-dimethylphenylhydrazine (15%), unreacted phenylhydrazine (50.7%), and minor oxidation products. Such behavior runs counter to how amines are expected to behave and can only be explained by a contribution from the α-effect. Alkylation of hydrazines has long been a difficult problem due to issues with reactivity, quaternization, and regioselectivity and should serve to inform the prospective chemist that similar issues may arise in acylation reactions.[69]

Scheme 1.2. Alkylation of phenylhydrazine.[27]

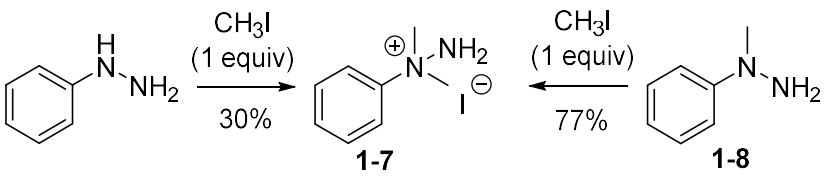

1.5 Acylation of hydrazines

Acylation of hydrazines can prove difficult to control. Regioselectivity and efficient pathways to desired products take center stage in the quest for specific acylhydrazines. This section will focus on the current knowledge of acylating techniques and what conditions will produce desired products or polyacylation.

1.5.1 Acylation of hydrazines by acid chlorides and acid anhydrides.

Acylation regioselectivities differ between unhindered alkylhydrazines and arylhydrazines, but performing reactions with a bulky substituent as in *tert*-butylhydrazine requires its own analysis. A closer inspection of the discovery synthesis of 1,2-diacyl-1-tert-butylhydrazines (Scheme 1.3), possesses a preference for reacting with anhydrides on the distal nitrogen.[42] It is also possible to synthesize **1-10a-b** by direct acylation of *tert*-butylhydrazine with acid chlorides without resorting to unbalanced stoichiometric ratios or using pyridine.[70-72] The steric bulk of the tert-butyl group affords better control with reactive acylating compounds than methylhydrazine or arylhydrazines, and thereby allows less sophisticated syntheses to get desired outcomes.

Scheme 1.3. Acylation of *tert*-butylhydrazine to 1,2-diacyl-1-*tert*-butylhydrazine.[70, 72]

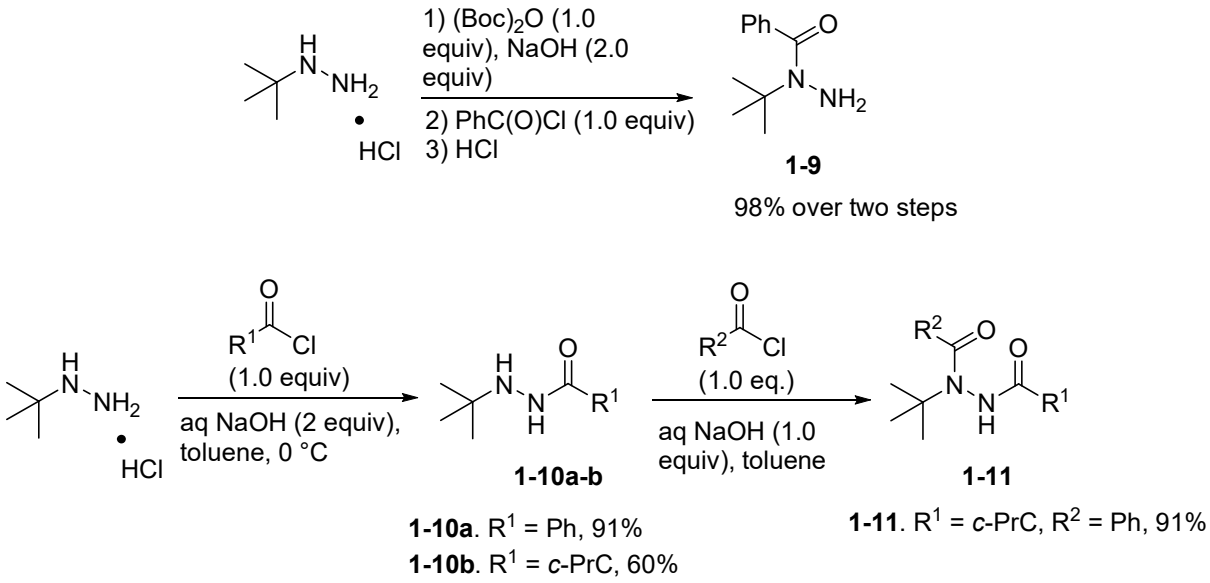

Less bulky alkylhydrazines present a challenge to acylation reactions, even in the case of **1-12**, where regiochemistry is not a factor: diacylation. Reaction of **1-12** with benzoyl chloride predominantly yields **1-13** (Scheme 1.4), despite attempts at slow addition, rigorously controlling temperature, changing the solvent system, and order of addition.[73]

Scheme 1.4. Reaction of 1,1-dimethylhydrazine with benzoyl chloride.[33, 73]

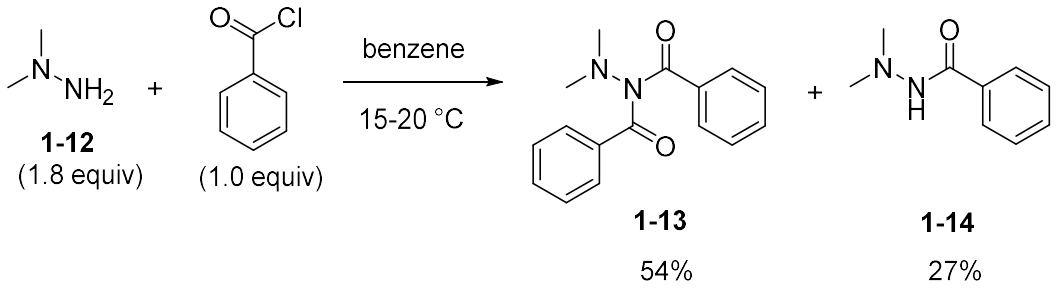

Accessing 1-acyl-2-alkylhydrazines via direct acylation via anhydrides or acid chlorides is less straightforward than it was with *t*-butylhydrazines, as the proximal nitrogen in the less hindered alkylhydrazines will preferentially react with electrophiles.[32-33] Taking this regiochemistry into

account, an example strategy to obtain the desired 1-acyl-2-alkylhydrazines can be seen in Scheme 1.5, using methylhydrazine and protection-deprotection with an acetyl group to finally give **1-18**.[32] The ever present complication with all acylation reactions with hydrazines is the tendency to diacylate rapidly, which is certainly true of methylhydrazine in this case. Peet shows that in the first step to install the acetyl group, 26% of the product is **1-16**, despite the fact that the solution is cold and the stoichiometry favors monoacylation.[32]

Scheme 1.5. Synthesizing 2-acyl-1-methylhydrazine.[32]

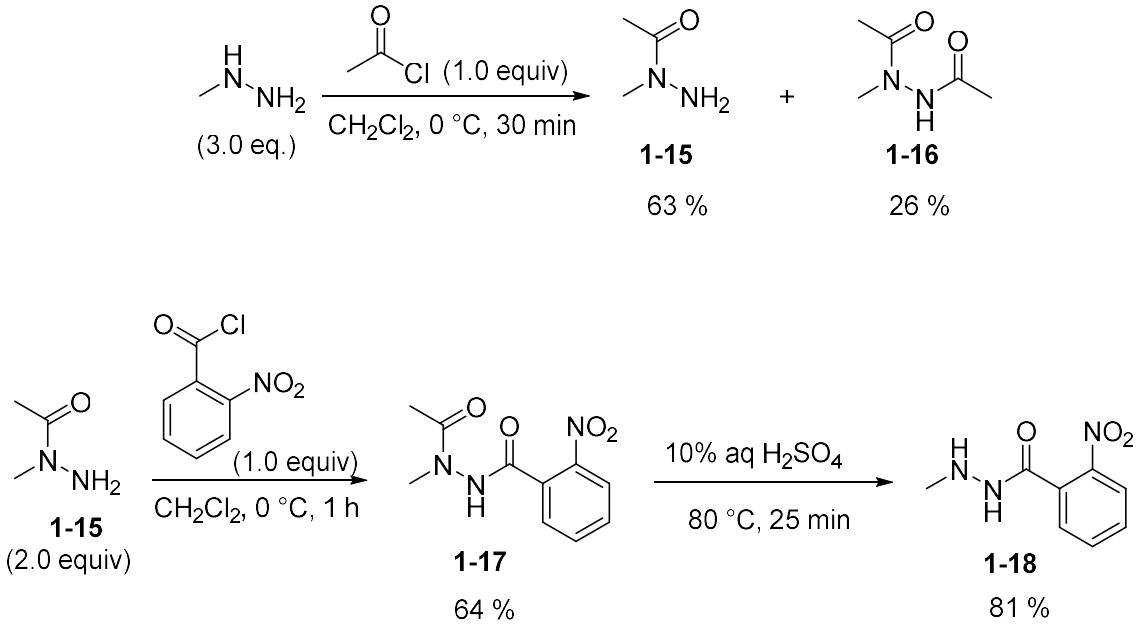

To synthesize 1-acyl-1-phenylhydrazines by acylating phenylhydrazine, the most reliable method in the literature is described in Scheme 1.6.[74-75] Preferential distal acylation of phenylhydrazine by di-*tert*-butyl dicarbonate yields **1-19** nearly quantitatively, which is then acylated by benzoyl chloride to **1-20** and then deprotected by HCl to give **1-21**. For alkylhydrazines, this same procedure is less successful as di-*tert*-butyl dicarbonate is likely to react with the proximal nitrogen; thus, a reductive amination strategy must be employed to install the alkyl group after acylation has been accomplished (Scheme 1.7).[74]

Scheme 1.6. Synthesizing 1-acyl-1-phenylhydrazines using di-*tert*-butyl dicarbonate protection-deprotection.[74-75]

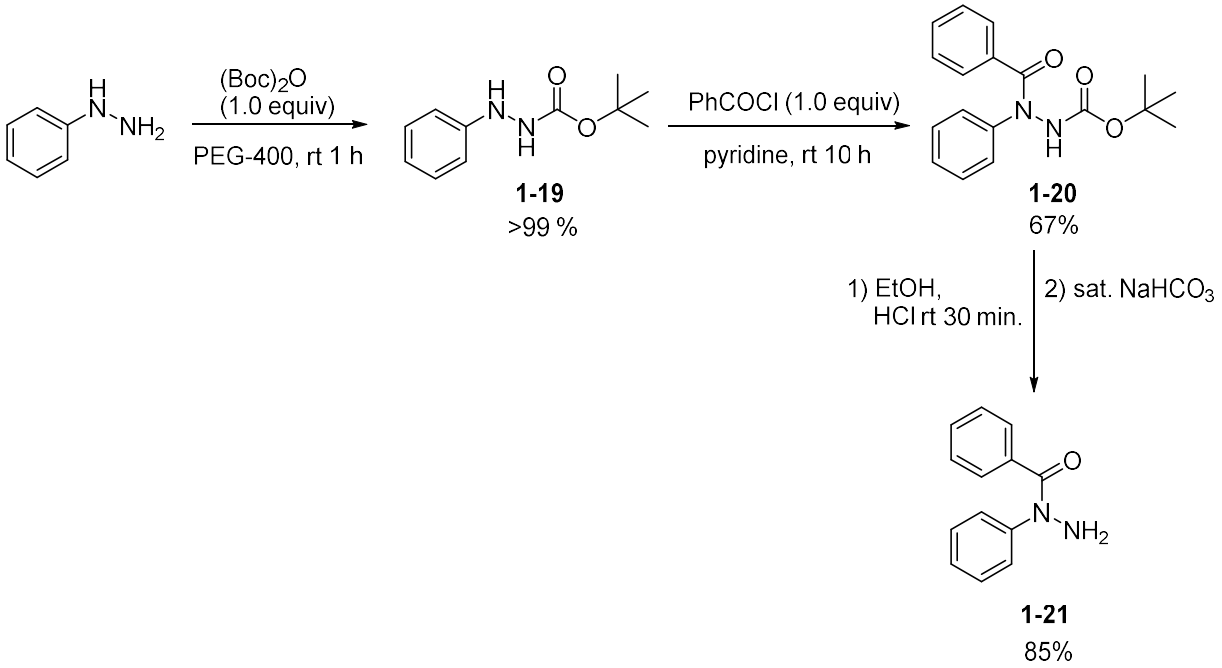

Scheme 1.7. Synthesis of 1-acyl-alkylhydrazines using reductive amination and di-*tert*-butyl dicarbonate protection-deprotection.[74]

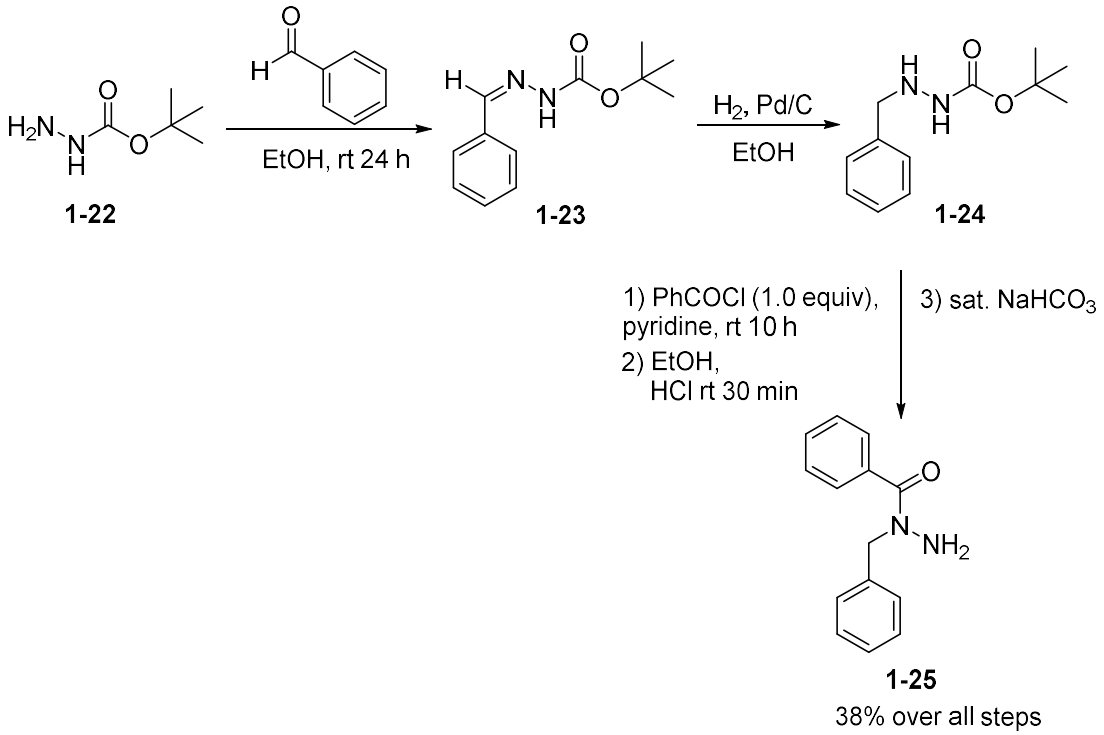

To do direct acylation of phenylhydrazines to make 1-acyl-2-phenylhydrazines, a simple strategy was to use acid chlorides in diethylether such that the desired distally acylated species would immediately precipitate, thereby avoiding 1,2-diacylation.[76] This method did not unerringly give the desired product as it was still quite possible to get the undesired diacylhydrazine **1-29** if the stoichiometry is not biased at least 3:1 in hydrazine to acid chloride (it was not quantified but implied to be the major product).[76] Moore was able to work around this by changing the order of addition, adding 1.0 equivalents of acid chloride slowly to a cold ethereal solution of 3.0 equivalents of **1-27**, obtaining **1-28** in 65% yield (Scheme 1.8).[76] The reaction is reliant on the insolubility of the product in diethylether, and thus, there was a need for different methods with more control and efficiency.

Scheme 1.8. Distal acylation of phenylhydrazines by acid chlorides.[76]

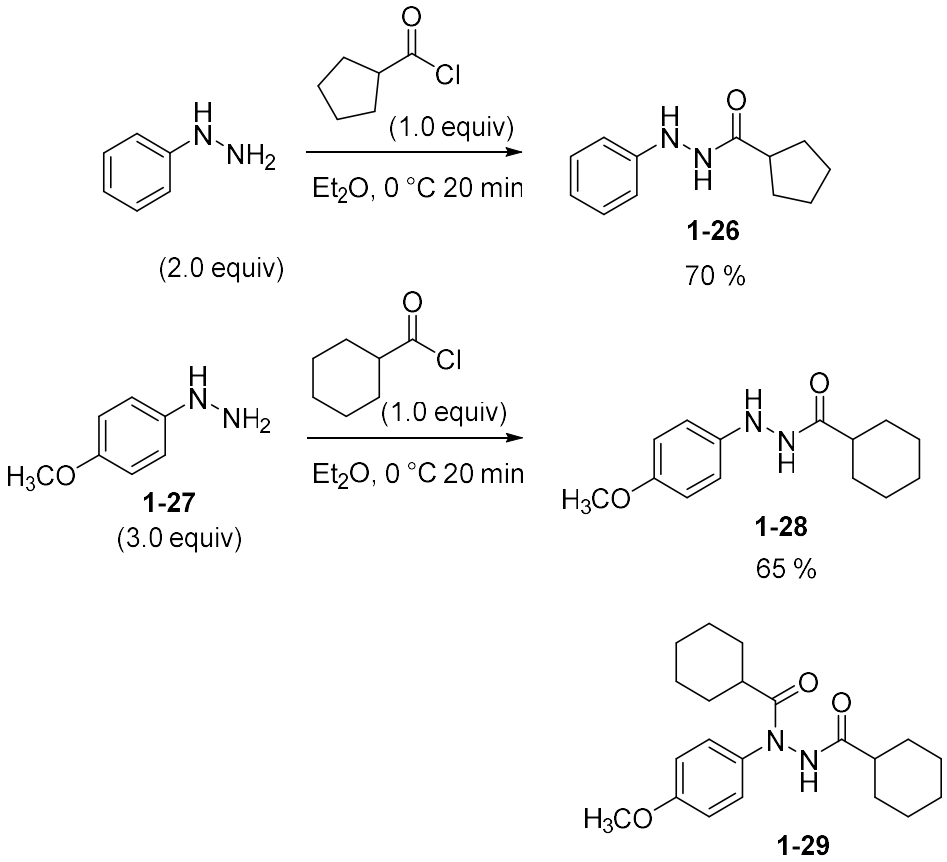

The first of these methods is the reaction of **1-30a-c** with an acid anhydride, usable in solvents from diethyl ether,[77] to ethanol,[78] to the polymeric PEG-400,[75] and water/organic mixtures (Table 1.6).[79] It is more efficient than Moore's method on a per mole basis, gives good to excellent yields, and is simple to carry out; however, anhydrides are not as commercially available as acid chlorides or esters, and are not as atom efficient as it could be, with half of the anhydride lost as a leaving group in each reaction. Acid chlorides (as seen previously) in direct reaction with hydrazines can be difficult to control, though with the addition of pyridine it appears that this can be tamed (Table 1.6). Using pyridine as a solvent allows one to synthesize **1-31d-e** using a 1:1 mole ratio of **1-30a** to acid chloride.[80-82] The reason for this selectivity will be discussed in Chapter 2. Table 1.6 shows some examples of some typical reaction yields.

Table 1.6. Acylation of arylhydrazines by anhydrides[78] and acid chlorides[82-83]

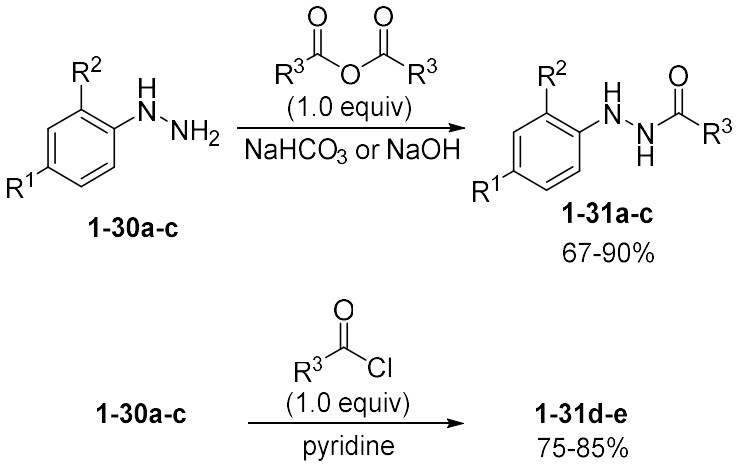

Entry	1-30	R^1	R^2	R^3	1-68	% Yield
1	**a**	H	H	Me	**a**	90[a]
2	**b**	Me	H	Ph	**b**	78[a]
3	**c**	NO_2	NO_2	Et	**c**	67[a]
4	**a**	H	H	Ph	**d**	85[b]
5	**a**	H	H	4-methoxyphenyl	**e**	75[b]

[a] Anhydride and inorganic base method. [b] Acid chloride and pyridine method used.

Obtaining 1,2-diacyl-1-arylhydrazine products is a desirable goal for their own worth as well as starting materials for heterocycle synthesis.[7] A consistent and successful method for this task is to use a 1-acyl-1-arylhydrazine like **1-32** derived from previous methodologies, and then perform a second acylation with an acid chloride, heated in toluene (Table 1.7).[7, 84] This reaction is relatively free of side reactions and gives moderate to good yields.[7, 84] While the literature examples use **1-32a-c**[6, 93] as their starting material, there is little reason to believe that this method cannot be applied to other 1-acyl-2-phenylhydrazines.

Table 1.7. Obtaining 1,2-diacyl-1-arylhydrazine products via acid chlorides.[84]

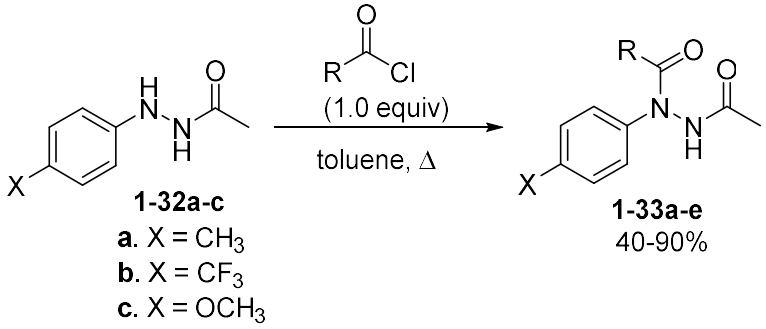

1-32a-c
a. X = CH_3
b. X = CF_3
c. X = OCH_3

1-33a-e
40-90%

Entry	X	R	1-33	% Yield
1	CH_3	CH_3	**a**	40
2	CH_3	*i*-Pr	**b**	90
3	CH_3	4-Me-C_6H_4	**c**	60
4	CF_3	4-Me-C_6H_5	**d**	60
5	OCH_3	4-Me-C_6H_6	**e**	86

1.5.2 Hydrazinolysis of esters.

Aminolysis of esters is a reaction that trained chemists will know well. The problem with reasoning by analogy from amines to predict hydrazine behavior is a conflation of properties that are not necessarily present in both. 1,1-Dimethylhydrazine is quite unreactive toward esters

larger than formates (Scheme 1.9).[33] Only ethyl formate reacted smoothly, while ethyl acetate and methyl benzoate under reflux returned starting materials.[33] Even after treatment with sodium hydride to activate methylhydrazine by metalation, reaction with methyl benzoate gave **1-35** in only 20% yield (Scheme 1.9).[33] Scheme 1.10 demonstrates the result of attempting to push the reaction with methylbenzoate in a sealed tube. Acylation never occurs, but instead reacts to give the quaternary salt **1-36** with incomplete conversion.[73]

Scheme 1.9. Reaction of 1,1-dimethylhydrazine with esters.[33, 85]

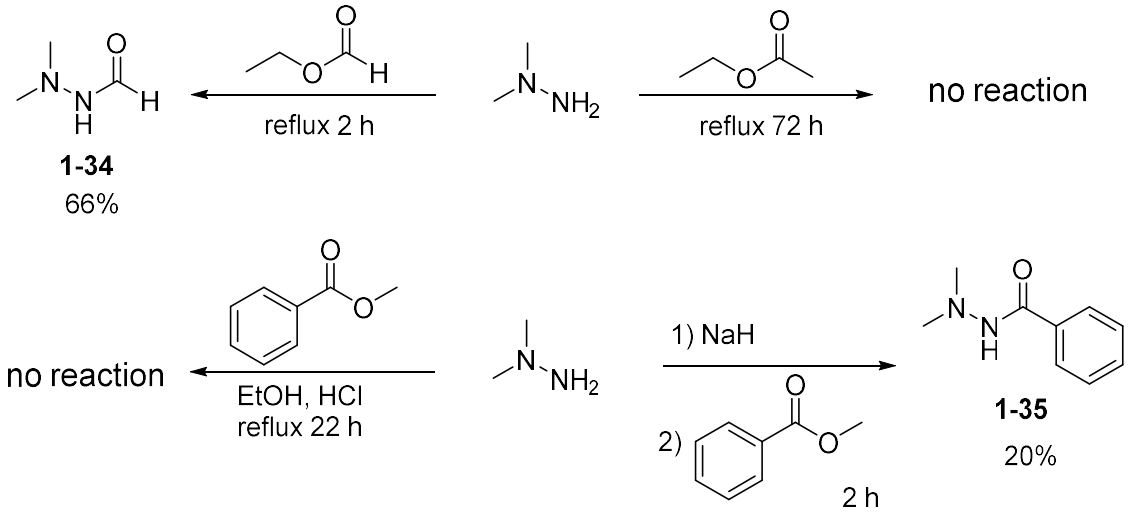

Scheme 1.10. Methylation of 1,2-dimethylhydrazines by methylbenzoate.[73]

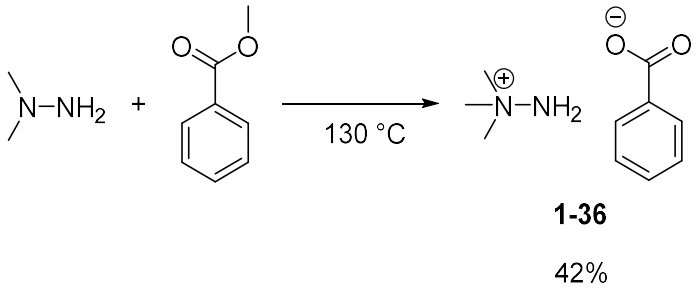

Scheme 1.11. Hydrazinolysis of esters by phenylhydrazine.[86-87]

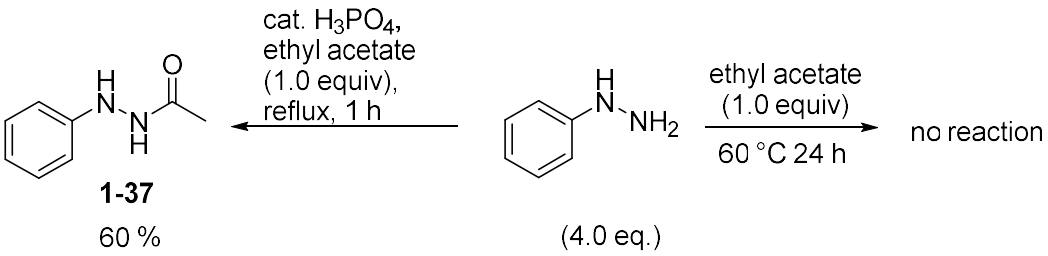

Phenylhydrazine is similarly disinclined toward reaction with esters (Scheme 1.11), requiring sealed tube conditions,[86] phosphoric acid activation,[86] or organometallic activation (this will be discussed later in this section).[87]

Methylhydrazine in reaction with esters or anhydrides, will give a mixture of both monoacyl isomers **1-38a-d** and **1-39a-d** (Table 1.8).[33] Hinman and Fulton determined the ratio of isomers (as they were inseparable) by reacting the mixture with p-nitrobenzaldehyde to form hydrazone solids **1-40a-d** that could then be isolated.[33] In reaction with methylhydrazine, esters give **1-39a**,**b**, and **d** as the major product, whereas anhydrides give primarily **1-38a-d** (Table 1.8).[33]

Table 1.8. Acylation of methylhydrazine by esters and anhydrides and analysis by hydrazone formation with p-nitrobenzaldehyde.[33]

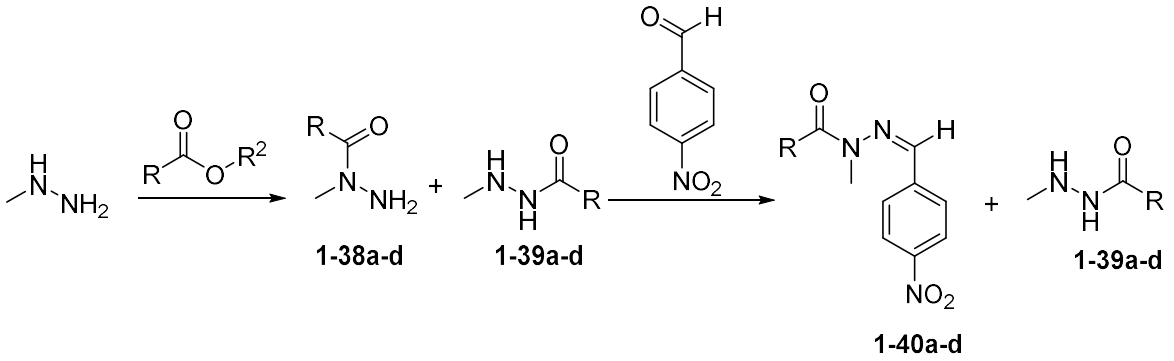

Entry	Compound	R^1	R^2	% yield of 1-40
1	**a**	Me	Me	20-23
2	**b**	Pr	Me	11-13
3	**c**	*i*-Pr	Me	>2%
4	**d**	Ph	Me	5
5	**a**	Me	MeC(O)	63
6	**b**	*n*-Pr	*n*-PrC(O)	55
7	**d**	Ph	PhC(O)	80-83

As previously shown, hydrazinolysis of esters with some hydrazines is nearly impossible without activation or a catalyst. At Rohm and Haas in 1988, Benderly showed an approach (Table 1.9) to get past this lack of reactivity by an activation strategy using trimethylaluminum.[87] Activation by deprotonation of hydrazines like 1,1-dimethylhydrazine and phenylhydrazine create nucleophiles that are strong enough to react with esters. Metalated with aluminum, the activated hydrazine will preferentially coordinate with the carbonyl oxygen of the ester through aluminum's empty p-orbital, activating the ester as a Lewis acid. The ester was unlikely to react at all with unactivated hydrazine, thus diacylation is far less likely. Table 1.9, Entry 2 shows that methyl 4-methylbenzoate reacts with the activated 1,1-dimethylhydrazine to an 87% yield, in stark contrast to no reaction with methyl benzoate as seen in Scheme 1.9. Similarly,

phenylhydrazine reacts with ethyl hexanoate and ethyl β-carboline 3-carboxylate (part of a family of anxiogenic and convulsant allosteric modulators of GABAA receptors),[88] forming **1-42d-e** with excellent yields. With **1-42a-e** as the major product by far, this indicates that any dimethylalkoxyaluminum produced in initial acylations are not adequate Lewis acids to catalyze further acylations. The obvious downside to this strategy is that functional groups that are sensitive to bases or to Lewis acid catalysis could be incompatible with this approach. The optimal ratio of activated hydrazine to ester found by Benderly was 2.5:1, which is not as atom efficient as previous paths (such as using pyridine with acid chlorides in Table 1.6).[87]

Table 1.9. Acylation of hydrazines via esters using trimethylaluminum.[87]

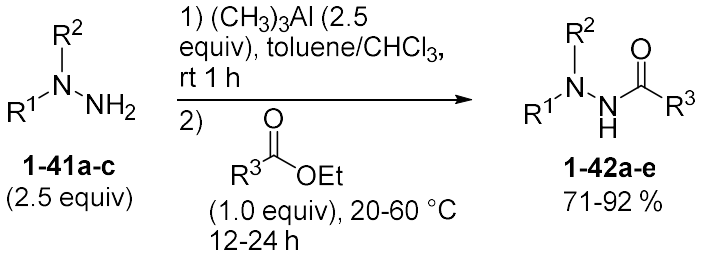

Entry	1-41	R^1	R^2	R^3	1-42	% Yield
1	**a**	Me	Me	*n*-Hex	**a**	82
2	**a**	Me	Me	4-Me-C_6H_4	**b**	87
3	**b**	Pyr	H	4-Me-C_6H_4	**c**	71
4	**c**	Ph	H	*n*-Hex	**d**	91
5	**c**	Ph	H	β-carboline 3-carboxylate	**e**	92

Referring to phenylhydrazine as an ambident nucleophile, Rosamilia uses what he called an ambident electrophile, dimethyl carbonate as a means to see what kind of electrophile the nitrogens prefer.[89]

Table 1.10. Arylhydrazine reactions with dimethyl carbonate as a function of base.[89-90]

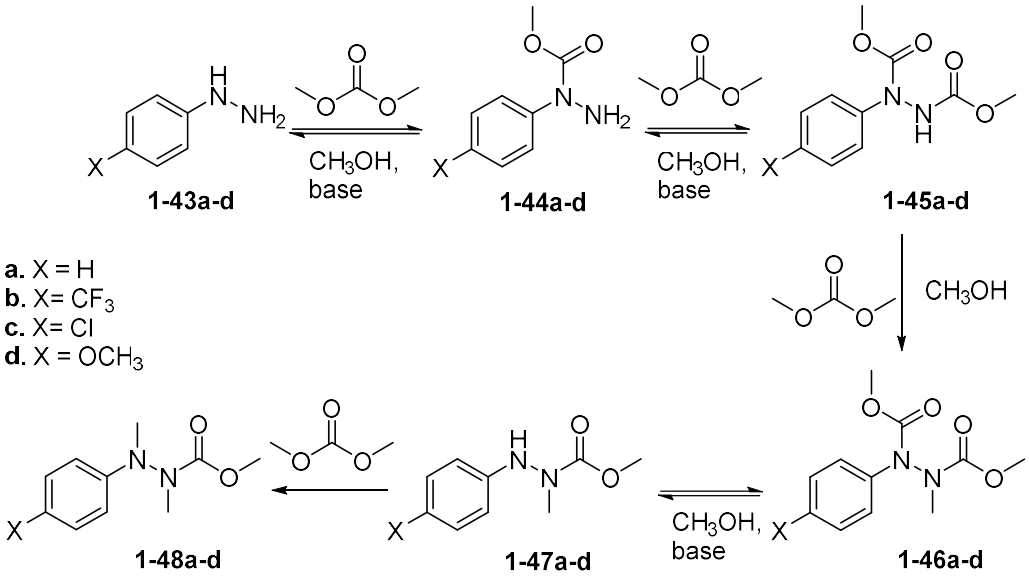

Entry	1-43	base	time (min.)	conversion to I-44 (%)	other products (%)
1	**a**	KO-*t*-Bu	25	85	0
2	**b**	NaOMe	15	0	0
3	**b**	NaOMe	40	68	0
4	**b**	NaOMe	70	70	0
5	**b**	NaOMe	110	79	0
6	**b**	NaOMe	1140	84	0
7	**b**	KO-*t*-Bu	2	78	0
8	**b**	KO-*t*-Bu	15	80	0
9	**b**	KO-*t*-Bu	40	83	0
10	**c**	NaOMe	15	0	0
11	**c**	NaOMe	40	18	0
12	**c**	NaOMe	70	78	3 (**1-45**)
13	**c**	NaOMe	110	88	5 (**1-45**)
14	**c**	NaOMe	160	92	6 (**1-45**)
15	**c**	KO-*t*-Bu	2	>99	0
16	**c**	KO-*t*-Bu	15	>99	0
17	**d**	NaOMe	15	0	0
18	**d**	NaOMe	40	26	0
19	**d**	NaOMe	70	85	5 (**1-46)**
20	**d**	NaOMe	110	89	10 (**1-46)**
21	**d**	NaOMe	160	84	11 (**1-46**), 4 (**1-47**)
22	**d**	KO-*t*-Bu	2	66	0
23	**d**	KO-*t*-Bu	15	>99	0

Table 1.10 shows that potassium tert-butoxide consistently resulted in faster reactions to give **1-44a-d** versus sodium methoxide. Compare Entry 5 to Entry 7, Entry 14 to Entry 15, and Entry 21 to Entry 23, and it is clear that potassium *tert*-butoxide as base decreased reaction times relative to the sodium methoxide and also increased conversion to **1-44a-d** simultaneously. Seeking to use hard-soft acid-base chemistry to explain the difference between the two nitrogens, Rosamilia shows that acylation on the proximal nitrogen is the first reaction to occur regardless of the alkoxide base he utilized (Table 1.10).[90] He proposed that deprotonation of the proximal nitrogen of phenylhydrazine by an alkoxide base facilitates reaction with dimethylcarbonate's carbonyl carbon.[89] Ring electronic effects were insufficient to influence the regioselectivities or hard-soft preferences of arylhydrazines toward dimethyl carbonate.[90] Other compounds within the reaction scheme of Table 1.10 could be accessed with reflux temperatures and time, though **1-45c**, **1-46d**, and **1-47d** were also observed at room temperature only when sodium methoxide was utilized.[90]

1.5.3 Acylation of hydrazines by carboxylic acids.

Acylation of hydrazines via carboxylic acids is also possible, though with some caveats. Phenylhydrazine and other arylhydrazines are capable of direct reaction with carboxylic acids, but only if those acids are liquids at the reaction temperature and thus, can be used neat.[91-93] While the protocol is simple (Scheme 1.12), the scope of this process is limited by the melting point of the carboxylic acid, and acid sensitive functional groups on the hydrazine, such as a *tert*-butyl carbonate or trityl group. When successful, this method can give access to 1-acyl-2-arylhydrazines in moderate to good yield.

Scheme 1.12. Acylation of phenylhydrazine via carboxylic acids.[91, 94]

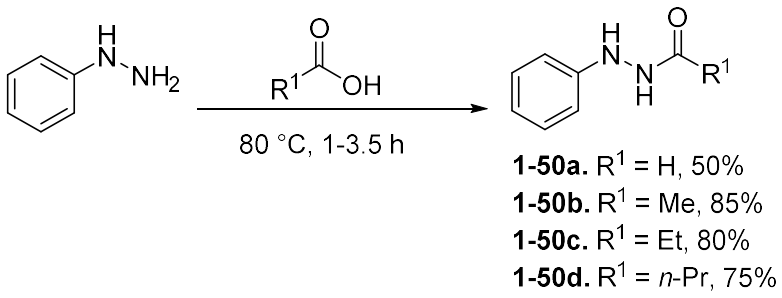

Scheme 1.13. Acylation of arylhydrazines by carboxylic acids using Katritzky benzotriazole and 1-ethyl-3-(3-dimethylaminopropyl)carbodiimide.[94-95]

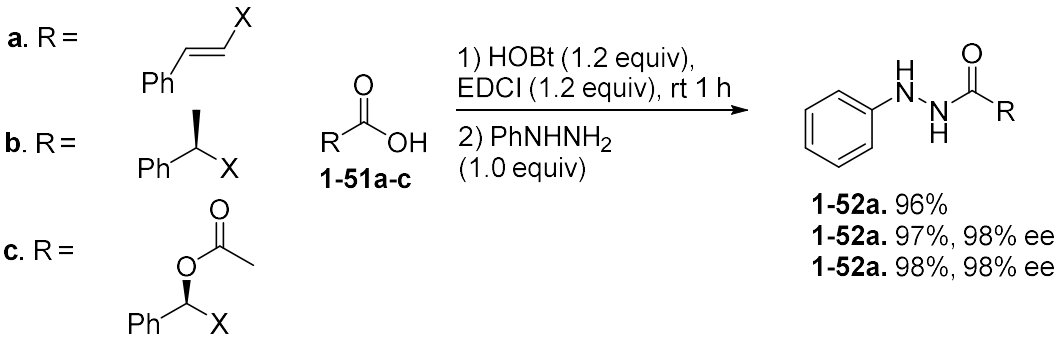

A more complex strategy is that of using carbodiimides to activate the carboxylic acid toward nucleophilic attack from hydrazines (Scheme 1.13). Borrowing from peptide synthesis techniques, dicyclohexylcarbodiimide (DCC) was the first[73] to be tried with hydrazines, but a more effective route has been found, using 1-ethyl-3-(3-dimethylaminopropyl)carbodiimide (EDCI).[94] The reaction conditions will tolerate many functional groups and the temperatures required are only small deviations from room temperature. The downsides to using these peptide coupling reagents however, is that carbodiimides are known to be potent allergens[96] that sensitize subjects upon repeated exposure. In addition benzotriazoles have environmental concerns[97] as they possess high water solubility while also having low biodegradability. These are not large

concerns for researchers, but are troubling to chemical manufacturers who wish use this technique.

1.6 Conformational isomerism

1.6.1 Rotation about the N-N bond.

The primary structural feature of hydrazine and its derivatives is the N-N bond, its rotation, and the conformations it imposes based on substitution. This rotational isomerism can be observed via X-ray crystallography, as shown in Figure 1.9.[98-99] If one or more of the conformational minima is a twist conformation, then it is possible to have helicity (*M*)- or (*P*)- and thus, axial chirality, with racemization that proceeds by N-N bond rotation.

Figure 1.9. Diformylhydrazine and 1,2-diformyl-1,2-dimethylhydrazine crystal structures (FOMHAZ02 and DMDFHZ).[98-99]

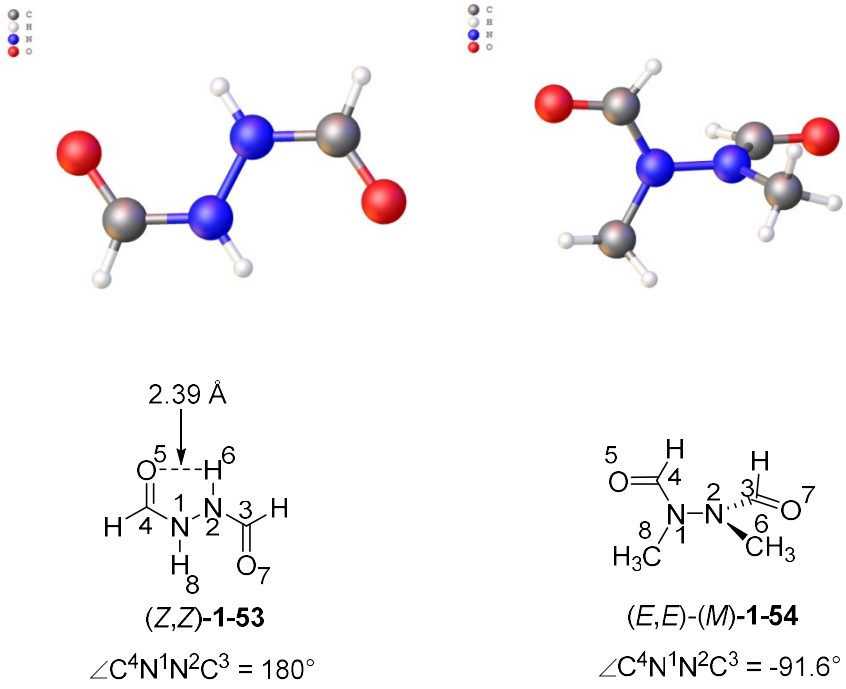

These X-ray structures show a planar conformation for 1,2-diformylhydrazine (**1-53**) and a twist conformation that is nearly orthogonal in 1,2-diformyl-1,2-dimethylhydrazine (**1-54**) (Figure

1.9). The planar structure of **1-53** is due to crystal packing that maximizes intermolecular hydrogen-bonding between other molecules of **1-53** and intramolecularly with the $\angle C^4N^1N^2C^3$ dihedral angle of 180°.[40] Note that the formyl groups in **1-53** are both in the (*Z*)-conformation, as this is suggested to be a significant factor for the relative stability of planar **1-53** in Table 1.11.[40] **1-54**, being fully substituted, has no favorable intramolecular or intermolecular hydrogen-bonding with another molecule of **1-54**, and thus adopts the (*E*)-conformation in both acyl groups, presumably to decrease steric repulsion from the oxygen lone pairs. Figure 1.10 shows that when a hydrogen-bond donor such as 18-crown-6 is crystallized with **1-53**, planarity is lost and a twist conformation is adopted, though both the acyl groups remain as (*Z*)-.[100]

Figure 1.10. 1-53 complex with 18-Crown-6 (CEJVIW).[100]

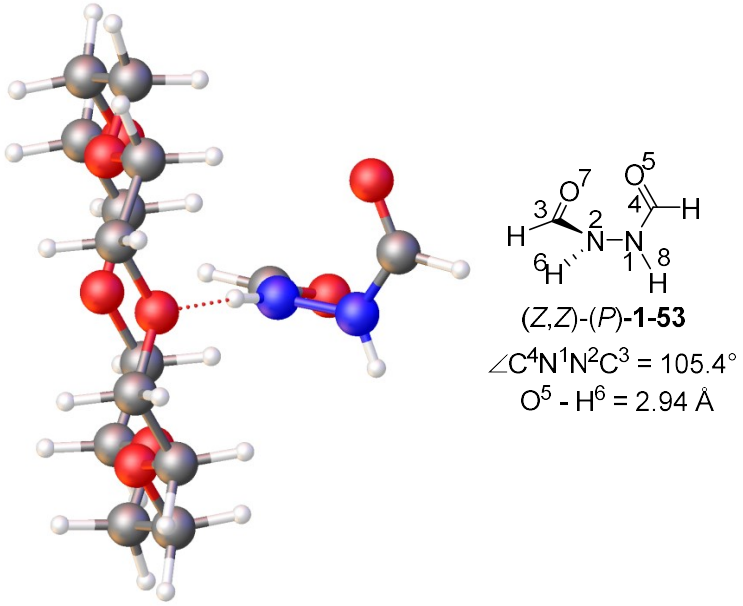

Table 1.11 shows calculated relative energies for 0, 90, and 180 degree dihedrals for each of possible rotational isomers of the formyl groups of **1-53**.[40] The computation predicts that that 90° is the most stable conformation, and 180° is nearly the same energy in (*Z*,*Z*)-, but incrementally higher in (*E*,*Z*)- (losing one favorable H-bonding interaction during rotation) and

yet higher in the (*E*,*E*)-isomer. The (*E*,*E*)-isomer would point the carbonyl oxygens O^5 and O^7 away from H^6 and H^8, which points to the importance of H-bonding to lowering the N-N rotational barrier and lends credence to H-bonding being the reason for planar X-ray crystal structures for diformylhydrazine.

Table 1.11. Calculated energies of 1-53 isomers as a function of dihedral angle (MP2/6-31+G).[40]**

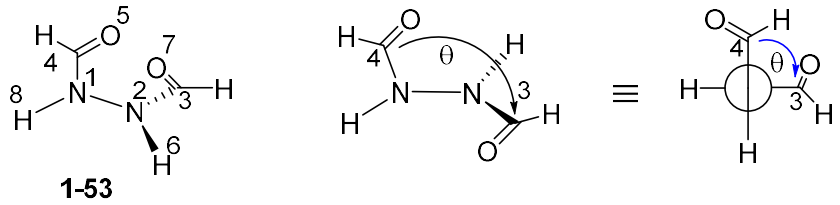

Conformation	∠$C^4N^1N^2C^3$ θ	ΔE_{rel} (kcal/mol)
(*Z*,*Z*)-	90	0.0
	0	17.0
	180	0.8
(*E*,*Z*)-	90	1.0
	0	11.8
	180	8.3
(*E*,*E*)-	90	1.3
	0	16.1
	180	13.3

NMR provides good evidence for the N-N bond-twist resulting in a chiral axis. While doing a conformational analysis of 1,2-diacyl-1-benzylhydrazines using ^{1}H NMR spectroscopy, Bishop saw that the barrier to N-N bond rotation (torsional barrier) was high enough at room temperature that the benzylic protons of the benzyl group were magnetically non-equivalent (see Table 1.12).[39] Barriers were quite high, around 23 kcal/mol, except for (*M*)-**1-55d** and (*P*)-**1-55d** as the presence of an N-H proton lowered the barrier to 13.2 kcal/mol, a drop of 10 kcal/mol (this

is perhaps due to a drop in steric hindrance, going from a benzyl group to a hydrogen).[39] The fact that the benzylic protons of the N-benzyl group were diastereotopic (Table 1.12 shows H^a's immediate environment contains R^2 in (*M*)-**1-55d**, but has a carbonyl oxygen in (*P*)-**1-55d**) can only mean that they were adjacent to a source of chirality, the N-N bond axis.[39] The conformational minima for these 1,2-diacyl-1-benzylhydrazines were described as a twist conformation, where the two substituents of N^1 are in one plane, and the two substituents of N^2 are in another plane that is nearly orthogonal relative to N^1's substituent groups (Table 1.12).[39] No information is provided on the (*E*)/(*Z*)-stereochemistry of the acyl groups, so **1-55d** is depicted as (*Z*,*Z*)- in the context of the energetically preferred conformation of **1-53** given in Table 1.11.

Table 1.12. N-N bond rotational barriers and corresponding coalescence temperatures of 1,2-diacyl-1-benzylhydrazines..[39]

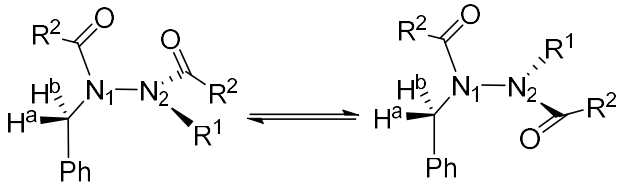

Entry	Compound	R^1	R^2	T_c (°C)	$\Delta G^{\ddagger}$ at T_c (kcal/mol)
1	**a**	CH_2Ph	OCH_3	192	23.5
2	**b**	CH_2Ph	CH_3	188	23.4
3	**c**	CH_2Ph	CH_2Ph	190	23.3
4	**d**	H	CH_2Ph	4	13.2

One might propose that nitrogen inversion, not just rotation, may be responsible for the barriers seen above; however, the NMR-derived barriers are much higher than typical inversion

barriers for amines, such as 6.7 kcal/mol for dimethylbenzylamine, and 1.4 kcal/mol for triisopropylamine.[101-102]

Figure 1.11. Changing substituents to increase N-N rotation barrier height.[38]

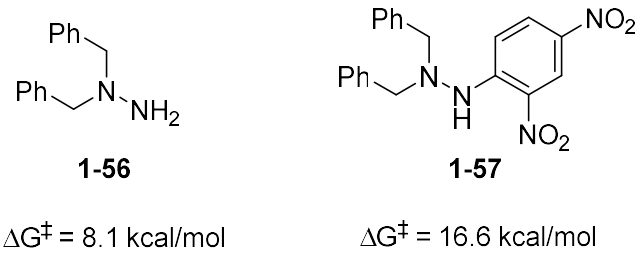

1-56 **1-57**

$\Delta G^{\ddagger}$ = 8.1 kcal/mol $\Delta G^{\ddagger}$ = 16.6 kcal/mol

Experiments with changing substituents, such as from 1,1-dibenzylhydrazine **1-56** ($\Delta G^{\ddagger}$ = 8.1 kcal/mol) to 1,1-dibenzyl-2-(2,4-dinitrophenyl)-hydrazine **1-57** ($\Delta G^{\ddagger}$ = 16.6 kcal/mol), support the N-N bond rotation hypothesis (Figure 1.11). An increase in a rotational barrier fits the data better than of an inversion barrier, as substituents on an adjacent group should not impact inversion to such a large degree.[38]

1.6.2 E/Z isomerism in acyl hydrazines

Another structural feature of acylhydrazines are the (*E*)- and (*Z*)-isomers that arise from the hindered rotation of their acyl group(s).[31] (*E*)- and (*Z*)- are determined in the same way as peptides, in that the amide resonance trigonalizes the nitrogen of the acylhydrazine, and priorities are assigned to the respective groups. Figure 1.12 shows how this is done with diacylhydrazines: four different (*E*)/(*Z*)-configurations, (*Z*,*Z*)-, (*E*,*Z*)-, (*Z*,*E*)-, and (*E*,*E*)-are possible along N^1-C^4 and N^2-C^3 while, monacylhydrazines can have only two possible configurations, (*E*)- or (*Z*)-.

Figure 1.12. E/Z isomerism of amide groups in mono- and diacylhydrazines.

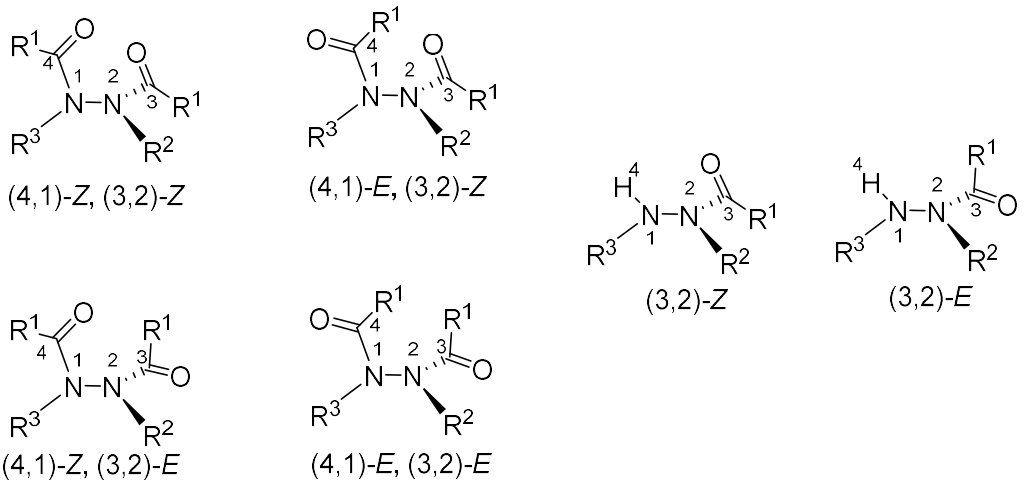

This (*E*)/(*Z*)-isomerism can potentially impact the rotational barrier of the N-N axis (suggested in calculations in Table 1.11, but we will explore this in depth in Chapter 4).[40] (*E*)/(*Z*)-Isomerism may be important for drug molecules and/or azapeptides for fitting into active sites or for structural features such as increased collagen thermal stability (azapeptides will be covered in more detail in **1.7.2**).[14] It is not hard to imagine that the (*E*)/(*Z*)-isomerism, as well as the N-N bond rotation, could be crucial in the action of ecdysone agonists like the RH series of compounds (Figure 1.1), as attempting to make cyclic diacylhydrazines like **1-59** (Figure 1.13) negated their toxicity, just as alkyl substitution does **1-58**.[15, 41]

Figure 1.13. Substitution effects on insecticidal action.[15, 41]

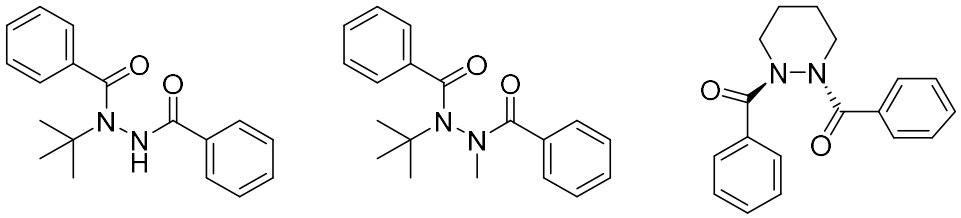

The presence of N-H is essential to insecticidal action of diacylhydrazines such as RH-5849 (Figure 1.13), and could be due to a simple hydrogen-bonding in the active site for ecdysone receptors;[41] however, there is room to argue that perhaps the presence of N-H allows a (*Z*)-conformation on the proximal acyl group (such as we saw with **1-53** versus the fully substituted **1-54** in Figure 1.9) and allows these molecules to rotate into a form that will fit into the ecdysone active site (since diacylhydrazines are not at all similar to steroid hormones in structure).

1.7 Applications of acylhydrazines

1.7.1 Synthesis of heterocycles and macrocycles from acylhydrazines.

While the number of synthetic techniques to make acylhydrazines may not be large, the number of possible heterocycles that can be formed from them are considerable. Majumdar et al wrote a review that describes the transformation of acylhydrazines into a host of heterocycles, including pyrazoles, imidazes, oxadiazoles, thiazoles, triazoles, pyridines, pyrazines, pyrimidines, oxadiazines, triazines and many more.[103] Acylhydrazines are an important synthetic jump-off point to a sizable number of heterocyclic molecules that find use in medicine and material science.[103] A few examples: Scheme 1.14 shows an alternative route to indoles **1-61a-b** by reaction of trisubstituted monoacylhydrazine **1-60a-b** and a triphenyl phosphonium ylide to access the key Fischer Indole synthesis intermediate.[103]

Scheme 1.14. Indole synthesis utilizing acylhydrazines.[103]

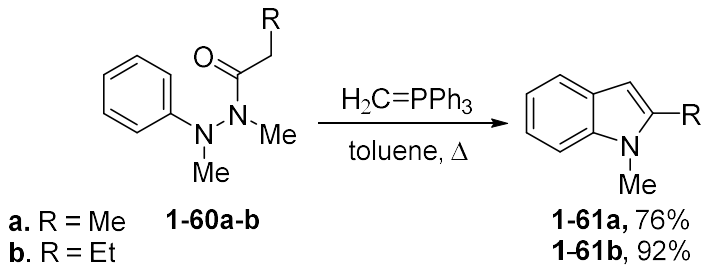

a. R = Me **1-60a-b**
b. R = Et

1-61a, 76%
1-61b, 92%

Scheme 1.15 offers routes to pyrazoles **1-64** and **1-65**, and pyrazolidinone **1-66** in good yields from simple relatively starting materials.[104]

Scheme 1.15. Pyrazole, pyrazoline, and pyrazolidinone syntheses utilizing acylhydrazines.[103]

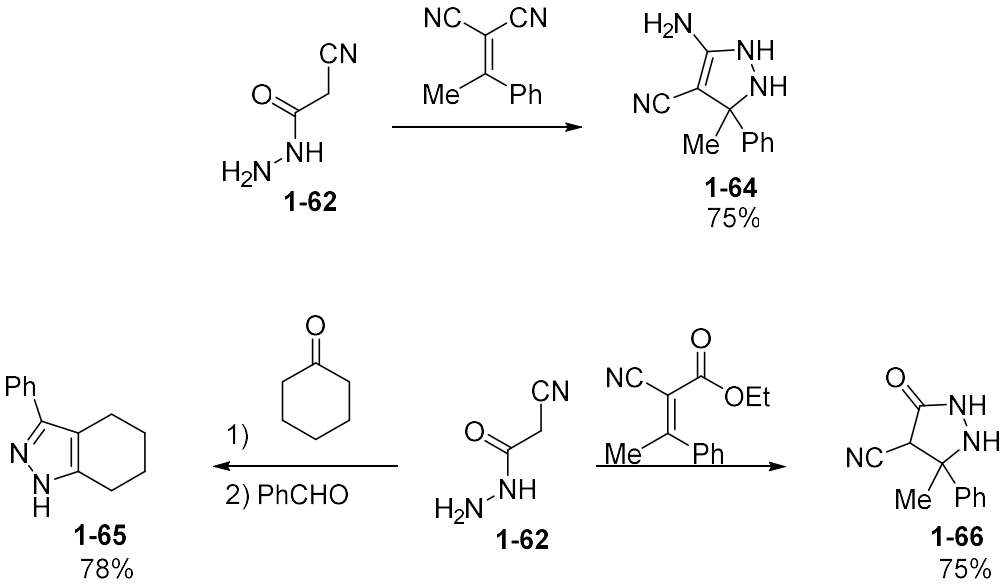

Scheme 1.16. 1,3,4-Oxadiazole syntheses utilizing acylhydrazines.[103]

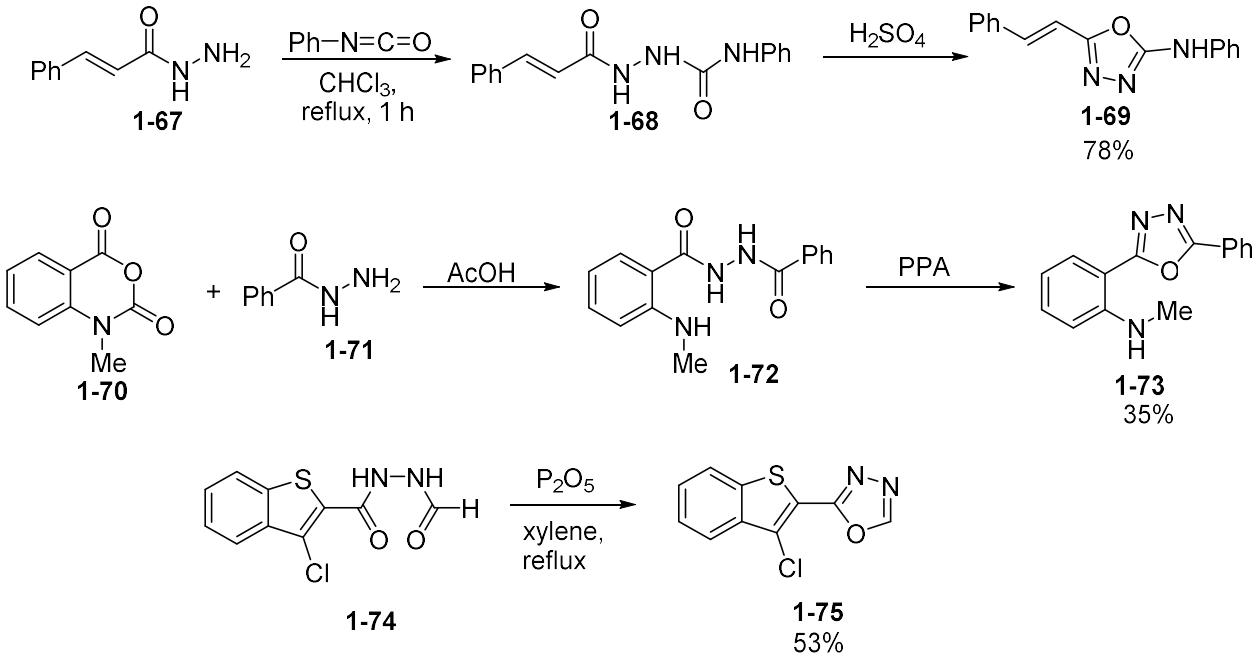

Scheme 1.16 showcases two 1,3,4-oxadiazoles (**1-69** and **1-73**) that are accessible from monoacylhydrazines, and **1-75** from diacylhydrazine **1-74** by ring closure using phosphorus pentaoxide.[103] Figure 1.17 presents a way to synthesize 1,5-disubstituted 3-amino-1H-1,2,4-triazoles like **1-78** can be made from a 1,2-diacylarylhydrazine **1-76** utilizing HPF_6 (older reactions use $HClO_4$ which has risks of explosion) and acetic anhydride to form oxadiazolium salt **1-77** that can safely react with cyanamide to produce the desired aminotriazole.[7] Lastly, Figure 1.17 also features a way to obtain disubstituted 1,2,4-triazole **1-81** from simply refluxing monoacylhydrazine **1-79** and benzimidamide **1-78** in chlorobenzene and ethanol with a moderate yield.

Scheme 1.17. 1,2,4-triazole synthesis utilizing acylhydrazines.[7, 103]

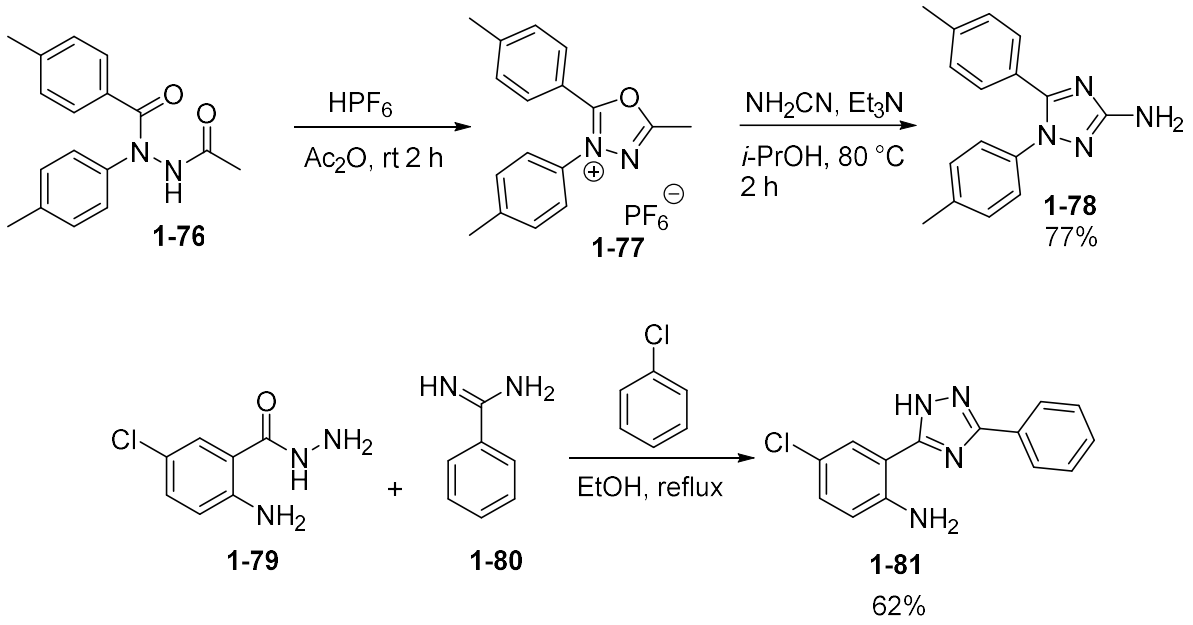

Synthetic applications of acylhydrazines are not solely in the sphere of heterocycles. The twisted N-N axis of acylhydrazines can be used to facilitate ring closing metathesis and thereby produce macrocycles (ring sizes ≥8-membered).[105] Due to the hindered rotation of the N-N bond and preference for twist-conformations of the N-N bond, vicinal substituents on the hydrazine nitrogens are preorganized into a gauche-like orientation that aids olefin metathesis and consequently, macrocyclization, as seen in Scheme 1.18.[105] This allows relatively simple access to macrolide-like molecules like **1-85** that are similar to cores of some antibiotics like spiramycin and erythromycin.[106]

Scheme 1.18. Macrocyclization via olefin metathesis and diacylhydrazine .[105]

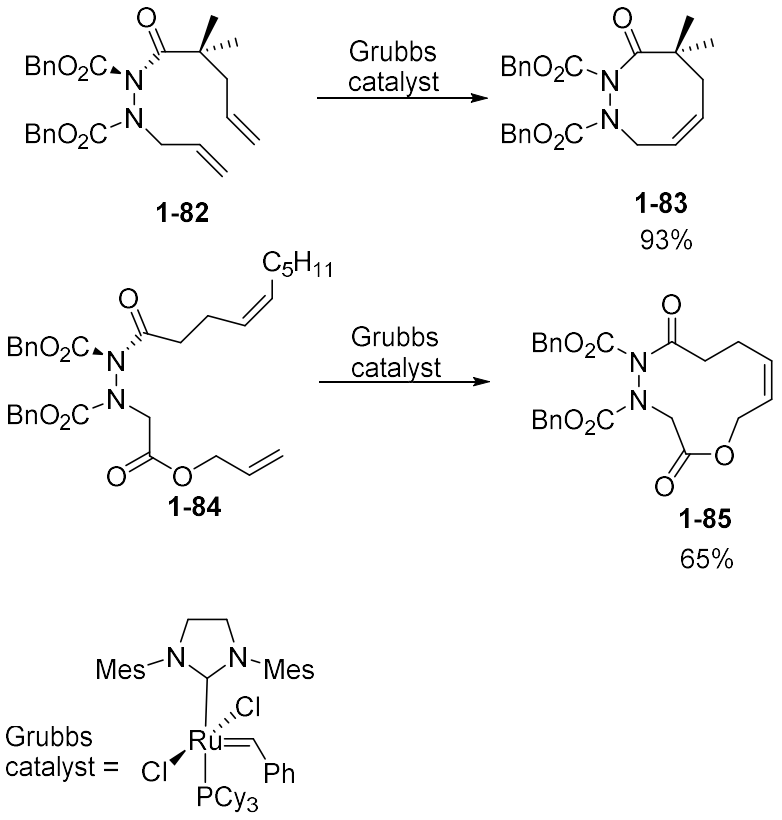

Another utilization of the N-N chiral axis in acylhydrazines is found in Enders' creative variation on the Evans-type chiral auxiliary, using 1-acyl-2,2-dialkylsubstituted hydrazine **1-86** (Scheme 1.19) .[107] The synthetic goal was to access 2-substituted lactams of multiple ring sizes with stereocontrol through an easily removable auxiliary unit.[107] After performing a cyclization on **1-86**, the stereoselectivity of the alkylation of **1-87** leading to **1-88a-b** is reinforced by intramolecular chelation of the lithium ion by both the methoxy group and nitrogen of the chiral auxillary.[107] The N-N bond in **1-88a-b** can then be reduced using lithium metal in ammonia, yielding **1-89a-b** with good yields and good to excellent ee.[107]

Scheme 1.19. Acylhydrazines as chiral auxiliaries for the synthesis of chiral lactams.[107]

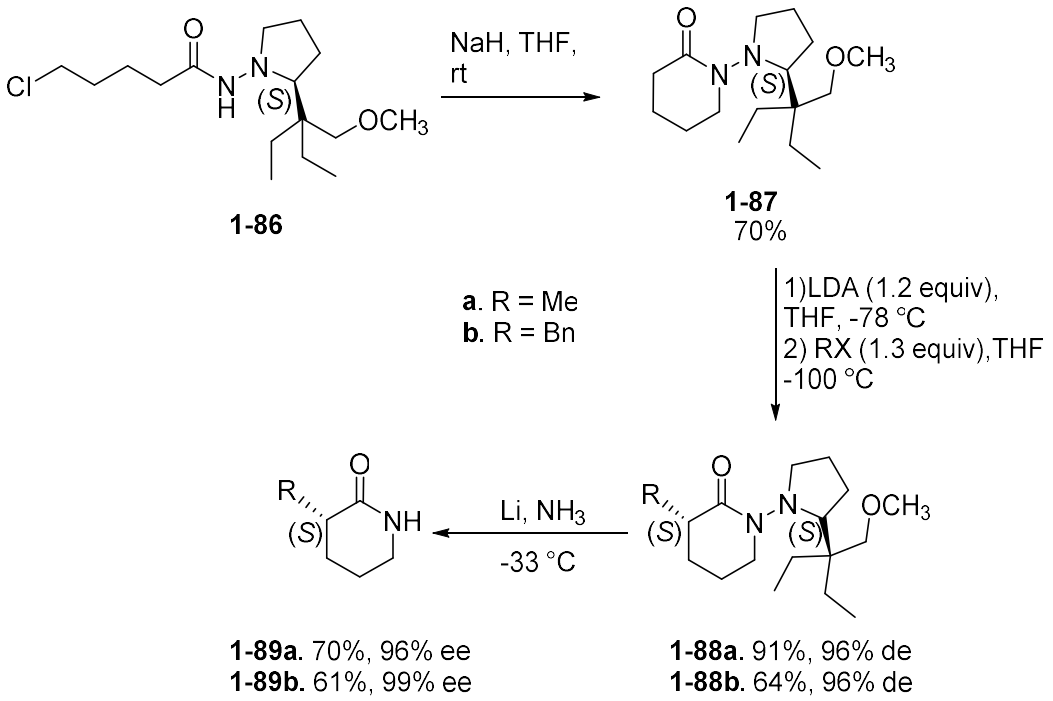

1.7.2 Utility of acylhydrazine intermediates in protein synthesis and as protein probes

Acylhydrazines are useful tools for protein synthesis that have such benefits as minimizing racemization (no oxazolone formation), while setting up conditions for ligation to another peptide strand using a one-pot procedure that cuts down the number of potential purification steps (see Scheme 1.20).[108] Treatment of peptide-derived acylhydrazine **1-90** provides easy access to the corresponding azide **1-91** via oxidation by sodium nitrite. Subsequent reaction with 5-thio-2-nitrobenzoic acid[109] (though other thiols can fill this role, this one is particularly effective) generates a thioester for coupling with the amino terminus of peptide 2 (**1-93**).[108] The thioester **1-92** is made because aminolysis of acyl azide is a slow reaction and the azide can be unstable at higher temperatures required to speed up the aforementioned aminolysis reaction and can undergo rearrangement, whereas the thioester is formed at lower temperatures, can undergo quantitative aminolysis by **1-93**, but will not exchange with other carboxylic acid

groups.[108] Also, while sodium nitrite can oxidize cysteine during the conversion of the acylhydrazine **1-90** to azide **1-91**, thiols can reduce cysteine back to its native form and thus, addition of excess thiol in the conversion of **1-91** to **1-92** solves two problems simultaneously.[108]

Scheme 1.20. Protein ligation via acylhydrazines.[108]

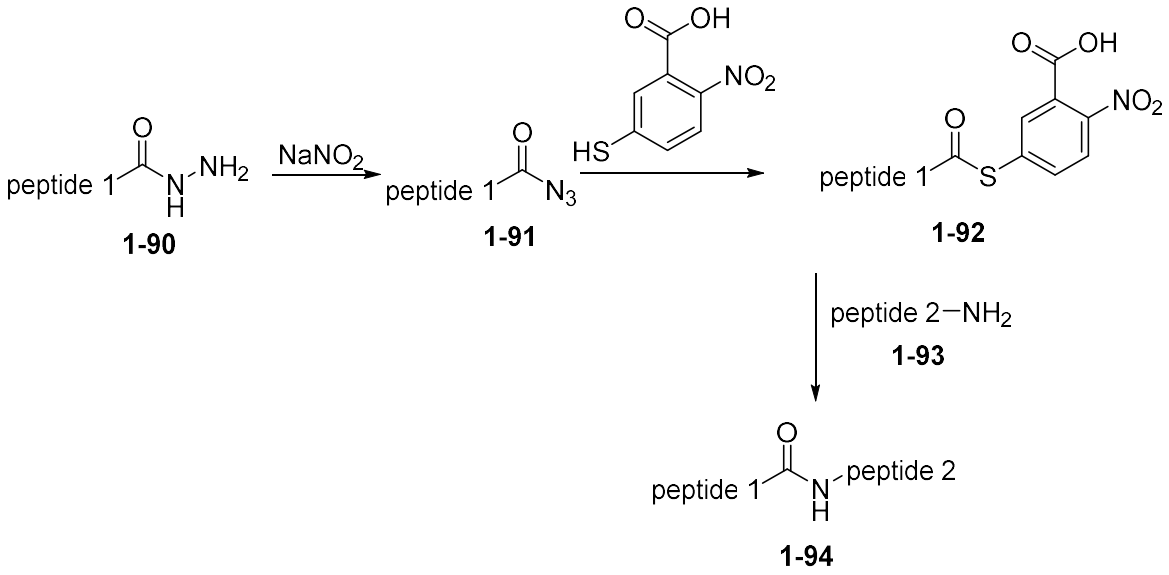

1-90 **1-91** **1-92** **1-93** **1-94**

Additionally, acylhydrazines such as BODIBY hydrazide and biotin hydrazide (Figure 1.14) on solid supports have been used to conjugate glycoproteins through condensation to glycohydrazones to form isolatable solids.[108] In doing so, glycoproteins can be enriched out of a mixture easily and allows quicker throughput for analysis.[108] Attachment of a -Leu-Cys-Tr-Pro-Ser-Arg- tag and selective oxidation of Cys in the tag to formyl glycine allows probing of a specific protein out of a mixture of proteins. These reactions are possible in the buffer solutions needed for biochemical experiments because acylhydrazines are weaker bases than amines but are still good nucleophiles at pH 7 due to the α-effect.[108]

Figure 1.14. Acylhydrazide protein probes.[108]

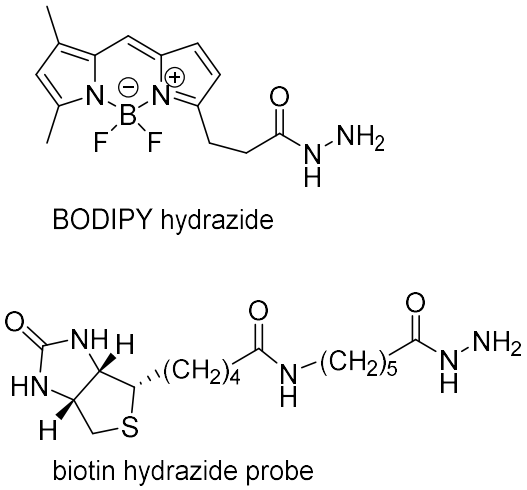

Acylhydrazines, in the form of azapeptides, find their way into biology precisely because of their conformational and chemical properties.[108] Azapeptides, just as any acylhydrazine, exhibit a twist conformation with hindered rotation. In addition, the replacement of tetrahedral C_α with a trigonal nitrogen embeds three changes to a peptide backbone: a) rigidity is increased by replacing a freely rotating C_α-N bond with an N-N bond that prefers twist conformations, b) removes the C_α chiral center, and adds another hydrogen-bond donor that can serve to increase interstrand forces.[40] Figure 1.15 describes how a single methyl substitution of the hydrazine of an azapeptide like **1-96** to generate **1-97** and **1-97** to **1-98** can change the preference for the (*E*)/(*Z*)-conformation of its acyl groups and thereby change the structure of a protein that it is incorporated into (note that this same phenomenon was observed in the crystal structures of **1-53** and **1-54** in Figure 1.9).[110] Methyl substitution not only changes the (*E*)/(*Z*) preference, it also increases the barrier of rotation for the N-N bond from 17.4 kcal/mol in **1-97** to 28.0 kcal/mol in **1-98** (just as we saw in Table 1.12).

Figure 1.15. Influencing protein shape via acylhydrazine conformational isomerism.[110]

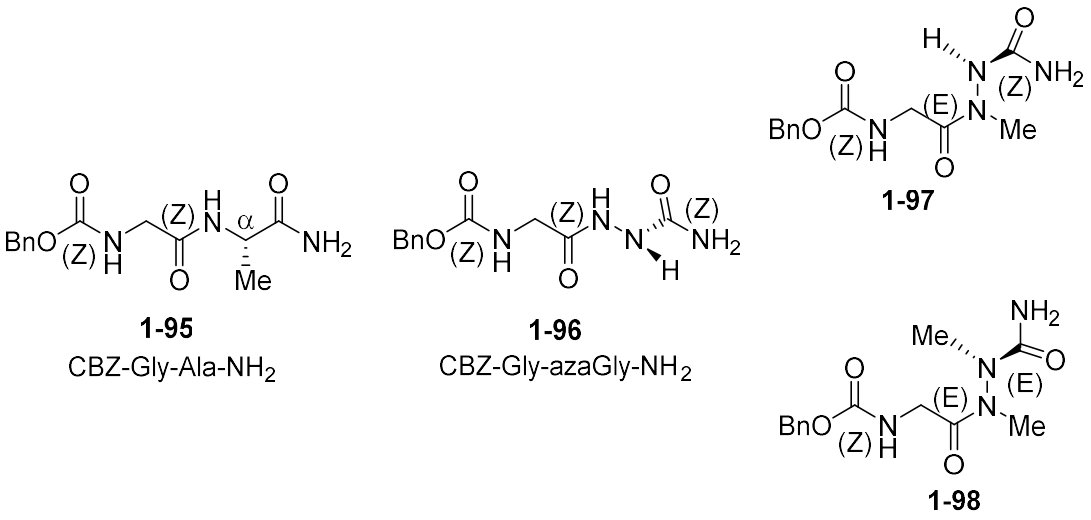

The fact that azapeptides have the same hindered rotation of the N-N bond as other acylhydrazines means that the number of conformations is more limited than for natural amino acids. The consequences of changes in peptide structure can be quite dramatic. Proteases such as chymotrypsin require their peptide substrates to adopt extended conformations in order to carry out peptide hydrolysis. Azapeptides force folded conformations to maximize hydrogen bonding and minimize lone pair electron repulsion, and as a result, are more slowly hydrolyzed by proteases.[11, 37] Using azaglycine in collagen also increased the protein's thermal stability via hydrogen-bonding between strands and thereby increasing the T_m of collagen by 10 °C or more and decreasing the time needed to thermodynamically refold (Table 1.13).[14]

Table 1.13. Azaglycine incorporation to collagen and changes in thermal stability.[14]

peptide	central triplet	T_m (°C) 12 °C/h	ΔG (kcal/mol)	folding $t_{1/2}$ (min)
1	-Pro-Pro-Gly-	37	-11	33 ± 2
2	-Pro-Hyp-Gly-	40	-12	24 ± 6
3	-Pro-Pro-azGly-	47	-13	27 ± 6
4	-Pro-Hyp-azGly-	51	-15	14 ± 3

1.7.3 Acylhydrazines as natural products.

Though very rare, hydrazines, hydrazones, and acylhydrazines are in fact found in some natural products.[111] Examples of these compounds can be found in a review by Le Goff, (with selected examples shown in Figure 1.16).[111]

Figure 1.16. Hydrazine containing natural products.[111]

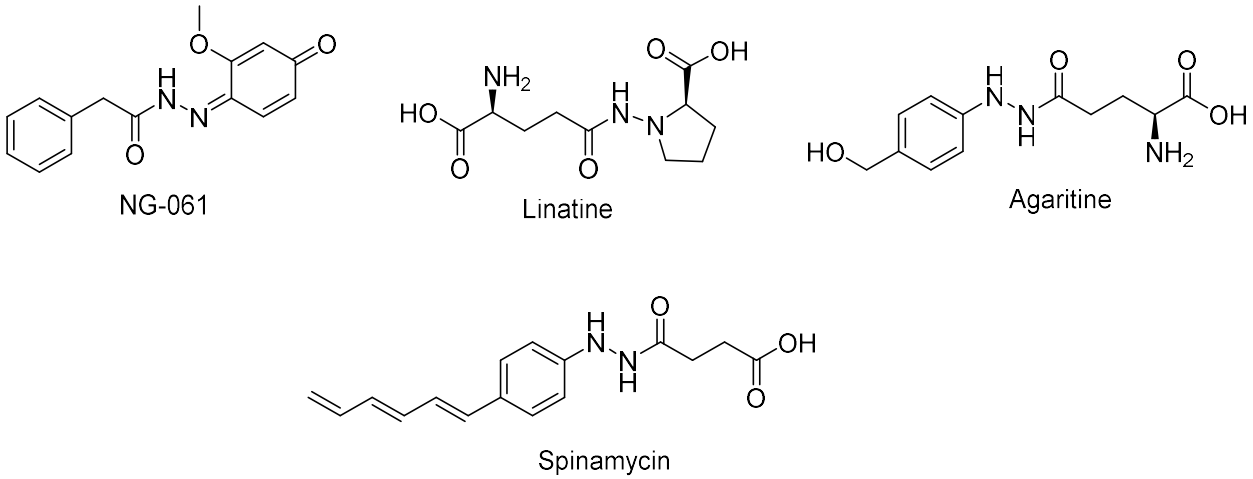

The acylhydrazone NG-061 has been shown to act as a nerve growth factor in rat pheochromocytoma cell line P12.[111-112] Linatine is a monoacylhydrazine that is not only antimicrobial,[111] but also a vitamin B6 antagonist in juvenile chickens[113] (thus, one would not use Linatine in poultry agriculture but investigate antimicrobial efficacy in mammals perhaps).[111] Agaritine is found in the common mushroom cultivar *Agaricus bisporus*, and has been seen to possess antileukemia properties without affecting normal lymphatic cells.[114] Spinamycin has been found to have anticancer and antifungal properties. Deducing the mechanism of action for each of these molecules, as well as their pharmacological effects on different organisms could prove useful in the design of synthetic acylhydrazines for biological application.

1.8 Conclusion

Acylhydrazines possess a number of properties that set them apart from diamines and other functional groups, such as being α-nucleophiles, and their twisted N-N bond axis. While it is possible to deduce the answers to some questions about acylhydrazines from the literature, uncertainty lingers about others. What is the regioselectivity preference in acylation for phenylhydrazines precisely? What kinds of synthesis techniques are most effective at the bench when attempting to make a diverse collection of 1,2-diacyl aryl- and benzylhydrazines? Will 1,2-diacylhydrazines prove toxic to *Anopheles gambiae*, presumably by K^+-channel disruption? What are the preferred conformations of 1,2-diacylhydrazines and can their various rotational isomerisms be observed by NMR and X-ray crystallography, as well as modelled computationally? These are questions that my work seeks to answer in the coming chapters.

Chapter 2. Synthesis of a Library of Potential Mosquitocides and Subsequent Toxicity Screening: Mono- and Diacyl-, Benzyl and Phenylhydrazines

2.1 Purpose of library generation, goals, toxicity benchmarks, and definition.

As alluded to in Chapter 1, the basis for our group exploring the chemical space of hydrazine substitution comes from the work of Hsu[15, 42, 70] and Salgado[23-24, 46] on the insecticidal activity of 1,2-diacyl-*tert*-butylhydrazines. With the goal of developing an effective mosquitocide against *Anopheles gambiae*, it was logical to explore different alkyl- and aryl-substituted hydrazines, as well as their mono- and diacylated derivatives. This chapter concerns the synthesis techniques employed for producing the library, as well as the mosquito toxicities of the individual compounds. The chosen hydrazine starting materials for this project were benzylhydrazine and phenylhydrazine (as well as arylhydrazines). The LC_{50} benchmarks we hoped to improve upon were set by the leads, RH-5849 and RH-1266 (Figure 2.1).[16]

Figure 2.1. Lead compounds of the RH-series, *Anopheles gambiae* topical toxicity values and possible structural modifications (CI denotes confidence interval).[16]

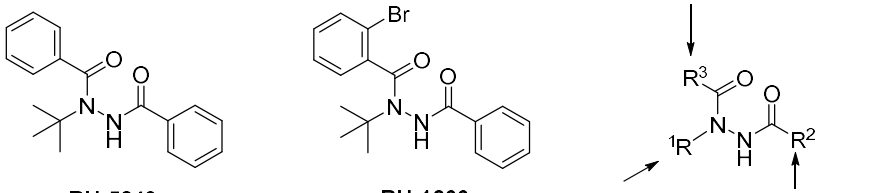

Since the lead compounds had LC_{50} values of 735 (583-945) and 504 (393-648) ng/insect respectively, we sought new compounds that show lethality or incapacitation of 100% of all

mosquitoes tested at a dose of 500 ng/insect, to be considered for LD_{50} measurements and further study. All toxicity testing was done by collaborators in the Bloomquist group at the Department of Entomology and Nematology at the University of Florida: Drs. Rafique Islam and Fan Tong. The assay consisted of gathering 20 *Anopheles gambiae*, (female, non-blood fed, 2-5 days old) and anesthetizing them by cooling briefly. A 500 ng solution of a test compound in 200 nL of ethanol was topically administered to the dorsal thorax by a glass microapplicator. Mosquitoes were then revived by warming, transferred to a chamber that provided free access to sugar water and monitored after 24 hours.[115] Mortality was scored as a fraction of immobile mosquitoes after 24 hours. Toxicity, as it is referred to here is not necessarily an affirmative statement on the mechanism of action being K^+-channel disruption, as this analysis was done in parallel for a group of select compounds only. Each compound was given a systematic number and letter designation based on the points of modification; a legend can be found in Figure 2.2 that applies to all mono- and diacylhydrazines synthesized for this project.

Figure 2.2. Compound ID scheme for all synthesized acylhydrazines.

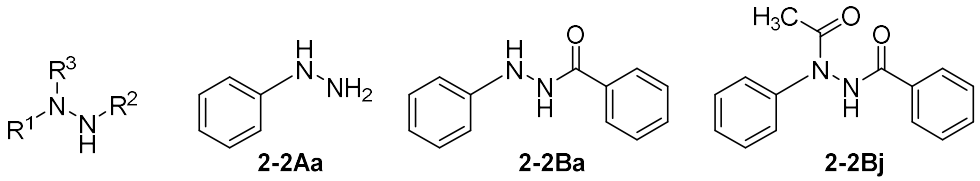

1; R^1 = benzyl
2; R^1 = Ph
3; R^1 = 4-fluorophenyl
4; R^1 = 4-methoxyphenyl
5; R^1 = 4-bromophenyl
6; R^1 = *t*-Bu

A; R^2 = H
B; R^2 = benzoyl
C; R^2 = 4-methylbenzoyl
D; R^2 = 4-fluorobenzoyl
E; R^2 = 4-methoxybenzoyl
F; R^2 = 4-chlorobenzoyl
G; R^2 = 2-bromobenzoyl
H; R^2 = 2-fluorobenzoyl
I; R^2 = cyclopropanecarbonyl
J; R^2 = acetyl
K; R^2 = trimethylacetyl
L; R^2 = dimethylacetyl
M; R^2 = phenylacetyl
N; R^2 = nicotinoyl
O; R^2 = isonicotinoyl
P; R^2 = Boc

a; R^3 = H
b; R^3 = Benzoyl
c; R^3 = 4-methylbenzoyl
d; R^3 = 4-fluorobenzoyl
e; R^3 = 4-methoxybenzoyl
f; R^3 = 4-chlorobenzoyl
g; R^3 = 2-bromobenzoyl
h; R^3 = 2-fluorobenzoyl
i; R^3 = cyclopropanecarbonyl
j; R^3 = acetyl
k; R^3 = trimethylacetyl
l; R^3 = dimethylacetyl
m; R^3 = phenylacetyl
n; R^3 = nicotinoyl
o; R^3 = isonicotinoyl
p; R^3 = Boc
q; R^3 = trifluoroacetyl
r; R^3 = propanoyl
s; R^3 = isovaleryl
t; R^3 = methyl carboxylate

2.2 Benzylhydrazine and its acyl derivatives.

The first choice of modification to diverge from the RH-series was to change R^1 (Table 2.1) from *t*-Bu to the less hindered benzyl group. To our knowledge, acylbenzylhydrazines have received limited investigation insecticides before now, and even then, they were used as agents against *Lepidoptera*, *Coleoptera*, and *Nematoda* (moths/butterflies, beetles, and nematode worms respectively), not mosquitoes like *Anopheles gambiae*.[70, 116] Initial attempts at synthesizing monoacylbenzylhydrazines followed the methodology described for *tert*-butylhydrazines in Chapter 1. However, due to the reduced steric bulk of the benzyl group relative to *tert*-butyl, acylation regioselectivity in reaction with acid chlorides was poorly controlled, as was noted in

Chapter 1 for methylhydrazine.[32] Utilizing the same reaction conditions (Schotten-Baumann) that produced controllable monoacylation for *tert*-butylhydrazine, benzylhydrazine yielded the diacylbenzylhydrazine as the major product. Entries 1 and 2 of Table 2.1 are of particular note, in that the only products observed were **2-1Ll** and **2-1Kk**, respectively.

Table 2.1. Unintentional benzylhydrazine diacylation.

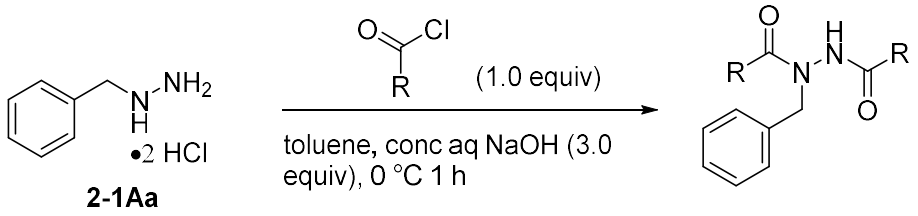

Entry	Product ID	R	Isolated Yield[a] (%)
1	**2-1Ll**	isobutyryl	50
2	**2-1Kk**	*tert*-butyl	50
3	**2-1Bb**	Ph	35
4	**2-1Ee**	4-$MeOC_6H_4$	27
5	**2-1Dd**	4-F-C_6H_4	28
6	**2-1Hh**	2-F-C_6H_4	22

[a] Isolated by recrystallization.

In these two cases acid chlorides were completely consumed to make only the diacyl product, and while Entries 4-6 of Table 2.1 were less biased toward the 1,2-diacylbenzylhydrazine, it was still a major product. Though complete characterization of the products was not performed, it was clear that even if the stoichiometric ratios of starting materials were further biased toward forming monoacyl products, the reaction would still give mixtures that require purification. It was clear that a different strategy was needed in order to more efficiently produce unsymmetric diacylbenzylhydrazines.

In order to produce a library of diacylbenzylhydrazines with differing acyl groups, the lack of selectivity in the acylation reaction had to be tamed or bypassed. The method that we settled on was that of a reductive amination-style approach. Starting with **2-7** and reacting with benzaldehyde to synthesize **2-8**[30], and subsequent reduction[117] with sodium cyanoborohydride gave **2-1Ba** in 81 % yield over the two steps (see Scheme 2.1). This strategy eliminated the generation of regioisomers and undesired diacyl products, and paved the way for the synthesis of a number of unsymmetric diacylbenzylhydrazines for toxicity screening.

Scheme 2.1. Hydrazone formation for the installation of the benzyl group.[30, 117]

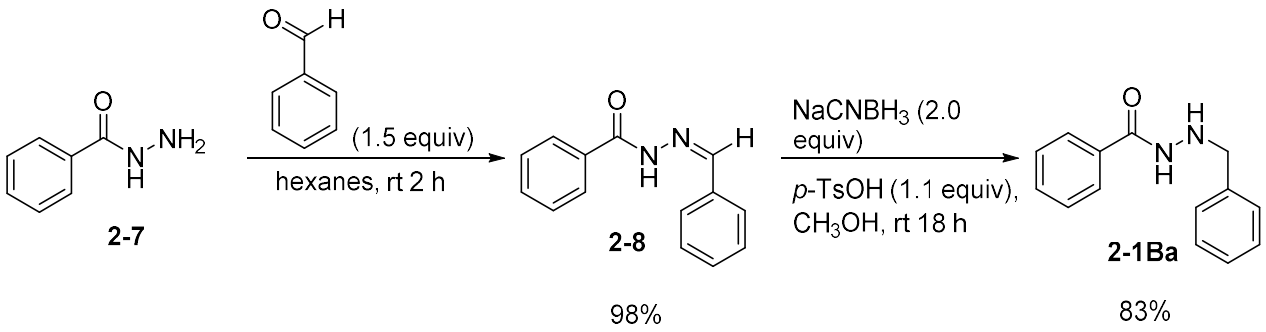

Diacylbenzylhydrazines were synthesized by utilizing three methods (Scheme 2.2). Method **A** describes the synthesis of unsymmetrical diacylbenzylhydrazines using **2-1Ba** as the starting material. Methods **B** and **C** are variant paths to symmetrical diacylhydrazines (two of the same acyl group) starting from benzylhydrazine dihydrochloride, with **B** being a single organic phase reaction and **C** derived from the Schotten-Baumann conditions of Hsu.[42]

Scheme 2.2. Diacylbenzylhydrazine synthesis Methods A, B, and C[42] and corresponding isolated yields.

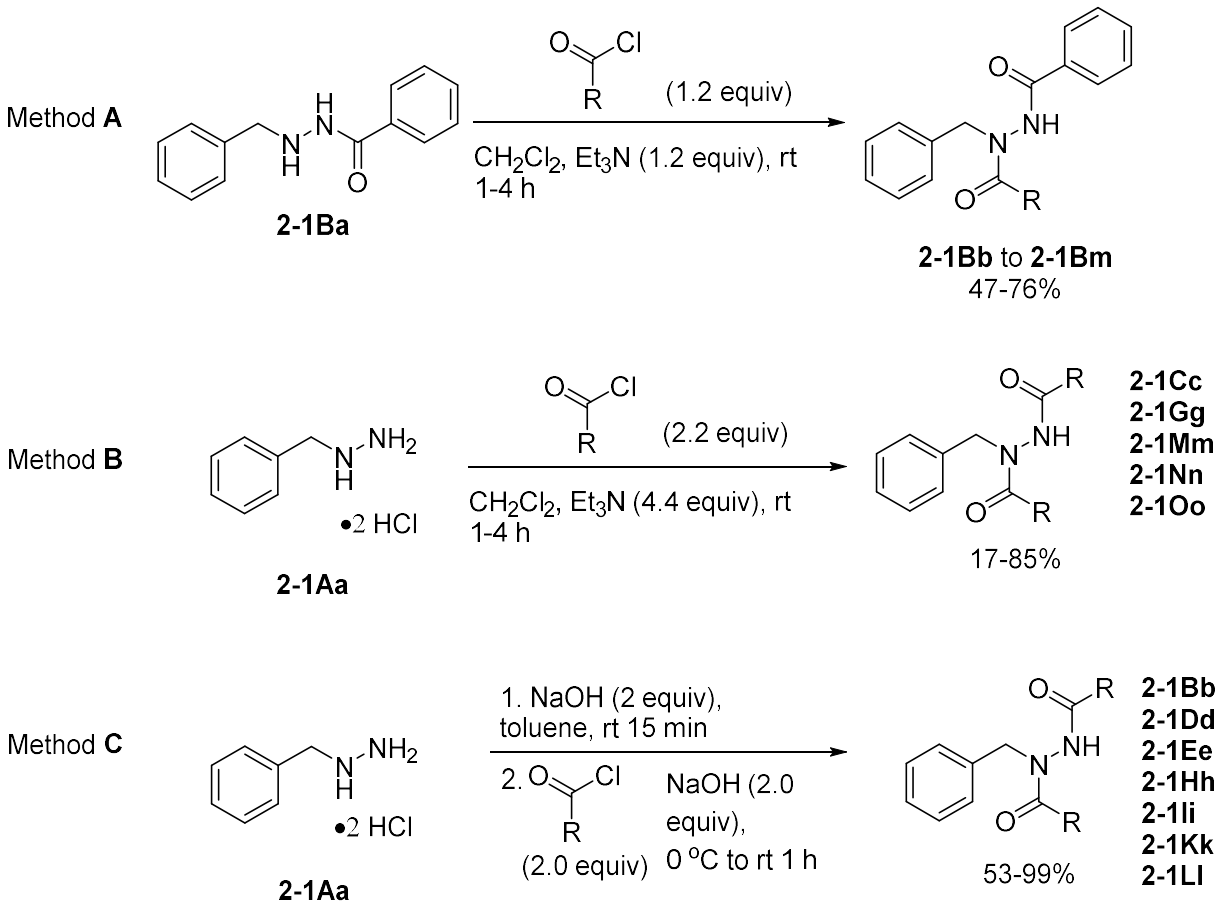

As shown in Scheme 2.2 and Table 2.2, unsymmetrical diacylbenzylhydrazines **2-1Bb** to **2-1Bm** were prepared by Method A in 47-76% yield. Symmetrical diacylbenzylhydrazines were prepared by Methods B and C in 17-85 and 53-99% yield respectively. In each case, the products were isolated by recrystallization, so the yields reflect both reaction selectivity and product solubility. The lowest yields were for **2-1Nn** and **2-1Oo** (35 and 17% respectively), and we attribute these low yields to hydrolytic sensitivity of the nicotinoyl and isonicotinoyl groups. When Method C was applied to the synthesis of **2-1Nn** and **2-1Oo**, the desired compounds were not observed (Entries 4 and 6, Table 2.2), possibly because of the aqueous base employed.

Table 2.2. Synthesis of symmetrical *N*,*N*′-diacylbenzylhydrazines, comparing Methods B and C.

Entry	Product ID	R	Synthesis Method	Isolated Yield[a] %
1	**2-1Mm**	**$PhCH_2$**	**B**	72
2	**2-1Mm**	**$PhCH_2$**	**C**	28
3	**2-1Nn**	**3-pyridyl**	**B**	35
4	**2-1Nn**	**3-pyridyl**	**C**	0
5	**2-1Oo**	**4-pyridyl**	**B**	17
6	**2-1Oo**	**4-pyridyl**	**C**	0

[a] Isolated by recrystallization.

Using these methods, 20 diacylbenzylhydrazines, as well as **2-8** and **2-1Ba**, were synthesized and submitted for assay to test their mosquitocidal properties (see Table 2.3). The most potent *N*,*N*′-diacylbenzylhydrazines tested were **2-1Dd** and **2-1Hh** (Entries 12 and 15 in Table 2.3), each showing 85% mortality of tested mosquitoes at 500 ng/insect after 24 hours. As none of the benzylhydrazines met the benchmark (100% mortality at this dose) no further testing on these compounds were performed. Note that toxicity curves are rather steep. We estimate that had they been tested, 2-1Dd and 2-1Hh would have had LD_{50} values in the range of 300-400 ng/insect. Thus, the desired significant improvement in toxicity relative to the lead compounds had not been realized. It was then decided to move on to acylphenylhydrazine derivatives.

Table 2.3. Acylbenzylhydrazine synthetic yields using Methods A-C and toxicity assay results (see Figure 2.2 for product legend).

Entry	Product ID	R^2	R^3	Synthesis Method	Isolated Yield %[a]	% Mortality at 500 ng/insect
1	**2-1Ba**	benzoyl	H	NA	83	30
2	**2-8**	NA	NA	NA	98	40
3	**2-1Bb**	benzoyl	benzoyl	**C**	70	65
4	**2-1Bc**	benzoyl	4-Me-benzoyl	**A**	54	30
5	**2-1Bd**	benzoyl	4-F-benzoyl	**A**	64	50
6	**2-1Be**	benzoyl	4-MeO-benzoyl	**A**	76	30
7	**2-1Bh**	benzoyl	2-F-benzoyl	**A**	71	10
8	**2-1Bi**	benzoyl	*c*-Pr-C(O)	**A**	67	20
9	**2-1Bk**	benzoyl	trimethylacetyl	**A**	84	50
10	**2-1Bl**	benzoyl	dimethylacetyl	**A**	47	30
11	**2-1Bm**	benzoyl	phenylacetyl	**A**	56	40
12	**2-1Cc**	4-Me-benzoyl	4-Me-benzoyl	**B**	85	80
13	**2-1Dd**	4-F-benzoyl	4-F-benzoyl	**C**	75	85
14	**2-1Ee**	4-MeO-benzoyl	4-MeO-benzoyl	**C**	53	75
15	**2-1Gg**	2-Br-benzoyl	2-F-benzoyl	**B**	52	60
16	**2-1Hh**	2-F-benzoyl	2-F-benzoyl	**C**	86	85
17	**2-1Ii**	*c*-Pr-C(O)	*c*-Pr-C(O)	**C**	69	30
18	**2-1Kk**	trimethylacetyl	trimethylacetyl	**C**	99	70
19	**2-1Ll**	trimethylacetyl	trimethylacetyl	**C**	76	25
20	**2-1Mm**	phenylacetyl	phenylacetyl	**B**	72	30
21	**2-1Nn**	nicotinoyl	nicotinoyl	**B**	35[b]	70
22	**2-1Oo**	isonicotinoyl	isonicotinoyl	**B**	17[b]	20

[a] Isolated by recrystallization. [b] The low yields are attributed to the hydrolytic sensitivity of the nicotinoyl and isonicotinoyl groups.

2.3 Phenylhydrazines and acyl derivatives.

The move to phenylhydrazines from benzylhydrazine was accompanied by a moderate increase in steric hindrance around the proximal nitrogen as well as the possible electronic effects of the aromatic substituent. Two phenylhydrazines were used as the starting materials for the vast majority of this part of the library: phenylhydrazine (**2-2Aa**) and 4-

fluorophenylhydrazine (**2-3Aa**). The decision to include **2-3Aa** derivatives to the library was based on the idea that oxidative detoxification mechanisms (via enzymes like cytochrome P450s)[118] might be mitigated by the presence of fluorine on the phenylhydrazine ring and thereby possibly increasing mosquito toxicity.

Synthesis efforts with phenylhydrazine and 4-fluorophenylhydrazine hydrochloride proved challenging at first. Phenylhydrazine chemical behavior most certainly shows a break from the chemistry of amines (see Chapter 3), and the reductive amination strategy (Scheme 2.3) could not be applied here. I focused on acylation reactions for synthesizing the desired products we desired, rather than coupling reactions,[119] as acylation appeared to be a shorter path.

Two early reports in the literature noted that acylation of arylhydrazines requires specific acylation techniques in order to control this process, or else polyacylation is likely to occur.[74, 76] In Chapter 1, work by Benderly was presented which showed that selective distal monoacylation of 1,1-dimethylhydrazine and phenylhydrazine in good yields could be achieved by a Me_3Al-mediated activation reaction with esters of those same hydrazines (see Chapter 1).[87] A related amine activation strategy using DIBAL-H was successfully utilized to synthesize amides from esters and lactones.[120] Aminolysis by DIBAL-mediated activation allowed reaction at lower temperatures, with shorter time, and higher yields (Table 2.4).

Table 2.4. Method D optimization.

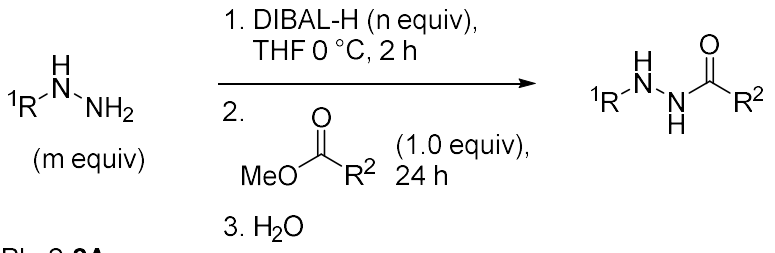

^{1}R = Ph, 2-**2Aa**
^{1}R = 4-F-C_6H_4, **2-3Aa**
^{1}R = *t*-Bu, **2-6Aa**

Entry	Hydrazine	m	n	T (°C)	R^2	Product ID	% Yield[a]
1	**2-2Aa**	5.0	0	50	Ph	**2-2Ba**	0[b]
2	**2-2Aa**	5.0	5.0	rt	Ph	**2-2Ba**	96
3	**2-2Aa**	2.0	2.0	50	Ph	**2-2Ba**	96
4	**2-2Aa**	1.2	1.2	50	Ph	**2-2Ba**	99
5	**2-2Aa**	1.2	1.2	50	4-Me-C_6H_4	**2-2Ca**	98
6	**2-2Aa**	2.0	2.0	50	4-F- C_6H_4	**2-2Da**	72
7	**2-2Aa**	5.0	0	50	2-F-C_6H_4	**2-2Ha**	0[b]
8	**2-2Aa**	2.0	2.0	50	2-F- C_6H_4	**2-2Ha**	99
9	**2-2Aa**	2.0	2.0	50	4-MeO- C_6H_4	**2-2Ea**	67
10	**2-2Aa**	5.0	0	50	2-Br- C_6H_4	**2-2Ga**	0[b]
11	**2-2Aa**	2.0	2.0	50	2-Br- C_6H_4	**2-2Ga**	94
12	**2-6Aa**· HCl[c]	5.0	0	50	Ph	**2-6Ba**	0[b]
13	**2-6Aa**· HCl[c]	5.0	5.0	rt	Ph	**2-6Ba**	91
14	**2-3Aa**· HCl[c]	2.0	2.0	50	Ph	**2-3Ba**	70

[a] Isolated by recrystallization. [b] No product detected by TLC. [c] Activation of hydrazine·HCl salts were preceded by a neutralization step by addition of m equiv of MeLi in hexanes.

In Table 2.4, we show both the problem with standard hydrazinolysis of esters and the clear efficacy of DIBAL-mediated activation; even with multiple equivalents of *tert*-butylhydrazine or phenylhydrazine with mild heating, no desired product was detectable (Table 2.4, Entries 1, 7, 10, and 12), while the addition of DIBAL-H affords excellent yields of >90% (Table 2.4, Entries 2, 3, 4, 5, 8, 11, and 13). To improve the atom economy on Huang's[120] technique of using 5.0 equivalents of amine and DIBAL-H, we show that the reaction can be completed with fewer equivalents and mild heating, with yields that are nearly quantitative in

some cases (Table 2.4, entry 4, 5, and 8). Aqueous workups of organoaluminum reactions are well known for voluminous emulsions of aluminum hydroxide that are difficult to break. After an aqueous quench of the reaction mixture and addition of ethyl acetate, the emulsion mixture can be filtered through Celite, leaving two clear layers of liquid that may then proceed to normal extraction. Filtering eliminates the need for adding salts or adjusting pH, and the products can be obtained by concentration and recrystallization.

Scheme 2.2. Possible mechanism for DIBAL-H activation of *tert*-butyl and arylhydrazines.

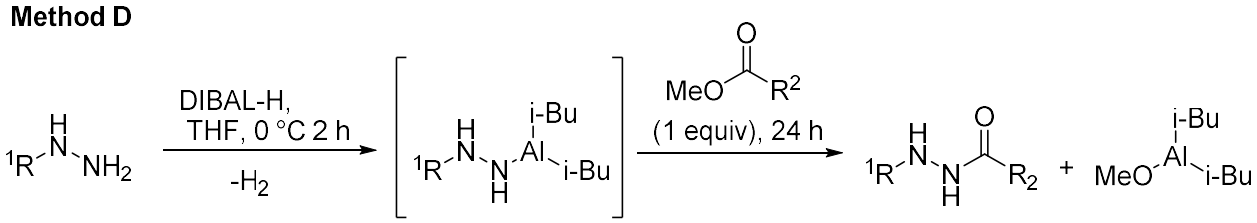

Method D (see Scheme 2.2) of regioselective distal acylation is proposed to work by alumination of arylhydrazines by diisobutylaluminum hydride (DIBAL-H) and subsequent electrophilic trapping by an ester. As shown in Table 2.4, aryl esters were practically unreactive toward *tert*-butyl and arylhydrazines, so the risk of polyacylation was greatly reduced. Apparently, the presence of di-isobutylaluminum methoxide (or other aluminum species) in solution was not sufficient to catalyze esters to react with **2-2Aa**, **2-3Aa**, or **2-6Aa** on the proximal nitrogen.

Regioselective monoacylation of arylhydrazines via anhydrides[77-78] was also an attractive option, as the reaction conditions are mild[75, 79] and the protocol is simple (Table 2.5).

Table 2.5. Regioselective acylation of phenylhydrazines via anhydrides.[75, 79]

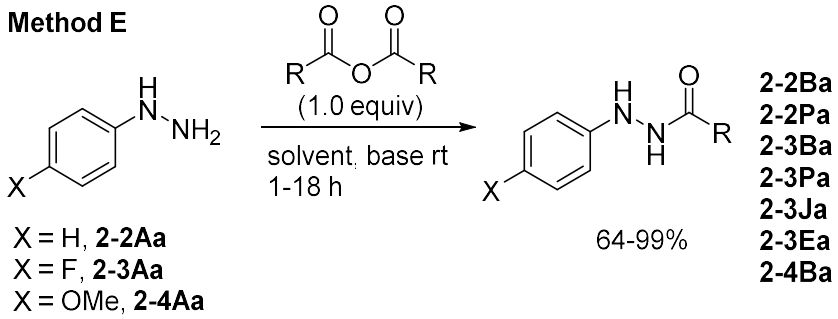

Entry	Hydrazine	Solvent	Base	R	Product ID	% Yield[a]
1	**2-2Aa**	PEG-400	none	Ph	**2-2Ba**	99
2	**2-2Aa**	PEG-400	none	O*t*-Bu	**2-2Pa**	76
3	**2-3Aa·HCl**	H_2O/EtOH	NaOH	Ph	**2-2Ba**	94
4	**2-3Aa·HCl**	H_2O/EtOH	NaOH	O*t*-Bu	**2-3Pa**	73
5	**2-3Aa·HCl**	H_2O/EtOH	NaOH	CH_3	**2-3Ja**	69
6	**2-3Aa·HCl**	H_2O/EtOH	NaOH	OMe	**2-3Ea**	68
7	**2-4Aa·HCl**	H_2O/EtOH	NaOH	Ph	**2-4Ba**	64

a) Isolated by recrystallization.

The selectivity of these reactions was rather good, and the product could be isolated via recrystallization in most cases. As can be seen, aryl hydrazines **2-2Aa**, **2-3Aa**, and **2-4Aa** with various anhydrides (including di-*tert*-butyl dicarbonate) under these conditions give distal monoacyl hydrazines in 64-99% yield. A possible disadvantage of this method was the low commercial availability of anhydrides as compared to acid chlorides or esters. Typically, Method E employed PEG-400[75] or H_2O/EtOH as solvent, and aqueous NaOH[79] to produce the hydrazine free base when needed.

Scheme 2.3. Acylation of arylhydrazines via Method F.[81]

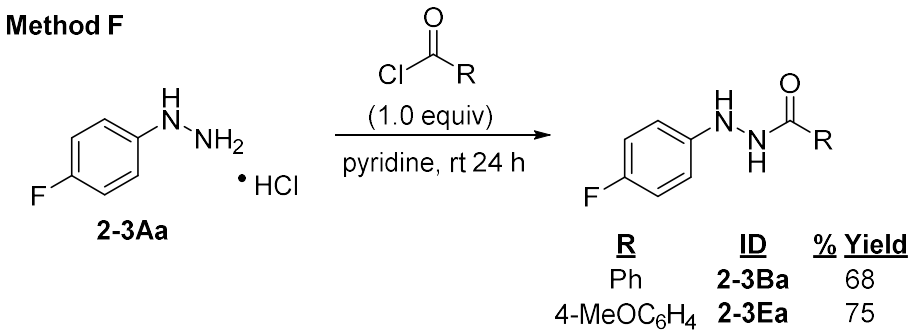

R	ID	% Yield
Ph	**2-3Ba**	68
4-MeOC$_6$H$_4$	**2-3Ea**	75

The final method for distal monoacylation, used more sparingly as it was the last to be explored, was Method F (Scheme 2.3). The use of pyridine as a solvent or as an additive is critical to achieve regioselective acylation of arylhydrazines via acid chlorides with an even stoichiometry (see Chapter 1).[80-82] We explore the effect of base selection and pyridine on the regioselectivity of this reaction in Chapter 3.

After we successfully synthesized distal monoacylarylhydrazines, the next step was to perform a second acylation reaction on the proximal nitrogen. This second acylation was revealed to be tougher to perform after the first, as the *N'*-acyl-*N*-arylhydrazines are less reactive toward acid chlorides on the proximal nitrogen. This was an unexpected problem, as polyacylation was previously the primary complication to regioselective acylation of arylhydrazines[74, 76] (we study this problem in Chapter 3). We explored a variety of conditions to accomplish this task (see Table 2.6 for selected examples), which proved to be less straightforward than it would initially appear. Comparison of Entries 2 and 3 show that there was nearly a two-fold increase in product yield when moving to toluene with no base versus dichloromethane and triethylamine. Similarly, Entry 5 shows a sizable increase in yield of **2-2Bc** over Entry 4 (70% vs 48%) and again with Entries 7 and 8 (43% and 78% respectively). Though many conditions were tested, the most consistently high yields were obtained when using toluene

with mild heating and no soluble base. Entries 9 and 10 would seem to throw that conclusion into doubt, but the evolution of HCl gas is most likely responsible for the loss of the Boc group in Entry 10; however, Entry 11 shows that the simple addition of an insoluble, inorganic base was sufficient to counteract this problem, as well as deliver a yield for **2-2Pb** that is more than two-fold higher than in Entry 9.

Table 2.6. Comparison of conditions for the second acylation of *N′*-acylphenylhydrazines.

Entry	Hydrazide	Solvent	Base equiv	RC(O)Cl equiv	Temp (°C)	Time (h)	Product ID	% Yield[a]
1	**2-2Ba**	CH_2Cl_2	Et_3N; 1.0	1.0	rt	24	**2-2Bk**	27
2	**2-2Ba**	CH_2Cl_2	Et_3N; 1.0	1.0	rt	24	**2-2Bi**	48
3	**2-2Ba**	toluene	none	1.0	80	6	**2-2Bi**	84
4	**2-2Ba**	toluene	Et_3N; 1.1	1.1	50	24	**2-2Bc**	48
5	**2-2Ba**	toluene	none	1.0	80	6	**2-2Bc**	70
6	**2-2Ba**	toluene	none	1.0	80	6	**2-2Bb**	74
7	**2-2Ba**	THF	Et_3N; 1.2	1.2	50	24	**2-2Bl**	43
8	**2-2Ba**	toluene	none	1.0	80	6	**2-2Bl**	78
9	**2-2Pa**	THF	Et_3N; 1.1	1.1	50	24	**2-2Pb**	41
10	**2-2Pa**	toluene	none	1.0	80	6	**2-2Pb**	0
11	**2-2Pa**	toluene	$NaHCO_3$; 1.0	1.0	80	6	**2-2Pb**	84

a) These products were isolated by recrystallization.

The fact that a soluble amine base is associated with lower yields in multiple cases suggests that perhaps an *O*-acylation side reaction was consuming the acid chloride. Deprotonation of the hydrazide N-H proton would provide the carbonyl oxygen enough nucleophilic strength to compete with the proximal nitrogen. Upon aqueous workup, the *O*-acylated product would immediately hydrolyze into the starting material, which is consistent with our observations on thin layer chromatography, showing that reactions with lower yields returned some unconverted starting material.

When using no soluble base, mild heating, and a solvent in which HCl has low solubility, we managed to synthesize asymmetric 1,2-diacylarylhydrazides with good yields and reactions clean enough that recrystallization was a logical choice for purification. Thus, Method G emerged as the preferred route of making unsymmetric diacylarylhydrazines (Table 2.7).[7] Our results were consistent with literature yields for similar compounds.[7] Table 2.6, Entry 11 revealed the problem of HCl gas with acid sensitive groups, such as the Boc group. With relief, we saw that the addition of dry sodium bicarbonate ameliorated this problem without compromising product formation.

Table 2.7. Acylation of monoacylphenylhydrazines via Method G and selected results.

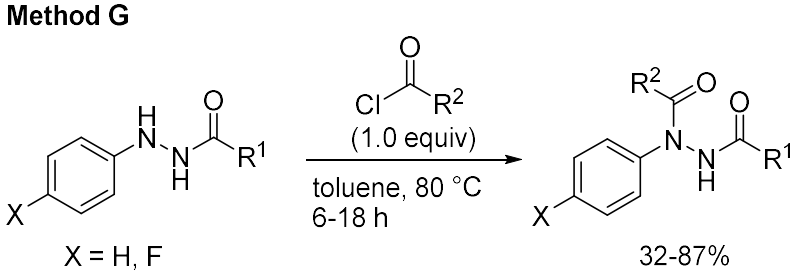

Entry	X	R^1	R^2	Product ID	Isolated % Yield
1	H	Ph	4-Me-C_6H_4	**2-2Bc**	70
2	H	Ph	4-F-C_6H_4	**2-2Bd**	68
3	H	Ph	2-Br-C_6H_4	**2-2Bg**	74
4	H	Ph	2-F-C_6H_4	**2-2Bh**	80
5	H	Ph	*i*-Pr	**2-2Bl**	78
6	H	CH_3	Ph	**2-2Jb**	70
7	H	CH_3	4-MeO-C_6H_4	**2-2Je**	87
8	H	CH_3	2-F-C_6H_4	**2-2Jh**	75
9	H	CH_3	*t*-Bu	**2-2Jk**	70
10	H	O*t*-Bu	Ph	**2-2Pb**	85[a]
11	H	O*t*-Bu	4-F-C_6H_4	**2-2Pd**	58[a]
12	H	O*t*-Bu	*t*-Bu	**2-2Pk**	74[a]
13	F	Ph	4-F-C_6H_4	**2-3Bd**	65
14	F	Ph	4-MeO-C_6H_4	**2-3Be**	74
15	F	Ph	CH_3	**2-3Bj**	70
16	F	Ph	CF_3	**2-3Bq**	69
17	F	Ph	Et	**2-3Br**	37
18	F	Ph	*i*-Bu	**2-3Bs**	64

[a] Dry $NaHCO_3$ was added into the reaction mixture before heating and acid chloride addition.

With reliable techniques to perform controlled acylation reactions on phenylhydrazines, the business of producing the library could proceed with speed. For symmetric diacylphenylhydrazines, Method B would suffice to synthesize them. Tables 2.8, 2.9, and 2.10 contain synthetic yields (with the Method indicated) for individual compounds, as well as results of first round of the toxicity assay.

Table 2.8. Monoacylphenylhydrazine synthetic yields and toxicity assay results.

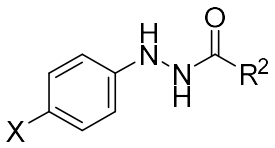

Entry	Product ID	X	R^2	Synthesis Method	Isolated % Yield[a]	% Mortality at 500 ng/insect
1	**2-2Ba**	H	Ph	**D**	99	20
2	**2-2Ca**	H	4-Me-C_6H_4	**D**	98	20
3	**2-2Da**	H	4-F-C_6H_4	**D**	72	40
4	**2-2Ea**	H	4-MeO-C_6H_4	**D**	99	60
5	**2-2Ga**	H	2-Br-C_6H_4	**D**	94	20
6	**2-2Ha**	H	2-F-C_6H_4	**D**	67	50
7	**2-2Pa**	H	O*t*-Bu	**E**	76	27
8	**2-3Ba**	F	Ph	**D**	70	**100**
9	**2-3Ea**	F	4-MeO-C_6H_4	**E**	68	0
10	**2-3Ka**	F	*t*-Bu	**B**	99	55
11	**2-3Pa**	F	O*t*-Bu	**D**	73	27
12	**2-4Ba**	OMe	Ph	**E**	64	0

[a] Isolated by recrystallization.

Table 2.9. Diacylphenylhydrazine synthetic yields and toxicity assay results.

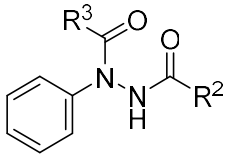

Entry	Product ID	R^2	R^3	Synthesis Method	Isolated Yield %[a]	% Mortality at 500
1	**2-2Bc**	benzoyl	4-Me-benzoyl	**G**	70	20
2	**2-2Bd**	benzoyl	4-F-benzoyl	**G**	68	0
3	**2-2Be**	benzoyl	4-MeO-benzoyl	**G**	70	21
4	**2-2Bg**	benzoyl	2-Br-benzoyl	**G**	74	33
5	**2-2Bh**	benzoyl	2-F-benzoyl	**G**	80	0
6	**2-2Bi**	benzoyl	*c*-Pr-C(O)	**G**	84	7
7	**2-2Bj**	benzoyl	acetyl	**G**	80	0
8	**2-2Bk**	benzoyl	trimethylacetyl	**A**[a]	27	30
9	**2-2Bl**	benzoyl	dimethylacetyl	**G**	78	**100**
10	**2-2Bm**	benzoyl	phenylacetyl	**G**	60	7
11	**2-2Bq**	benzoyl	trifluoroacetyl	**G**	69	20
12	**2-2Br**	benzoyl	propanoyl	**G**	74	20
13	**2-2Bs**	benzoyl	isovaleryl	**G**	59	20
14	**2-2Bt**	benzoyl	methyl carboxylate	**G**	77	25
15	**2-2Dk**	4-F-benzoyl	trimethylacetyl	**A**[a]	68	20
16	**2-2Gg**	2-Br-Benzoyl	2-Br-benzoyl	**B**	99	0
17	**2-2Gj**	2-Br-benzoyl	acetyl	**A**[a]	80	27
18	**2-2Gk**	2-Br-benzoyl	trimethylacetyl	**A**[a]	60	0
19	**2-2Gl**	2-Br-benzoyl	dimethylacetyl	**GA**[a]	7830	23
20	**2-2Jb**	acetyl	benzoyl	**G**	70	15
21	**2-2Je**	acetyl	4-MeO-benzoyl	**G**	87	0
22	**2-2Jh**	acetyl	2-F-benzoyl	**G**	75	13
23	**2-2Jk**	acetyl	trimethylacetyl	**G**	70	7
24	**2-2Jl**	acetyl	dimethylacetyl	**G**	70	7
25	**2-2Pb**	Boc	benzoyl	**G**	85	**100**
26	**2-2Pd**	Boc	4-F-benzoyl	**G**	58	31
27	**2-2Pe**	Boc	4-MeO-benzoyl	**G**	59	7
28	**2-2Ph**	Boc	2-F-benzoyl	**G**	62	17
29	**2-2Pk**	Boc	trimethylacetyl	**G**	74	42
30	**2-2Pm**	Boc	phenylacetyl	**G**	71	9
31	**2-2Pq**	Boc	trifluoroacetyl	**G**	58	60
32	**2-2Pr**	Boc	propanoyl	**G**	44	7

[a] Used THF instead of CH_2Cl_2 for solvent, and heated to 50 °C.

Table 2.10. Diacyl-(4-fluorophenyl)hydrazine and 3-5Ab synthetic yields and toxicity assay results.

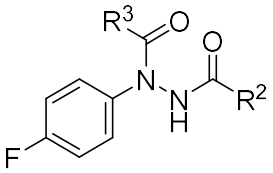

Entry	Product ID	R^2	R^3	Synthesis Method	Isolated Yield %	% Mortality at 500 ng/insect
1	**2-3Bd**	benzoyl	4-F-benzoyl	**G**	65	0
2	**2-3Be**	benzoyl	4-MeO-benzoyl	**G**	74	8
3	**2-3Bj**	benzoyl	acetyl	**G**	70	10
4	**2-3Bk**	benzoyl	trimethylacetyl	**A**[a]	74	0
5	**2-3Bl**	benzoyl	dimethylacetyl	**A**[a]	49	18
6	**2-3Br**	benzoyl	propanoyl	**G**	37	0
7	**2-3Bs**	benzoyl	isovaleryl	**G**	64	18
8	**2-3Bt**	benzoyl	methyl carboxylate	**G**	70	18
9	**2-3Dd**	4-F-benzoyl	4-F-benzoyl	**A**[a]	65	7
10	**2-3Kk**	trimethylacetyl	trimethylacetyl	**B**	46	60
11	**2-3Ll**	dimethylacetyl	dimethylacetyl	**B**	82	70
12	**2-3Pb**	boc	benzoyl	**G**	72	5
13	**2-4Bb**	benzoyl	benzoyl	**B**	99	10

[a] Used THF instead of CH_2Cl_2 for solvent, and heated to 50 °C.

2.4 Toxicity Analysis.

Inspection of the data from Tables 2.3 and 2.8, 2.9, and 2.10 show that only three compounds managed to meet the goal of 100% lethality at 500 ng/insect after administration: **2-3Ba**, **2-2Pb**, and **2-2Bl**. These three compounds were studied further to determine their LD_{50} values (Figure 2.3) and then compared to their close analogues that were produced in the library in an attempt to ascertain molecular features that increased or decreased mosquito toxicity.

Figure 2.3. Mosquito mortality after 24 hours at 500 ng/insect and calculated or estimated LD_{50} values (with 95% confidence interval) for the compounds with the greatest efficacy and their close analogs.

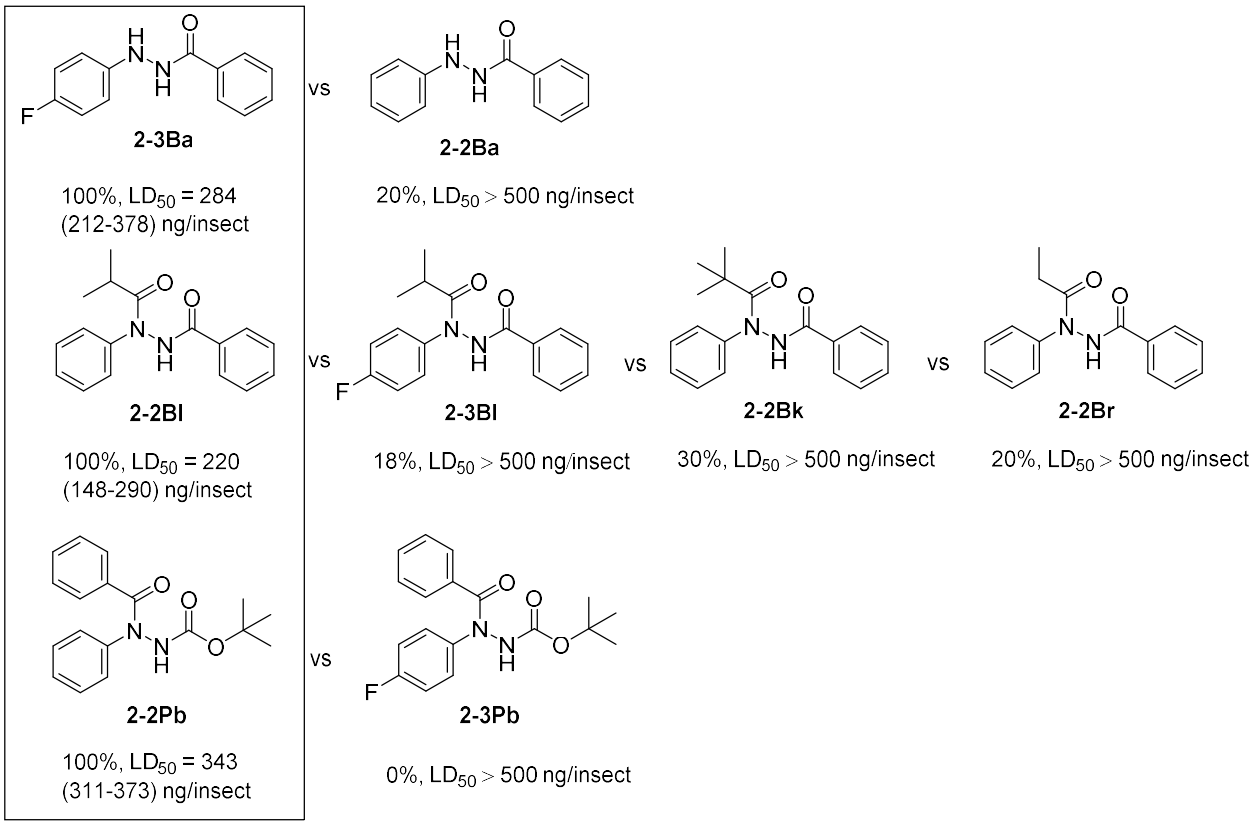

As seen in Figure 2.3, three compounds (**2-3Ba**, **2-2Bl**, and **2-2Pb**) met the criterion of 100% mosquito mortality after 24 hours at a dose of 500 ng/insect. Further testing of these three compounds showed that each possessed LD_{50} values lower than that of RH-1266 (LD_{50} = 504 (393-648 ng/insect), with non-overlapping 95% confidence intervals; **2-2Bl**, in particular, was twice as toxic to mosquitoes as compared to RH-1266. Examination of the mosquito toxicity of the close analogs of these compounds reveals that mosquito toxicity is very sensitive to the structure of the compound. Compound **2-3Ba**, derived from 4-fluorophenylhydrazine (**2-3Aa**) is appreciably more toxic than **2-2Ba** which lacks a fluorine substituent. However, fluorine-bearing

2-3Bl is appreciably less toxic than **2-2Bl**. Toxicity also dropped in the case of **2-2Pb** versus **2-3Pb**. Thus, there is no general trend to suggest that the presence of a fluorine in the 4-position of the arylhydrazine ring reduces metabolic detoxification. Secondly, analogs **2-2Bk** and **2-2Br** differ from **2-2Bl** in methyl substitution of the proximal acyl substituent; both addition of a methyl group (**2-2Bk**) and removal of a methyl group (**2-2Bq**) reduce mosquito toxicity.

There are several factors that may explain the differences in efficacy, despite the seemingly small alterations in molecular structure. The first addresses a possible issue for fluorinated vs non-fluorinated diacylphenylhydrazines: drug absorption. Differences in polarity between **2-2Bl** and **2-3Bl** (with the latter showing as more polar on TLC) may make the latter more difficult to absorb through the insect cuticle or past certain membranes. A drug that cannot find its way to a target, no matter how sensitive the target may be to the drug, is not a good drug.

The second is the possible sensitivity of the target protein's binding sites. It is possible that the size of these binding pockets is highly tuned such that substrates must be a specific shape in order to bind properly. An increase in the size of the proximal acyl group may make the molecule too big to bind (e.g. **2-2Bk**), whereas being too small (e.g. **2-2Br**) would not allow the molecule to properly anchor inside to produce a sufficiently large change in protein conformation for toxic effects to emerge.

The third possible explanation is that these compounds may be binding to different targets. If this is true, then an alternation, such as the presence of a fluorine atom, may change where the compound goes in the insect's body and what it eventually binds to. If the mechanism of action is different in fluorinated vs non-fluorinated diacylarylhydrazines, then there cannot be an expectation of increased toxicity when molecular features on one protein target are introduced

to a different protein target. As mentioned earlier, RH-5849 and RH-1266 served as the prototypes of the candidate K^+ channel-blocking insecticides described in this chapter. Ideally, each new compound prepared would be assessed not only for their contact toxicity but also for their K^+ channel-blocking potency and selectivity. However, this ideal was not realized in practice. Stable heterologous expression of *An. gambiae* Kv2.1 channels was achieved in HEK293 (human embryonic kidney) cells according to the Bloomquist group's published procedure.[121] Expression of human Kv2.1 channels was induced in SH-Sy5y (human neuroblastoma) cells by addition of retinoic acid, according to the literature procedure.[122] However, the patch clamp assays proved quite time-consuming, and thus only reference compounds and the most contact toxic diacylhydrazines were assayed. Secondly, as data from my compounds and those of other Carlier group members began to be collected, it became clear that there was no direct relationship between *An. gambiae* Kv2.1 inhibition potency and *An. gambiae* topical toxicity. With that said, the three most mosquito-toxic compounds to emerge from my research (compounds **2-2Pb**, **2-2Bl**, and **2-3Ba**) were characterized for K^+ channel-blocking activity, and compared to the RH lead compounds (Table 2.11; work performed by Dr. Baonan Sun of the Bloomquist group at the University of Florida).

Table 2.11. Mosquito and Human Kv2.1 IC_{50} values, selectivity ratios, and correlation to measured *Anopheles gambiae* LD_{50} values.

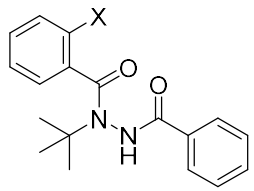

RH-5849 (PRC642): X = H
RH-1266 (PRC643): X = Br

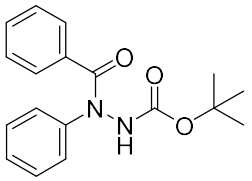

2-2Pb
(PRC960)

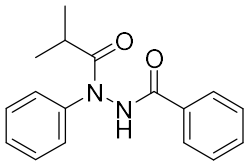

2-2Bl
(PRC1069)

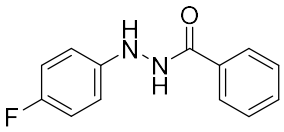

2-3Ba
(PRC1134)

Compound	*An. gambiae* Kv2.1 IC_{50} µM[a] (95% CI)	Human Kv2.1 IC_{50} µM[b] (95% CI)	Selectivity *An. gambiae* vs human[c]	*An. gambiae* topical LD_{50} ng/insect (95% CI)[d]
RH-5849 (PRC642)	12 (10-15)	39 (22-67)	3.3	735 (583-945)[e]
RH-1266 (PRC643)	7 (2.3-22)	13 (10-20)	1.9	504 (393-648)[e]
2-2Pb (PRC960)	63 (28-142)	135 (110-166)	2.1	343 (311-373)
2-2Bl (PRC1069)	28 (19-39)	40 (8-203)[f]	1.4	220 (148-390)
2-3Ba (PRC1134)	355 (227-555)[g]	1103 (557-2187)[h]	3.1	287 (212-376)

[a] *An gambiae* Kv2.1 was expressed in HEK-203 cells, and ion currents were measured according to the published procedure.[121] Unless otherwise noted, >90% inhibition of current was achieved. [b] Human Kv2.1 was expressed in SH-Sy5y cells according to the published procedure[122] and ion currents were measured under conditions similar to those for the *An. gambiae* channel. [c] Selectivity = IC_{50} (human)/IC_{50} (*An. gambiae*). [d] Determined according to Pridgeon et al.[123] [e] Topical toxicity data have been published.[124] [f] Only 66% inhibition achieved at 1 mM. [g] Maximum inhibition of 80% seen at 1 mM. [h] Only 50% inhibition achieved at 1 mM

None of the compounds tested have high *An. gambiae* vs human selectivity for inhibition of the Kv2.1 channel. Thus, some on-target mammalian toxicity would be expected from these compounds. Secondly as can be seen, in although **2-2Pb**, **2-2Bl** and **2-3Ba** are roughly twice as toxic to *An. gambiae* as RH-5849, they are weaker blockers of the *An. gambiae* Kv2.1 channel. In the case of **2-3Ba**, the K+ channel blocking potency is nearly 30-fold weaker than that of RH-5949. Admittedly this is a small data set, but the lack of correlation of the two activities could be rationalized in at least two ways. Firstly, differential ADME of these compounds could explain the poor correlation of K^+ channel-blocking potency and mosquito topical toxicity. In the

absence of any correlation of the activities of similar compounds, one has to consider the possibility that the topical mosquito toxicity of these compounds is due to engagement of a target other than *An. gambiae* Kv2.1.

2.5. Conclusion

The most toxic compounds in the library we synthesized were derived from phenylhydrazine (**2-2Aa**) and 4-fluorophenylhydrazine (**2-3Aa**), namely **2-2Bl**, **2-2Pb**, and **2-3Ba**. All three of these mosquitocidal compounds met the benchmark and also surpassed the leads, RH-5849 and RH-1266, with LD_{50} values that less than 504 ng/insect, with **2-2Bl** as the standout compound with a slightly greater than 2-fold decrease in LD_{50} with non-overlapping confidence intervals. Biological assay revealed that there was no correlation between mosquito mortality and inhibition of *An. gambiae* Kv2.1. In contrast to the arylhydrazines, no acylbenzylhydrazines were found that could meet the benchmark value for toxicity. We were able to both invent a new method and employ modified literature methods to selectively acylate benzyl- and phenylhydrazines with good to excellent yields for individual steps.

Chapter 3. A Streamlined Route to Proximal Aroyl Aromatic Hydrazines Revealed by ^{19}F NMR Studies of 4-Fluorophenylhydrazine Acylation

3.1 Premise of regioselectivity study and probing by ^{19}F NMR

Chapter 2 details our efforts to prepare a range of monoacyl and diacyl arylhydrazines, for investigation of their mosquitocidal properties; with emphasis to prepare and isolate as many compounds as possible at >95% purity. In the process of synthesizing our acylhydrazine library, it was imperative to seek out techniques with which to regioselectively acylate benzyl- and arylhydrazines. Chapter 1 described the methods already existent to synthesize acylhydrazines, possible pitfalls (e.g. polyacylation), and the α-effect but there was no connection made between these topics to allow prediction of a particular hydrazine's regiochemistry toward acylating agents. We decided to perform a follow-up study to gain insight into the synthetic results we observed in Chapter 2. The acylation of monoarylhydrazines appears simple, but its regioselectivity is poorly understood. Using 4-fluorophenylhydrazine (we will use the same naming scheme as was seen in Chapter 2 here in Figure 3.1, **3**-**3Aa**) as a probe, we determined the approximate kinetic selectivities for distal to proximal *N*-acylation using a range of acid chlorides and the corresponding acid anhydrides. These selectivities were determined by ^{19}F NMR spectroscopic analysis of reactions of **3**-**3Aa** with limiting (0.2 equiv) acylating agent in the presence of various bases. Acid anhydrides gave consistent preference for distal acylation, but the selectivity of acylation by acyl chlorides was unexpectedly found to depend upon the base employed. Use of triethylamine or aqueous base in conjunction with aroyl chlorides showed

a moderate preference for proximal acylation (Scheme 3.1). This observation yielded a convenient one-step method to synthesize proximal aroylarylhydrazines in yields comparable or superior to that provided by the standard three-step literature approach.

Figure 3.1. Compound ID legend for all acylhydrazines.

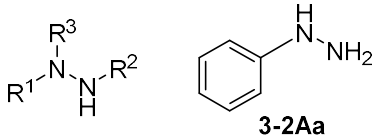

3-2Aa

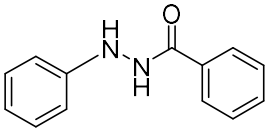

3-2Ba

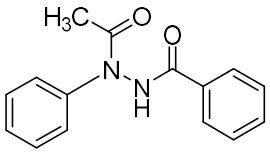

3-2Bj

1; R^1 = benzyl
2; R^1 = Ph
3; R^1 = 4-fluorophenyl
4; R^1 = 4-methoxyphenyl
5; R^1 = 4-bromophenyl
6; R^1 = *t*-Bu

A; R^2 = H
B; R^2 = benzoyl
C; R^2 = 4-methylbenzoyl
D; R^2 = 4-fluorobenzoyl
E; R^2 = 4-methoxybenzoyl
F; R^2 = 4-chlorobenzoyl
G; R^2 = 2-bromobenzoyl
H; R^2 = 2-fluorobenzoyl
I; R^2 = cyclopropanecarbonyl
J; R^2 = acetyl
K; R^2 = trimethylacetyl
L; R^2 = dimethylacetyl
M; R^2 = phenylacetyl
N; R^2 = nicotinoyl
O; R^2 = isonicotinoyl
P; R^2 = Boc

a; R^3 = H
b; R^3 = Benzoyl
c; R^3 = 4-methylbenzoyl
d; R^3 = 4-fluorobenzoyl
e; R^3 = 4-methoxybenzoyl
f; R^3 = 4-chlorobenzoyl
g; R^3 = 2-bromobenzoyl
h; R^3 = 2-fluorobenzoyl
i; R^3 = cyclopropanecarbonyl
j; R^3 = acetyl
k; R^3 = trimethylacetyl
l; R^3 = dimethylacetyl
m; R^3 = phenylacetyl
n; R^3 = nicotinoyl
o; R^3 = isonicotinoyl
p; R^3 = Boc
q; R^3 = trifluoroacetyl
r; R^3 = propanoyl
s; R^3 = isovaleryl
t; R^3 = methyl carboxylate

Scheme 3.1. Overview of acylation regioselectivity of 4-fluorophenylhydrazine toward acid chlorides.

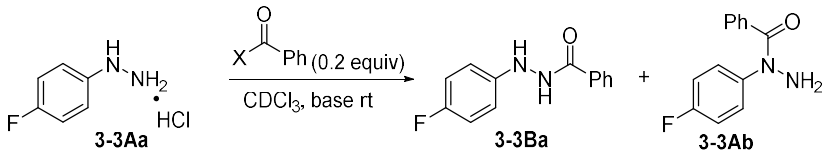

X:	Base:	distal:proximal
OC(O)Ph	Et_3N	94:6
Cl	Et_3N	36:64
Cl	pyridine	94:6
Cl	aq. NaOH	37:63

Acylhydrazines feature prominently in organic chemistry as starting materials for heterocycles,[7, 93, 125] as pharmaceuticals,[12-13] and insecticides,[15] and as azapeptide building blocks for protein engineering.[10, 110, 126] Recent exploration of acylhydrazine natural products[111] as anticancer[127] and antimicrobial[128] agents show the promise of this structural unit for further medicinal investigations. As discussed in Chapters 1 and 2, our interest in acylhydrazines originally grew out of the success of diacyl-*tert*-butylhydrazines (Figure 3.2) as agricultural insecticides; acting as ecdysone receptor agonists,[22-23, 129-130] they cause insect larvae to undergo a premature and fatal molt. Diacylhydrazines have also shown efficacy against human filarial parasitic nematodes.[131]

Figure 3.2. RH diacylhydrazine insecticides.[22]

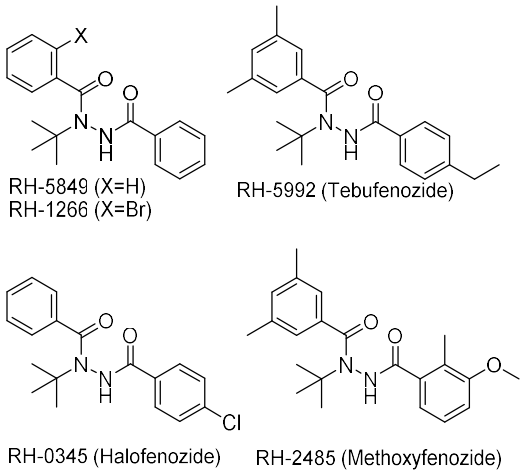

Interestingly, this class of compounds were observed to exhibit neurotoxic[24] symptoms in adult insects during field testing of RH-5849,[25] a diacyl-*tert*-butylhydrazine. Salgado[23-24] demonstrated that these compounds block voltage-dependent potassium channels, and attributed the observed neurotoxicity to this mechanism. Since potassium channels have not been extensively explored as insecticidal targets[16, 26] we thought to investigate the ability of diacylhydrazines to control the African vector of malaria, *Anopheles gambiae*. Note that the toxicity of diacyl-*tert*-butylhydrazines to mosquito larvae has been investigated.[132-133] We began our work with the intent of synthesizing a diverse collection of analogues of the RH series (Figure 3.2), in particular those derived from arylhydrazines.

Scheme 3.2. Regioselectivity of acetylation of methyl- and phenylhydrazine by acetic anhydride.[34, 134]

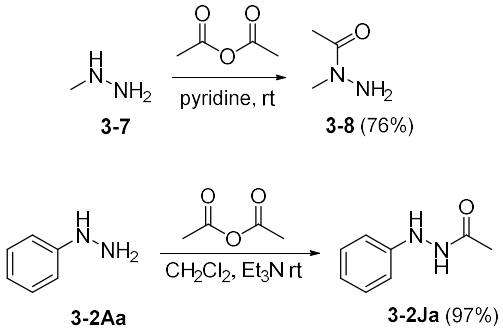

Whereas *t*-butylhydrazine is known to undergo selective acylation at the distal[42, 70] nitrogen, the situation with methyl-, 1° alkyl-, and arylhydrazines is known to be more complex.[33, 135] Methylhydrazine **3-7** is reported to react with acetic anhydride preferentially to form the proximally acetylated compound **3-8**,[34] but phenylhydrazine **3-2Aa** preferentially reacts with this reagent to form the distally acetylated product **3-2Ja** (Scheme 3.2).[77, 84 134]

Phenylhydrazine **3-2Aa** is also reported to form distally acetylated products in good yield on reaction with acid chlorides in pyridine (see Chapter 1).[80-82, 136] To our surprise however, we found that the distal selectivity with acid chlorides obtained with pyridine was substantially degraded when other bases (Et_3N, NaOH) were employed instead. To the best of our knowledge, no systematic study of the regioselectivity of acylation of arylhydrazines by acid anhydrides and acid chlorides has been reported. Several techniques could be employed to assess selectivity, but we chose ^{19}F NMR spectroscopy, due to its sensitivity and its ability to easily discriminate between proximally- and distally-acylated products.

3.2 Synthesis of ^{19}F NMR standards and determination ^{19}F NMR chemical shift values

Our first task was to prepare samples of the proximal monoacyl, distal monoacyl, and *N*,*N*′-diacylated derivatives of **3-3Aa** (Tables 3.1, 3.2, and 3.3 respectively). Distal acylated compounds were prepared by reaction of **3-3Aa** with the corresponding anhydrides (**3-9a**, **3-9b**, **3-9d**, and **3-9e**), or by treatment of **3-3Aa** with an acid chloride in pyridine (**3-9c**). Yields of distal acylarylhydrazines ranged from moderate to excellent (see Table 3.1).

Table 3.1. Preparation of distal acylated ^{19}F NMR standards.

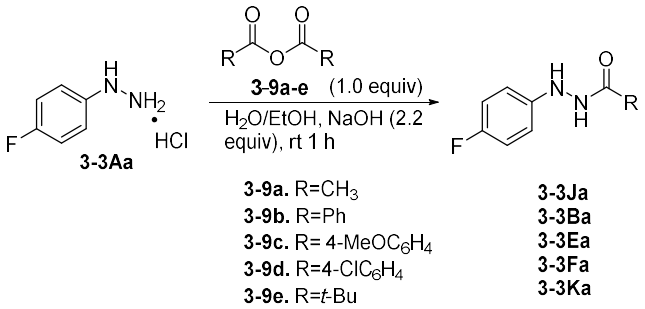

Entry	Product ID	R	% Yield
1	**3-3Ja**	Me	69
2	**3-3Ba**	Ph	94
3	**3-3Ea**	4-MeO-C_6H_4	75[a]
4	**3-3Fa**	4-Cl-C_6H_4	92
5	**3-3Ka**	*t*-Bu	99

[a] This compound was prepared by combining pyridine, acid chloride **3-10c** at room temperature for 16 hours.

Proximal monoacylhydrazines **3-3Aj**·HCl, **3-3Ab**·HCl, **3-3Ae**·HCl, **3-3Ad**·HCl and **3-3Ak**·HCl were prepared in three steps (see Table 3.2). Starting with **3-3Aa**, the distal nitrogen was protected with di-*tert*-butyl dicarbonate, followed by acylation of the proximal nitrogen with acid chlorides **3-10a-e**, followed by deprotection with HCl. The ^{1}H NMR spectra of proximal monoacylhydrazines (HCl salt) lack an acyl N-H signal, and often exhibit a broad singlet for the -NH_2·HCl moiety (relative integral of 3H) at approximately 10 ppm (DMSO-d_6).

Table 3.2. Preparation of proximal acylated ^{19}F NMR standards.

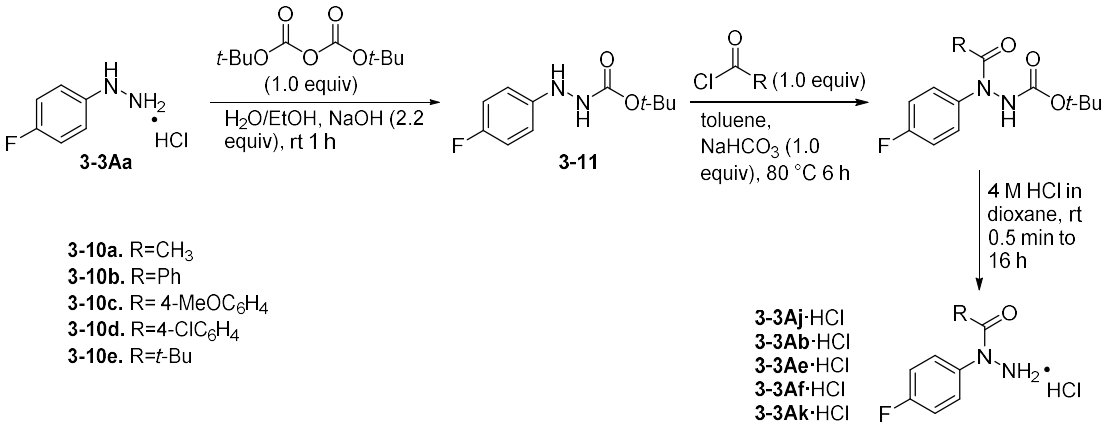

Entry	Acylating agent	Product ID	R	% Yield[a]
1	**3-10a**	**3-3Aj·HCl**	Me	67
2	**3-10b**	**3-3Ab·HCl**	Ph	47
3	**3-10c**	**3-3Ae·HCl**	4-MeO-C_6H_4	57
4	**3-10d**	**3-3Af·HCl**	4-Cl-C_6H_4	47
5	**3-10e**	**3-3Ak·HCl**	*t*-Bu	38

[a] This is the yield over all three steps.

Finally, the diacylhydrazines **3-3Bb**, **3-3Ee**, **3-3Ff**, and **3-3Kk** were trivially synthesized by reaction with two equivalents of acid chloride. Compound **3-3Jj** could not be synthesized in this manner due to competitive triacylation (**3-3Aa** reacting with **3-10a** to give the triacetylhydrazine); thus, we employed a different protocol,[137] combining **3-3Aa**·HCl with neat acetic anhydride (**3-9a**) at 80 °C.

Table 3.3. Preparation of diacylarylhydrazine ^{19}F NMR standards.

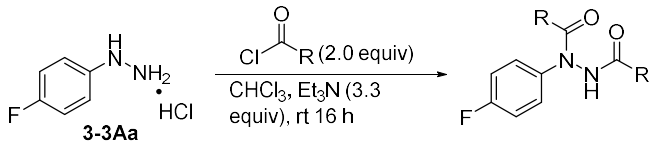

3-10a. R=CH_3
3-10b. R=Ph
3-10c. R= 4-$MeOC_6H_4$
3-10d. R=4-ClC_6H_4
3-10e. R=*t*-Bu

3-3Jj
3-3Bb
3-3Ee
3-3Ff
3-3Kk

Entry	Acylating agent	Product ID	R	% Yield
1	**3-10a**	**3-3Jj**	Me	99[a]
2	**3-10b**	**3-3Bb**	Ph	91
3	**3-10c**	**3-3Ee**	4-MeO-C_6H_4	57
4	**3-10d**	**3-3Ff**	4-Cl-C_6H_4	57
5	**3-10e**	**3-3Kk**	*t*-Bu	46

[a] This compound was prepared by combining **3-3Aa**·HCl with neat acetic anhydride at 80 °C for 1 hour.

Table 3.4. ^{19}F NMR chemical shifts of various acylated 4-fluorophenylhydrazines ($CDCl_3$, with 5.0 equivalents Et_3N).

Entry	Compound ID	δ (^{19}F)
1	**3-3Aa**	-129.9
2	**3-3Ja**[a]	-126.21, -126.51 (25:75)[a]
3	**3-3Ba**	-126.26
4	**3-3Ea**	-126.46
5	**3-3Fa**	-126.02
6	**3-3Ka**	-126.5
7	**3-3Aj**[a]	-116.32, -118.67 (89:11)[a]
8	**3-3Ab**	-117.86
9	**3-3Ae**	-118.14
10	**3-3Af**	-117.19
11	**3-3Ak**	-116.8
12	**3-3Jj**[a]	-114.72, -117.24 (60:40)[a]
13	**3-3Bb**	-116.82
14	**3-3Ee**	-117.32
15	**3-3Ff**	-115.73
16	**3-3Kk**	-115.5

[a] These compounds exist as a mixture of rotamers at room temperature with integral ratios listed in parentheses. These ratios are corroborated by ^{1}H NMR ratios of the NH protons: **3-3Ja** (25:75); **3-3Jj** (42:58); ^{1}H NMR ratios of the methyl protons **3-3Ja** (25:75), **3-3Aj** (86:14, DMSO-d_6).

To prepare for ^{19}F NMR studies of acylation regioselectivity in **3-3Aa**, ^{19}F NMR chemical shifts were determined for all compounds in $CDCl_3$ in the presence of 5.0 equivalents of Et_3N. As shown in Table 3.4, the ^{19}F chemical shifts follow an expected trend: distal acylated products (Entries 2-6) have ^{19}F chemical shift values similar to that of the starting material **3-3Aa** (Entry 1) but downfield, typically 3-4 ppm. In contrast, proximal acylated products (Entries 7-11) show a significant (11-13 ppm) shift downfield from Entry 1, with *N*,*N*′-diacyl products (Entries 12-16) appearing 1-2 ppm further downfield from proximal acylated products. Interestingly, for the acetyl derivatives (Entries 2, 7, and 12)**,** major and minor peaks were seen in the ^{19}F NMR spectra, which we attribute to the presence of amide rotamers. This proposal is

corroborated by the appearance of major and minor N-H signals in the ^{1}H NMR spectra that have similar relative integrals (see Figure 3.3); note that we discuss this type of isomerism in depth in Chapter 4. These ^{19}F chemical shifts show a large enough difference in ppm value that each species could be conveniently identified and quantified in solution.

Figure 3.3. Example of acetyl group rotamers in ^{1}H and ^{19}F NMR spectra from 3-3Ja.

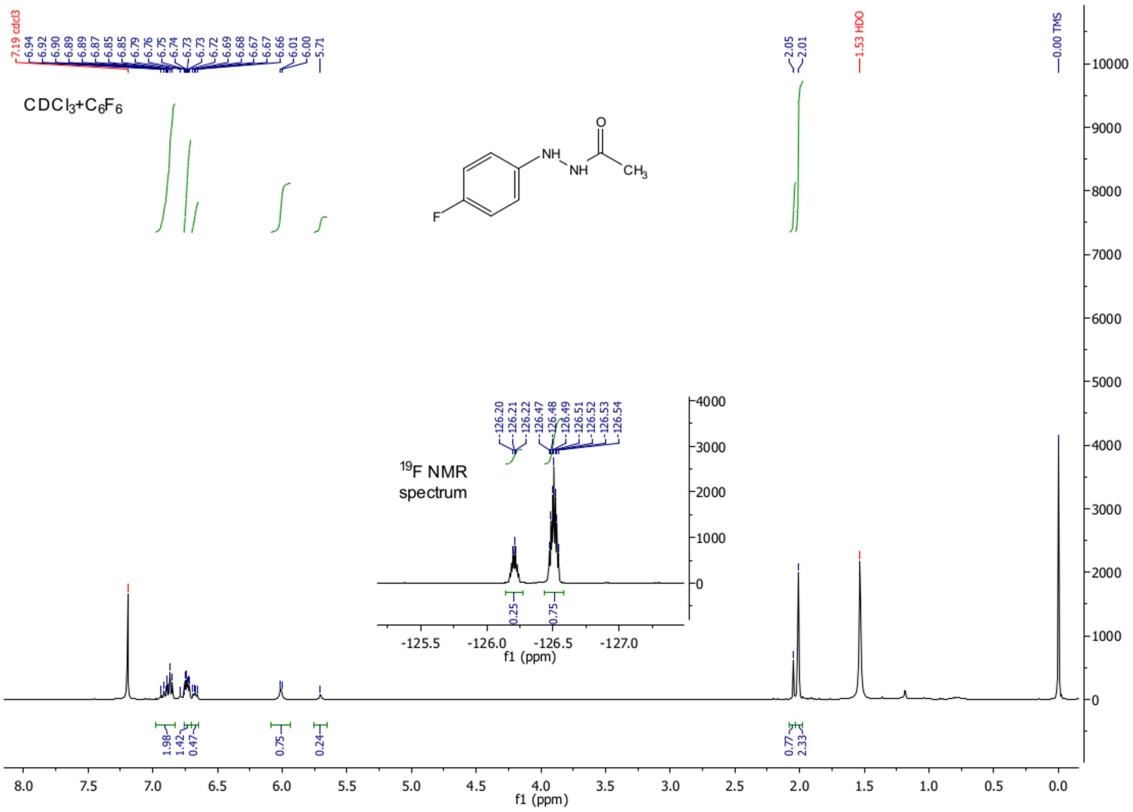

3.3 Determination of acylation regioselectivity in 4-fluorophenylhydrazine

With the authentic samples of the predicted possible distal and proximal monoacyl products in hand, we undertook ^{19}F NMR studies of the acylation of **3-3Aa**·HCl by acid chlorides **3-10a-e** and anhydrides **3-9a-e**. Reactions were carried out in $CDCl_3$ under inert atmosphere conditions, using 0.2 equivalents of the acylating agent and 5.0 equivalents of Et_3N. By limiting the acylating agent to only 0.2 equivalents, we hoped to avoid formation of diacyl

product. Note that **3-3Aa**·HCl is not appreciably soluble in $CDCl_3$; we selected Et_3N as base in large part because addition of 5.0 equivalents resulted in a homogenous solution. Furthermore, if oxygen was not rigorously excluded from the reactions, multiple trace oxidation products were visible by ^{19}F NMR spectroscopy. Distal:proximal monoacyl product ratios were determined by ^{19}F NMR integration and are reported in Table 3.5; since the reaction was allowed to proceed to only 20-30% conversion, the integral ratios will approximate the ratio of second-order rate constants leading to their respective products. As hoped, the formation of diacyl products was not observed under these conditions.

Table 3.5. Regioselectivity of acylation of 3-3Aa by acid chlorides and anhydrides.

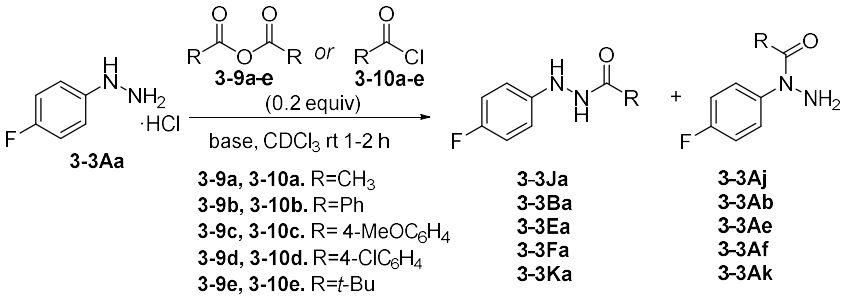

Entry	Acylating Agent	Base	% Conversion[a]	Distal : Proximal ratio[a]
1	**3-9a**	Et_3N[b]	29	89:11
2	**3-9b**	Et_3N[b]	17	94:6
3	**3-9c**	Et_3N[b]	19	90:10
4	**3-9d**	Et_3N[b]	12	92:8
5	**3-9e**	Et_3N[b]	16	>98:2
6	**3-10a**	Et_3N[b]	24	52:48
7	**3-10b**	Et_3N[b]	22	36:64
8	**3-10c**	Et_3N[b]	22	34:66
9	**3-10d**	Et_3N[b]	19	34:66
10	**3-10e**	Et_3N[b]	27	>98:2
11	**3-10a**	C_5H_5N/Et_3N[c]	16	81:19
12	**3-10b**	C_5H_5N/Et_3N[c]	17	94:6
13	**3-10c**	C_5H_5N Et_3N[c]	14	86:14
14	**3-10d**	C_5H_5N/Et_3N[c]	14	86:14
15	**3-10e**	C_5H_5N/Et_3N[c]	20	>98:2
16	**3-10a**	aq. NaOH[d]	27	30:70
17	**3-10b**	aq. NaOH[d]	27	37:63
18	**3-10c**	aq. NaOH[d]	18	33:66
19	**3-10d**	aq. NaOH[d]	25	36:64
20	**3-10e**	aq. NaOH[d]	29	>98:2

[a] Conversion calculated on the basis of integration of ^{19}F peaks from starting hydrazine **3-3Aa** and monoacyl products. The variation seen in conversion is most likely the result of dispensing errors of small volumes. Ratios of products were determined by ^{19}F NMR integration. [b] 5.0 equivalents of triethylamine was used. [c] 5.0 equivalents of pyridine was added and allowed to stir with **3-3Aa** and **3-10a-e** for 1 hour, followed by 2.5 equivalents of triethylamine and stirred for 2 hours. [d] 1.2 equivalents of 1.0 M aqueous NaOH were added to the solution.

As shown in Table 3.5, reactions of **3-3Aa** with anhydrides **3-9a-e** with Et_3N as the base offer excellent selectivity (89:11 to >98:2), as expected from the literature.[77-78, 138] However, the regioselectivities of reactions with acid chlorides were found to depend strongly on the identity

of the base. The presence of Et_3N as base, acetyl chloride (**3-10a**) offered no selectivity for distal vs proximal acylation (see Entries 6, 1). For reaction of aroyl chlorides **3-10b-d** in the presence of Et_3N, surprisingly, there was a preference for proximal acylation (ratios 36:64 - 33:66). The measured kinetic selectivity of benzoyl chloride **3-10b** in the presence of Et_3N is consistent with the literature observation that reaction of **3-3Aa** and **3-10b** in Et_3N/THF gives the distal monoacyl product **3-3Ba** in only 34% yield.[125] However for the bulky pivaloyl chloride, selectivity is not affected by the choice of base, and the distal:proximal acylation ratio was >98:2 (Table 3.5, entry 10).

The selectivities observed in reactions of acid chlorides **3-10a-d** with **3-3Aa** in the presence of Et_3N were much lower than we observed for acylation with anhydrides **3-9a-d** under the same conditions. Furthermore these results confirmed our earlier observations that Et_3N was not an adequate substitute for pyridine for the synthesis of distal monoacyl products from arylhydrazines and acid chlorides. We thus studied reaction in the presence of pyridine: acid chlorides **3-10a-e** (0.2 equiv) were allowed to stir with pyridine (5.0 equiv) and **3-3Aa** (1 equiv) in $CDCl_3$ at room temperature for 1 hour, after which triethylamine (2.5 equiv) was added to dissolve unreacted **3-3Aa** (thus allowing % conversion to be determined by ^{19}F NMR). Interestingly under these conditions, selectivity for the distal acylated products was much improved compared to the reaction in the presence of Et_3N alone (distal:proximal of 81:19 to 94:6, cf. entries 11-14 and 6-9). The high selectivity seen for reaction of **3-3Aa** and pivaloyl chloride (**3-10e**) with Et_3N as base (>98:2, entry 10) remained largely unchanged upon addition of pyridine (>98:2, entry 15).

Since we had also observed that Schotten-Baumann conditions did not work well to prepare distal monoacyl arylhydrazines from acid chlorides, we explored selectivity in the

presence of an inorganic base (aq. NaOH). As can be seen in Table 3.5, reactions of acid chlorides **3-10a-d** in this system favored the proximal acylation product (entries 16-19, distal:proximal ranged from 37:63 to 30:70). The 30:70 selectivity seen for acid chloride **3-10a** is particularly noteworthy in view of the fact that Table 3.5, Entry 6 shows no selectivity for acetyl chloride when triethylamine is the base. Lastly, as seen in the Et_3N and pyridine/Et_3N experiments, pivaloyl chloride **3-10e** favored the distal product with >98:2 selectivity.

To confirm that the selectivities reported in Table 3.5 are kinetic in origin, we noted that the ^{19}F NMR standard samples of **3-3Ja**, **3-3Ba**, **3-3Ea**, **3-3Fa**, and **3-3Ka**, as well as **3-3Aj**, **3-3Ab**, **3-3Ae**, **3-3Af**, and **3-3Ak** in $Et_3N/CDCl_3$ gave no indication of conversion to regioisomeric products after 72 hours at room temperature in solution. Similarly we confirmed that samples of **3-3Ab** and **3-3Af** in pyridine/$Et_3N/CDCl_3$ remained pure over 48 h at room temperature. Thus pyridine does not serve to equilibrate the proximal monoacyl products to distal monoacyl products. It would appear therefore that the different kinetic selectivities observed under various conditions reflect differences in the reactive intermediates.

In principle, triethylamine[139] and pyridine[140] can both provide nucleophilic catalysis of acylation of **3-3Aa** by anhydrides and acid chlorides and thereby generate a range of potential reactive intermediates (Scheme 3.3).

Scheme 3.3. The role of nucleophilic catalysis in the acylation of 3-3Aa.

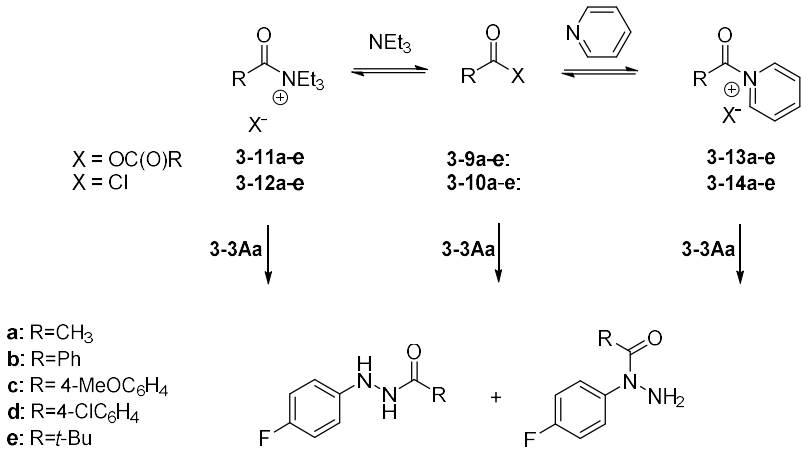

In contrast, NaOH can only act as a Brønsted base. The extent to which nucleophilic catalysis would affect the reaction would depend not only on relative abundance of the acylammonium (**3-11a-e**, **3-12a-e**) and acylpyridininum (**3-13a-e**, **3-14a-e**) salts, but on their second-order rate constants for acylation of **3-3Aa**, relative to direct reaction of **3-3Aa** with acid anhydrides and acid chlorides. These relative abundances and rate constants would in turn depend on the identity of the amine (Et_3N, pyridine), the R group, and the counterion X^- (Cl^- or RCO_2^-). Using Scheme 3.3 to interpret the results of Table 3.5, in the presence of Et_3N as base, anhydrides **3-9a-d** and acid chlorides **3-10a-d** give substantially different selectivities; therefore similar reactive acylammonium intermediates (e.g. **3-11a-d**, **3-12b-d**) are likely *not* involved in this reaction. We propose that in $Et_3N/CDCl_3$, the majority of products result from direct attack of **3-3Aa** on **3-9a-e** and **3-10b-e**. This proposal is supported by the observation that acid chlorides **3-10b-d** give similar product ratios using either Et_3N or NaOH as base. However in the presence of pyridine, since acid chlorides **3-10a-d** give substantially different selectivities than seen in the presence of Et_3N, it appears that different reactive intermediates are involved in this case, specifically acylpyridiniums 3-**14a-d**.

We further propose that the larger leaving group in acid anhydrides **3-9a-d** and acylpyridiniums **3-14a-d** (relative to Cl in **3-10a-d**) results in a steric preference for distal acylation of **3-3Aa**. Direct reaction of **3-3Aa** with acid chlorides **3-10b-e** occurs when Et_3N or aq. NaOH are used as base in place of pyridine, and reduced steric bulk in the electrophile can actually lead to a moderate preference for proximal monoacylation (i.e. aromatic acid chlorides **3-10b-d**, Table 3.5, Entries 7-9 and 17-19). For the very sterically hindered pivaloyl chloride **3-10e**, high distal selectivities are obtained no matter what base is used (Table 3.5, entries 10, 15, 20). The fact that the selectivity of acetyl chloride **3-10a** varies significantly when using Et_3N and NaOH (Table 3.5, entries 6, 16) suggests reaction of **3-3Aa** with **3-10a** in Et_3N proceeds in part through the acylammonium intermediate **3-12a**.

3.4 Synthetic application of regioselectivities of arylhydrazines toward aroyl chlorides

Observing the kinetic preference for the proximal acylation of **3-3Aa** by acid chlorides **3-10a-d** under Schotten-Baumann conditions (entries 16-19, Table 3.5), and the proximal acylation of **3-3Aa** by **3-10b-d** in the presence of Et_3N (entries 7-9, Table 3.5), we sought to develop a convenient one-step synthesis of proximal monoacylarylhydrazines. We thus explored the use of triethylamine (2.2 equiv) as base in CH_2Cl_2 and found that aroyl chlorides **3-10b-d** reacted with **3-3Aa** to give **3-3Ab**, **3-3Ae**, and **3-3Af** in 59-64% yield following chromatography. This protocol was then applied to phenylhydrazine (**3-2Aa**), 4-methoxyphenylhydrazine (**3-4Aa**), and 4-bromophenylhydrazine (**3-5Aa**). As can be seen in Table 3.6, reactions of aroyl chlorides **3-10b-d** with hydrazines **3-3Aa, 3-2Aa,** and **3-4Aa** were also quite successful, yielding the proximal monoaroyl hydrazines in 51-70% yield (Entries 1-9). Yields of the proximal monoaroyl hydrazines derived from 4-bromophenylhydrazine **3-5Aa** were somewhat lower, ranging from 40-47%. Yet in comparison to the traditional three-step literature protocol (illustrated in **Table**

3.2) our one-step route offers competitive yields. As shown in Table 3.6, one-step yields for **3-3Ab** and **3-3Ae** were comparable or superior to the three-step yields, with a considerable time saved and greater atom economy (Entries 1,2). Similarly, one-step yields for **3-2Ab**, **3-2Ad**, **3-4Ab**, and **3-4Ad** were superior to yields reported in the literature for the three-step approach (Table 3.6, Entries 4, 6, 7, and 9).

Table 3.6. One-step synthesis of proximal monoaroyl arylhydrazines.

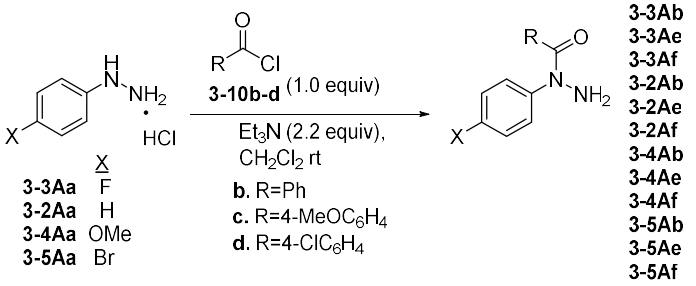

Entry	Hydrazine	Acylating Agent	Product	One-step method Yield (%)	Three-step method[a] Yield (%)
1	**3-3Aa**	**3-10b**	**3-3Ab**	59	47[b]
2	**3-3Aa**	**3-10c**	**3-3Ae**	60	57[b]
3	**3-3Aa**	**3-10d**	**3-3Af**	64	47[b]
4	**3-2Aa**	**3-10b**	**3-2Ab**	51	36[74]
5	**3-2Aa**	**3-10c**	**3-2Ae**	54	-
6	**3-2Aa**	**3-10d**	**3-2Af**	51	16[141]
7	**3-4Aa**	**3-10b**	**3-4Ab**	53	20[141]
8	**3-4Aa**	**3-10c**	**3-4Ae**	63	-
9	**3-4Aa**	**3-10d**	**3-4Af**	70	52[141-142]
10	**3-5Aa**	**3-10b**	**3-5Ab**	47	-
11	**3-5Aa**	**3-10c**	**3-5Ae**	40	-
12	**3-5Aa**	**3-10d**	**3-5Af**	43	-

[a] The three step method involves protection of the distal N, acylation at the proximal N, and deprotection, as shown for the synthesis of proximal acylarylhydrazine standards in Table 3.2. [b] These compounds were synthesized in our study.

These results raise the following question: given the favorable kinetic selectivity seen for proximal acetylation of **3-3Aa** under Schotten-Baumann conditions (Table 3.6, entry 16), could acceptable yields of **3-3Aj** and other proximal primary or secondary alkanoyl derivatives of aryl

hydrazines be obtained in a one step? Work by a colleague (Maryam Ghavami) showed that this is not practical, as reaction to higher conversion results in significant amounts of *N*,*N*′-diacylation products, with an approximate 1:1 ratio of the proximal and distal monoacyl products. It appears that as the proximal acetyl derivative is formed, its subsequent second acylation is competitive with acylation of the parent hydrazine itself, and is faster than acylation of the distal acetyl hydrazine.

3.5 Interpretation of experimental results utilizing the α-effect

Finally, the implications of arylhydrazine's acylation preference in the proximal position with acid chlorides prompts the following question: what is the basis for the regiochemistry observed? We suspect that α-effect (see Chapter 1) is the major contributing factor; it is defined by Edwards and Pearson as the breakdown of correlation between basicity and nucleophilicity in nucleophiles which possess an electronegative atom with one or more lone pairs adjacent to the nucleophilic atom.[51] Hydrazines fit this description and in the past, the α-effect has been used to compare the rates of reaction between α-nucleophiles and their normal counterparts.[52, 61, 66]

The underlying phenomenon to give predictive capability to these α-nucleophiles and their reactivity toward certain electrophiles comes from Hoz's proposal of single electron transfer (SET).[56] After SET, the nucleophile and electrophile would be bound in a high-spin, zwitterionic transition state that then collapses to a low-spin and charge-neutral product (Figure 3.4).[56] Molecular features that are capable of stabilizing the radical cation that the α-nucleophile becomes after SET would favor higher rates of reaction relative to nucleophilic centers which lack these same features.

Figure 3.4. Single electron transfer in reaction of α-nucleophiles and transition state stabilization.

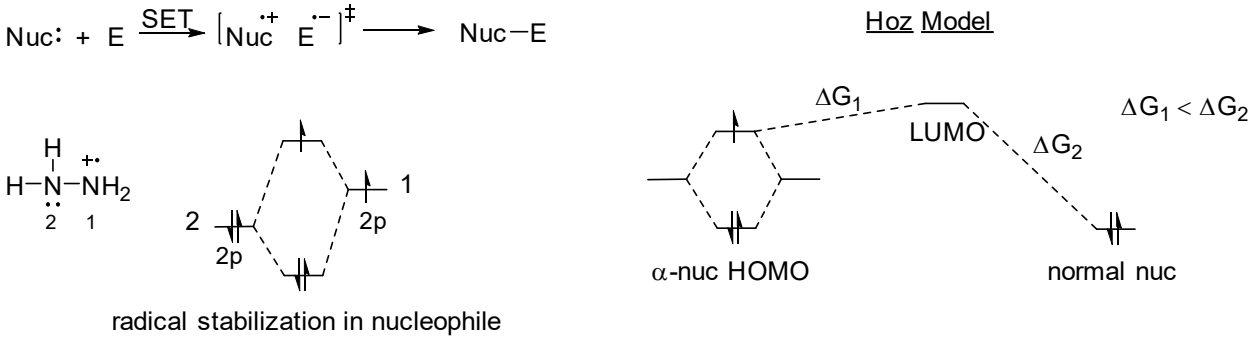

Figure 3.5. ^{1}H NMR spectrum of 3-3Aa in (DMSO-d_6, 400 MHz).

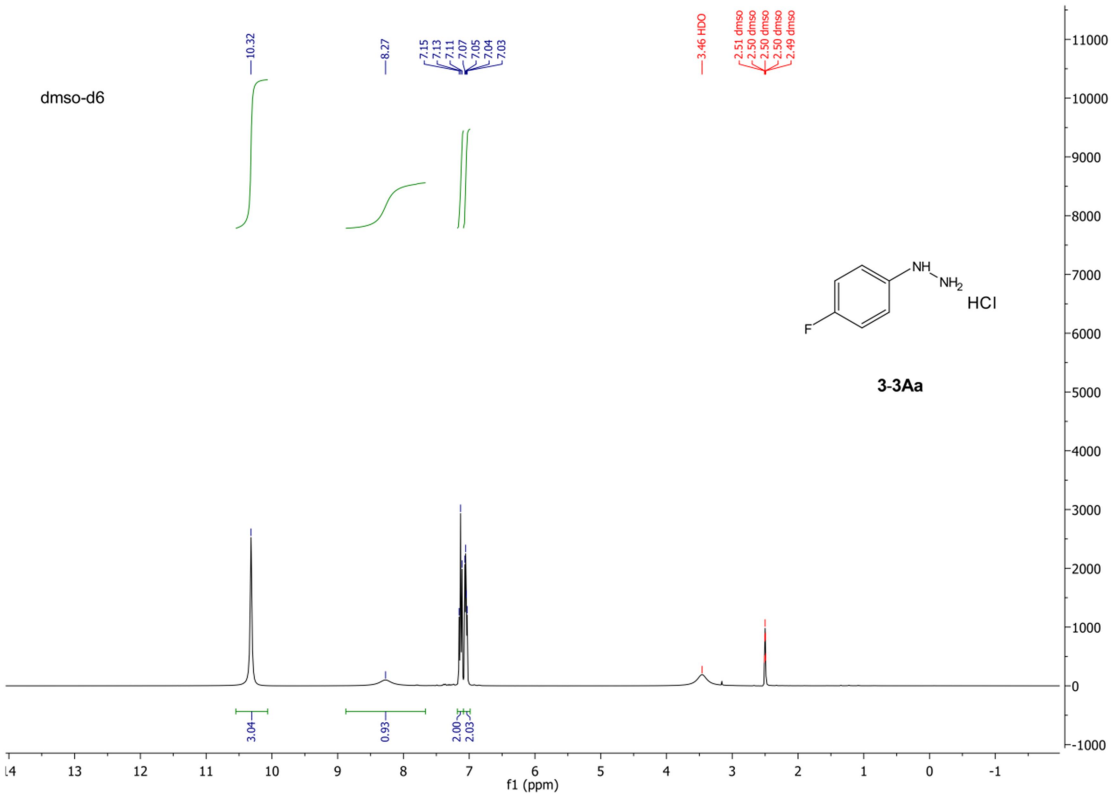

Thus according to Hoz, the model system of using pK_a values to predict nucleophilicity is less appropriate than estimating the first ionization energy or oxidation potential of the α-nucleophile.[56] The ^{1}H NMR spectrum 3-3Aa·HCl in DMSO-d_6 revealed that the distal nitrogen unambiguously is the stronger base (Figure 3.5). The sharp singlet peak at 10.32 ppm has an integration of 3H, while another broad singlet seen at 8.27 ppm integrating to 1H. As the other peaks represent the 4 hydrogens on the aryl ring, the only conclusion is that the distal nitrogen possesses a significantly larger pK_a value. This held true for **3-2Aa**·HCl, **3-4Aa**·HCl, and **3-5Aa**·HCl across two non-exchanging solvents, and with electron-donating and electron withdrawing substituents on the aryl ring (see Table 3.7).

Table 3.7. ^{1}H NMR determination of the relative base strength of arylhydrazine nitrogens in DMSO-d_6 and DMF-d_7.

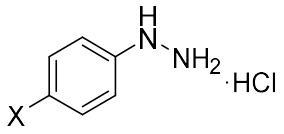

Hydrazine	X	Solvent	Distal NH δ (ppm)	Distal NH rel. integral	Proximal NH δ (ppm)	Proximal NH rel. integral
3-3Aa·HCl	F	DMSO-d_6	10.31	3.09	8.27	1.00
3-2Aa·HCl	H	DMSO-d_6	10.28	3.02	8.29	1.00
3-4Aa·HCl	OMe	DMSO-d_6	10.14	3.00	7.93	0.93
3-5Aa·HCl	Br	DMSO-d_6	10.29	3.04	8.45	1.03
3-3Aa·HCl	F	DMF-d_7	10.9	3.09	8.45	0.88[a]
3-2Aa·HCl	H	DMF-d_7	10.93	3.08	8.53	0.85[a]
3-4Aa·HCl	OMe	DMF-d_7	10.75	3.02	8.17	0.78[a]
3-5Aa·HCl	Br	DMF-d_7	10.97	2.94	8.70	0.95

[a] The DMF solvent peak was partially overlapping the proximal N-H peak and necessitated an estimation of the integral value based on subtraction of the solvent peak area.

Table 3.7 identifies the distal nitrogen as the more basic nitrogen. Combined with the results of our single-step synthesis of proximal acylarylhydrazines (Table 3.6), this confirms that acid-base

chemistry analogies are not necessarily predictive of acylation regiochemistry in arylhydrazines. We wish to use these insights to explain our experimental observations; not by comparing our arylhydrazines to corresponding amines, but to examine possible radical cations formed by our arylhydrazines and predict regiochemistry outcomes. As can be seen in Figure 3.6, assuming a SET-based process, it is clear that the proximal nitrogen is the position that allows the greatest stabilization of the radical cation via resonance from the aryl ring and the distal nitrogen. In contrast, if the distal nitrogen is the radical cation, it can only be stabilized through the proximal nitrogen.

Figure 3.6. Resonance forms of phenylhydrazine radical cation.

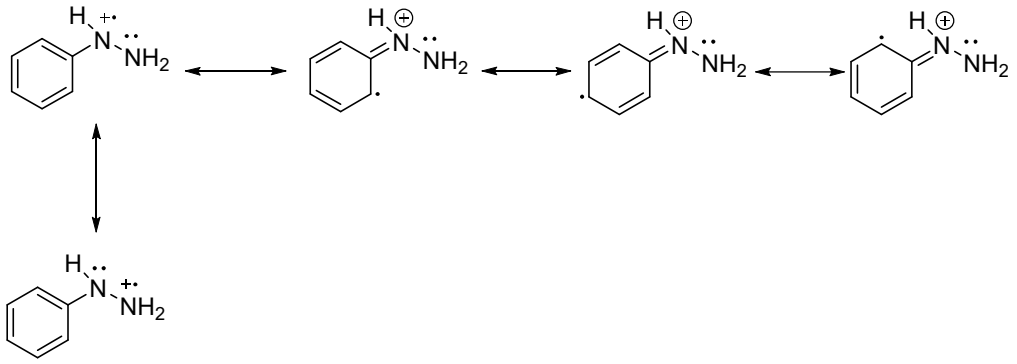

With this prediction in hand, we can propose a mechanism of arylhydrazine reaction with acid chlorides (see Figure 3.7).

Figure 3.7. Proposed mechanism of arylhydrazine acylation by acid chlorides via single electron transfer.

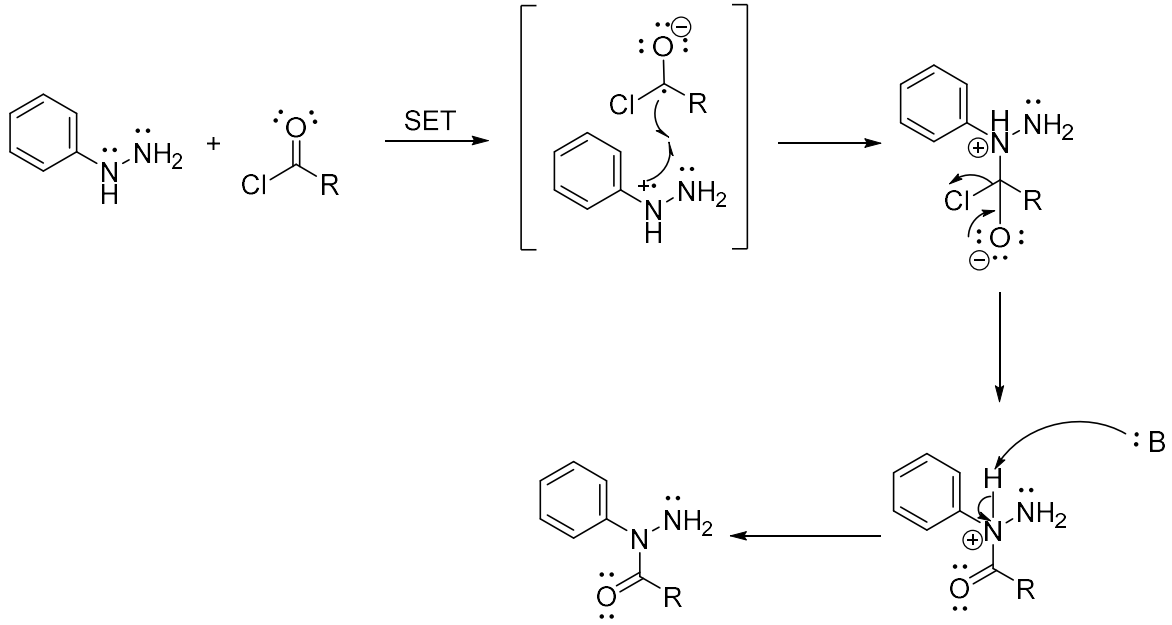

After an initial SET step, a zwitterionic biradical intermediate can be envisioned that is held together by electrostatic attraction (whether this is a transition state or an reactive intermediate is unknown). Combining the two radicals forms a bond that results in the canonical tetrahedral intermediate seen in carboxylic acid derivative chemistry. Facile ejection of chloride ion and deprotonation of the hydrazine nitrogen by a base gives the proximal monoacylarylhydrazine product. By invoking the SET hypothesis, our experimental results from Table 3.6 are now quite predictable, with the electron withdrawing bromine of **3-5Aa** reducing the radical stabilizing capability of the aryl ring and thereby lowering the proximally acylated product yield and vice versa for **3-4Aa**.

3.6 Conclusion

In conclusion, we showed that the selectivity of acid chloride acylation of 4-fluorophenylhydrazine is remarkably dependent on the base employed. With pyridine as base,

selectivity for the distal product is high, as reported in the literature for other arylhydrazines. This selectivity is likely steric in origin. However in Et_3N, or under Schotten-Baumann conditions, selectivity is lower in four out of five cases studied, and moderately favors the proximal acylation product. We attributed this base-dependent regioselectivity to the formation of different reactive acylating species under the various conditions. Pivaloyl chloride differed from this trend in giving high selectivity for the distal acylation product regardless of the base employed, also likely due to steric hindrance. We confirmed high distal acylation selectivity in reactions of 4-fluorophenylhydrazine with anhydrides, as would be expected based on the high yields of distal monoacyl product that can be obtained under these conditions. We utilized the regioselective preference for proximal acylation for aroyl chlorides in reaction with arylhydrazines to make a variety of proximal monoaroyl arylhydrazines in a single step and in better yield than the standard three-step procedure. Finally, we proposed a mechanism that uses single electron transfer to more adequately predict the regiochemistry of arylhydrazines toward acid chlorides when basicity could not predict the product outcome.

Chapter 4. Analysis of Diacylbenzylhydrazine Conformational Isomerisms Through X-Ray Crystallography, Variable Temperature NMR, and Computation

4.1 NMR analysis of diacylbenzylhydrazine conformations

While pursuing the synthesis of acylbenzylhydrazines, an observation was made: the benzylic protons of **4-1** were an extremely broad set of two signals, very close to coalescence (see Figure 4.1).

Figure 4.1. ^{1}HNMR spectrum of 4-1 at room temperature ($CDCl_3$, 400 MHz).

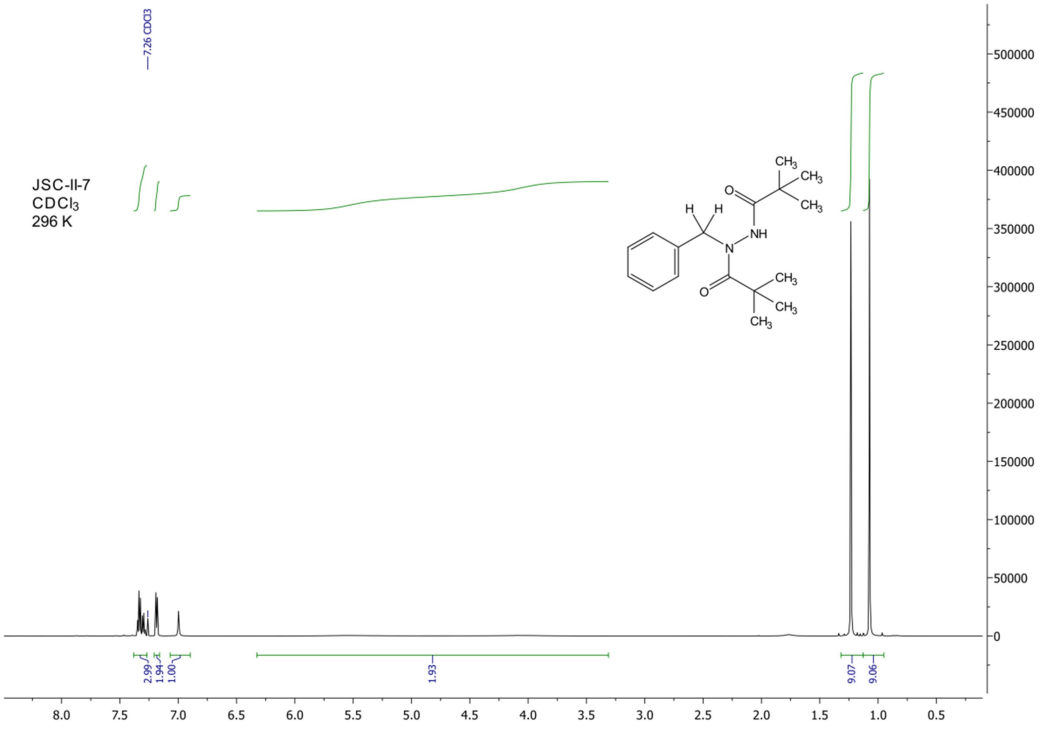

Variable temperature ^{1}H NMR experiments revealed the coalescence temperature (T_c) to be 311 K (Figure 4.2). Temperature calibration was accomplished through the δ of methanol-d4.

Figure 4.2. Determining the coalescence temperature for the benzylic protons of 4-1. ($CDCl_3$, 600 MHz).

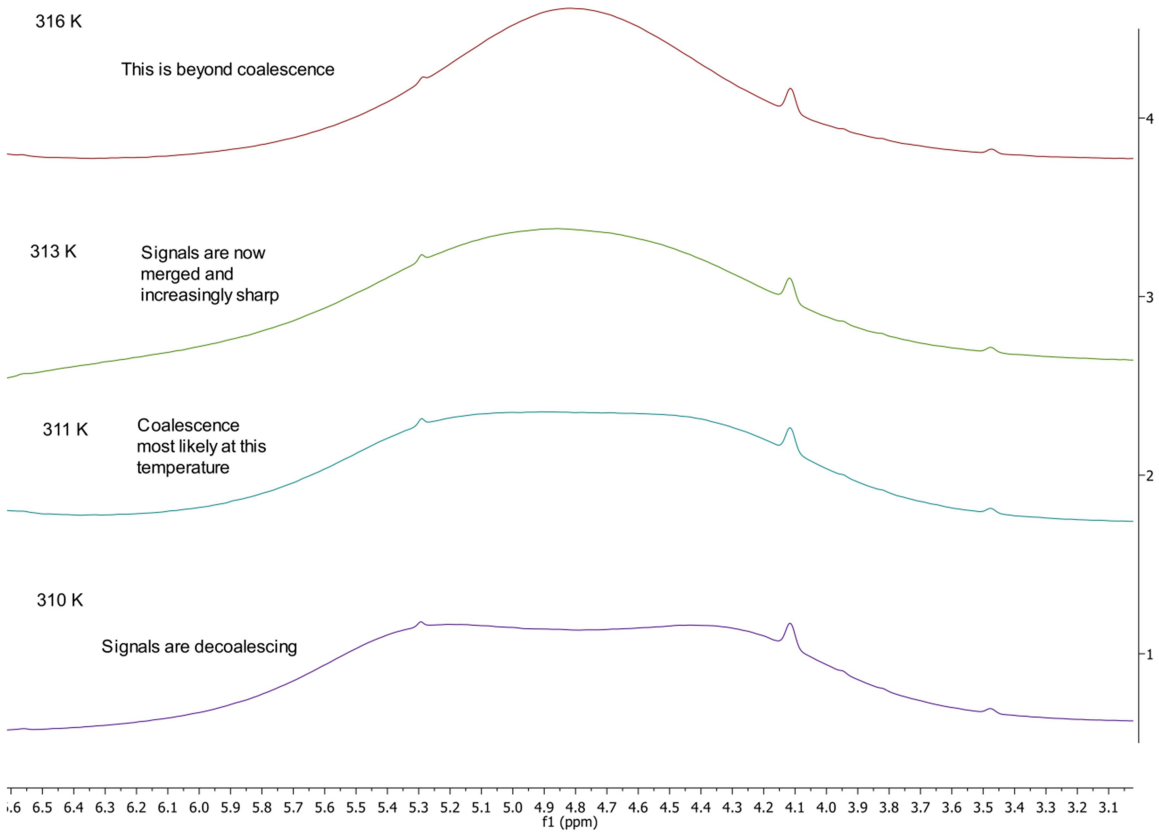

Upon steady cooling to -20 °C, the signals resolved and revealed diastereotopic protons with an integration of one proton each and a coupling constant of 14.4 Hz, consistent with $^{2}J_{HH}$ (Figure 4.3).

Figure 4.3. Variable temperature ^{1}HNMR spectrum of 4-1 and decoalescence of benzylic protons ($CDCl_3$, 600 MHz).

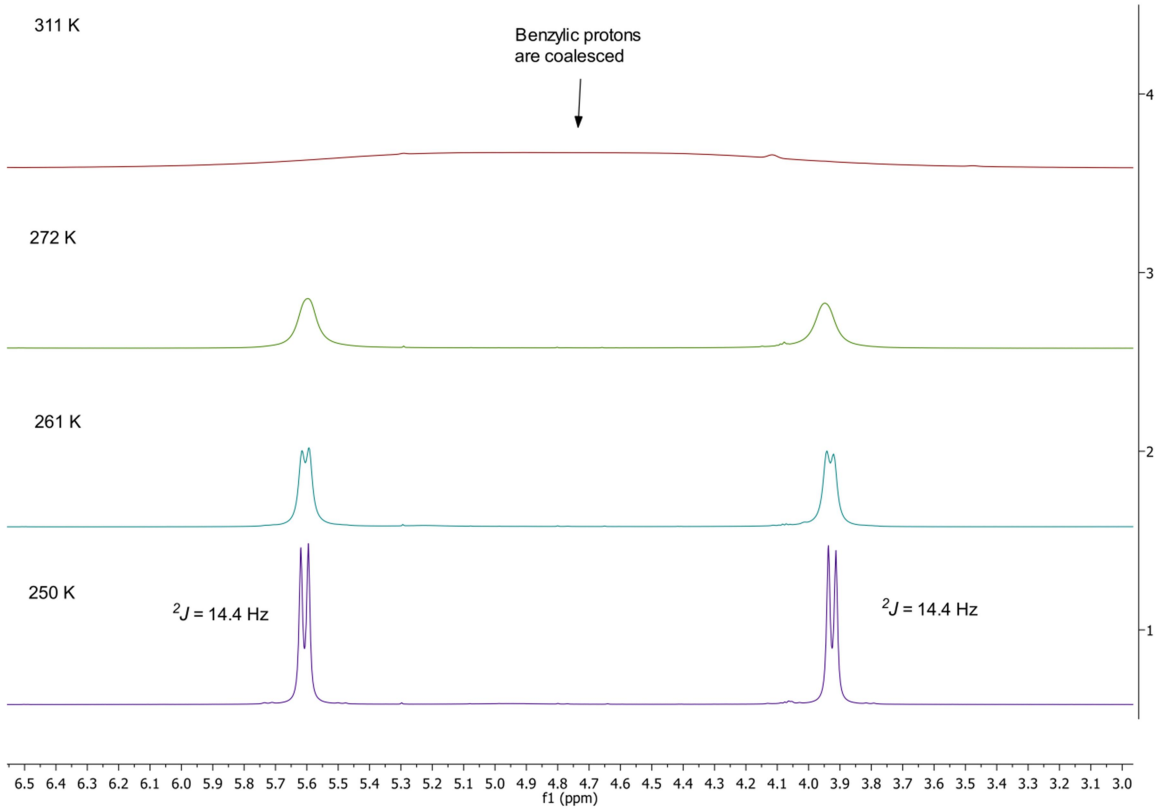

The lack of a stereogenic center in the molecule, combined with signal decoalescence at lower temperatures, points to axial chirality in the N-N bond of benzylhydrazine as the source of signal nonequivalence.[39, 143] Figure 4.3 illustrates how this is possible, as rotation of the N-N bond converts (*M*)-**4-1** to (*P*)-**4-1**. In this process, H^a's chemical environment changes with respect to the N-H proton, as H^a (proximal to N^2-H in (*M*)) and H^b (distal to N^2-H in (*M*)) interchange.

Figure 4.4. Axial chirality in 4-1 and 4-2, and interconversion between enantiomers.

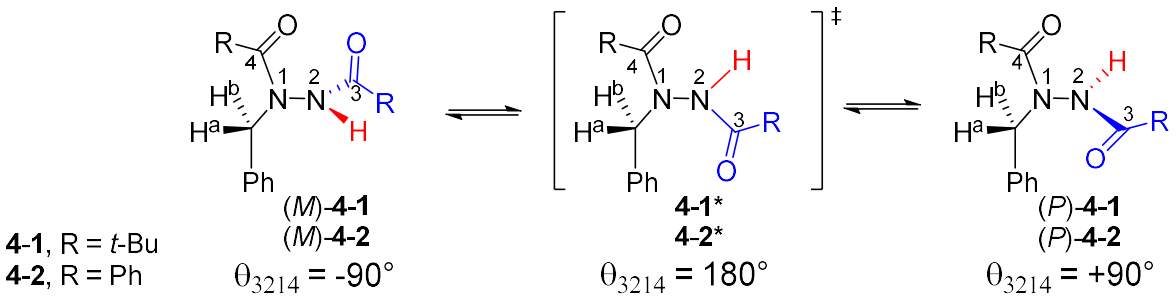

Furthermore, the only structures in which H^a and H^b could be equivalent are those that feature coplanar placement of the N substituents, such as **4-1*** in Figure 4.4. As mentioned in Chapter 1, the energetically preferred conformations of diacylhydrazines feature a twist around the N-N bond that place the N-substituents nearly orthogonal.[15, 40] Thus, H^a and H^b should be different when the N-N bond rotation is slow relative to the NMR timescale. Using Equations 4.1 and 4.2, the barrier to rotation was calculated to be 13.5 ± 0.2 kcal/mol, using T = 311 K, ν_{AB} = 1009.4 Hz and J_{AB} = 14.4 Hz. Error in $\Delta G^{\ddagger}$ was calculated based on an error in T_c of ± 3 K.

Equation 4.1. Calculation of the first-order rate constant for two coupled nuclei at coalescence.[144]

$$k = \frac{\pi}{\sqrt{2}}\sqrt{{\nu_{AB}}^2 + {J_{AB}}^2}$$

Equation 4.2. The Eyring-Polanyi equation.

$$k = \frac{k_B T}{h} e^{\frac{-\Delta G^{\ddagger}}{RT}}$$

As discussed in Chapter 1, a conformational analysis of 1,2-diacyl-1-benzylhydrazines by Bishop using ^{1}H NMR spectroscopy determined that the barrier to N-N bond rotation was high enough at room temperature that the benzylic protons of the *N*-benzyl group were magnetically

non-equivalent (see Table 4.1).[39] Tetrasubstituted compounds **4-5a-c** featured barriers at approximately 23 kcal/mol each, while tri-substituted compound **4-3d**, had a barrier of 13.2 kcal/mol, a drop of 10 kcal/mol.[39] **4-3d** is quite similar to compounds **4-1** and **4-2**, as is the value of their rotational barriers (13.2 kcal/mol, compared to 13.5 and 12.3 kcal/mol respectively).

Table 4.1. Measured N-N rotational barriers of 1,2-diacyl-1-benzylhydrazines and benzylic proton nonequivalence.[39]

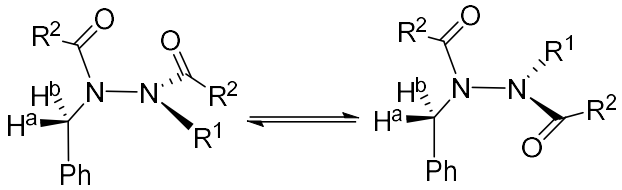

(*M*)-**4-3a-d** (*P*)-**4-3a-d**

Entry	Compound	R^1	R^2	T_c (°C)	$\Delta G^{\ddagger}$ at T_c (kcal/mol)
1	**a**	CH_2Ph	OCH_3	192	23.5
2	**b**	CH_2Ph	CH_3	188	23.4
3	**c**	CH_2Ph	CH_2Ph	190	23.3
4	**d**	H	CH_2Ph	4	13.2

Diacylbenzylhydrazines described by Bishop[39, 145] exhibit this benzyl signal broadening behavior, and **4-2** is no different in this regard. In Figure 4.5, we find a familiar circumstance in which the benzylic protons of **4-2** are totally coalesced at room temperature (T_c = 283 K for **4-2**) but resolve at lower temperatures (T = 250 K), ν_{AB} = 849.8 Hz and J_{AB} = 14.4 Hz with a calculated N-N torsional barrier of 12.3 ± 0.2 kcal/mol. There are, however, important differences with **4-2** and **4-1**; upon cooling, another peak arises at lower temperatures as a sharp singlet, representing approximately 18% of the total methylene proton signal integration (see

Figure 4.6). Note that the N-H region of the spectrum (δ = 8.5-9.0 ppm) also features two signals in a 0.17:0.80 ratio.

Figure 4.5. Variable temperature ^{1}HNMR comparison of 4-2 at 298 K, 283 K, 250 K, and 218 K ($CDCl_3$, 600 MHz).

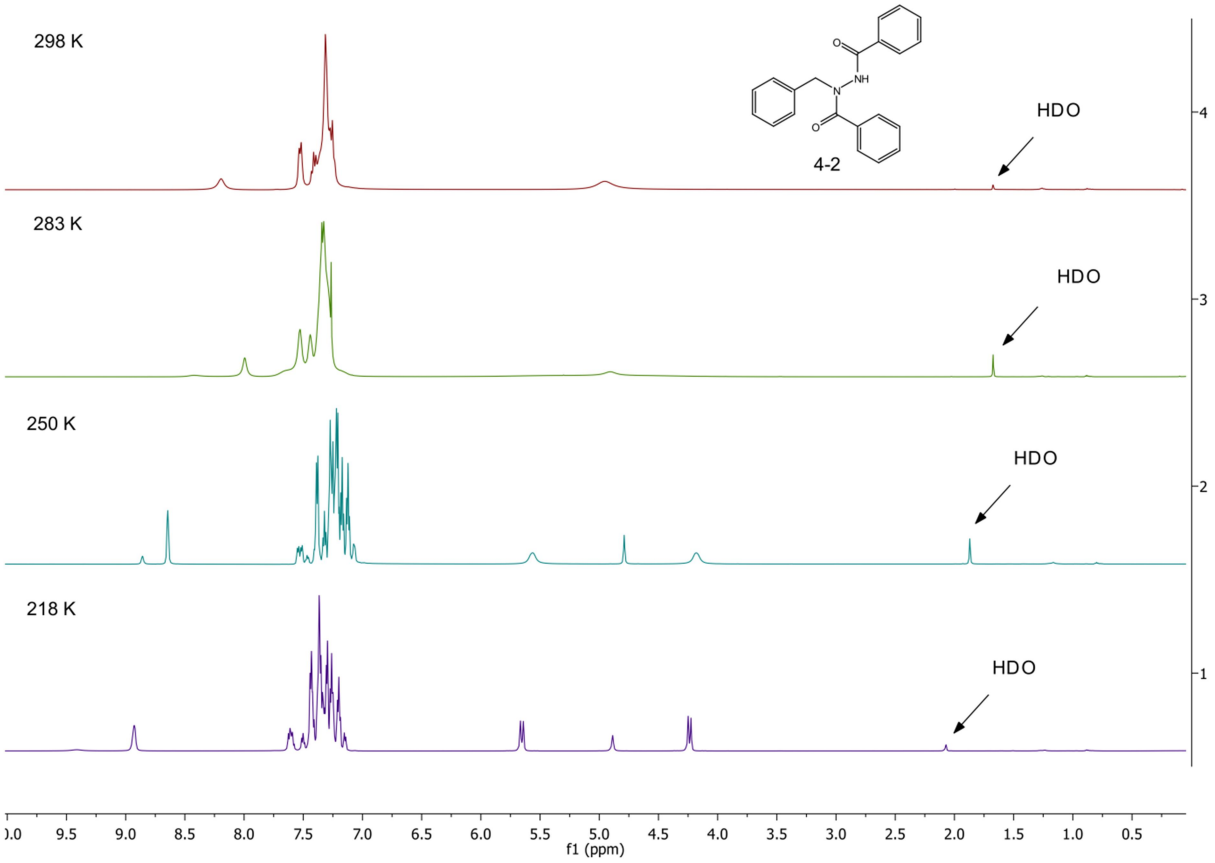

Figure 4.6. Benzylic proton decoalescence in 4-2 using variable temperature ^{1}HNMR ($CDCl_3$, 600 MHz).

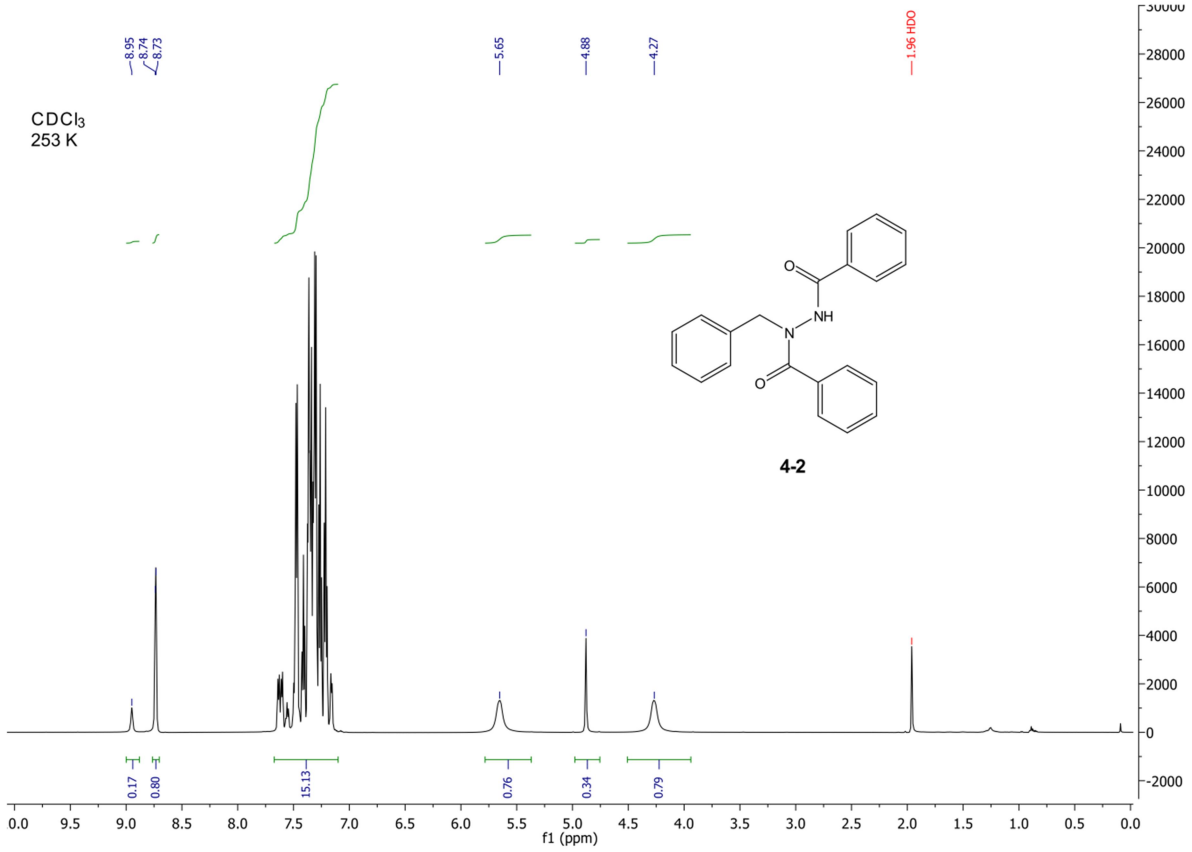

Another important observation is at room temperature (298 K) in $CDCl_3$, the ^{13}C NMR spectrum shows that both the benzylic carbon (~51 ppm) and one of the carbonyl carbon signals (~173 ppm) are very broad and barely visible. However, upon cooling to 250 K, each of these carbons resolved into a pair of major and minor signals (see inset in Figure 4.7).

Figure 4.7. Benzylic carbon signal decoalescence in 4-2 using variable temperature ^{13}CNMR ($CDCl_3$, 151 MHz).

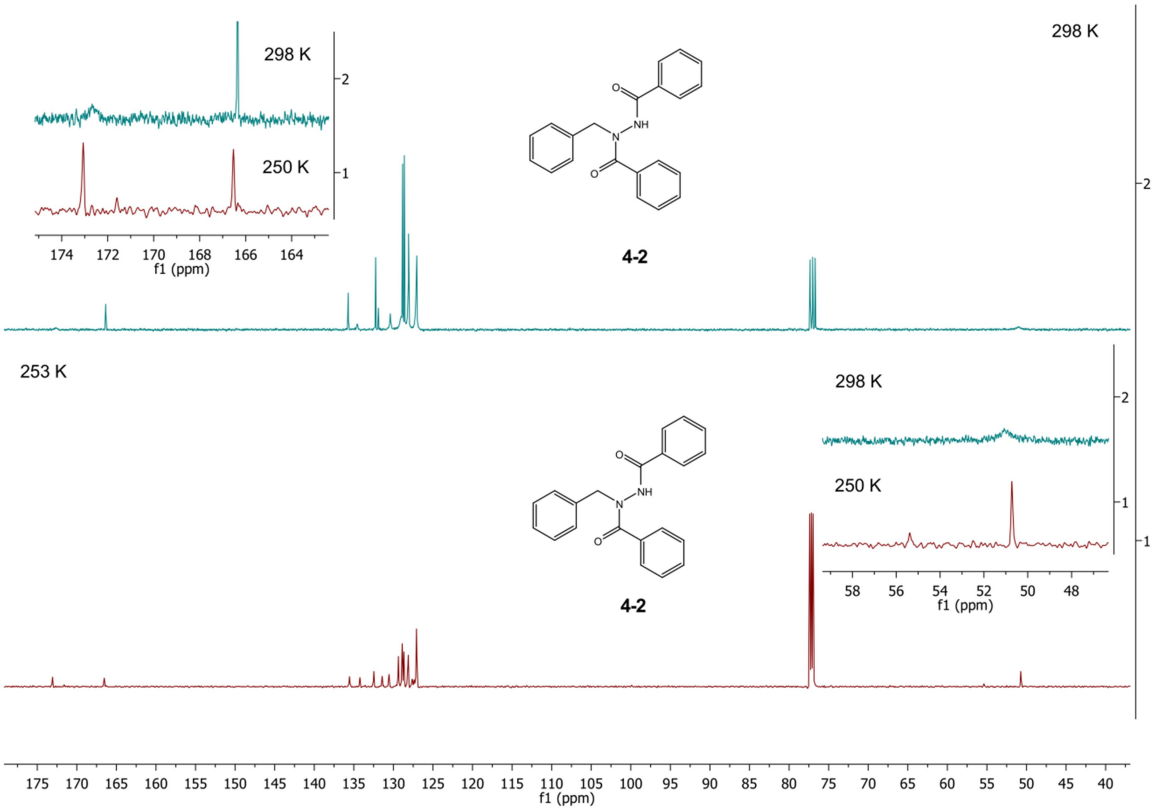

The signal broadening of the benzylic and carbonyl carbons in **4-2** cannot be due to slow N^1-N^2 bond rotation on the NMR timescale, since the benzylic and carbonyl carbons of **4-1** and **4-2** experience identical environments in the (*M*)- and (*P*)-enantiomers (Figure 4.4). Furthermore, the compounds have similar N-N torsional barriers ($\Delta G^{\ddagger}_{rot}$ = 12.3 kcal/mol and T_c = 283 K for **4-2** and $\Delta G^{\ddagger}_{rot}$ = 13.6 kcal/mol and T_c = 313 K for **4-1**). Slow conformational interchange of (*E*) and (*Z*)-isomers across the N^1-C^4 bond could explain this signal broadening and subsequent resolution at low temperatures (see Figure 4.9). If that is true, at 253 K the sharp singlet at 4.88 ppm in the ^{1}H NMR spectrum should correspond to the small carbon signal at 55.4 ppm in the ^{13}C NMR spectrum in the same way that the major resolved ^{1}H signals at 5.58

and 4.18 ppm should correlate to the major ^{13}C resonance at 50.7 ppm. HSQC at 250 K clearly reveals these correlations in Figure 4.8.

Figure 4.8. HSQC of 4-2 at 250 K ($CDCl_3$, 600 MHz for ^1H and 151 MHz for ^{13}C).

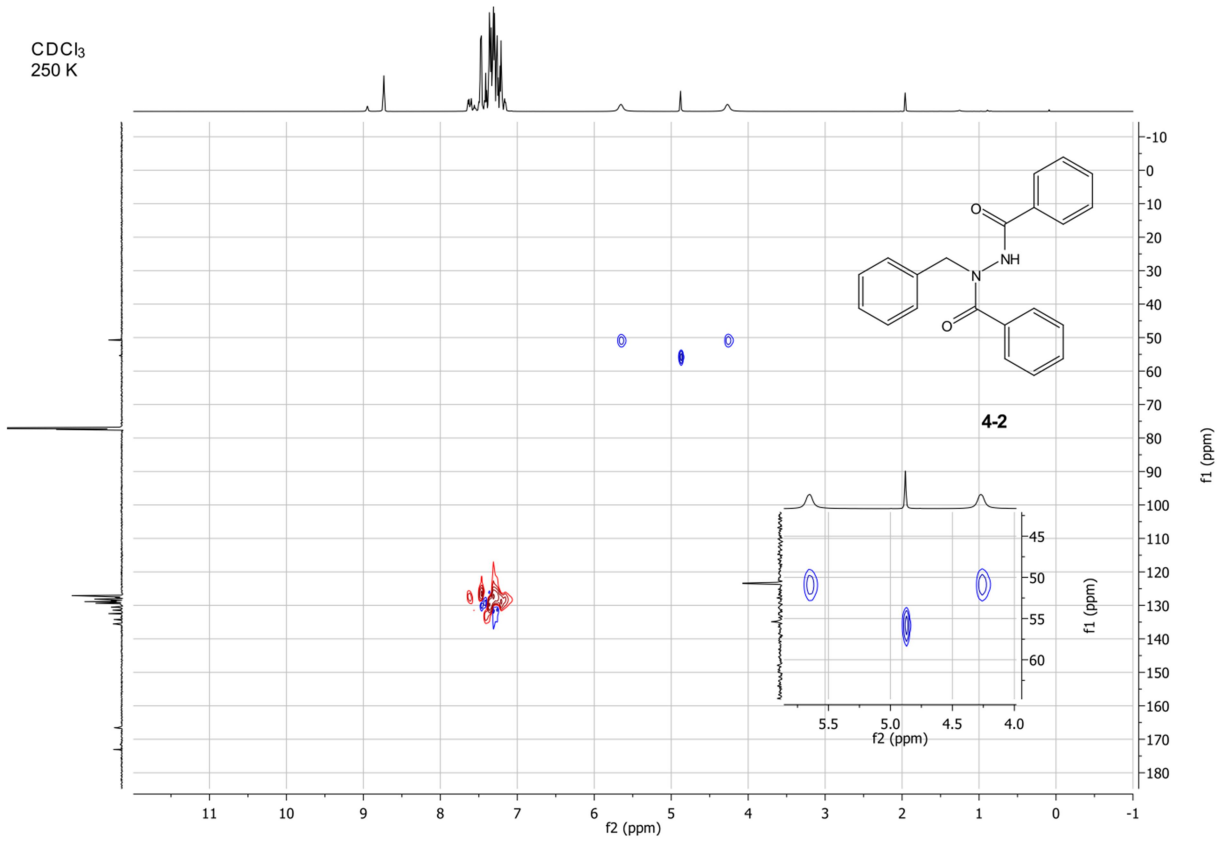

Figure 4.9 shows what we believe are the essential variables to understand the NMR spectra we have presented. As can be seen, H^a and H^b are diastereotopic in both (*Z*)-(*M*)-**4-2** and (*E*)-(*M*)-**4-2**. The rate constants for N^1-N^2 bond rotation of the *E*- and *Z*-isomers are k_Z and k_E (where $k_Z \neq k_E$) with corresponding barriers $\Delta G^{\ddagger}_Z$ and $\Delta G^{\ddagger}_E$. The fact that **4-2** has a sharp 4.88 ppm signal that did not decoalesce at 218 K leads us to estimate that one of these barriers is <10 kcal/mol (Figure 4.5).[38] We will address this point below in Section 4.3.3.

Figure 4.9. Free energy barrier of N-N bond rotation from a given (*E*)- or (*Z*)-isomer of 4-2.

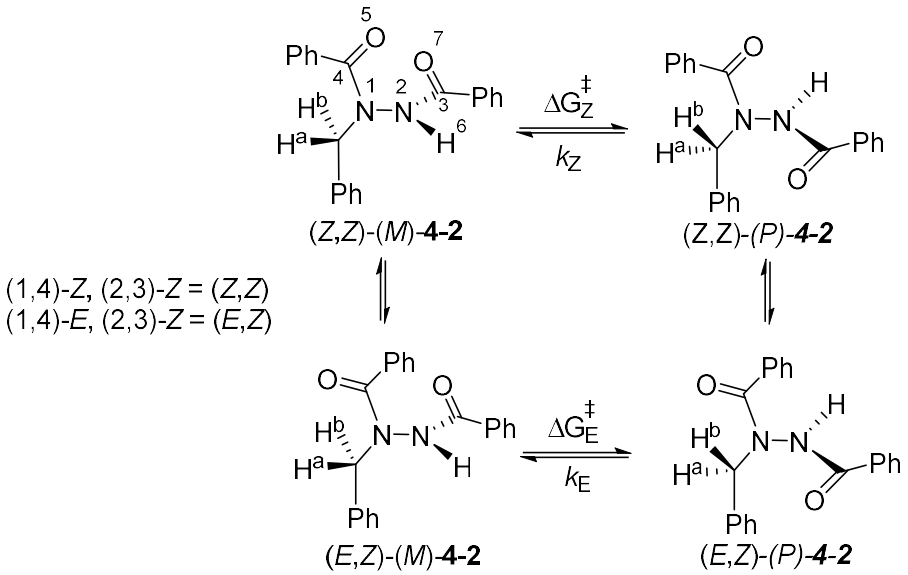

Upon cooling to 218 K, the 4.88 ppm signal did not resolve into two separate signals, nor did it broaden (Figure 4.5). NMR data obtained here cannot determine for certain whether this signal is sharp due to accidental equivalence or a very low N-N torsional barrier. The hypothesis of (*E*)/(*Z*)-isomerism causing carbon signal broadening would be strengthened with additional evidence from other techniques distinct from NMR.

Figure 4.10. E/Z assignment for diacylbenzylhydrazines.

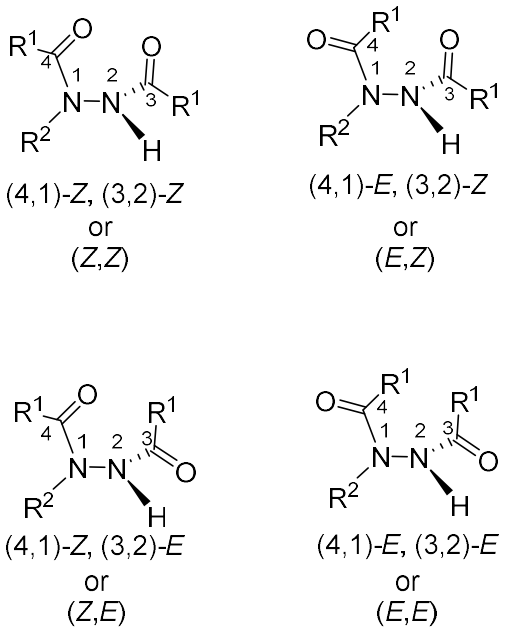

4.2 X-ray crystallography of diacylhydrazines

With the idea of both N^1-N^2 slow bond rotation and (*E*)/(*Z*)-isomerism being the cause of signal broadening in NMR spectra of **4-1** and **4-2**, the natural place to follow up on these hypotheses would be X-ray crystallography. Designations for (*E*)/(*Z*) assignment can be seen in Figure 4.10. Crystals showing a twist conformation and signs of (*E*)- and (*Z*)-isomerism about the N^1-C^4 bond would strengthen the argument formulated from the NMR analysis. After synthesizing the compounds initially (see Chapter 2), crystals were grown by vapor diffusion over a two week span, using ethyl acetate and hexane. After screening crystal quality, X-ray crystal diffraction was conducted by Dr. Carla Slebodnick. Figures 4.11 and 4.12 feature the X-ray crystallography results, showing that **4-1** and **4-2** exhibit the expected twist conformation, as well as that the proximal acyl group is the (*E*)-conformation, while the distal is (*Z*).

Figure 4.11. Anisotropic ellipsoid drawing (50%) of (*P*)-4-1. A) Orientation matching line drawing. B) View down N^1-N^2 axis.

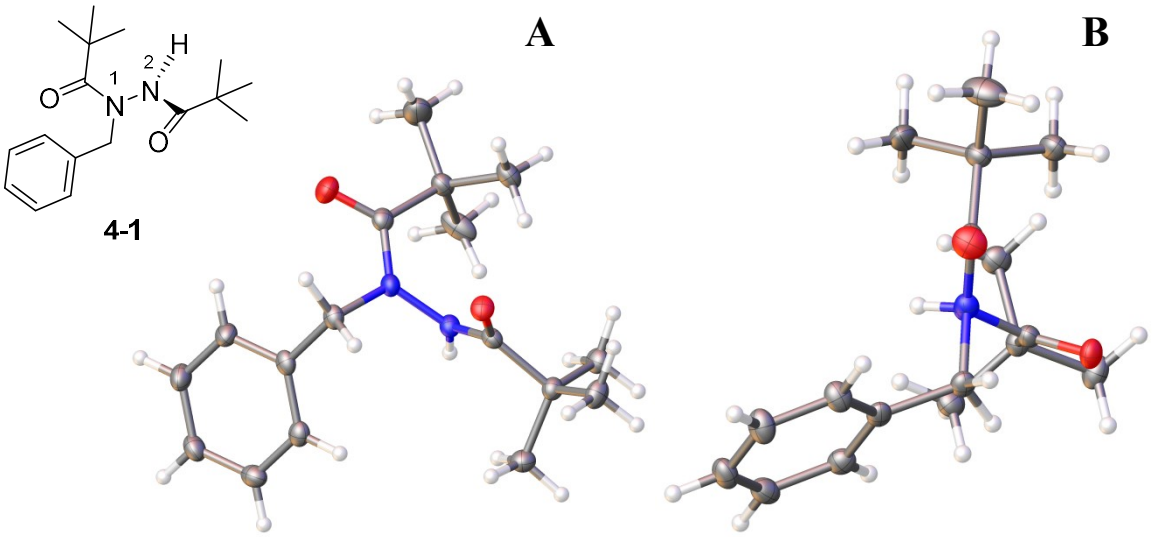

Figure 4.12. Anisotropic ellipsoid drawing (50%) of (*P*)-4-2. A) Orientation matching line drawing. B) View down N^1-N^2 axis.

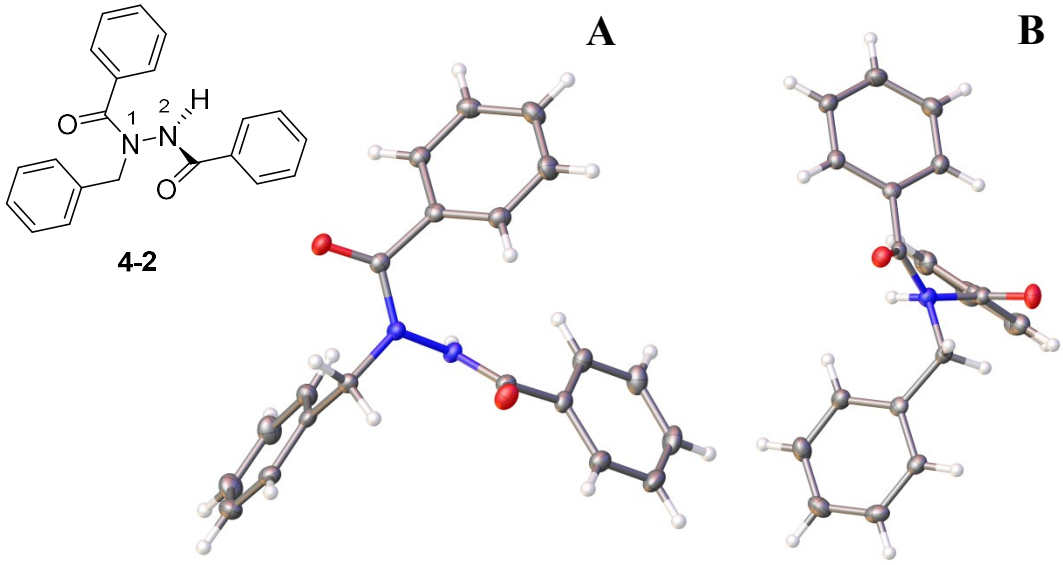

Diacylphenylhydrazines **4-3** and **4-4** also yielded crystal structures for this study (Figures 4.13 and 4.14 respectively), with **4-3** also being (*E*,*Z*)- but **4-4** (complexed with *N*′-phenylbenzohydrazide) is (*Z*,*Z*)-, both displaying the predicted twist conformation.

Figure 4.13. Anisotropic ellipsoid drawing (50%) of (*P*)-4-4. A) Orientation matching line drawing. B) View down N^1-N^2 axis.

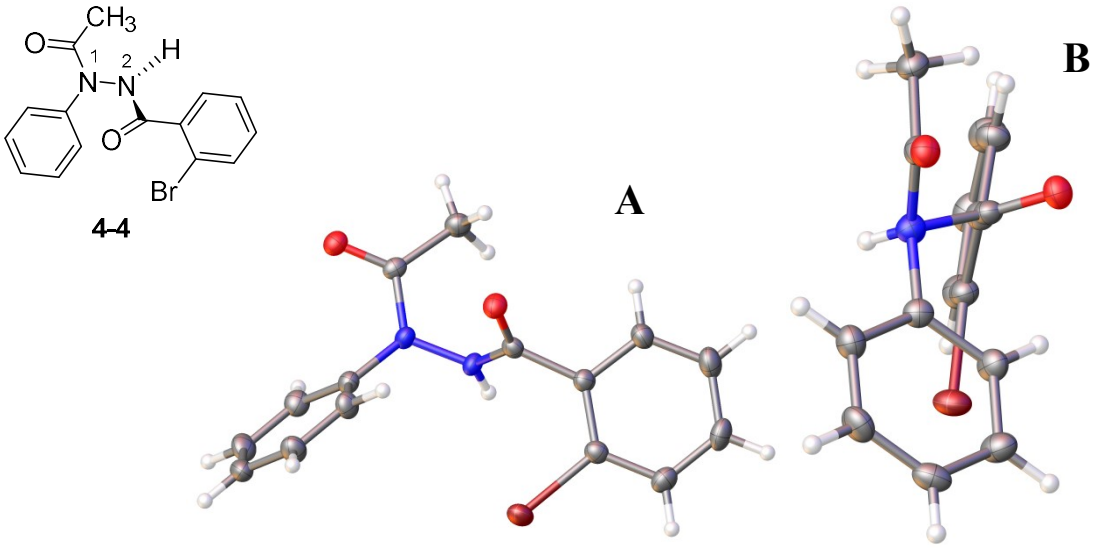

Figure 4.14. Anisotropic ellipsoid drawing (50%) of (*P*)-4-5 complexed with *N′*-phenylbenzohydrazide. A) Orientation matching line drawing. B) View down N^1-N^2 axis.

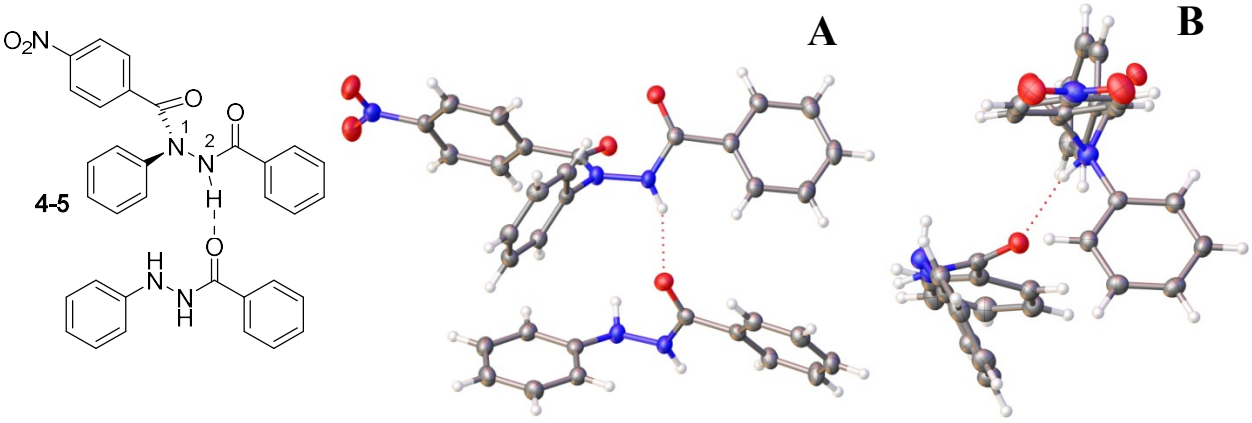

Table 4.2 gives details of the crystal geometries of **4-1**, **4-2**, **4-4**, to **4-5**, with all crystals appearing with (*P*)-stereochemistry and as the (*E*,*Z*)-conformation, save for **4-5** which was (*Z*,*Z*). Intermolecular hydrogen bonding in **4-5** is likely distorting the geometry enough that the O^5-H^6 distance is slightly too long for internal hydrogen bonding (typical distance[146] being 1.9-2.6 Å

versus 3.02 Å from Entry 4, Table 4.2). Internal hydrogen-bonding in the (*E*,*Z*)-conformation is not feasible, as the O^5 is pointed away from H^6.

Table 4.2. Geometric parameters derived from the X-ray crystal diffraction of 4-1, 4-2, 4-4, and 4-5.

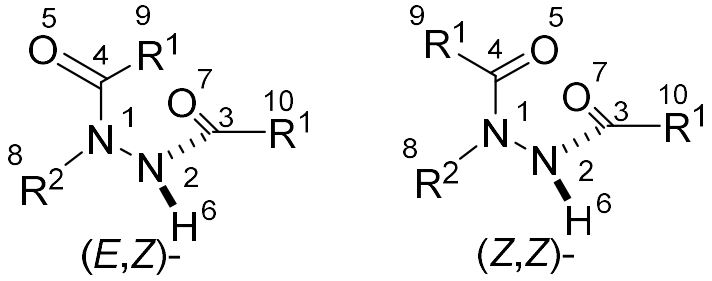

Entry	Compound	Stereochemistry	Amide Geometry	∠$N^2N^1C^4O^5$ (°)	∠$N^1N^2C^3O^7$ (°)	∠$C^4N^1N^2C^3$ (°)	O^5-H^6 (Å)
1	**4-1**	P	(*E*,*Z*)	176.8	-7.0	110.1	3.94
2	**4-2**	P	(*E*,*Z*)	158.53	2.8	119.0	3.71
3	**4-4**	P	(*E*,*Z*)	-171.85	-4.8	73.6	4.07
4	**4-5**	P	(*Z*,*Z*)	4.53	10.5	64.3	3.02

Thus, from the four X-ray structures, we can make the following observations:

1) The N-N bond always features the twist conformation, with the $C^4N^1N^2C^3$ dihedral angle between 64.3°-110.1°, which is within 26° of being orthogonal.

2) The proximal amide bond ($N^2N^1C^4O^5$ dihedral) is (*E*)- in **4-1**, **4-2**, and **4-4**, but (*Z*)- in one case (**4-5** complexed to *N′*-phenylbenzohydrazide).

3) The distal amide bond ($N^1N^2C^3O^7$ dihedral) is always (Z)-.

These crystal structures bolster the argument that (*E*)/(*Z*) interconversion of the proximal amide bond is the source of line broadening in the ^{13}C NMR spectrum for **4-2**, as it is this amide conformation that is shown in the crystals as being variable (Table 4.2, Entries 1-3 versus Entry 4). This evidence is not definitive, however, as crystal packing forces may distort the (*E)*/(*Z)* conformation ratio in order to better facilitate crystal formation. Computing the lowest energy conformations and the N-N torsion transition structures would provide a strong basis to argue for how representative the crystal structures are of solution-phase diacylbenzylhydrazines, and the identity of most probable conformers in solution.

4.3 Computational analysis of diacylbenzylhydrazine conformations

4.3.1 Interpreting NMR spectra via 4-1 and 4-2 (*E*)/(*Z*)-isomer's equilibrium geometries, and the Boltzmann distribution

To get a sense of which of what the major conformers are in solution, I set out to optimize the 4 possible amide bond conformers of **4-1** and **4-2**. All calculations were performed on the (*P*)-conformations of **4-1** and **4-2** using the density functional B3LYP with the 6-31G(d) basis set with the default conditions in gas phase at 298.15 K and 1.0 atm. Optimized structures were obtained and a Boltzmann distribution (Equation 4.3) was calculated from them using their relative energies to estimate the population of each conformer (Table 4.3) to see if the predictions matched our experimental observations.

Equation 4.3. The Boltzmann Distribution.

$$\frac{N_i}{N_{Total}} = \frac{e^{\frac{-E_i}{RT}}}{\sum_{k=1}^{Total} e^{\frac{-E_k}{RT}}}$$

As shown in Table 4.3, the most stable amide bond conformation of **4-1** is (*E*,*Z*)-, which matches the crystal structure in Figure 4.11. The (*Z*,*Z*)-conformation is 2.3 kcal/mol higher in energy and is expect to represent only 2% of the population. The (*Z*,*E*)- and (*E*,*E*)-conformations are even higher in energy (+10.5 and +9.1 respectively). Thus, calculation explains why the ^{1}H and ^{13}C NMR spectra of **4-1** gave evidence of only one amide conformation.

The energies of the amide conformers of **4-2** follow that of **4-1**, though the energy differences are smaller. Again, the (*E*,*Z*)-conformation is predicted to be the most stable conformation, but the calculated relative free energy of (*Z*,*Z*)-**4-2** is only +1.7 kcal/mol. The predicted (*E*,*Z*)-/(*Z*,*Z*)- population ratio is 94:6. So it seems possible that amide bond isomerism could be detected in **4-2** by NMR spectoscopy.

Table 4.3. Optimized conformations of 4-1 and 4-2 and population analysis, B3LYP/6-31G(d).

Entry	Compound	Conformer	ΔG_{rel} (kcal/mol, 298 K)	N_i	N_i/N_{total}
1	**4-1**	**(*E*,*Z*)**	0.0	1.00000	0.98
2	**4-1**	**(*Z*,*Z*)**	2.3	0.02233	0.02
3	**4-1**	**(*Z*,*E*)**	10.5	0.00000	0.00
4	**4-1**	**(*E*,*E*)**	9.1	0.00000	0.00
5	**4-2**	**(*E*,*Z*)**	0.0	1.00000	0.94
6	**4-2**	**(*Z*,*Z*)**	1.7	0.06050	0.06
7	**4-2**	**(*Z*,*E*)**	5.8	0.00006	0.00
8	**4-2**	**(*E*,*E*)**	5.0	0.00022	0.00

The calculated values of the population of (*E*,*Z*)- and (*Z*,*Z*)-**4-1** represents a 0.6 kcal/mol difference in energy versus the experimentally determined value, which we consider acceptable. Computation suggests that **4-2** exists in solution as the (*E*,*Z*) and (*Z*,*Z*)-conformations (with (*E*,*Z*)

as the major conformer) and the crystal structure of **4-2** (Figure 4.11) shows the (*E*,*Z*)-conformation as well. If this is true, therefore, the signal broadening seen in Figure 4.5 and Figure 4.7 is due to interconversion between the (*E*)- and (*Z*)-isomers along the N^1-C^4 bond axis (Figure 4.15). The next task was to determine the reason for the sharp 4.88 ppm signal in the ^{1}H NMR spectrum at 250 K; is it a small N-N bond rotational barrier or some other phenomenon that could cause accidental equivalence?

Figure 4.15. Structures of predicted major conformational isomers, (*P*)-(*E*,*Z*)-4-2 and (*P*)-(*Z*,*Z*)-4-2.

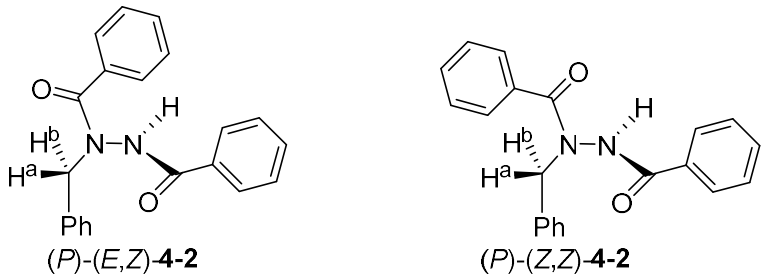

(*P*)-(*E*,*Z*)-**4-2** (*P*)-(*Z*,*Z*)-**4-2**

We propose that the presence of the sharp 4.88 ppm peak in the ^{1}H NMR spectrum of **4-2** at 250 K is due to the N-N bond rotation of the (*Z*,*Z*)-conformation. The associated rotational barrier is much smaller than for the (*E*,*Z*)-conformation due to a favorable hydrogen-bonding interaction between O^5 and H^6 over the N-N bond rotation . The (*E*,*Z*)-conformation is prevented from this, as O^5 in (*E*,*Z*)- is pointed into space, away from the rest of the molecule. This would result in a higher barrier that is easily decoalesced in comparison to (*Z*,*Z*)-. In addition, our calculations suggest that this sharp peak would be minor, as the (*Z*,*Z*)-conformation of **4-2** is higher in energy than (*E*,*Z*)- by at least 1.7 kcal/mol, which is confirmed in the 250 K ^{1}H NMR spectrum of **4-2**.

Table 4.4. Calculated energies of 1,2-diformylhydrazine isomers as a function of dihedral angle (MP2/6-31+G).[40]**

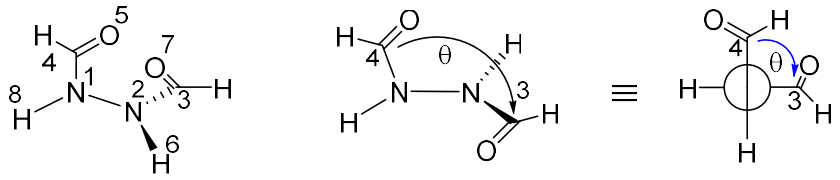

Conformation	∠$C^4N^1N^2C^3$ θ	ΔE_{rel} (kcal/mol)
(*Z*,*Z*)-	90	0.0
	0	17.0
	180	0.8
(*E*,*Z*)-	90	1.0
	0	11.8
	180	8.3
(*E*,*E*)-	90	1.3
	0	16.1
	180	13.3

Computational studies into diformylhydrazine by Reynolds and Hormann showed a lower N-N potential energy at the 180° dihedral of diformylhydrazine was (*Z*,*Z*) (0.8 kcal/mol) versus (*E*,*Z*) (10.8 kcal/mol) or (*E*,*E*) (12.0 kcal/mol). Table 4.4 shows that the constrained energy of (*Z*,*Z*)-diformylhydrazine is 7.5 kcal/mol smaller than (*E*,*Z*)-diformylhydrazine at the $C^4N^1N^2C^3$ 180° dihedral. The authors state that this must be due to a favorable hydrogen-bonding interaction between O^5 and H^6 at 180° that is possible for (*Z*,*Z*)-, but impossible for (*E*,*E*)-diformylhydrazine.[39-40] If the reason for the sharp signal for **4-2** in the ^{1}HNMR was due to the (*Z*,*Z*)-conformation allowing hydrogen-bonding at the 180° $C^4N^1N^2C^3$ dihedral, then N-N torsional barrier must be smaller than (*E*,*Z*)-. Performing a coordinate scan of the dihedral angle

θ (Figure 4.16) should reveal probable transition state structures for 4-2 and test our hydrogen-bonding hypothesis, as well as give values for the possible rotational barriers

Figure 4.16. Angle definition and possible transition structures.

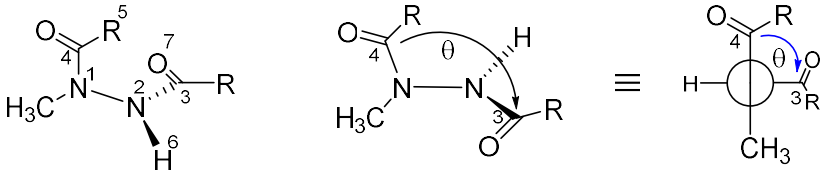

4-6: R = CH_3
4-7: R = Ph

Figure 4.17. Predicted transition state structures for diacylmethylhydrazines.

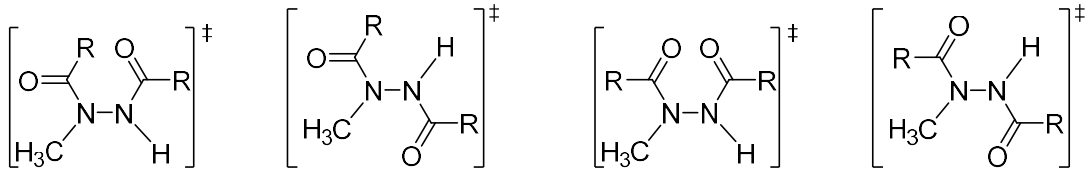

(*E*,*Z*)-θ = 0° (*E*,*Z*)-θ = 180° (*Z*,*Z*)-θ = 0° (*Z*,*Z*)-θ = 180°

As shown in Figure 4.17, two possible N-N bond rotation transition structures could be envisioned; one with the $C^4N^1N^2C^3$ dihedral angle θ near 0, and one with θ near 180. At the outset it seemed likely that the potential maxima near θ = 0° would be higher than that nearer to θ = 180°, due to increased steric repulsion. In addition, these computations would yield a distance measurement between O^5 and H^6 that would either suggest or eliminate the possibility of hydrogen-bonding as a hypothesis for barrier height. If the barrier of the (*Z*,*Z*)-isomer is comparable to the (*E*,*Z*)-isomer, then the sharp signal could then be ruled as due to accidental equivalence (whatever the cause might be).

4.3.2 Coordinate scan search for transition structure starting geometries

In computing N-N bond rotational barriers, **4-6** and **4-7** were used as model systems to shorten computing time. Use of a methyl group in place of benzyl would eliminate conformational complexity about the N^1-CH_2Ph bond and allow focus on the positions of the acyl groups. Geometry optimization of the four amide conformational isomers of **4-2** revealed (Figure 4.18) that the phenyl ring of the benzyl group was normally pointed into space away from the rest of the molecule, and thus, should not impact the N^1-N^2 rotational barrier.

Figure 4.18. Benzyl group position in the various amide bond conformers of 4-2 (B3LYP/6-31G(d)).

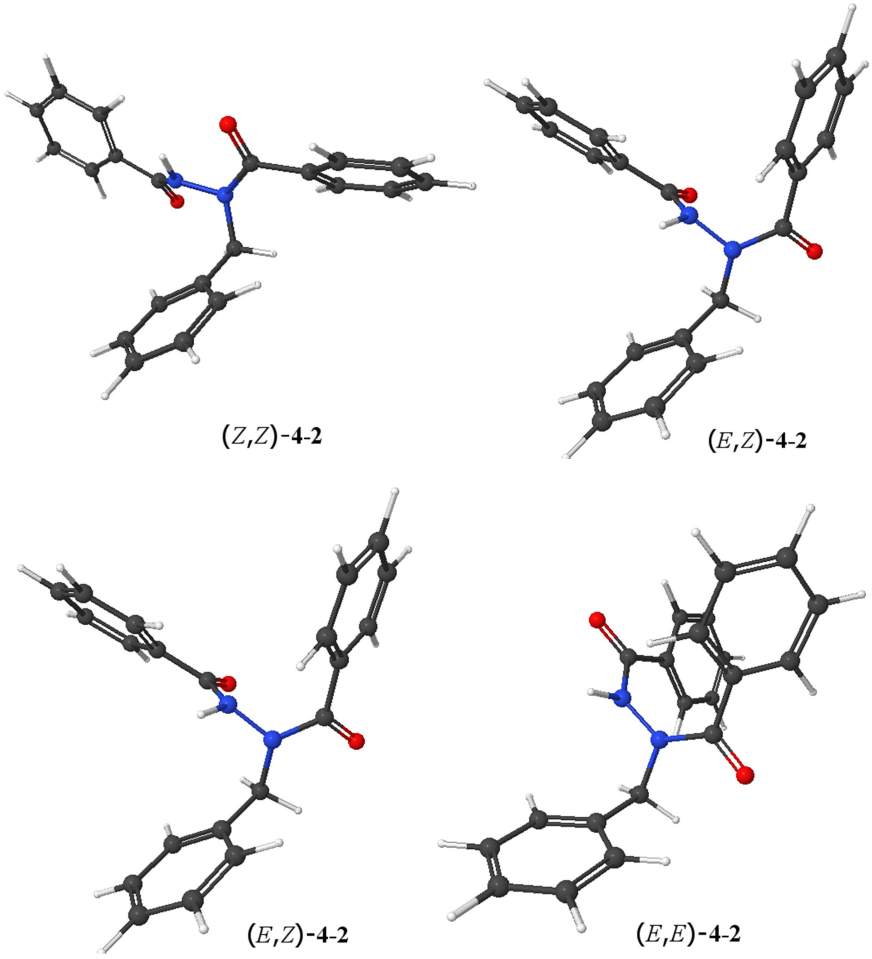

To search for starting geometries for transition state optimization, coordinate scans were performed by scanning the dihedral angle θ in the (*Z*,*Z*) and (*E*,*Z*) isomers in the clockwise (-180° to +180°) and anticlockwise (+180° to -180°) directions in 10° increments, optimizing the geometry with this fixed dihedral angle, and measuring the energy of the structure at each increment. The presence of the chiral axis could also yield asymmetric curves from clockwise and anticlockwise rotations.[147]

Figure 4.19. Coordinate scan of θ for (*Z*,*Z*)-4-6, at B3LYP/6-31G(d).

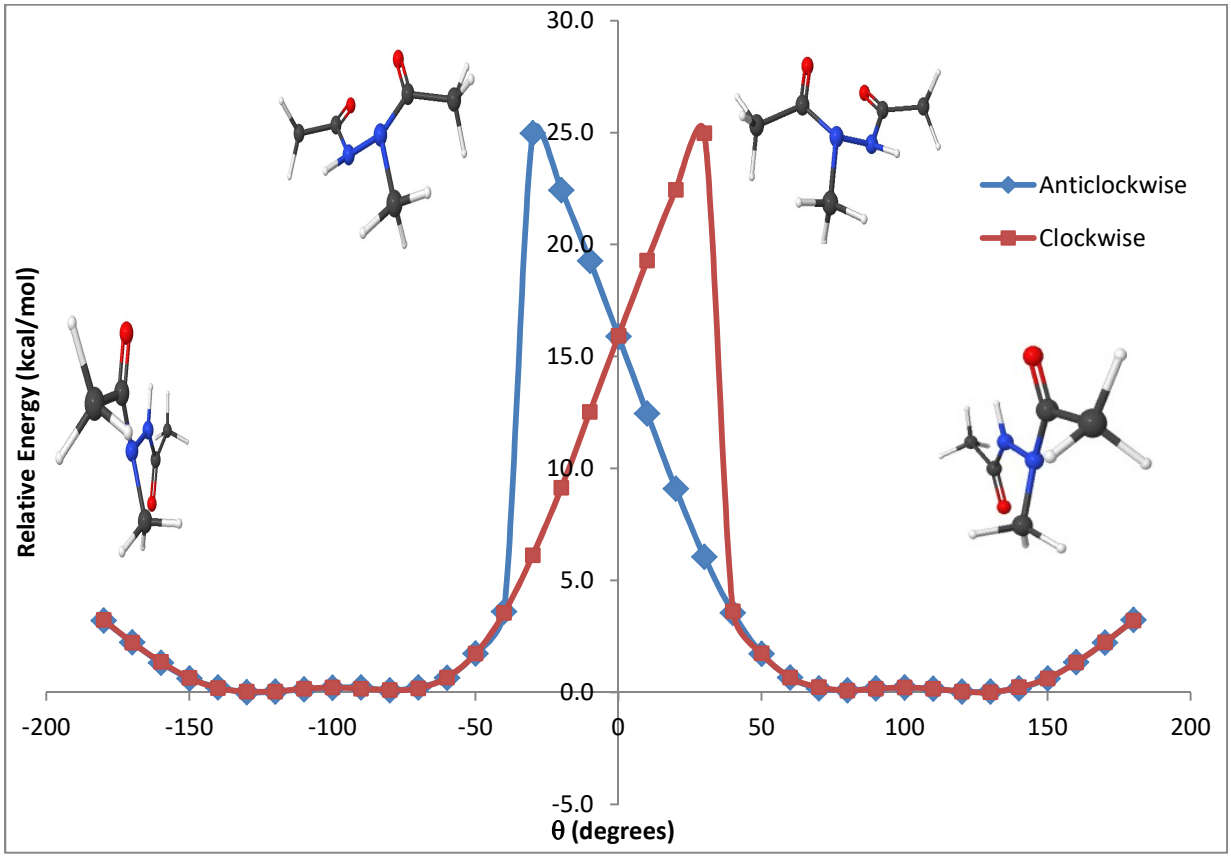

Figure 4.20. Coordinate scan of θ for (*E*,*Z*)-4-6, B3LYP 6-31G(d).

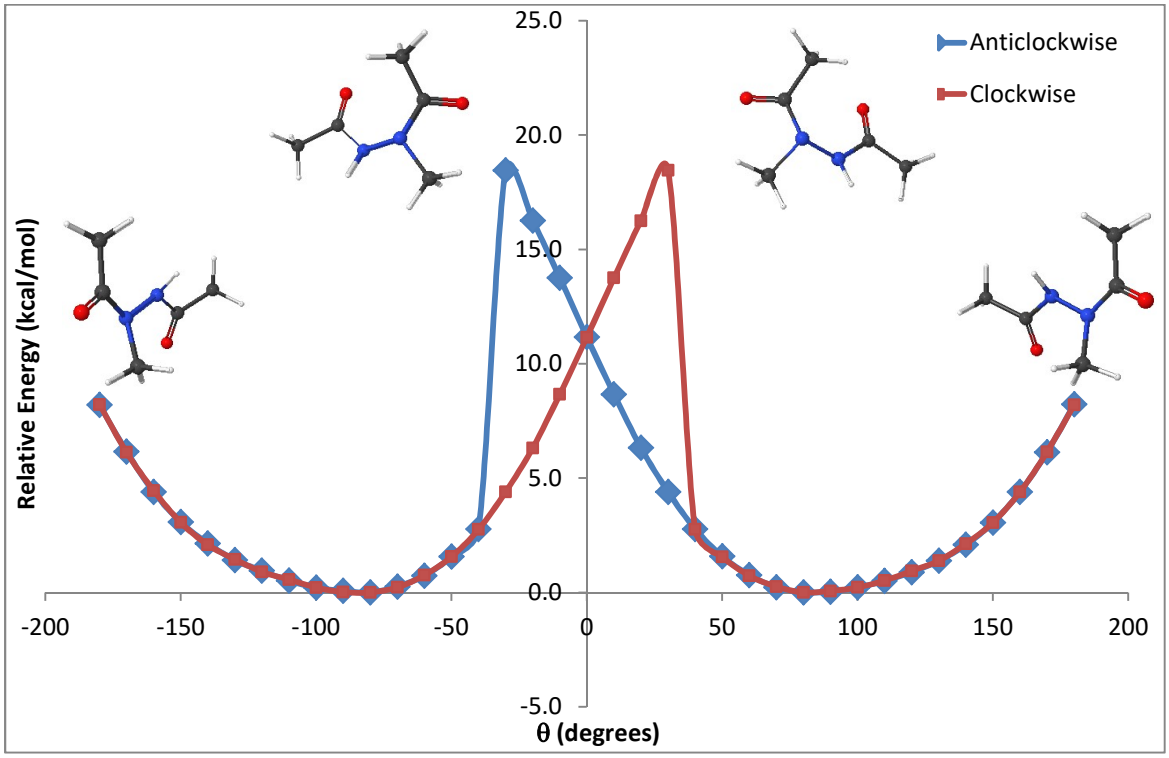

Several features of these plots are notable. First, as expected, Figures 4.19 and 4.20 show the energy of the potential maximum near θ = 0° was considerably higher than the maximum near θ = 180°, most likely due to steric effects. Second, the potential energy maxima for the coordinate scans of (*Z*,*Z*)-**4-6** and (*E*,*Z*)- **4-6** does not occur at exactly θ = 0°; rather there are two enantiomeric maxima at -30° and +30°. Similarly, the low energy potential maximum occurs as a second pair of enantiomeric maxima at –180° and +180° with structures that are not C_s symmetric. The enantiomerization of axially chiral compounds via enantiomeric transition structures such as (*M*)-**4-9*** (rather than through a C_s-symmetric, achiral transition state) has been observed by the Carlier group for a number of benzodiazepines, with an example shown in Figure 4.21.[148]

Figure 4.21. Benzodiazepine 4-9 enantiomerization through the chiral transition state (M)-4-9*.[148]

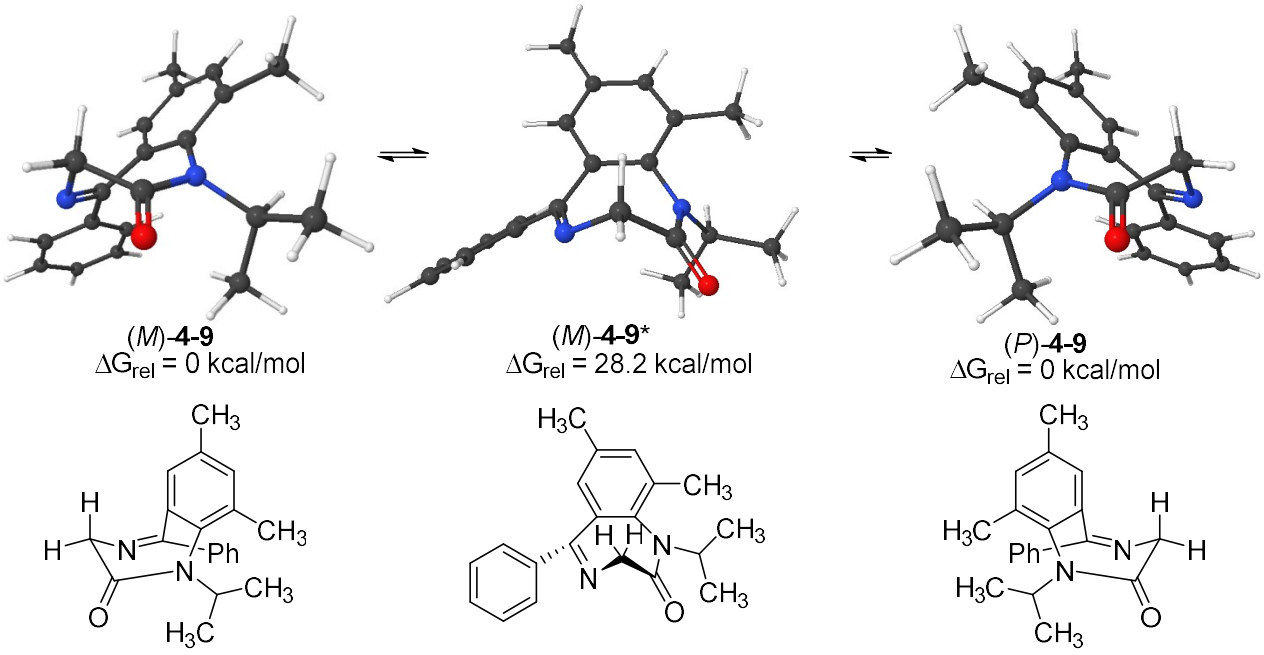

The curves for **4-6** show (*Z*,*Z*)**-4-6** with a barrier near 180° of 3.2 kcal/mol (Figure 4.19), while (*E*,*Z*)**-4-6** possesses a much higher barrier of 8.2 kcal/mol (Figure 4.20). The barriers at -30° and +30° for (*Z*,*Z*)**-4-6** were 25.0 kcal/mol, and somewhat lower for (*E*,*Z*)**-4-6** at 18.5 kcal/mol. The large barriers near +30° and -30° drop off precipitously in each case, indicating that something different than simple rotation is occurring here, such as inversion of N^1. This phenomenon was witnessed by Carlier and co-workers in an earlier study of bond rotation in N-methyl tacrine hydrochloride.[147] Figure 4.22 shows these asymmetric curves, with the large drops in energy attributed to pyramidalization and subsequent inversion of N^2 in protonated N-methyl tacrine.[147]

Figure 4.22. Coordinate scan of the dihedral angle (C^1-N^2-C^3-C^4) of protonated N-methyl tacrine.[147]

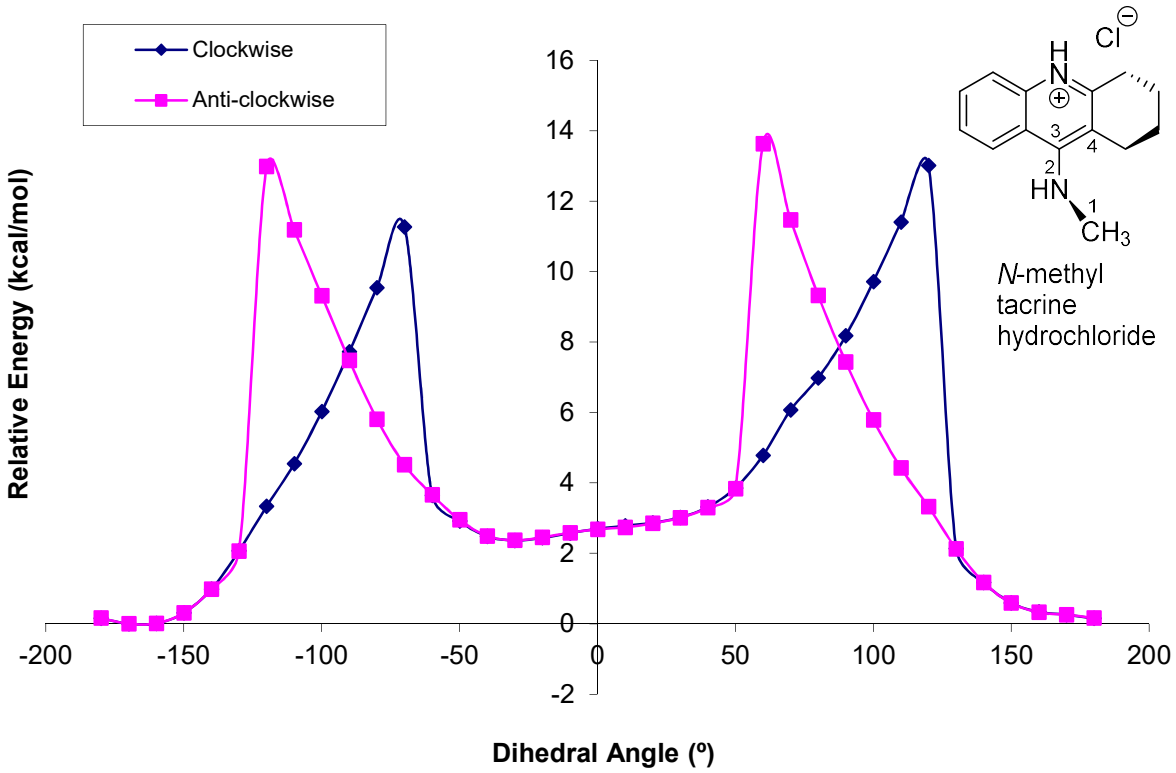

In the tacrine study (Figure 4.22), structures in the ranges θ = 60° to 130° (and θ = -60 to -130 °) featured differences in the sense of pyramidalization of the exocyclic nitrogen, depending on whether the structures were generated by clockwise or anticlockwise rotations. Thus it seemed likely that the different energies of (*Z*,*Z*)-**4-6** at θ = - 30° obtained from clockwise and anticlockwise rotation might be due to pyramidalization at N^1 and N^2. As shown in Figure 4.23, this is indeed the case, as pyramidalization is most likely relieving strain associated with close proximity of the carbonyl oxygens.

Figure 4.23. Pyramidalization of (*Z*,*Z*)-4-6 in the anticlockwise rotation going from θ = - 30° to θ = - 40° (N^1 is in front).

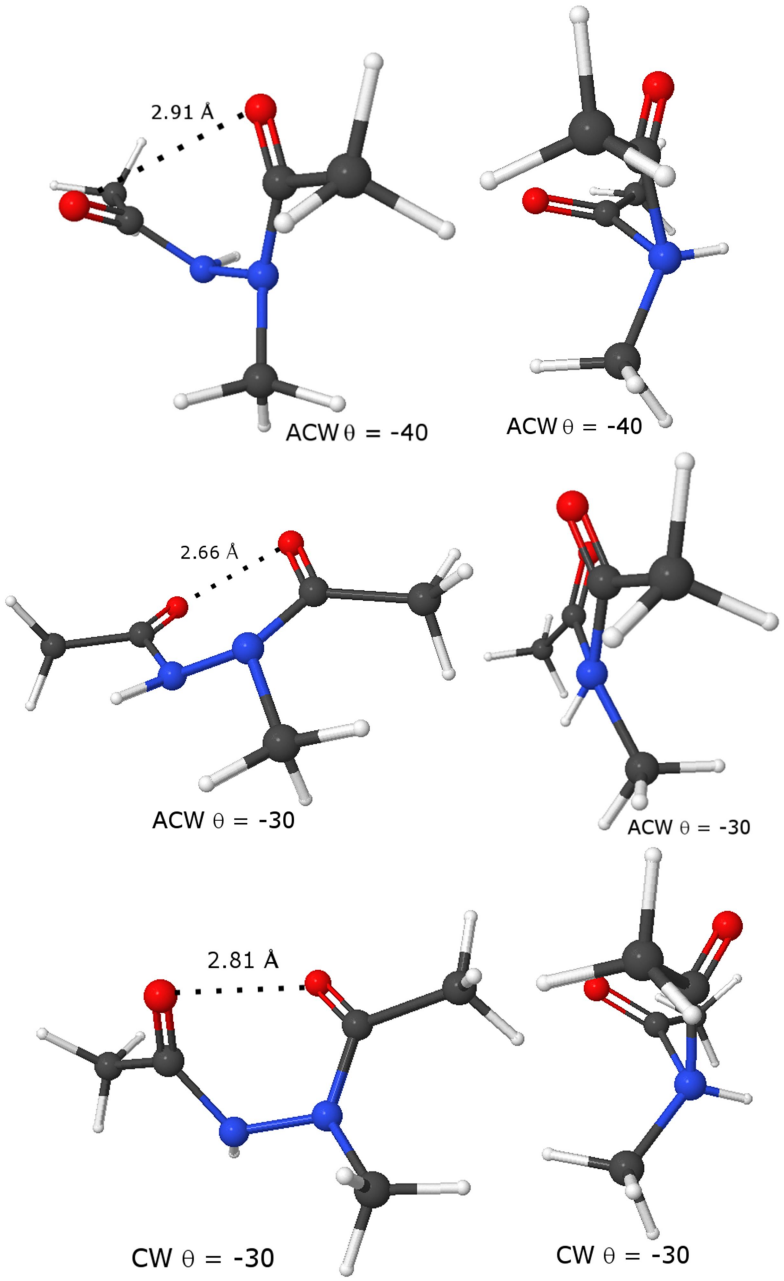

A prudent question to ask in the wake of the computed curves in Figures 4.19 and 4.20 is: why are the energies of **4-6** at a given dihedral angle θ different when rotating clockwise (CW)

or anticlockwise (ACW)? To answer this, we examined the distance of O^5-O^7 in (*Z*,*Z*)-**4-6** and C^9-O^7 in (*E*,*Z*)-**4-6** and attempted to see their correlation to relative energy. For brevity, we examined the 0° to -60° range in Tables 4.5 and 4.6 with data from Figures 4.19 and 4.20 respectively.

Table 4.5. Correlation of the O^5-O^7 distance parameter and relative energy in CW and ACW rotations of (*Z*,*Z*)-4-6 from 0° to -60° (B3LYP/6-31G(d)).

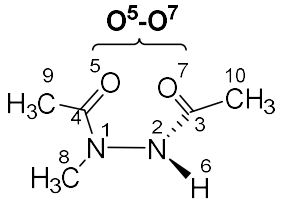

(*Z*,*Z*)-**4-6**

Dihedral angle (°)	ΔE_{CW} (kcal/mol)	$(O^5\text{-}O^7)_{CW}$ (Å)	ΔE_{ACW} (kcal/mol)	$(O^5\text{-}O^7)_{ACW}$ (Å)	$\Delta\Delta E^a$ (kcal/mol)	$\Delta(O^5\text{-}O^7)^b$ (Å)
0	15.9	2.66	15.9	2.66	0.0	0.00
-10	12.5	2.69	19.3	2.64	6.7	-0.05
-20	9.1	2.74	22.4	2.64	13.3	-0.10
-30	6.1	2.81	25.0	2.66	18.9	-0.15
-40	3.5	2.91	3.6	2.91	0.1	0.00
-50	1.7	3.03	1.7	3.03	0.0	0.00
-60	0.7	3.20	0.6	3.20	0.0	0.00

a) $\Delta\Delta E = \Delta E_{ACW} - \Delta E_{CW}$. b) $\Delta(O^5\text{-}O^7) = (O^5\text{-}O^7)_{ACW} - (O^5\text{-}O^7)_{CW}$.

What we found was a negative, linear relationship between relative distance (ΔO^5-O^7 and ΔC^9-O^7) relative energy ($\Delta\Delta E$) from 0° to -30°. Looking at Table 4.5, both since the CW and ACW curves overlap at 0°, the relative energies (+15.9 kcal/mol) at this dihedral angle are identical. The O^5-O^7 distance of 2.66 Å is well within the sum of the van der Waals radii of 3.04 Å and thus repulsive non-bonded contact of these atoms likely is a major determinant of the high potential energy. In the CW curve, the relative energy decreases uniformly from 0 to -60°; the concurrent increase in the O^5-O^7 bond distance suggests relief of O^5-O^7 non-bonded interactions

lowers the energy. However, in the ACW curve, energies increase from 0 to -30°. The fact that the O^5-O^7 distance remains between 2.66 and 2.64 Å over this range suggests O^5-O^7 steric compression has reached an unsurmountable limit. Whatever is driving the increase in energy in the ACW curve from 0 to -30°, the large energy difference between the CW -30° and ACW -30° structures ($\Delta\Delta E$ =18.9 kcal/mol!) is accompanied by a large difference in the O^5-O^7 distance ($\Delta(O^5\text{-}O^7)$ = 0.15 Å). Therefore, different *N*-pyramidalization in the CW -30° affords a dramatically lower energy because it significantly increases the O^5-O^7 distance.

These same phenomena are found in Table 4.6 for (*E*,*Z*)-**4-6**, with the C^9-O^7 distance being similarly predictive of higher energy structures between 0° and -30° for the ACW rotation than that of the CW rotation. The $\Delta\Delta E$ value for (*E*,*Z*)-**4-6** is less than that of (*Z*,*Z*)-**4-6** (14.1 kcal/mol versus 18.9 kcal/mol respectively) and is likely the result of less electron-electron repulsion between C^9-O^7 that was present in O^5-O^7.

Table 4.6. Correlation of the C^9-O^7 distance parameter and relative energy in CW and ACW rotations of (*E*,*Z*)-4-7 from 0° to -60° (B3LYP/6-31G(d)).

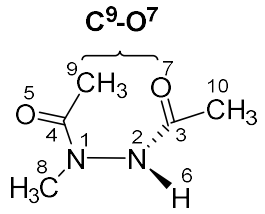

(*E*,*Z*)-**4-6**

Dihedral angle (°)	ΔE_{CW} (kcal/mol)	$(C^9\text{-}O^7)_{CW}$ (Å)	ΔE_{ACW} (kcal/mol)	$(C^9\text{-}O^7)_{ACW}$ (Å)	$\Delta\Delta E^a$ (kcal/mol)	$\Delta(C^9\text{-}O^7)^b$ (Å)
0	11.2	2.79	11.2	2.79	0.0	0.00
-10	8.7	2.83	13.8	2.77	5.1	-0.06
-20	6.3	2.88	16.3	2.76	9.9	-0.12
-30	4.4	2.94	18.5	2.76	14.1	-0.18
-40	2.8	3.03	2.8	3.03	0.0	0.00
-50	1.6	3.12	1.6	3.12	0.0	0.00
-60	0.8	3.22	0.7	3.22	0.0	0.00

a) $\Delta\Delta E = \Delta E_{ACW} - \Delta E_{CW}$. b) $\Delta(C^9\text{-}O^7) = (C^9\text{-}O^7)_{ACW} - (C^9\text{-}O^7)_{CW}$.

The curves of the coordinate scans for **4-7** were similar to that of **4-6**, but more complex. Figures 4.24 and 4.25 highlight the asymmetry of the two curves across the y-axis, showing the utility exploring the clockwise and anticlockwise rotations. The energy maxima around -180° and +180° reveal that they are not the same, as is the case with the minima, particularly in the case of (*E*,*Z*)-**4-7** (Figure 4.25). Maxima in Figure 4.24 appeared at -170° in the anticlockwise rotation and +170° for the clockwise rotation, with a barrier value of 5.8 kcal/mol. As was the case for **4-6**, the barriers near 180° were smaller than the barriers near 0° and thus will be more likely representative of the NMR observed rotation barriers. (*Z*,*Z*)-**4-7** barriers near 0° appeared at -20° and +20° with a value of 24.6 kcal/mol and showed the same precipitous drop as seen in **4-7**. Structures were provided for the higher energy of the two 180° barriers in Figure 4.25, as the nitrogen inversion near 0° causes (*E*,*Z*)-**4-7** to isomerize to (*Z*,*Z*)-**4-7**. We suspect that the slight

differences in the orientation of the benzoyl phenyl rings of (*E*,*Z*)-**4-7** , combined with this isomerization to (*Z*,*Z*)-**4-7** were the reasons the CW and ACW curves are not mirror images.

Figure 4.24. Coordinate scan of θ for (*Z*,*Z*)-4-7, B3LYP 6-31G(d).

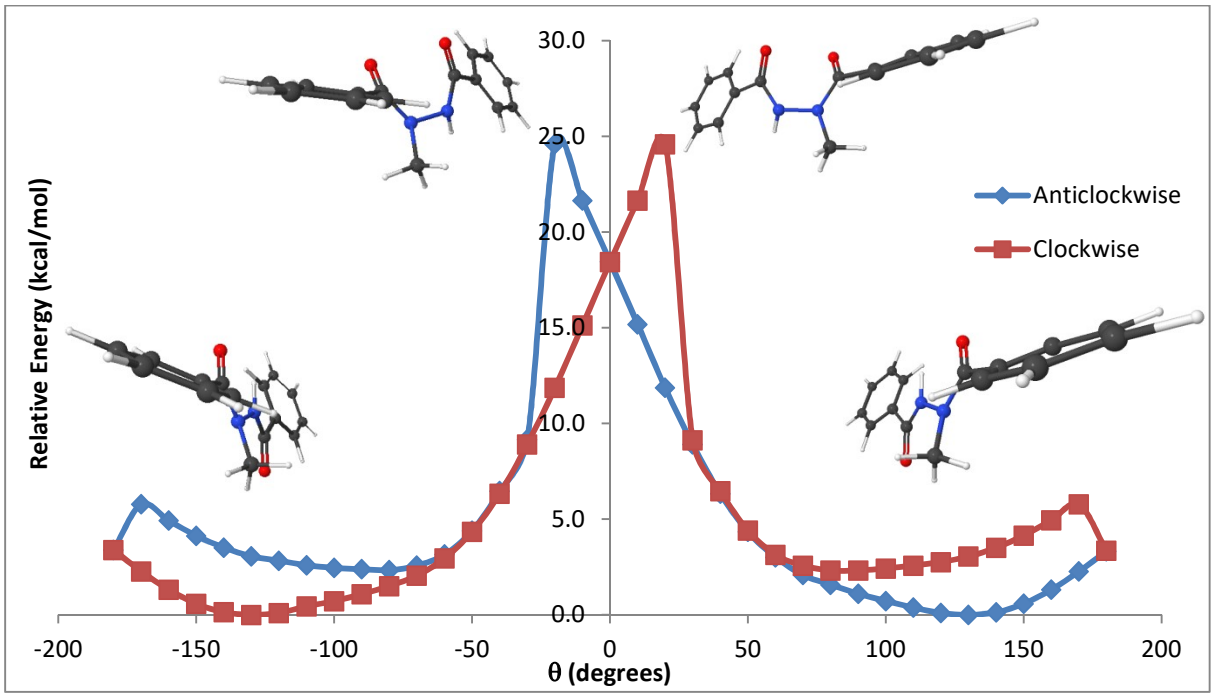

Figure 4.25. Coordinate scan of θ for (*E*,*Z*)-4-7, B3LYP 6-31G(d).

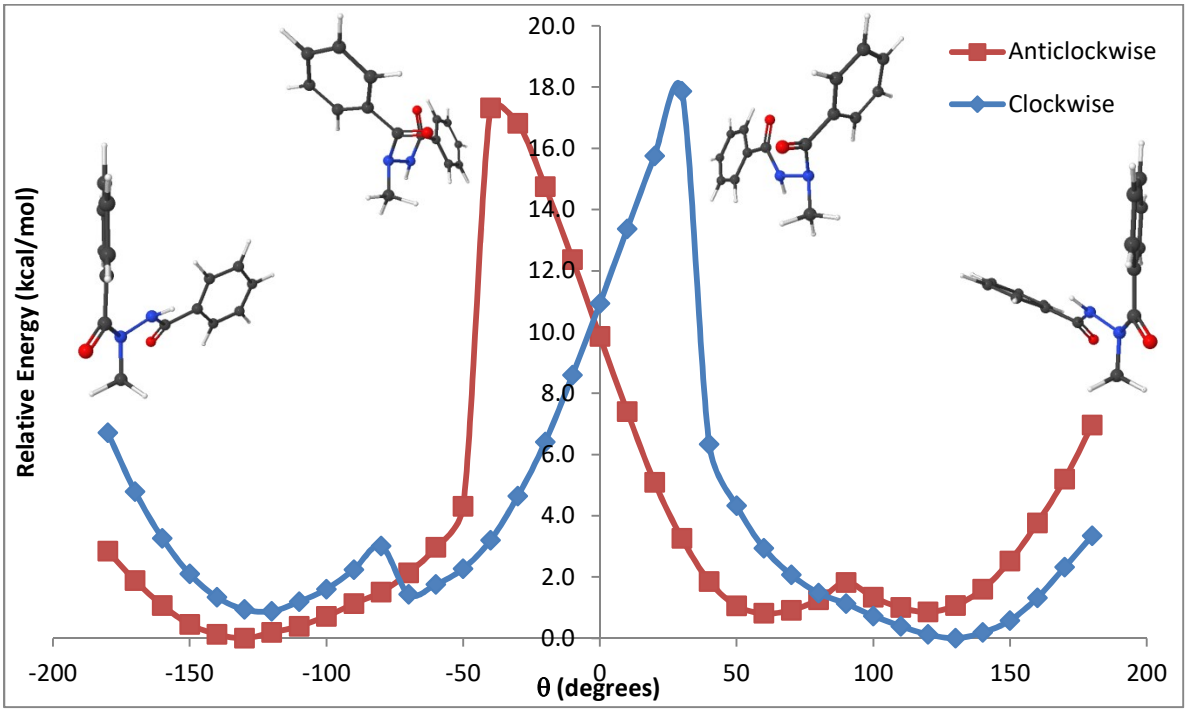

4.3.3 Transition structure analysis and interpretation of N-N bond rotation in (*E*,*Z*)- and (*Z*,*Z*)-4-6 and 4-7

The highest energy structures for **4-6** and **4-7** generated in the coordinate scans of θ were used as starting geometries in calculating N^1-N^2 bond rotation transition structures. These transition structures were calculated using the B3LYP functional with a 6-31G(d) basis set and were not constrained optimizations, but allowed full movement on all parameters. N-N bond rotation transition structures were verified by two criteria: they possessed a single imaginary vibrational frequency, and that the vibration showed a rocking movement of the groups around the N^1-N^2 bond, resembling a very short sweep of θ. Once the free energies of formation for each transition structure were known, they provided three pieces of information. The first was an estimate of the free energy barrier of rotation to compare to the experimentally determined values. The second was to imply a set of probable conformers that could give rise to each of the

benzylic proton signals seen in Figure 4.5. The third is the O^5-H^6 distance for (*Z*,*Z*)-**4-6** and (*Z*,*Z*)-**4-7** isomers to evaluate if internal hydrogen-bonding is occurring and thus could provide an explanation of the sharp signal at 4.88 ppm in Figure 4.5. A survey of the Cambridge Crystallographic Database by Bilton et al, showed that for NH---O hydrogen-bonding, the most common distances fell between 1.9-2.6 Å and had an OHN angle of >75°.[146] Table 4.7 for **4-6** and Table 4.8 for **4-7** show the results, with the dihedral angle θ, ΔG_{rel} of each species with respect to the lowest energy ground state conformer, O^5-H^6 distance in Å, and the OHN angle for each species with an O^5-H^6 distance between 1.9 and 2.6 Å. Figures 4.26 and 4.27 contain the structure results of the transition state calculations in Table 4.7 in a graphical representation of dihedral angle versus energy for the (*E*)/(*Z*)-isomer outlined. We located the enantiomeric transition structures for each conformation, and obtained the same ΔG_{rel} at a given dihedral angle. They have been omitted for brevity.

Table 4.7. Transition state and ground-state geometries and accompanying relative free energies of 4-6 at B3LYP/6-31G(d) at 298 K.

Entry	Amide Geometry	Starting Dihedral θ	Final dihedral θ	# of imaginary frequencies	ΔG_{rel} (kcal/mol)	O^5-H^6 (Å)	OHN angle Φ
1	(*Z*,*Z*)	-30.0	-20.8	1	25.9	3.84	-
2	(*Z*,*Z*)	-170.0	-180.0	1	6.0	1.98	111.92
3	(*E*,*Z*)	-30.0	-16.3	1	19.4	4.22	-
4	(*E*,*Z*)	-170.0	-177.6	1	12.5	3.73	-
5	(*E*,*Z*)	-90.0	-84.0	0	0.0	3.17	-
6	(*Z*,*Z*)	-90.0	-127.5	0	1.0	2.11	106.43
7	(*Z*,*E*)	-90.0	-77.0	0	2.9	2.78	-
8	(*E*,*E*)	-90.0	-111.5	0	0.7	4.05	-

Figure 4.26. Calculated transition state structures of (*Z*,*Z*)-4-6, B3LYP 6-31G(d).

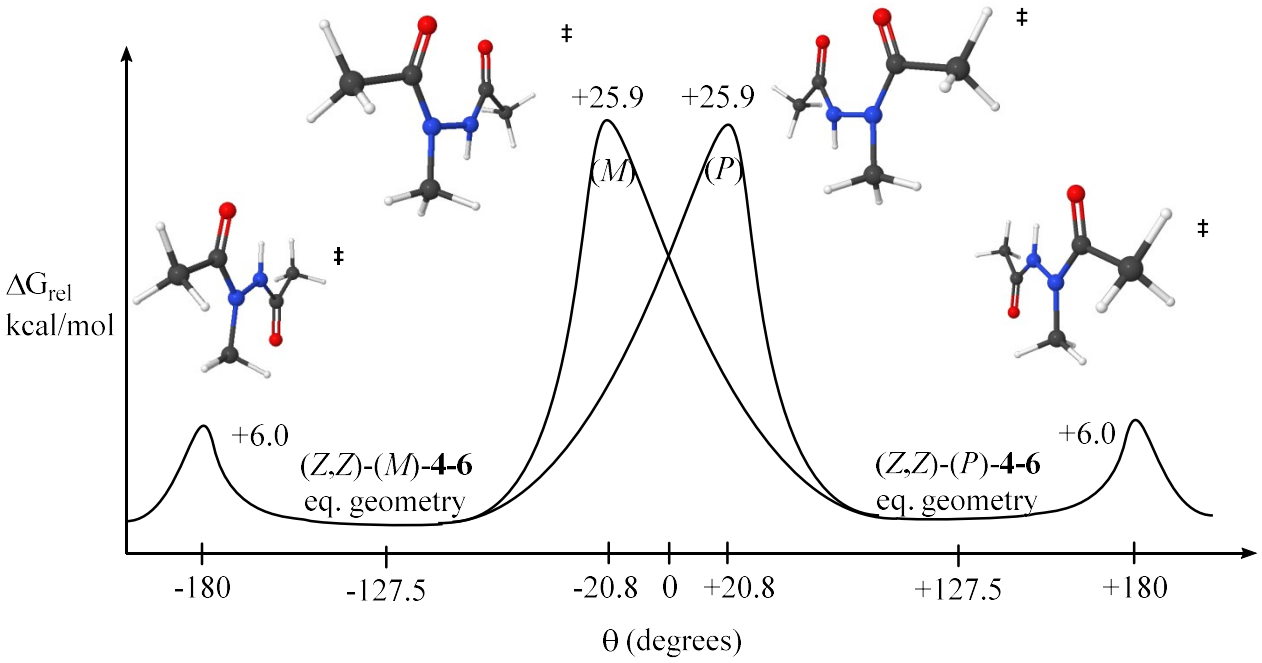

Figure 4.27. Calculated transition state structures of (*E*,*Z*)-4-6, B3LYP 6-31G(d).

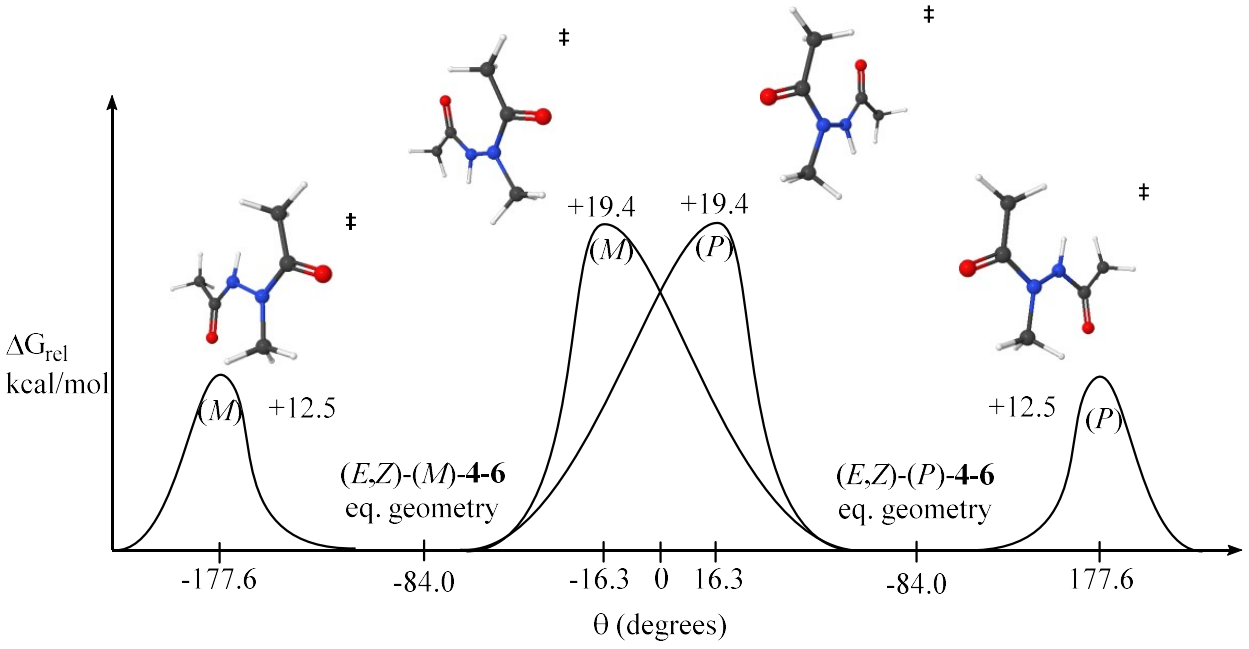

In Table 4.7, the data for the (*Z*,*Z*)-**4-6** and (*E*,*Z*)-**4-6** unconstrained transition structures versus their optimized geometries show some key pieces of information. First, the observation from the coordinate scans that the enantiomeric energy barriers near 180° are much smaller than the barriers near 0° is corroborated by the calculated transition structures and matches the description from the literature (see Table 4.4).[40] Next, (*Z*,*Z*)-isomer transition structure at -14.7° in Entry 1 of Table 4.7 has a much higher relative free energy (+6.4 kcal/mol higher) than the corresponding transition structure for the (*E*,*Z*)-isomer at -35.5° in Entry 3. This is likely due to repulsion of the lone pair electrons of carbonyl oxygens O^5 and O^7 being quite unfavorable compared to the lower repulsion of the methyl group and O^7 in the case of (*E*,*Z*). Concomitantly, the (*Z*,*Z*)-conformer transition structure in Entry 2 near 180° is nearly 6.5 kcal/mol lower than that of (*E*,*Z*)- (Entry 4), with an O^5-H^6 distance of 1.98 Å and OHN angles >75°, which fits the Bilton et al, description of intramolecular hydrogen-bonding.[146] While there is no particular rotational direction implied in Figures 4.26 and 4.27, they do indicate that the most likely path of interconversion of (*M*) and (*P*) is through the smaller barrier near 180°.

Table 4.8. Transition state and ground-state geometries and relative free energies for 4-7 at B3LYP/6-31G(d) at 298 K.

Entry	Amide Geometry	Starting Dihedral θ	Final dihedral θ	# of imaginary frequencies	ΔG_{rel} (kcal/mol)	O^5-H^6 (Å)	OHN angle Φ
1	(*Z*,*Z*)	-20.0	-14.7	1	24.3	3.86	-
2	(*Z*,*Z*)	-160.0	-162.5	1	5.7	1.97	112.4
3	(*E*,*Z*)	-35.5	-35.5	1	18.2	3.96	-
4	(*E*,*Z*)	-170.0	-165.0	1	10.5	3.69	-
5	(*E*,*Z*)	90.0	75.9	0	0.3	4.24	-
6	(*Z*,*Z*)	90.0	130.9	0	0.0	2.07	107.2
7	(*Z*,*E*)	90.0	75.8	0	4.1	2.57	82.4
8	(*E*,*E*)	90.0	110.0	0	4.7	4.18	-

Figure 4.28. Calculated transition state structures of (*Z*,*Z*)-4-7, B3LYP 6-31G(d).

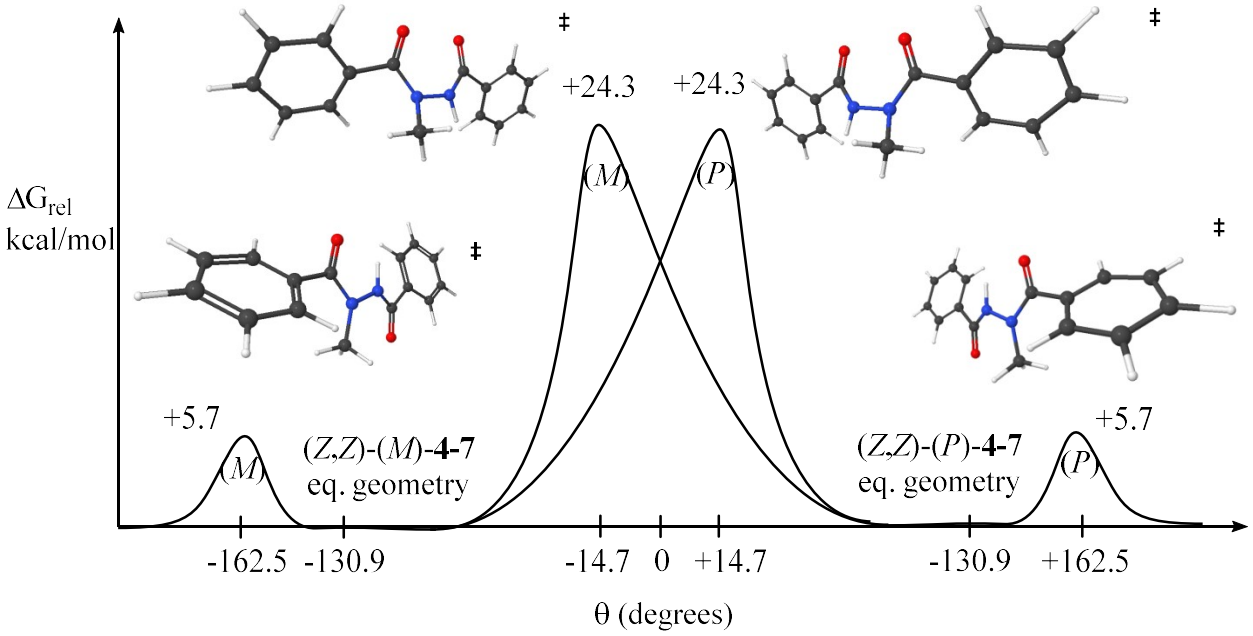

Figure 4.29. Calculated transition state structures of (*E*,*Z*)-4-7, B3LYP 6-31G(d).

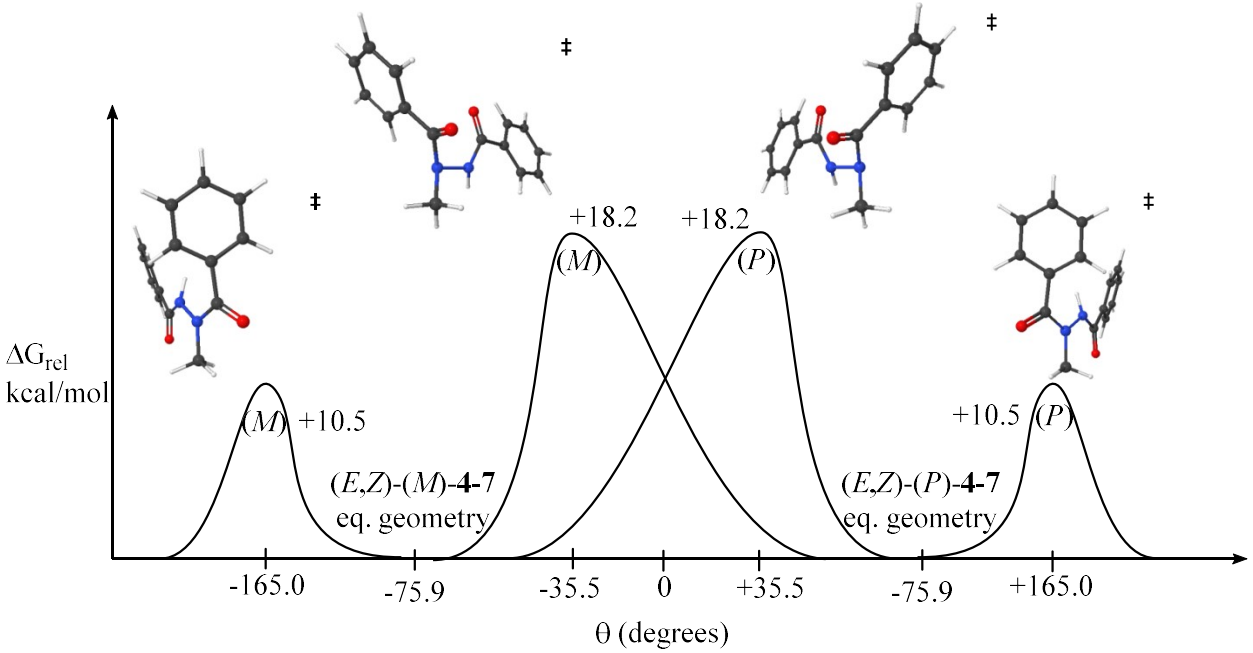

Table 4.8's data concerning **4-7** shows much of the same trends as Table 4.7. The coordinate scan data is corroborated by located unconstrained transition structures; (*Z*,*Z*)-**4-7** once again shows a higher barrier at near 0° (Entry 1) than (*E*,*Z*)-**4-7** (Entry 3) but a lower energy barrier at near 180° (compare Entry 2 and 4). The difference in energy between the (*E*,*Z*)- and (*Z*,*Z*)-isomers are closer near 180° (+4.6 kcal/mol) for **4-7** than for **4-6**, but still significantly different. The O^5-H^6 distance in Entry 2 of Table 4.8 is nearly the same value as the distance in Table 4.7, and thus, hydrogen-bonding is likely the reason for the large difference in energy between (*Z*,*Z)*-**4-7** and (*E*,*Z*)-**4-7** for their near-180° transition structures. The barrier for (*E*,*Z*)-**4-7** is 1.8 kcal/mol less than the NMR determined free energy barrier of 12.3 kcal/mol for **4-2**. The most realistic estimation of the barrier determined by NMR would predictably come from the lowest energy transition structures, which we see here. To estimate the coalescence temperature for **4-2** in the (*Z*,*Z*)-conformation, Equations 4.1 and 4.2 can be utilized with two assumptions: the (*Z*,*Z*)-**4-7** free energy barrier of rotation in Table 4.8, Entry 2 is the actual barrier for (*Z*,*Z*)-**4-2** ($\Delta G^{\ddagger}$ = 5.7 kcal/mol), and ν_{AB} has a value of 849.8 Hz (just as it was for (*E*,*Z*)-**4-2**). After iteration of the value of *T*, the coalescence temperature for (*Z*,*Z*)-**4-2** is estimated to be 135 K. If the estimate is close, that means that (*Z*,*Z*)-**4-2** would appear as a sharp singlet due to rapid rotation at 250 K or 218 K, which is precisely what is observed in the NMR spectra of Figure 4.4. After computational analysis, we conclude that the sharp 4.88 ppm signal seen for **4-2** is in fact its (*Z*,*Z*)-isomer, with the barrier being much smaller than the easily decoalesced (*E*,*Z*)-isomer, with internal hydrogen bonding between O^5 and H^6 lowering the barrier of rotation for (*Z*,*Z*)-**4-2** relative to (*E*,*Z*)-**4-2**.

With the context of our computational analysis suggesting the identity of the conformations seen in via NMR, we can also attempt to estimate the barrier to rotation of

(*E*,*Z*)/(*Z*,*Z*) interconversion in **4-2** (Figure 4.30) using the same methodology as previously demonstrated. It should be possible to calculate using the Δδ to estimate the midpoint of the decoalesced (*E*,*Z*)-**4-2** benzylic proton peaks, and then use the Δν between the (*E*,*Z*)-**4-2** signal and the (*Z*,*Z*)-**4-2** signal (Figure 4.31) to calculate the rate constant (k_{iso}) and thus, isomerization free energy barrier using Equations 4.2 and 4.4.

Equation 4.4. Calculation of the first-order rate constant for two nuclei at coalescence.[144]

$$k = \frac{\pi \Delta v}{\sqrt{2}}$$

Figure 4.30. Free energy of isomerization between (*E*,*Z*)-4-2 and (*Z*,*Z*)-4-2.

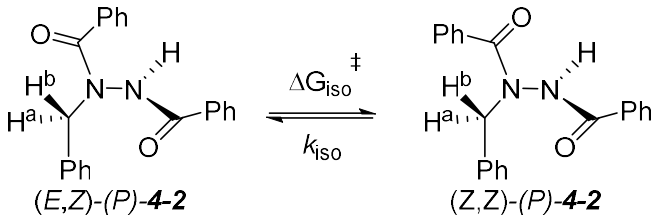

(*E*,*Z*)-*(P)*-***4-2*** (Z,Z)-*(P)*-***4-2***

Figure 4.31. ^{1}H NMR coalescence measurements of 4-2 (E,Z)/(Z,Z) barrier to isomerization.

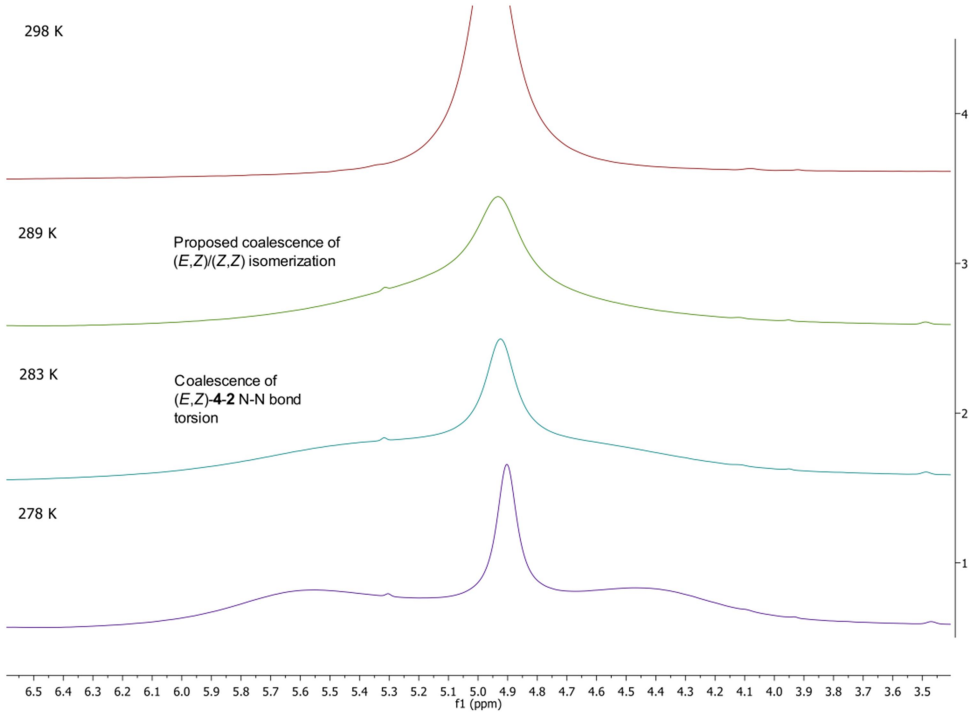

With our assumptions above, we measured Δν to be 51.9 Hz, and T_c to be 289 K. We calculate that k_{iso} = 115.3 s^{-1} and thus, the free energy barrier of isomerization was estimated to be 14.2 ± 0.2 kcal/mol, based on an error in T_c of ± 3 K.

4.4 Conclusion

A combination of NMR spectroscopy, X-ray crystallography, and computational modeling was used to deduce the probable conformations of diacylbenzylhydrazines in solution. These analysis techniques allowed spectroscopic identification and quantification of these conformational isomers within acceptable error. In addition, exploration of the conformer transition structures of model compounds **4-6** and **4-7** support the hypothesis that the (*Z*,*Z*)-conformation barrier is lower than the (*E*,*Z*)-conformation due to favorable interaction between

O^5 and H^6, and properly predicts observed NMR behavior. This analysis could give clues as to why certain compounds in a library of diacylhydrazines may possess more or less activity if that activity is a function of the population of (*E*,*Z*)- or (*Z*,*Z*)-conformations.[40, 126, 149] Such information could guide synthetic decision-making toward certain acyl groups or to constrained structures in pursuit of these conformational features for medicinal chemistry ends in future investigations of these systems.

Chapter 5. Experimental

Compounds were purchased from Sigma-Aldrich and were used without purification, unless otherwise noted. ^{1}H NMR spectra were recorded at 400 MHz; the corresponding ^{19}F and ^{13}C NMR resonant frequencies were 376 MHz and 101 MHz respectively. ^{19}F NMR regioselectivity experiments were performed in standard NMR tubes flushed with nitrogen, with the cap wrapped with parafilm; details are provided below. The solvent and internal standard for ^{1}H and ^{13}C NMR spectroscopy were $CDCl_3$ with TMS, and $CDCl_3$ with C_6F_6 (-164.90 ppm) for ^{19}F NMR spectroscopy. Due to solubility considerations, NMR analyses of hydrazine hydrochloride salts were typically performed in DMSO-d_6. Note that ^{19}F NMR spectra of these compounds could be obtained in $CDCl_3$ with added triethylamine. Preparative reactions were carried out in inert atmosphere under N_2 using standard techniques and oven-dried glassware unless otherwise specified. X-ray crystal structures are contained within .cif files that are available upon request. All computational chemistry calculations were carried out using Gaussian09 through the WebMO interface, with xyz coordinates are available below for each structure of interest (equilibrium geometries and transition states). Crystal structure data is available upon request and will be submitted to the Cambridge Crystallographic Data Centre.

5.1 Synthesis methodologies

Figure 5.1. Product Legend for all compounds synthesized in Chapters 2 and 3.

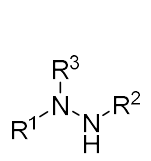

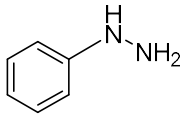

2Aa

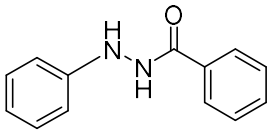

2Ba

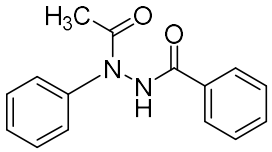

2Bj

1; R^1 = benzyl
2; R^1 = Ph
3; R^1 = 4-fluorophenyl
4; R^1 = 4-methoxyphenyl
5; R^1 = 4-bromophenyl
6; R^1 = *t*-Bu

A; R^2 = H
B; R^2 = benzoyl
C; R^2 = 4-methylbenzoyl
D; R^2 = 4-fluorobenzoyl
E; R^2 = 4-methoxybenzoyl
F; R^2 = 4-chlorobenzoyl
G; R^2 = 2-bromobenzoyl
H; R^2 = 2-fluorobenzoyl
I; R^2 = cyclopropanecarbonyl
J; R^2 = acetyl
K; R^2 = trimethylacetyl
L; R^2 = dimethylacetyl
M; R^2 = phenylacetyl
N; R^2 = nicotinoyl
O; R^2 = isonicotinoyl
P; R^2 = Boc

a; R^3 = H
b; R^3 = Benzoyl
c; R^3 = 4-methylbenzoyl
d; R^3 = 4-fluorobenzoyl
e; R^3 = 4-methoxybenzoyl
f; R^3 = 4-chlorobenzoyl
g; R^3 = 2-bromobenzoyl
h; R^3 = 2-fluorobenzoyl
i; R^3 = cyclopropanecarbonyl
j; R^3 = acetyl
k; R^3 = trimethylacetyl
l; R^3 = dimethylacetyl
m; R^3 = phenylacetyl
n; R^3 = nicotinoyl
o; R^3 = isonicotinoyl
p; R^3 = Boc
q; R^3 = trifluoroacetyl
r; R^3 = propanoyl
s; R^3 = isovaleryl
t; R^3 = methyl carboxylate

Method A. Monoacylhydrazine was added to a round bottom flask with magnetic stirrer and 5 mL of dichloromethane, and stirred. Triethylamine (2.0 equiv.) was then added, followed by an acid chloride (1.0 equiv.) which was then added dropwise (in the case of solid acid chlorides, a solution in 1 mL of dichloromethane was used), and the solution was allowed to stir for 2-4 hours. Water (10 mL) was then added, and the crude mixture was extracted with ethyl acetate (3

x 10 mL). After subsequent drying over Na_2SO_4, the solution was concentrated in vacuo and then purified by silica chromatography, or by recrystallization from ethyl acetate:hexane.

Method B. Benzylhydrazine dihydrochloride or phenylhydrazine (1.0 equiv.) was added to a round bottom flask with magnetic stirrer and 5 mL of dichloromethane, and stirred. Triethylamine (5.0 equiv.) was added and allowed to stir at room temperature for 15 minutes. An acid chloride (2.0 equiv.) was then added dropwise (in the case of solid acid chlorides, a solution in 1 mL of dichloromethane was used), and the solution was allowed to stir for 2-4 hours. Water (10 mL) was then added, and the crude mixture was extracted with ethyl acetate (3 x 10 mL). After subsequent drying over Na_2SO_4, the solution was concentrated in vacuo and then purified by silica chromatography, or by recrystallization from ethyl acetate:hexane.

Method C. Benzylhydrazine dihydrochloride (2.0 equiv.) was added to a round bottom flask with magnetic stirrer and 10 mL of toluene, and stirred. 50% NaOH in water (2.0 equiv.) was then added, and allowed to stir for 15 minutes. The solution was then cooled with an ice bath to 5 °C. Next, 50% NaOH in water (1.0 equiv.) and an acid chloride (1.0 equiv.) were added dropwise simultaneously (in the case of solid acid chlorides, a solution in 1 mL of toluene was used). The solution was allowed to warm to room temperature for 1 hour. Water (10 mL) was then added, and the crude mixture was extracted with ethyl acetate (3 x 10 mL). After subsequent drying over Na_2SO_4, the solution was concentrated in vacuo and then purified by silica chromatography, or by recrystallization from ethyl acetate:hexane.

Method **D**. Organic hydrazine (1.2-5 equiv.) was added to a round bottom flask with magnetic stirrer and distilled THF, and fitted with a rubber septum. The mixture was then cooled to 0 °C with an ice bath. If the organic hydrazine was a hydrochloride salt, an equimolar amount (1.2-5 equiv.) of 1.0 M methyllithium in THF was added dropwise to generate the free base. Next, an equimolar amount (1.2-5 equiv.) 1.0 M DIBAL-H in THF or hexane was added dropwise to the solution, taking care that the liberated H_2 gas was not produced too rapidly. After DIBAL-H addition, the ice bath was removed and the solution was allowed stir and warm to room temperature over 2 hours. The solution may turn a color, depending on the hydrazine. Then, an ester (1.0 equiv.) was added dropwise (in the case of solid esters, a solution of ester in 1 mL of THF was used). The solution may take on a color here as well. If the reaction used 5 equivalents of activated hydrazine, then it is run at room temperature overnight; if it is less than 5 equivalents, the solution was warmed with an oil bath to 50 °C and allowed to stir overnight. The reaction was then cooled with an ice bath and quenched with slow addition of water (10 mL). The mixture was then concentrated in vacuo to remove THF. Then, 1.0 M HCl can added to the solution until the aluminum emulsion is broken. Acid sensitive products can be filtered through Celite after addition of ethyl acetate. After aqueous extraction with ethyl acetate and subsequent drying over Na_2SO_4, the solution was concentrated in vacuo and then purified by chromatography, or by recrystallization.

Method **E**[79]: organic hydrazine (0.70 mmol), 1.0 M aqueous NaOH (1.67 equiv), and ethanol (0.4 mL/mmol) were combined in a round bottom flask with a magnetic stir bar and allowed to stir for 5 minutes in open air. The desired anhydride (1.0 equiv) was added and allowed to stir for up to 18 hours. Water was added to the reaction, followed by extraction with ethyl acetate. The

combined organic extracts were dried, filtered, and concentrated in vacuo. Recrystallization from ethyl acetate and hexane, afforded the desired distally acylated arylhydrazine.

Method **F**[150]: organic hydrazine (0.90 mmol), pyridine (3.0 mL/mmol), and the desired acid chloride (1.0 equiv) were combined in a round bottom flask with magnetic stir bar. After 3 hours, the reaction was concentrated in vacuo, 1 M HCl (5.0 mL/mmol) was added, and the mixture was extracted with ethyl acetate. The combined organic extracts were dried, filtered, and concentrated in vacuo to afford the desired distally acylated arylhydrazine.

Method G[7]. Monoacylhydrazine (1.0 equiv.) was added to a round bottom flask with magnetic stirrer and 5.0 mL of toluene, and fitted with a rubber septum (if acid sensitive groups are present, add solid sodium bicarbonate (1.0 equiv.)). Then, an acid chloride (1.0 equiv.) was added dropwise (in the case of solid acid chlorides, a solution in 1 mL of toluene was used). The solution was warmed with an oil bath to 80 °C and allowed to stir for 6-16 hours. The reaction was then cooled to room temperature and quenched with the addition of water (10 mL). After aqueous extraction with ethyl acetate and subsequent drying over Na_2SO_4, the solution was concentrated in vacuo and then purified by chromatography, or by recrystallization.
Compounds **3-3Aj**, **3-3Ab**, **3-3Ae, 3-3Af,** and **3-3Ak**, were prepared by a general procedure (Method **H**) based on existing literature methods[7, 74, 79] with modification. **Method H**: *tert*-butyl-2-(4-fluorophenyl)hydrazine-1-carboxylate (prepared in 73% yield from **3-3Aa·HCl**)[79] (0.30 mmol), the requisite acid chloride (1.0 equiv.), and solid $NaHCO_3$ (1.0 equiv.) were combined in toluene, heated to 80 °C and stirred for 6-16 hours. After heating, the reaction mixture was removed from heat and water was added and allowed to stir for 45 minutes. The mixture was

then extracted with ethyl acetate, dried over Na_2SO_4, and concentrated in vacuo. These intermediates were typically recrystallized with hexane or toluene and hexane. Deprotection was accomplished by addition 4 M HCl in dioxane (16 equiv.) was added and a drop of methanol (to trap *t*-butyl cation; in the case of **3-3Aj**, methanol was omitted due to acetyl group reactivity), and stirring at room temperature for 0.5-16 hours. Trituration with diethyl ether then afforded a solid that was isolated by filtration.

***N′*-benzylbenzohydrazide (2-1Ba)**. *N′*-benzylidenebenzohydrazide (1.003 g, 0.44 mmol) and methanol (5 mL) were combined in open air at room temperature and set to stir. Next, sodium cyanoborohydride (0.0553 g, 0.88 mmol) was added and then finally p-toluenesulfonic acid (0.0860 g, 0.495 mmol). The solution was allowed to stir for 18 hours or until TLC showed total conversion of starting material. Then, a saturated solution of sodium carbonate was cautiously added to the solution and the crude product was extracted with dichloromethane, dried over sodium sulfate and concentrated under reduced pressure. The crude product was then recrystallized from ethyl acetate:hexane and yielded **2-1Ba** as a white powder (0.0888 g, 83%), mp 124-126 °C. This compound is known.[30, 151] ^{1}H NMR (400 MHz, DMSO-d_6) δ 10.07 (d, J = 6.1 Hz, 1H), 7.80 (d, J = 7.1 Hz, 2H), 7.51 (t, J = 7.3 Hz, 1H), 7.44 (t, J = 7.5 Hz, 2H), 7.42 – 7.35 (m, 2H), 7.33 (t, J = 7.4 Hz, 2H), 7.26 (t, J = 7.2 Hz, 1H), 5.43 (q, J = 5.8 Hz, 1H), 3.99 (d, J = 5.4 Hz, 2H); ^{13}C NMR (101 MHz, DMSO-d_6) δ 165.6 , 138.5 , 133.2 , 131.2 , 128.6 , 128.3 , 128.2 , 127.1 , 127.0 , 54.8. HRMS(ESI) m/z calculated for $C_{14}H_{15}N_2O$ [M + H^+] 227.1179, found 227.1171.

***N′*-benzoyl-*N*-benzyl-benzohydrazide(2-1Bb)**. Synthesized using Method C from benzylhydrazine dihydrochloride (1.9992 g, 10.2 mmol), toluene (10 mL), 50% NaOH in water (1.6 mL, 30.6 mmol) and benzoyl chloride (1.2 mL, 10.2 mmol). After workup the crude product was recrystallized from ethyl acetate and hexane, affording **2-1Bb** as a white powder (1.1798 g, 70%), mp 146-147 °C. This compound is known.[152] ^{1}H NMR (400 MHz, DMSO-d_6) δ 11.00 (s, 1H), 7.58 (d, J = 6.8 Hz, 2H), 7.49 (t, J = 6.6 Hz, 3H), 7.44 – 7.25 (m, 9H), 5.37 (s, 1H), 4.36 (s, 1H); ^{13}C NMR (101 MHz, DMSO-d_6) δ 172.0 , 165.3 , 136.5 , 134.9 , 132.0 , 131.9 , 130.1 , 128.6 , 128.3 , 127.7 , 127.4 , 127.2 , 127.2 , 51.6. HRMS(ESI) m/z calculated for $C_{21}H_{18}N_2NaO_2$ [M + Na^+] 353.1260, found 353.1240.

***N′*-benzoyl-*N*-benzyl-4-methylbenzohydrazide (2-1Bc)**. Synthesized using Method A from **2-1Ba** (68.1 mg, 0.29 mmol), dichloromethane (5 mL), triethylamine (61 μL, 0.44 mmol) and 4-methylbenzoyl chloride (58 μL, 0.44 mmol). After workup the crude product was recrystallized from ethyl acetate and hexane, affording **2-1Bc** as a white solid (54.3 mg, 54%), 156-157 °C. ^{1}H NMR (400 MHz, DMSO-d_6) δ 10.99 (s, 1H), 7.96 – 7.48 (m, 5H), 7.47 – 7.21 (m, 7H), 7.16 (d, J = 7.7 Hz, 2H), 5.36 (s, 1H), 4.33 (s, 1H), 2.27 (s, 3H); ^{13}C NMR (101 MHz, DMSO-d_6) δ 171.9 , 165.2 , 139.9 , 136.6 , 131.9 , 131.8 , 128.7 , 128.4 , 128.3 , 128.2 , 127.4 , 127.3 , 127.3 , 51.7 , 20.9. HRMS(ESI) m/z calculated for $C_{22}H_{21}N_2O_2$ [M + H^+] 345.1598, found 345.1608.

***N′*-benzoyl-*N*-benzyl-(4-fluorobenzo)hydrazide (2-1Bd)**. Synthesized using Method A from **2-1Ba** (70.6 mg, 0.31 mmol), dichloromethane (5 mL), triethylamine (48 μL, 0.34 mmol) and 4-fluorobenzoyl chloride (34 μL, 0.34 mmol). After workup the crude product was recrystallized from ethyl acetate and hexane, affording **2-1Bd** as a white solid (69.9 mg, 64%), 201-202 °C. ^{1}H

NMR (500 MHz, DMSO-d_6) δ 11.04 (s, 1H), 7.65 (dd, J = 8.4, 5.4 Hz, 2H), 7.51 (t, J = 7.2 Hz, 3H), 7.47 – 7.39 (m, 4H), 7.36 (t, J = 7.6 Hz, 3H), 7.30 (t, J = 7.2 Hz, 1H), 7.20 (t, J = 8.6 Hz, 2H), 5.33 (s, 1H), 4.35 (s, 1H); ^{13}C NMR (126 MHz, DMSO-d_6) δ 168.00 , 165.76 , 158.08 (d, $^1J_{CF}$ = 247.8 Hz), 136.19 , 131.98 , 131.94 , 128.46 , 128.36 , 128.33 , 127.43 , 127.31 , 123.87 (d, J_{CF} = 3.2 Hz), 123.62 (d, J_{CF} = 16.7 Hz), 115.54 (d, J_{CF} = 21.2 Hz), 51.39 . ^{19}F NMR (376 MHz, DMSO-d_6) δ -112.46. HRMS(ESI) m/z calculated for $C_{21}H_{18}FN_2O_2$ [M + H^+] 349.1347, found 349.1355.

***N′*-benzoyl-*N*-benzyl-(4-methoxybenzo)hydrazide (2-1Be)**. Synthesized using Method A from **2-1Ba** (63.9 mg, 0.28 mmol), dichloromethane (5 mL), triethylamine (40 μL, 0.28 mmol) and 4-methoxybenzoyl chloride (47.8 mg, 0.28 mmol). After workup the crude product was recrystallized from ethyl acetate and hexane, affording **2-1Be** as a white solid (76.7 mg, 76%), 190 °C. ^{1}H NMR (500 MHz, DMSO-d_6) δ 11.02 (s, 1H), 7.64 – 7.54 (m, 4H), 7.51 (t, J = 7.4 Hz, 1H), 7.43 – 7.38 (m, 4H), 7.36 (t, J = 7.5 Hz, 2H), 7.29 (t, J = 7.2 Hz, 1H), 6.90 (d, J = 8.3 Hz, 2H), 5.34 (s, 1H), 4.31 (s, 1H), 3.73 (s, 3H); ^{13}C NMR (126 MHz, DMSO-d_6) δ 171.4 , 165.2 , 160.7 , 136.7 , 132.1 , 132.0 , 129.5 , 128.7 , 128.4 , 128.3 , 127.4 , 127.3 , 126.6 , 113.0 , 55.2 , 51.8. HRMS(ESI) m/z calculated for $C_{22}H_{21}N_2O_3$ [M + H^+] 361.1547, found 361.1551.

***N′*-benzoyl-*N*-benzyl-(2-fluorobenzo)hydrazide (2-1Bh)**. Synthesized using **Method A** from **2-1Ba** (70.8 mg, 0.31 mmol), dichloromethane (5 mL), triethylamine (51 μL, 0.31 mmol) and 2-fluorobenzoyl chloride (33 μL, 0.31 mmol). After workup the crude product was recrystallized from ethyl acetate and hexane, affording **2-1Bh** as a white solid (76.5 mg, 71%), 142-143 °C. This compound exists as a mixture of conformers at room temperature. ^{1}H NMR (400 MHz, DMSO-d_6) δ 11.06 (s, 0.93*1H), 10.92 (s, 0.07*1H), 7.90 – 7.27 (m, 12H), 7.23 (t, J = 9.2 Hz,

1H), 7.15 (t, J = 7.5 Hz, 1H), 5.37 (d, J = 15.1 Hz, 0.92*1H), 4.64 (s, 0.16*2H), 4.42 (d, J = 15.5 Hz, 0.92*1H); ^{13}C NMR (126 MHz, DMSO-d_6) δ 171.10 , 165.28 , 162.90 (d, $1J_{CF}$ = 247.5 Hz), 136.39 , 132.05 , 131.91 , 131.21 (d, J_{CF} = 3.0 Hz), 129.90 (d, J_{CF} = 8.7 Hz), 128.74 , 128.46 , 128.37 , 127.45 , 127.24 , 114.77 (d, J_{CF} = 21.6 Hz), 51.74 , 45.71; ^{19}F NMR (376 MHz, DMSO-d_6) δ -116.94 (dt, J = 11.2, 6.1 Hz, 0.92*1F), -117.18 (0.8*1F). HRMS(ESI) m/z calculated for $C_{21}H_{18}FN_2O_2$ [M + H^+] 349.1347, found 349.1354.

***N′*-benzyl-*N′*-(cyclopropanecarbonyl)benzohydrazide (2-1Bi)**. Synthesized using Method A from **2-1Ba** (78.21 mg, 0.35 mmol), dichloromethane (5 mL), triethylamine (54 μL, 0.39 mmol) and cyclopropane carbonyl chloride (35 μL, 0.39 mmol). After workup the crude product was recrystallized from ethyl acetate and hexane, affording 2**-1Bi** as a white solid (67.8 mg, 67%), mp 122-123 °C. ^{1}H NMR (500 MHz, DMSO-d_6) δ 11.08 (s, 1H), 7.83 (d, J = 6.9 Hz, 2H), 7.58 (t, J = 7.3 Hz, 1H), 7.49 (t, J = 7.6 Hz, 2H), 7.42 – 7.21 (m, 5H), 5.25 (d, J = 14.9 Hz, 1H), 4.19 (d, J = 14.9 Hz, 1H), 1.95 (p, J = 6.2 Hz, 1H), 0.75 (s, 4H); ^{13}C NMR (126 MHz, DMSO-d_6) δ 174.8 , 165.5 , 136.9 , 132.1 , 132.1 , 128.6 , 128.5 , 128.3 , 127.6 , 127.3 , 50.9 , 10.0 , 7.9 , 7.8. HRMS(ESI) m/z calculated for $C_{18}H_{19}N_2O_2$ [M + H^+] 295.1441, found 295.1444.

***N′*-benzyl-*N′*-pivaloylbenzohydrazide (2-1Bk)**. Synthesized using Method A from **2-1Ba** (36.5 mg, 0.16 mmol), dichloromethane (5 mL), triethylamine (25 μL, 0.18 mmol) and pivaloyl chloride (22 μL, 0.18 mmol). After workup the crude product was recrystallized from ethyl acetate and hexane, affording **2-1Bk** as a white solid (41.6 mg, 84%), 223-224 °C . ^{1}H NMR (400 MHz, DMSO-d_6) δ 10.83 (s, 1H), 7.82 (d, J = 7.1 Hz, 2H), 7.59 (t, J = 7.4 Hz, 1H), 7.50 (t, J = 7.6 Hz, 2H), 7.31 (t, J = 7.2 Hz, 2H), 7.29 – 7.21 (m, 3H), 5.32 (s, 1H), 4.10 (s, 1H), 1.20 (s,

9H); ^{13}C NMR (101 MHz, DMSO-d_6) δ 178.2 , 166.5 , 137.2 , 132.2 , 128.5 , 128.2 , 128.2 , 127.7 , 127.1 , 52.6 , 38.8 , 27.7. HRMS(ESI) m/z calculated for $C_{19}H_{23}N_2O_2$ [M + H^+] 311.1754, found 311.1763.

***N′*-benzyl-*N′*-isobutyrylbenzohydrazide (2-1Bl)**. Synthesized using Method A from **2-1Ba** (39.5 mg, 0.17 mmol), dichloromethane (5 mL), triethylamine (27 μL, 0.19 mmol) and isobutyryl chloride (20 μL, 0.19 mmol). After workup the crude product was recrystallized from ethyl acetate and hexane, affording **2-1Ba** as a white solid (23.6 mg, 47%), 162-164 °C. ^{1}H NMR (500 MHz, DMSO-d_6) δ 10.93 (s, 1H), 7.79 (d, J = 7.0 Hz, 2H), 7.59 (t, J = 7.4 Hz, 1H), 7.49 (t, J = 7.7 Hz, 2H), 7.38 – 7.29 (m, 2H), 7.30 – 7.22 (m, 3H), 5.26 (d, J = 15.0 Hz, 1H), 4.17 (d, J = 15.0 Hz, 1H), 2.84 (hept, J = 6.8 Hz, 1H), 1.07 (s, 3H), 0.97 (s, 3H); ^{13}C NMR (101 MHz, DMSO-d_6) δ 178.3 , 165.7 , 136.9 , 132.1 , 128.5 , 128.4 , 128.3 , 127.5 , 127.2 , 50.5 , 29.3. HRMS(ESI) m/z calculated for $C_{18}H_{21}N_2O_2$ [M + H^+] 297.1598, found 297.1610.

***N′*-benzoyl-*N*-benzyl-(phenylaceto)hydrazide (2-1Bm)**. Synthesized using Method A from **2-1Ba** (83.6 mg, 0.37 mmol), dichloromethane (5 mL), triethylamine (57 μL, 0.41 mmol) and phenylacetyl chloride (54 μL, 0.41 mmol). After workup the crude product was recrystallized from ethyl acetate and hexane, affording **2-1Bm** as a white solid (70.8 mg, 56%), 168-169 °C. This compound exists as a mixture of conformers at room temperature. ^{1}H NMR (500 MHz, DMSO-d_6) δ 11.04 (s, 0.95*1H), 10.66 (s, 0.05*1H), 7.87 – 7.77 (m, 2H), 7.62 – 7.57 (m, 1H), 7.50 (t, J = 7.6 Hz, 2H), 7.38 – 7.13 (m, 10H), 5.22 (s, 0.95*1H), 4.88 (s, 0.05*1H), 4.19 (d, J = 75.2 Hz, 0.95*1H), 3.90 (s, 0.05*1H), 3.80 (s, 1H), 3.61 (s, 1H); ^{13}C NMR (101 MHz, DMSO-d_6) δ 172.5 , 165.5 , 136.6 , 135.2 , 132.2 , 132.0 , 129.6 , 128.6 , 128.5 , 128.3 , 128.1 , 127.6 ,

127.3 , 126.4 , 50.7 , 38.2. HRMS(ESI) m/z calculated for $C_{22}H_{20}N_2NaO_2$ [M + Na^+] 367.1417, found 367.1426.

***N′*-(4-methylbenzoyl)-*N*-benzyl-(4-methylbenzo)hydrazide (2-1Cc)**. Synthesized using Method B from benzylhydrazine dihydrochloride (0.2033 g, 1.0 mmol), dichloromethane (5 mL), triethylamine (0.42 mL, 3.0 mmol) and 4-methylbenzoyl chloride (0.28 mL, 2.0 mmol). After workup the crude product was recrystallized from ethyl acetate and hexane, affording **2-1Cc** as a white solid (0.3157 g, 85%), mp 170-171 °C. ^{1}H NMR (400 MHz, DMSO-d_6) δ 10.90 (s, 1H), 7.54 – 7.43 (m, 4H), 7.43 – 7.33 (m, 4H), 7.32 – 7.25 (m, 1H), 7.20 (d, J = 7.8 Hz, 2H), 7.15 (d, J = 7.7 Hz, 2H), 5.36 (s, 1H), 4.31 (s, 1H), 2.29 (s, 3H), 2.26 (s, 3H); ^{13}C NMR (101 MHz, DMSO-d_6) δ 171.9 , 165.0 , 142.1 , 139.9 , 136.6 , 131.9 , 129.1 , 128.9 , 128.6 , 128.3 , 128.2 , 127.4 , 127.3 , 51.7 , 20.9. HRMS(ESI) m/z calculated for $C_{23}H_{23}N_2O_2$ [M + H^+] 360.1786, found 360.1791.

***N′*-(4-fluorobenzoyl)-*N*-benzyl-(4-fluorobenzo)hydrazide (2-1Dd)**. Synthesized using Method C from benzylhydrazine dihydrochloride (0.4703 g, 2.55 mmol), toluene (10 mL), 50% NaOH in water (1.20 mL, 15.3 mmol) and 4-fluorobenzoyl chloride (0.60 mL, 5.1 mmol). After workup the crude product was recrystallized from ethyl acetate and hexane, affording **2-1Dd** as a white powder (0.7043 g, 75%), mp 200-201 °C. ^{1}H NMR (400 MHz, DMSO-d_6) δ 11.05 (s, 1H), 7.69 – 7.56 (m, 4H), 7.45 – 7.34 (m, 4H), 7.31 (d, J = 7.1 Hz, 1H), 7.25 (t, J = 8.9 Hz, 2H), 7.20 (t, J = 8.9 Hz, 2H), 5.35 (s, 1H), 4.35 (s, 1H); ^{13}C NMR (101 MHz, DMSO-d_6) δ 171.00 , 164.78 (d, $^1J_{CF}$ = 137.1 Hz), 164.22 , 162.31 (d, $^1J_{CF}$ = 136.0 Hz), 136.35 , 131.14 , 130.01 , 129.89 , 129.79 , 128.67 , 128.33 , 127.43 , 115.51 (d, $^2J_{CF}$ = 22.0 Hz), 114.77 (d, $^2J_{CF}$ = 22.2 Hz), 51.69; ^{19}F

NMR (376 MHz, DMSO-d_6) δ -109.94 (s, 1F), -112.39 (s, 1F). HRMS(ESI) m/z calculated for $C_{21}H_{17}F_2N_2NaO_2$ [M + Na^+] 389.1072, found 389.1094.

***N'*-(4-methoxybenzoyl)-*N*-benzyl-(4-methoxybenzo)hydrazide (2-1Ee)**. Synthesized using Method C from benzylhydrazine dihydrochloride (1.9697 g, 10.1 mmol), toluene (10 mL), 50% NaOH in water (1.6 mL, 30.3 mmol) and 4-methoxybenzoyl chloride (1.7224 g, 10.1 mmol). After workup the crude product was recrystallized from ethyl acetate and hexane, affording **2-1Ee** as a white powder (1.0522 g, 53%), mp 166-168 °C.^{1}H NMR (400 MHz, DMSO-d_6) δ 10.84 (s, 1H), 7.60 (d, J = 8.6 Hz, 13H), 7.43 – 7.32 (m, 4H), 7.29 (t, J = 7.0 Hz, 17H), 6.94 (d, J = 8.5 Hz, 2H), 6.88 (d, J = 8.4 Hz, 2H), 5.35 (s, 1H), 4.29 (s, 1H), 3.77 (s, 3H), 3.73 (s, 3H); ^{13}C NMR (101 MHz, DMSO-d_6) δ 171.5 , 164.5 , 162.1 , 160.6 , 136.8 , 129.5 , 129.2 , 128.6 , 128.3 , 127.3 , 126.7 , 124.1 , 113.7 , 113.0 , 55.4 , 55.2 , 51.9. HRMS(ESI) m/z calculated for $C_{23}H_{23}N_2NaO_4$ [M + Na^+] 392.1684, found 392.1685.

***N'*-(2-bromobenzoyl)-*N*-benzyl-(benzo)hydrazide (2-1Gg)**. Synthesized using Method B from benzylhydrazine dihydrochloride (0.2066 g, 1.1 mmol), dichloromethane (5 mL), triethylamine (0.56 mL, 4.4 mmol) and 2-bromobenzoyl chloride (0.3825 g, 2.2 mmol). After workup the crude product was recrystallized from ethyl acetate and hexane, affording **2-1Gg** as a white solid (0.1480 g, 35%), 177-178 °C.^{1}H NMR (400 MHz, DMSO-d_6) δ 11.34 (s, 1H), 8.75 (d, J = 2.2 Hz, 1H), 8.68 (dd, J = 4.9, 1.6 Hz, 1H), 8.62 (s, 1H), 8.61 – 8.55 (m, 1H), 7.95 (dt, J = 8.0, 1.9 Hz, 1H), 7.85 (d, J = 7.9 Hz, 1H), 7.51 – 7.42 (m, 3H), 7.42 – 7.35 (m, 3H), 7.35 – 7.29 (m, 1H), 5.37 (d, J = 14.8 Hz, 1H), 4.41 (d, J = 14.8 Hz, 1H); ^{13}C NMR (101 MHz, DMSO-d_6) δ 170.0 , 164.0 , 152.7 , 151.0 , 148.0 , 147.6 , 136.0 , 135.0 , 134.8 , 130.6 , 128.8 , 128.4 , 127.6 , 127.5 ,

123.7 , 123.0 , 51.6. HRMS(ESI) m/z calculated for $C_{21}H_{17}Br_2N_2O_2$ [M + H^+] 488.9632, found 488.9656.

***N′*-(2-fluorobenzoyl)-*N*-benzyl-(2-fluorobenzo)hydrazide (2-1Hh)**. Synthesized using Method C from benzylhydrazine dihydrochloride (0.4964 g, 2.5 mmol), toluene (10 mL), 50% NaOH in water (0.408 mL, 7.8 mmol) and 2-fluorobenzoyl chloride (0.31 mL, 2.5 mmol). After workup the crude product was recrystallized from ethyl acetate and hexane, affording **2-1Hh** as a white powder (0.3888 g, 86%), 126-128 °C. This compound exists as a mixture of rotamers at room temperature. ^{1}H NMR (400 MHz, DMSO-d_6) δ 11.04 (s, 0.95*1H), 10.78 (s, 0.04*1H), 10.43 (s, 0.02*1H) 7.51 – 7.10 (m, 12H), 6.96 (td, J = 7.3, 1.8 Hz, 1H), 5.38 (d, J = 64.8 Hz, 1H), 4.56 (s, 1H); ^{13}C NMR (101 MHz, DMSO-d_6) δ 167.8 , 163.1 , 159.7 (d, J_{CF} = 80.1 Hz), 157.21 (d, J_{CF} = 76.7 Hz), 135.95 , 132.95 (d, J_{CF} = 8.2 Hz), 131.64 (d, J_{CF} = 8.1 Hz), 129.27 (d, J_{CF} = 2.9 Hz), 128.40 , 128.37 , 128.33 , 127.44 , 124.24 (d, J_{CF} = 3.6 Hz), 123.87 , 123.47 (d, J_{CF} = 16.8 Hz), 121.62 (d, J_{CF} = 15.2 Hz), 116.04 (d, J_{CF} = 21.2 Hz), 115.51 (d, J_{CF} = 21.1 Hz), 51.22; ^{19}F NMR (376 MHz, DMSO-d_6) δ -115.30 – -115.44 (m, 0.04*1F), -115.47 (s, 0.05*1F), -116.69 (dt, J = 11.6, 6.1 Hz, 0.91*1F), -117.12 (dt, J = 11.6, 6.1 Hz, 1F). HRMS(ESI) m/z calculated for $C_{21}H_{17}F_2N_2O_2$ [M + H^+] 367.1253, found 367.1265.

***N′*-cyclopropanoyl-*N*-benzyl-cyclopropanecarbohydrazide(2-1Ii)**. Synthesized using Method C from benzylhydrazine dihydrochloride (0.9942 g, 5.1 mmol), toluene (10 mL), 50% NaOH in water (1.20 mL, 15.3 mmol) and cyclopropane carbonyl chloride (0.93 mL, 10.2 mmol). After workup the crude product was recrystallized from ethyl acetate and hexane, affording **2-1Ii** as a white powder (0.9154 g, 69%), mp 159-160 °C. This compound exists as a mixture of rotamers

at room temperature. ^{1}H NMR (400 MHz, DMSO-d_6) δ 10.61 (s, 0.92*1H), 10.21 (s, 0.05*1H), 9.82 (s, 0.03*1H), 7.35 (t, J = 7.3 Hz, 2H), 7.29 (d, J = 7.0 Hz, 1H), 7.27 – 7.19 (m, 2H), 5.22 (s, 0.44*2H), 4.88 (s, 0.05*2H), 4.78 (d, J = 14.3 Hz, 0.05*2H), 4.66 (d, J = 14.4 Hz, 0.02*2H), 3.96 (s, 0.44*2H), 1.90 (p, J = 6.2 Hz, 1H), 1.59 (tt, J = 7.3, 5.1 Hz, 1H), 0.91 – 0.62 (m, 8H); ^{13}C NMR (101 MHz, Acetone-d_6) δ 206.1 , 175.8 , 173.0 , 138.2 , 129.5 , 129.2 , 128.2 , 51.4 , 12.7 , 10.7 , 8.1 , 7.3. HRMS(ESI) m/z calculated for $C_{15}H_{18}N_2NaO_2$ [M + Na^+] 281.1260, found 281.1248.

***N′*-pivaloyl-*N*-benzyl-pivalohydrazide (2-1Kk)**. Synthesized using **Method C** from benzylhydrazine dihydrochloride (1.9916 g, 10.2 mmol), toluene (10 mL), 50% NaOH in water (1.60 mL, 30.6 mmol) and pivaloyl chloride (1.26 mL, 10.2 mmol). After workup the crude product was recrystallized from ethyl acetate and hexane, affording **2-1Kk** as yellow crystals (1.4731 g, 99%), mp 132-133 °C. This compound exists as a mixture of rotamers at room temperature. ^{1}H NMR (400 MHz, Chloroform-*d*) δ 7.42 – 7.27 (m, 3H), 7.18 (d, J = 6.7 Hz, 2H), 6.98 (s, 1H), 6.11 – 3.35 (m, 2H), 1.24 (s, 9H), 1.07 (s, 9H); ^{13}C NMR (101 MHz, $CDCl_3$) δ 179.1 , 177.0 , 136.3 , 129.1 , 129.0 , 128.1 , 50.7 , 39.3 , 38.5 , 27.8 , 27.3. HRMS(ESI) m/z calculated for $C_{17}H_{26}N_2NaO_2$ [M + Na^+] 313.1886, found 313.1867.

***N′*-isobutryl-*N*-benzyl-isobutyrohydrazide (2-1Ll)**. Synthesized using **Method C** from benzylhydrazine dihydrochloride (0.9945 g, 5.1 mmol), toluene (10 mL), 50% NaOH in water (1.7 mL, 15.3 mmol) and isobutyryl chloride (0.53 mL, 5.1 mmol). After workup the crude product was recrystallized from ethyl acetate and hexane, affording **2-1Jd** as a white solid (0.5091 g, 76%), mp 112-113 °C. This compound exists as a mixture of rotamers at room

temperature. ^{1}H NMR (400 MHz, Chloroform-*d*) δ 7.73 (s, 1H), 7.30 – 7.20 (m, 3H), 7.15 (d, *J* = 7.0 Hz, 2H), 5.37 (s, 0.43*2H), 4.77 (s, 0.14*2H), 3.95 (s, 0.43*2H), 2.77 (hept, *J* = 6.8 Hz, 1H), 2.28 (hept, *J* = 6.9 Hz, 1H), 1.04 (d, *J* = 7.0 Hz, 13H); ^{13}C NMR (101 MHz, $CDCl_3$) δ 179.4 , 175.9 , 136.1 , 129.0 , 128.8 , 128.0 , 50.1 , 33.4 , 30.1 , 19.4 , 19.2. HRMS(ESI) m/z calculated for $C_{15}H_{22}N_2NaO_2$ [M + Na^+] 285.1573, found 285.1561.

***N′*-(phenylacetyl)-*N*-benzyl-(phenylaceto)hydrazide (2-1Mm)**. Synthesized using Method B from benzylhydrazine dihydrochloride (0.2048 g, 1.0 mmol), dichloromethane (5 mL), triethylamine (0.42 mL, 3.0 mmol) and phenylacetyl chloride (0.28 mL, 2.0 mmol). After workup the crude product was recrystallized from ethyl acetate and hexane, affording **2-1Mm** as a white solid (0.2704 g, 72%), 120-121 °C. ^{1}H NMR (400 MHz, Chloroform-*d*) δ 7.38 – 7.25 (m, 8H), 7.25 – 7.16 (m, 5H), 7.16 – 6.91 (m, 6H), 6.79 (s, 1H), 6.41 – 3.68 (br s, 2H), 3.58 (s, 2H), 3.47 (s, 2H); ^{13}C NMR (101 MHz, Chloroform-*d*) δ 173.0 , 169.3 , 135.6 , 134.6 , 133.2 , 129.4 , 129.1 , 129.1 , 128.9 , 128.8 , 128.1 , 127.9 , 127.0 , 50.3 , 42.0 , 40.4. HRMS(ESI) m/z calculated for $C_{23}H_{23}N_2O_2$ [M + H^+] 360.1786, found 360.1782.

***N′*-(nicotinoyl)-*N*-benzyl-(nicotino)hydrazide (2-1Nn)**. Synthesized using Method B from benzylhydrazine dihydrochloride (0.2066 g, 1.1 mmol), dichloromethane (5 mL), triethylamine (0.56 mL, 4.4 mmol) and nicotinoyl chloride (0.3825 g, 2.2 mmol). After workup the crude product was recrystallized from ethyl acetate and hexane, affording **2-1Nn** as a white solid (0.1480 g, 35%), 175-176 °C.^{1}H NMR (400 MHz, DMSO-d_6) δ 11.34 (s, 1H), 8.75 (d, *J* = 2.2 Hz, 1H), 8.68 (dd, *J* = 4.9, 1.6 Hz, 1H), 8.62 (s, 1H), 8.61 – 8.55 (m, 1H), 7.95 (dt, *J* = 8.0, 1.9

Hz, 1H), 7.85 (d, *J* = 7.9 Hz, 1H), 7.51 – 7.42 (m, 3H), 7.42 – 7.35 (m, 3H), 7.35 – 7.29 (m, 1H), 5.37 (d, *J* = 14.8 Hz, 1H), 4.41 (d, *J* = 14.8 Hz, 1H); ^{13}C NMR (101 MHz, DMSO-d_6) δ 170.0 , 164.0 , 152.7 , 151.0 , 148.0 , 147.6 , 136.0 , 135.0 , 134.8 , 130.6 , 128.8 , 128.4 , 127.6 , 127.5 , 123.7 , 123.0 , 51.6. HRMS(ESI) m/z calculated for $C_{19}H_{17}N_4O_2$ [M + H^+] 333.1346, found 333.1350.

***N′*-(isonicotinoyl)-*N*-benzyl-(isonicotino)hydrazide (2-1Oo)**. Synthesized using Method B from benzylhydrazine dihydrochloride (0.2093 g, 1.1 mmol), dichloromethane (5 mL), triethylamine (0.56 mL, 4.4 mmol) and isonicotinoyl chloride (0.3863 g, 2.2 mmol). After workup the crude product was recrystallized from ethyl acetate and hexane, affording **3-1Oo** as a yellow solid (.0731 g, 17%), 211-213 °C. ^{1}H NMR (400 MHz, DMSO-d_6) δ 11.41 (s, 1H), 8.69 – 8.58 (m, 4H), 7.54 – 7.27 (m, 10H), 5.32 (d, *J* = 14.7 Hz, 1H), 4.42 (d, *J* = 14.9 Hz, 1H); ^{13}C NMR (101 MHz, DMSO-d_6) δ 170.0 , 164.2 , 150.3 , 149.6 , 142.3 , 138.7 , 135.8 , 128.8 , 128.4 , 127.7 , 121.0 , 51.5. HRMS(ESI) m/z calculated for $C_{19}H_{17}N_4O_2$ [M + H^+] 333.1346, found 333.1352.

***N′*-phenylbenzohydrazide (2-2Ba)**. Synthesized using Method D from phenylhydrazine (0.12 mL, 1.2 mmol), and distilled THF (5.0 mL), 1.0 M DIBAL-H in THF (1.2 mL, 1.2 mmol), and methyl benzoate (0.13 mL, 1.0 mmol). After workup, the crude product was recrystallized from ethyl acetate:hexane yielding **2-2Ba** as a white powder (211.1 mg, 99%), mp 141-144 °C. This compound is known.[78, 153] ^{1}H NMR (400 MHz, DMSO-d_6) δ 10.36 (d, *J* = 3.0 Hz, 1H), 7.92 (d, *J* = 7.1 Hz, 2H), 7.88 (d, *J* = 2.9 Hz, 1H), 7.58 (t, *J* = 7.3 Hz, 1H), 7.50 (t, *J* = 7.5 Hz, 2H), 7.20 – 7.11 (t, 2H), 6.79 (d, *J* = 7.9 Hz, 2H), 6.72 (t, *J* = 7.3 Hz, 1H); ^{13}C NMR (101 MHz, DMSO-d_6) δ 166.81, 149.90, 133.43, 132.06, 129.16, 128.91, 127.70, 119.10, 112.76. HRMS(ESI) m/z calculated for C13H12N2NaO [M + Na^+] 235.0842, found 235.0836.

***N′*-(4-methylbenzoyl)-*N′*-phenylbenzohydrazide (2-2Bc)**. Synthesized using Method G from **2-2Ba** (41.1 mg, 0.30 mmol), 5.0 mL of toluene, and 4-methylbenzoyl chloride (46 μL, 0.33 mmol). After workup, the crude product was recrystallized from ethyl acetate:hexane, yielding **2-2Bc** as white crystals (69.4 mg, 70%), mp 160-161 °C. ^{1}H NMR (400 MHz, DMSO-d_6) δ 11.50 (s, 1H), 7.74 (d, J = 7.6 Hz, 2H), 7.57 (t, J = 7.4 Hz, 1H), 7.48 (d, J = 7.5 Hz, 4H), 7.37 (d, J = 4.7 Hz, 4H), 7.26 – 7.19 (m, 1H), 7.17 (d, J = 7.9 Hz, 2H), 2.28 (s, 3H); ^{13}C NMR (101 MHz, DMSO-d_6) δ 165.3 , 140.3 , 132.2 , 128.7 , 128.6 , 128.4 , 127.8 , 127.3 , 126.2 , 20.9. HRMS(ESI) m/z calculated for $C_{21}H_{18}N_2NaO_2$ [M + H^+] 353.1280, found 353.1260.

***N*'-benzoyl-4-fluoro-*N*-phenylbenzohydrazide (2-2Bd).** Synthesized using Method G from **2-2Ba** (64.0 mg, 0.30 mmol), 5.0 mL of toluene, and 4-fluorobenzoyl chloride (40 μL, 0.30 mmol). After workup, the crude product was recrystallized from ethyl acetate:hexane, yielding **2-2Bd** as white crystals (68.6 mg, 68%), mp 169-170 °C. ^{1}H NMR (400 MHz, DMSO-d_6) δ 11.56 (s, 1H), 7.72 (d, J = 7.6 Hz, 2H), 7.69 – 7.61 (m, 2H), 7.57 (t, J = 7.4 Hz, 1H), 7.47 (t, J = 7.6 Hz, 2H), 7.45 – 7.35 (m, 4H), 7.22 (t, J = 8.8 Hz, 3H); ^{13}C NMR (101 MHz, DMSO-d_6) δ 165.4 , 162.9 (d, $^{1}J_{CF}$ = 248.1 Hz), 141.8 , 132.3 , 131.6 , 130.3 , 130.2 , 128.8 , 128.6 , 127.3 , 126.3 , 124.1 ,

115.0 (d, $^{2}J_{CF}$ = 21.9 Hz); ^{19}F NMR (376 MHz, DMSO-d_6) δ -109.59. HRMS(ESI) m/z calculated for $C_{20}H_{15}FN_2NaO$ [M + Na^+] 357.1010, found 357.1032.

***N*'-benzoyl-4-methoxy-*N*-phenylbenzohydrazide (2-2Be).** Synthesized using Method G from **2-2Ba** (61.5 mg, 0.29 mmol), 5.0 mL of toluene, and 4-methoxybenzoyl chloride (49.9 mg, 0.29 mmol). After workup, the crude product was recrystallized from ethyl acetate:hexane, yielding **2-2Be** as white crystals (70.7 mg, 70%), mp 199-200 °C. ^{1}H NMR (400 MHz, DMSO-d_6) δ 11.50 (s, 1H), 7.77 (d, *J* = 7.6 Hz, 2H), 7.57 (d, *J* = 7.9 Hz, 3H), 7.48 (t, *J* = 7.6 Hz, 2H), 7.37 (d, *J* = 4.4 Hz, 4H), 7.27 – 7.16 (m, 1H), 6.91 (d, *J* = 8.7 Hz, 2H), 3.74 (s, 3H); ^{13}C NMR (101 MHz, DMSO-d_6) δ 169.3 , 165.3 , 160.9 , 142.4 , 132.2 , 131.8 , 129.9 , 128.7 , 128.6 , 127.3 , 126.9 , 126.0 , 124.2 , 113.2 , 55.2. HRMS(ESI) m/z calculated for $C_{21}H_{18}FN_2NaO_3$ [M + Na^+] 369.1210, found 369.1224.

***N*'-benzoyl-2-bromo-*N*-phenylbenzohydrazide (2-2Bg).** Synthesized using Method G from **2-2Ba** (53.3 mg, 0.25 mmol), 5.0 mL of toluene, and 2-bromobenzoyl chloride (33 μL, 0.25 mmol). After workup, the crude product was recrystallized from ethyl acetate:hexane, yielding **2-2Bg** as white crystals (73.1 mg, 74%), mp 165-166 °C. This compound exists as a mixture of rotamers at room temperature. ^{1}H NMR (400 MHz, DMSO-d_6) δ 11.53 (s, 0.40*1H), 11.49 (s, 0.59*1H), 7.97 (d, *J* = 7.6 Hz, 1H), 7.67 (d, *J* = 7.9 Hz, 1H), 7.61 (d, *J* = 8.0 Hz, 2H), 7.58 – 7.08 (m, 11H); ^{13}C NMR (101 MHz, DMSO-d_6) δ 168.8 , 166.3 , 165.3 , 141.9 , 140.7 , 137.5 , 132.7 , 132.2 , 131.7 , 130.8 , 129.3 , 128.8 , 128.5 , 127.6 , 127.3 , 127.0 , 126.5 , 126.0 , 123.5 , 119.3 , 118.3. HRMS(ESI) m/z calculated for $C_{20}H_{15}BrN_2NaO_2$ [M + Na^+] 417.0209, found 417.0236.

***N*'-benzoyl-2-fluoro-*N*-phenylbenzohydrazide (2-2Bh).** Synthesized using Method G from **2-2Ba** (32.5 mg, 0.15 mmol), 5.0 mL of toluene, and 2-fluorobenzoyl chloride (18 μL, 0.15 mmol). After workup, the crude product was recrystallized from ethyl acetate:hexane, yielding **2-2Bh** as white crystals (41.1 mg, 80%), mp 160-161 °C. ^{1}H NMR (400 MHz, DMSO-d_6) δ 11.56 (s, 1H), 7.72 (d, J = 7.6 Hz, 2H), 7.69 – 7.61 (m, 2H), 7.57 (t, J = 7.4 Hz, 1H), 7.47 (t, J = 7.6 Hz, 2H), 7.45 – 7.35 (m, 4H), 7.22 (t, J = 8.8 Hz, 3H); ^{13}C NMR (101 MHz, DMSO-d_6) δ 165.4 , 141.8 , 132.3 , 131.6 , 130.3 , 130.2 , 128.8 , 128.6 , 127.3 , 126.3 , 124.1 , 115.1 , 114.9; ^{19}F NMR (376 MHz, DMSO-d_6) δ -109.59. HRMS(ESI) m/z calculated for $C_{20}H_{15}FN_2NaO$ [M + Na^+] 357.1010, found 357.1032.

***N*′-(cyclopropanecarbonyl)-*N*′-phenylbenzohydrazide (2-2Bi).** Synthesized using Method G from **2-2Ba** (32.5 mg, 0.15 mmol), 5.0 mL of toluene, and cyclopropanecarbonyl chloride (16 μL, 0.15 mmol). After workup, the crude product was recrystallized from ethyl acetate:hexane, yielding **2-2Bi** as white crystals (42.6 mg, 84%), mp 215-216 °C. ^{1}H NMR (400 MHz, Chloroform-*d*) δ 9.12 (s, 1H), 7.78 (d, J = 7.6 Hz, 2H), 7.59 (d, J = 7.7 Hz, 2H), 7.37 (dt, J = 34.6, 7.8 Hz, 6H), 1.63 (s, 1H), 1.15 (dq, J = 6.7, 4.0 Hz, 2H), 0.81 (dq, J = 7.3, 4.0 Hz, 2H); ^{13}C NMR (101 MHz, Chloroform-*d*) δ 174.0 , 166.7 , 142.0 , 132.3 , 131.9 , 129.5 , 128.7 , 128.3 , 127.6 , 12.7 , 9.5. HRMS(ESI) m/z calculated for $C_{17}H_{17}N_2O_2$ [M + H^+] 281.1285, found 281.1293.

***N′*-acetyl-*N′*-phenylbenzohydrazide (2-2Bj)**. Synthesized using Method G from **3-2Ba** (83.1 mg, 0.39 mmol), 5.0 mL of toluene, and acetyl chloride (33 μL, 0.47 mmol). After workup, the crude product was recrystallized from ethyl acetate:hexane, yielding **2-2Bj** white crystals (79.5 mg, 80%), mp 113-114 °C. This compound exists as a mixture of rotamers at room temperature. ^{1}H NMR (400 MHz, Chloroform-*d*) δ 10.09 (s, 0.37*1H), 9.69 (s, 0.63*1H), 7.84 (d, *J* = 7.6 Hz, 0.35*2H), 7.72 (d, *J* = 7.6 Hz, 0.65*2H), 7.56 – 7.01 (m, 8H), 2.17 (s, 0.33*3H), 2.12 – 1.90 (m, 0.67*3H); ^{13}C NMR (101 MHz, Chloroform-*d*) δ 172.9 , 170.5 , 166.4 , 142.1 , 141.3 , 132.7 , 132.2 , 131.6 , 129.6 , 128.9 , 128.6 , 127.7 , 127.6 , 126.9 , 124.9 , 22.3 , 21.8. HRMS(ESI) m/z calculated for $C_{15}H_{14}N_2NaO_2$ [M + Na^+], 277.0947, found 277.0963.

***N′-tert*-butyl-*N′*-phenylbenzohydrazide (2-2Bk)**. Synthesized using Method B from **2-2Ba** (72.0 mg, 0.34 mmol), 5.0 mL of toluene, and pivaloyl chloride (42 μL, 0.34 mmol). After workup, the crude product was recrystallized from ethyl acetate:hexane, yielding **2-2Bk** as white crystals (27.0 mg, 27%), mp 201-204 °C. ^{1}H NMR (400 MHz, DMSO-d_6) δ 11.29 (s, 1H), 7.86 (d, *J* = 7.0 Hz, 2H), 7.61 (t, *J* = 7.4 Hz, 1H), 7.53 (t, *J* = 7.5 Hz, 2H), 7.42 (d, *J* = 7.0 Hz, 2H), 7.36 (t, *J* = 7.8 Hz, 2H), 7.22 (t, *J* = 7.2 Hz, 1H), 1.23 (s, 9H); ^{13}C NMR (101 MHz, DMSO-d_6) δ 177.5 , 166.1 , 143.5 , 132.4 , 132.0 , 128.8 , 128.5 , 127.6 , 126.6 , 126.1 , 28.0. HRMS(ESI) m/z calculated for $C_{18}H_{20}N_2NaO_2$ [M + Na^+], 319.1417, found 319.1418.

***N′*-isobutyryl-*N′*-phenylbenzohydrazide (2-2Bl)**. Synthesized using Method G from **2-2Ba** (38.1 mg, 0.18 mmol), 5.0 mL of toluene, and isobutyryl chloride (20 μL, 0.18 mmol). After workup, the crude product was recrystallized from ethyl acetate:hexane, yielding **2-2Bl** as white

crystals (40.5 mg, 78%), mp 190-191 °C. ^{1}H NMR (400 MHz, Chloroform-*d*) δ 9.30 (d, *J* = 114.1 Hz, 1H), 7.75 (d, *J* = 7.1 Hz, 2H), 7.55 (d, *J* = 7.6 Hz, 2H), 7.50 – 7.27 (m, 6H), 2.73 (s, 1H), 1.18 (s, 3H), 1.16 (s, 3H); ^{13}C NMR (101 MHz, Chloroform-*d*) δ 166.7 , 142.0 , 132.3 , 131.9 , 129.6 , 128.7 , 128.0 , 127.6 , 31.4 , 19.6. HRMS(ESI) m/z calculated for $C_{17}H_{18}N_2NaO_2$ [M + Na^+] 305.1260, found 305.1266.

***N′*-phenyl-*N′*-(2-phenylacetyl)benzohydrazide (2-2Bm).** Synthesized using Method G from **2-2Ba** (32.5 mg, 0.15 mmol), 5.0 mL of toluene, and phenylacetyl chloride (20 μL, 0.15 mmol). After workup, the crude product was recrystallized from ethyl acetate:hexane, yielding **2-2Bm** white crystals (30.0 mg, 60%), mp 192-194 °C. This compound exists as a mixture of rotamers at room temperature. ^{1}H NMR (400 MHz, DMSO-d_6) δ 11.62 (s, 0.75*1H), 11.14 (s, 0.25*1H), 7.94 (d, *J* = 7.6 Hz, 2H), 7.68 – 7.60 (m, 1H), 7.56 (d, *J* = 10.2 Hz, 2H), 7.48 (d, *J* = 7.6 Hz, 3H), 7.34 (dd, *J* = 32.8, 7.3 Hz, 4H), 7.24 (s, 3H), 3.94 (d, *J* = 16.1 Hz, 0.35*2H), 3.85 – 3.54 (m, 0.65*2H); ^{13}C NMR (101 MHz, DMSO-d_6) δ 172.3 , 166.2 , 142.0 , 135.5 , 132.9 , 132.1 , 130.0 , 129.2 , 129.0 , 128.6 , 128.1 , 127.0 , 126.4 , 124.2. HRMS(ESI) m/z calculated for $C_{21}H_{18}N_2NaO_2$ [M + Na^+] 353.1260, found 353.1289.

***N′*-phenyl-*N′*-(2,2,2-trifluoroacetyl)benzohydrazide (2-2Bq)**. Synthesized using Method G from **2-2Ba** (68.8 mg, 0.32 mmol), 5.0 mL of toluene, and trifluoroacetic anhydride (46 μL, 0.32 mmol). After workup, the crude product was recrystallized from ethyl acetate:hexane, yielding **2-2Bq** as white crystals (68.9 mg, 69%), mp 185-186 °C. This compound exists as a mixture of rotamers at room temperature. ^{1}H NMR (400 MHz, DMSO-d_6) δ 11.97 (s, 0.84*1H), 11.68 (s,

0.16*1H), 7.91 – 7.84 (m, 2H), 7.65 (q, J = 7.4 Hz, 1H), 7.61 – 7.54 (m, 4H), 7.49 (t, J = 7.8 Hz, 2H), 7.37 (t, J = 7.3 Hz, 1H); ^{13}C NMR (101 MHz, DMSO-d_6) δ 166.4 , 164.6 , 156.5 (d, J_{CF} = 35.2 Hz), 139.8 , 132.9 , 132.6 , 131.1 , 130.9 , 130.0 , 129.5 , 129.1 , 128.9 , 128.7 , 127.9 , 127.8 , 127.6 , 123.9 , 116.1 (q, $^1J_{CF}$ = 288.9 Hz); ^{19}F NMR (376 MHz, DMSO-d_6) δ -66.77 (s, 0.16*1F), -70.02 (s, 0.84*1F). HRMS(ESI) m/z calculated for $C_{15}H_{11}F_3N_2NaO_2$ [M + Na^+] 331.0665, found 331.0678.

***N′*-phenyl-*N′*-propionylbenzohydrazide (2-2Br).** Synthesized using Method G from **2-2Ba** (79.7 mg, 0.37 mmol), 5.0 mL of toluene, and propionyl chloride (33 µL, 0.37 mmol). After workup, the crude product was recrystallized from ethyl acetate:hexane, yielding **2-2Br** as white crystals (64.2 mg, 63%), 191-192. ^{1}H NMR (400 MHz, DMSO-d_6) δ 11.49 (s, 0.77*1H), 11.06 (s, 0.23*1H), 7.92 (d, J = 7.6 Hz, 2H), 7.63 (t, J = 7.4 Hz, 1H), 7.58 – 7.51 (m, 2H), 7.49 (d, J = 7.9 Hz, 2H), 7.45 – 7.32 (m, 2H), 7.21 (s, 1H), 2.60 (s, 1H), 2.34 (s, 1H), 1.04 (t, J = 7.4 Hz, 3H); ^{13}C NMR (101 MHz, DMSO-d_6) δ 174.1 , 165.6 , 141.7 , 132.4 , 131.7 , 128.7 , 128.5 , 127.5 , 125.7 , 123.5 , 26.1 , 8.8. HRMS(ESI) m/z calculated for $C_{16}H_{16}N_2NaO_2$ [M + Na^+] 291.1104, found 291.1119.

***N′*-(3-methylbutanoyl)-*N′*-phenylbenzohydrazide (2-2Bs).** Synthesized using Method G from **2-2Ba** (68.5 mg, 0.32 mmol), 5.0 mL of toluene, and isovaleryl chloride (40 µL, 0.32 mmol). After workup, the crude product was recrystallized from ethyl acetate:hexane, yielding **2-2Bs** as white crystals (59.1 mg, 59%), mp 157-158 °C. This compound exists as a mixture of rotamers at room temperature. ^{1}H NMR (400 MHz, DMSO-d_6) δ 11.49 (s, 0.75*1H), 11.04 (s, 0.25*1H),

7.91 (d, J = 7.6 Hz, 2H), 7.62 (t, J = 7.4 Hz, 1H), 7.55 (t, J = 7.6 Hz, 2H), 7.46 (d, J = 7.4 Hz, 2H), 7.37 (t, J = 7.9 Hz, 2H), 7.20 (t, J = 7.4 Hz, 1H), 2.44 (s, 1H), 2.16 (m, 2H), 0.99 – 0.79 (m, 6H); ^{13}C NMR (101 MHz, DMSO-d_6) δ 172.8 , 165.6 , 141.7 , 132.4 , 131.7 , 129.4 , 128.7 , 128.5 , 127.5 , 125.8 , 123.7 , 41.6 , 24.5 , 22.5. HRMS(ESI) m/z calculated for $C_{18}H_{20}N_2NaO_2$ [M + Na^+] 319.1417, found 319.1431.

methyl 2-benzoyl-1-phenylhydrazine-1-carboxylate (2-2Bt). Synthesized using Method G from **3-3Ba** (80.3 mg, 0.35 mmol), 5.0 mL of toluene, solid $NaHCO_3$ (35.0 mg, 0.35 mmol), and methyl chloroformate (29 μL, 0.35 mmol). After workup, the crude product was recrystallized from hexane, yielding **2-2Bt** white crystals (64.1 mg, 64%), mp 119-120 °C. This compound exists as a mixture of rotamers at room temperature. ^{1}H NMR (400 MHz, DMSO-d_6) δ 11.31 (s, 1H), 7.94 – 7.84 (m, 2H), 7.62 (t, J = 7.3 Hz, 1H), 7.57 – 7.43 (m, 4H), 7.22 (t, J = 8.8 Hz, 2H), 3.70 (s, 3H); ^{13}C NMR (101 MHz, DMSO-d_6) δ 165.5 , 159.8 (d, $^1J_{CF}$ = 238.9 Hz), 154.6 , 138.2 , 132.4 , 131.7 , 128.7 , 127.5 , 125.7 (br) , 115.4 (d, $^2J_{CF}$ = 22.8 Hz), 53.5; ^{19}F NMR (376 MHz, DMSO-d_6) δ -115.41 (0.38*1F), -116.84 (0.62*1F). HRMS(ESI) m/z calculated for $C_{15}H_{14}N_2NaO_3$ [M + Na^+], 293.0897, found 293.0907.

4-methyl-*N′*-phenylbenzohydrazide (2-2Ca). Synthesized using Method D from phenylhydrazine (0.49 mL, 5.0 mmol), and distilled THF (5.0 mL), 1.0 M DIBAL-H in THF (5.0 mL, 5.0 mmol), and methyl 4-methylbenzoate (0.13 mL, 1.0 mmol). After workup, the crude product was recrystallized from ethyl acetate:hexane, yielding **2-2Ca** as a white powder (221.1 mg, 98%), mp 176-177 °C. ^{1}H NMR (400 MHz, DMSO-d_6) δ 10.27 (s, 1H), 7.86 (s, 1H), 7.82

(d, J = 7.9 Hz, 2H), 7.30 (d, J = 7.9 Hz, 2H), 7.15 (t, 2H), 6.77 (d, J = 7.9 Hz, 2H), 6.71 (t, J = 7.3 Hz, 1H), 2.37 (s, 3H); ^{13}C NMR (101 MHz, DMSO-d_6) δ 166.63, 150.03, 141.97, 130.66, 129.40, 129.13, 127.72, 118.99, 112.74, 21.43. HRMS(ESI) m/z calculated for $C_{14}H_{14}N_2NaO$ [M + Na^+] 249.0998, found 249.0987.

4-fluoro-*N′*-phenylbenzohydrazide (2-2Da). Synthesized using Method D from phenylhydrazine (0.49 mL, 5.0 mmol), and distilled THF (5.0 mL), 1.0 M DIBAL-H in THF (5.0 mL, 1.2 mmol), and methyl 4-fluorobenzoate (0.13 mL, 1.0 mmol). After workup, the crude product was recrystallized from ethyl acetate:hexane yielding **2-2Da** as a white powder (166.3 mg, 72%), mp 182-184 °C. ^{1}H NMR (400 MHz, DMSO-d_6) δ 10.38 (s, 1H), 8.08 – 7.95 (m, 2H), 7.90 (s, 1H), 7.34 (t, J = 8.8 Hz, 2H), 7.22 – 7.07 (m, 2H), 6.78 (d, J = 7.9 Hz, 2H), 6.72 (t, J = 7.3 Hz, 1H); ^{13}C NMR (101 MHz, DMSO-d_6) δ 165.69, 164.52 (d, $^1J_{CF}$ = 249.0 Hz), 149.87, 130.39 (d, $^3J_{CF}$ = 9.0 Hz), 129.92 (d, J = 2.9 Hz), 129.16, 119.09, 115.87 (d, $^2J_{CF}$ = 21.8 Hz), 112.75; ^{19}F NMR (376 MHz, DMSO-d_6) δ -111.03 (td, J = 9.1, 4.7 Hz). HRMS(ESI) m/z calculated for $C_{13}H_{12}FN_2O$ [M + H^+] 231.0928, found 231.0923.

4-methoxy-*N′*-phenylbenzohydrazide (2-2Ea). Synthesized using Method D from phenylhydrazine (0.22 mL, 2.0 mmol), and distilled THF (5.0 mL), 1.0 M DIBAL-H in THF (2.0 mL, 2.0 mmol), and methyl 4-methoxybenzoate (0.1665 g, 1.0 mmol) dissolved in 1.0 mL of THF. After workup, the crude product was recrystallized from ethyl acetate:hexane yielding **2-2Ea** as a white powder (163.2 mg, 67%), mp 167-168 °C. ^{1}H NMR (400 MHz, DMSO-d_6) δ 10.21 (s, 1H), 7.91 (d, J = 8.8 Hz, 2H), 7.83 (s, 1H), 7.14 (dd, J = 8.5, 7.2 Hz, 2H), 7.03 (d, J =

8.8 Hz, 2H), 6.77 (d, J = 7.5 Hz, 2H), 6.71 (t, J = 7.3 Hz, 1H), 3.82 (s, 3H); ^{13}C NMR (101 MHz, DMSO-d_6) δ 166.24, 162.31, 150.14, 129.58, 129.14, 125.60, 118.97, 114.14, 112.75, 55.84. HRMS(ESI) m/z calculated for $C_{14}H_{14}N_2NaO_2$ [M + Na^+] 265.0947, found 265.0945.

2-bromo-*N*′-phenylbenzohydrazide (2-2Ga). Synthesized using Method D from phenylhydrazine (0.12 mL, 1.2 mmol), and distilled THF (5.0 mL), 1.0 M DIBAL-H in THF (1.2 mL, 1.2 mmol), and methyl 2-bromobenzoate (0.14 mL, 1.0 mmol). After workup, the crude product was recrystallized from ethyl acetate:hexane yielding **2-2Ga** as orange crystals (273.1 mg, 94%), mp 170-171 °C. ^{1}H NMR (400 MHz, DMSO-d_6) δ 10.19 (d, J = 2.6 Hz, 0.95*1H), 9.66 (s, 0.05*1H), 8.00 (d, J = 2.5 Hz, 0.95*1H), 7.87 (s, 0.07*1H), 7.71 (d, J = 7.9 Hz, 0.85*1H), 7.57 (d, J = 7.8 Hz, 0.11*1H), 7.54 – 7.45 (m, 2H), 7.42 (ddd, J = 9.0, 6.8, 2.5 Hz, 0.89*1H), 7.34 – 7.22 (m, 0.27*1H), 7.18 (t, J = 7.7 Hz, 0.94*2H), 7.13 (d, J = 7.8 Hz, 0.07*2H), 6.88 (d, J = 7.9 Hz, 2H), 6.74 (t, J = 7.4 Hz, 1H); ^{13}C NMR (101 MHz, DMSO-d_6) δ 167.54, 149.53, 137.84, 133.34, 131.81, 129.63, 129.16, 128.15, 119.68, 119.07, 112.79. HRMS(ESI) m/z calculated for $C_{17}H_{17}BrN_2NaO_2$ [M + Na^+] 291.0128, found 291.0134.

2-bromo-*N*'-(2-bromobenzoyl)-*N*'-phenylbenzohydrazide (2-2Gg). Synthesized using Method B from benzylhydrazine dihydrochloride (0.2066 g, 1.1 mmol), dichloromethane (5 mL), triethylamine (0.56 mL, 4.4 mmol) and 2-bromobenzoyl chloride (0.3825 g, 2.2 mmol). After workup the crude product was recrystallized from ethyl acetate and hexane, affording **2-1Gg** as an orange solid (0.1480 g, 35%), 157-159 °C. ^{1}H NMR (400 MHz, DMSO-d_6) δ 10.19 (s, 2H), 9.82 (s, 0H), 9.67 (s, 0H), 8.11 (s, 0H), 8.00 (s, 2H), 7.87 (s, 0H), 7.71 (d, J = 7.8 Hz, 2H), 7.57

(d, J = 7.8 Hz, 0H), 7.55 – 7.46 (m, 5H), 7.42 (ddd, J = 9.0, 6.7, 2.6 Hz, 2H), 7.34 – 7.23 (m, 1H), 7.18 (t, 5H), 7.13 (d, J = 8.4 Hz, 1H), 6.94 (d, J = 7.9 Hz, 1H), 6.87 (d, J = 7.9 Hz, 4H), 6.73 (t, J = 7.3 Hz, 3H); ^{13}C NMR (101 MHz, DMSO-d_6) δ 167.5 , 149.5 , 137.8 , 133.3 , 131.8 , 129.6 , 129.1 , 128.1 , 119.7 , 119.1 , 114.8 , 112.9 , 112.8. HRMS(ESI) m/z calculated for $C_{20}H_{14}Br_2N_2NaO_2$ [M + Na^+] 494.9314, found 494.9319.

***N*'-acetyl-2-bromo-*N*'-phenylbenzohydrazide (2-2Gj)**. Synthesized using Method G, from **2-2Ga** (63.3 mg, 0.23 mmol), 5.0 mL of toluene, and acetyl chloride (16 µL, 0.23 mmol). After workup, the crude product was recrystallized from ethyl acetate:hexane, yielding **2-2Gj** white crystals (75.9 mg, 80%), mp 160-161 °C. This compound exists as a mixture of rotamers at room temperature. ^{1}H NMR (400 MHz, DMSO-d_6) δ 11.5 (s, 0.85*1H), 10.9 (d, J = 27.4 Hz, 0.15*1H), 7.7 (d, J = 7.8 Hz, 1H), 7.5 (d, J = 8.1 Hz, 5H), 7.4 (t, J = 7.7 Hz, 2H), 7.3 (d, J = 7.6 Hz, 1H), 2.3 (s, 0.79*3H), 2.1 – 1.8 (m, 0.21*1H); ^{13}C NMR (101 MHz, DMSO-d_6) δ 170.9 , 166.2 , 141.0 , 135.8 , 133.2 , 132.1 , 129.1 , 128.6 , 127.9 , 126.0 , 123.7 , 119.1 , 22.1. HRMS(ESI) m/z calculated for $C_{15}H_{13}BrN_2NaO_2$ [M + Na^+] 355.0053, found 355.0059.

***N*'-*tert*-butyl-2-bromo-*N*'-phenylbenzohydrazide (2-2Gk)**. Synthesized using Method G, from **2-2Ga** (86.0 mg, 0.30 mmol), 5.0 mL of tetrahydrofuran, triethylamine (50 µL, 0.36 mmol), and pivaloyl chloride (50 µL, 0.36 mmol). After workup, the crude product was recrystallized from ethyl acetate:hexane, yielding **2-2Gk** as beige crystals (67.4 mg, 60%), mp 193-194 °C. This compound exists as a mixture of rotamers at room temperature. ^{1}H NMR (400 MHz, DMSO-d_6) δ 11.24 (s, 0.83*1H), 10.36 (s, 0.05*1H), 8.94 (s, 0.12*1H), 7.69 (d, J = 7.9 Hz, 1H), 7.56 – 7.47

(m, 1H), 7.47 – 7.32 (m, 6H), 7.32 – 7.18 (m, 1H), 1.28 (s, 0.83*9H), 1.20 (d, J = 8.9 Hz, 0.12*9H), 1.11 (s, 0.05*1H); ^{13}C NMR (101 MHz, DMSO-d_6) δ 177.3 , 166.2 , 143.1 , 135.9 , 133.3 , 132.0 , 129.1 , 128.7 , 128.4 , 127.8 , 126.9 , 126.7 , 119.2 , 112.4 , 27.9 , 27.8 , 27.1. HRMS(ESI) m/z calculated for $C_{18}H_{19}BrN_2NaO_2$ [M + Na^+] 397.0522, found 397.0516.

***N*'-*tert*-butyl-2-bromo-*N*'-phenylbenzohydrazide (2-2Gl)**. Synthesized using Method G, from **2-2Ga** (86.0 mg, 0.30 mmol), 5.0 mL of tetrahydrofuran, triethylamine (50 μL, 0.36 mmol), and isobutyryl chloride (40 μL, 0.36 mmol). After workup, the crude product was recrystallized from ethyl acetate:hexane, yielding **2-2Gl** as beige crystals (31.9 mg, 30%), mp 183-184 °C. This compound exists as a mixture of rotamers at room temperature. ^{1}H NMR (400 MHz, DMSO-d_6) δ 11.48 (s, 0.77*1H), 10.89 (s, 0.23*1H), 7.70 (d, J = 7.8 Hz, 1H), 7.57 – 7.26 (m, 7H), 7.22 (s, 1H), 3.14 (s, 1H), 1.10 (s, 6H); ^{13}C NMR (101 MHz, DMSO-d_6) δ 177.4 , 166.4 , 141.5 , 135.9 , 133.1 , 132.0 , 129.0 , 128.5 , 127.9 , 126.1 , 124.4 , 119.0 , 30.3 , 19.5 , 19.1. HRMS(ESI) m/z calculated for $C_{17}H_{17}BrN_2NaO_2$ [M + Na^+] 383.0366, found 383.0377.

2-fluoro-*N*′-phenylbenzohydrazide (2-2Ha). Synthesized using Method D from phenylhydrazine (0.22 mL, 2.0 mmol), and distilled THF (5.0 mL), 1.0 M DIBAL-H in THF (2.0 mL, 2.0 mmol), and methyl 2-fluorobenzoate (0.13 mL, 1.0 mmol). After workup, the crude product was recrystallized from ethyl acetate:hexane yielding **2-2Ha** as a white powder (228.6 mg, 99%), mp 141-142 °C. This compound exists as a mixture of rotamers. ^{1}H NMR (400 MHz, DMSO-d_6) δ 10.18 (d, J = 2.6 Hz, 0.95*1H), 9.66 (s, 0.5*1H), 8.00 (d, J = 2.6 Hz, 1H), 7.65 (td, J = 7.4, 1.8 Hz, 1H), 7.58 (tdd, J = 7.3, 5.3, 1.8 Hz, 1H), 7.33 (q, J = 8.2, 7.4 Hz, 2H), 7.22 –

7.09 (m, 2H), 6.82 (d, J = 7.9 Hz, 2H), 6.74 (t, J = 7.3 Hz, 1H). ^{13}C NMR (101 MHz, DMSO-d_6) δ 164.48, 159.58 (d, $^{1}J_{CF}$ = 248.9 Hz), 149.53, 133.08 (d, J = 8.4 Hz), 130.40 (d, J = 3.1 Hz), 129.19 , 125.04 (d, J = 3.5 Hz), 123.42 (d, J = 15.4 Hz), 119.10, 116.60 (d, J = 22.0 Hz), 112.67; ^{19}F NMR (376 MHz, DMSO-d_6) δ -116.23 (dt, J = 11.2, 6.3 Hz, 0.95*1F), -116.69 (dt, J = 10.0, 6.2 Hz, 0.5*1F). HRMS(ESI) m/z calculated for $C_{13}H_{12}FN_2O$ [M + H^+] 231.0928, found 231.0920.

***N*'-*tert*-butyl-2-bromo-*N*'-phenylbenzohydrazide (2-2Hk)**. Synthesized using Method G, from **2-2Ha** (74.1 mg, 0.32 mmol), 5.0 mL of tetrahydrofuran, triethylamine (60 µL, 0.38 mmol), and pivaloyl chloride (50 µL, 0.36 mmol). After workup, the crude product was recrystallized from ethyl acetate:hexane, yielding **2-2Hk** as beige crystals (68.8 mg, 68%), mp 147-148 °C. ^{1}H NMR (400 MHz, DMSO-d_6) δ 11.19 (s, 1H), 7.64 – 7.45 (m, 2H), 7.34 (ddd, J = 17.6, 13.2, 8.3 Hz, 6H), 7.21 (t, J = 7.1 Hz, 1H), 1.23 (s, 9H); ^{13}C NMR (101 MHz, DMSO-d_6) δ 177.3 , 163.7 , 159.2 (d, J = 250.4 Hz), 143.3 , 133.6 (d, J = 8.6 Hz), 130.0 (d, J = 2.7 Hz), 128.4 , 126.6 , 126.1 , 124.9 (d, J = 3.4 Hz), 121.6 (d, J = 14.7 Hz), 116.5 (d, J = 21.8 Hz), 27.7; ^{19}F NMR (376 MHz, DMSO-d_6) δ -112.89 (dt, J = 11.6, 6.3 Hz). HRMS(ESI) m/z calculated for $C_{18}H_{19}FN_2NaO_2$ [M + H^+] 337.1323, found 337.1325.

***N'*-acetyl-*N*-phenylbenzohydrazide (2-2Jb).** Synthesized using Method G from *N*'-phenylacetohydrazide (58.8 mg, 0.39 mmol), 5.0 mL of toluene, solid $NaHCO_3$ (33.3 mg, 0.39 mmol), and benzoyl chloride (46 µL, 0.39 mmol). After workup, the crude product was recrystallized from ethyl acetate:hexane, yielding **2-2Jb** as a white powder (69.9 mg, 70%), mp 111-113 °C. ^{1}H NMR (400 MHz, DMSO-d_6) δ 10.86 (s, 1H), 7.49 (d, J = 7.4 Hz, 2H), 7.47 – 7.25 (m, 7H), 7.21 (t, J = 6.9 Hz, 1H), 1.74 (s, 3H); 13C NMR (101 MHz, DMSO-d6) δ 169.7 ,

168.2 , 142.0 , 135.2 , 130.3 , 128.6 , 127.8 , 127.5 , 126.2 , 124.2 , 20.2. HRMS(ESI) m/z calculated for $C_{15}H_{14}N_2NaO_2$ [M + Na^+], 277.0947, found 277.0941.

***N′*-acetyl-4-fluoro-*N*-phenylbenzohydrazide (2-2Jd).** Synthesized using Method G from *N*'-phenylacetohydrazide (55.2 mg, 0.37 mmol), 5.0 mL of toluene, and 4-fluorobenzoyl chloride (44 μL, 0.37 mmol). After workup, the crude product was recrystallized from ethyl acetate:hexane, yielding **2-2Jd** white crystals (75.2 mg, 75%), mp 138-139 °C. ^{1}H NMR (400 MHz, DMSO-d_6) δ 10.88 (s, 1H), 7.55 (dd, J = 8.5, 5.5 Hz, 2H), 7.40 – 7.25 (m, 4H), 7.25 – 7.16 (m, 3H), 1.74 (s, 3H); ^{13}C NMR (101 MHz, DMSO-d_6) δ 168.8 , 168.3 , 162.9 (d, $^1J_{CF}$ = 247.6 Hz), 141.9 , 131.6 , 130.2 (d, $^3J_{CF}$ = 9.0 Hz), 128.7 , 126.3 , 124.2 , 114.9 (d, $^2J_{CF}$ = 21.9 Hz), 20.2; ^{19}F NMR (376 MHz, DMSO-d_6) δ -109.77 (tt, J = 9.3, 5.5 Hz). HRMS(ESI) m/z calculated for $C_{15}H_{13}FN_2NaO_2$ [M + Na^+], 295.0853, found 295.0849.

***N′*-acetyl-4-methoxy-*N*-phenylbenzohydrazide (2-2Je).** Synthesized using Method G from *N*'-phenylacetohydrazide (52.7 mg, 0.35 mmol), 5.0 mL of toluene, and 4-methoxybenzoyl chloride (55.8 mg, 0.35 mmol) in 0.5 mL of toluene. After workup, the crude product was recrystallized from ethyl acetate:hexane, yielding **2-2Je** as white crystals (75.2 mg, 75%), mp 135-136 °C. ^{1}H NMR (400 MHz, DMSO-d_6) δ 10.81 (s, 1H), 7.46 (d, J = 8.6 Hz, 2H), 7.32 (t, J = 7.7 Hz, 2H), 7.25 (d, J = 7.4 Hz, 2H), 7.18 (t, J = 7.3 Hz, 1H), 6.89 (d, J = 8.7 Hz, 2H), 3.76 (s, 3H), 1.76 (s, 3H); ^{13}C NMR (101 MHz, DMSO-d_6) δ 169.1 , 168.2 , 160.8 , 142.5 , 129.9 , 128.6 , 126.9 , 126.0 , 124.2 , 113.1 , 55.2 , 20.3. HRMS(ESI) m/z calculated for $C_{16}H_{16}N_2NaO_3$ [M + Na^+], 307.1053, found 307.1044.

***N′*-acetyl-4-methoxy-*N*-phenylbenzohydrazide (2-2Jh).** Synthesized using Method G from *N*'-phenylacetohydrazide (68.7 mg, 0.45 mmol), 5.0 mL of toluene, and isobutyryl chloride (47 µL, 0.45 mmol). After workup, the crude product was recrystallized from ethyl acetate:hexane, yielding **2-2Je** as white crystals (69.5 mg, 70%), mp 88-89 °C. ^{1}H NMR (400 MHz, DMSO-d_6) δ 10.85 (s, 0.74*1H), 10.39 (s, 0.26*1H), 7.68 – 6.99 (m, 5H), 2.87 (s, 1H), 2.17 – 1.69 (m, 3H), 1.35 – 0.66 (m, 6H); ^{13}C NMR (101 MHz, DMSO-d_6) δ 177.5 , 168.8 , 142.0 , 128.4 , 125.8 , 124.0 , 30.1 , 20.5 , 19.5 , 19.0. HRMS(ESI) m/z calculated for $C_{12}H_{16}N_2NaO_2$ [M + Na^+], 243.1104, found 243.1103.

***N′*-(tert-butyl)benzohydrazide (2-6Ba)**. Synthesized using Method D from *tert*-butylhydrazine hydrochloride (123.0 mg, 1.0 mmol), and distilled THF (5.0 mL), 1.0 M methyllithium in THF (1.0 mL, 1.0 mmol), 1.0 M DIBAL-H in THF (1.0 mL, 1.0 mmol), and methyl benzoate (24 µL, 0.2 mmol). After workup, the crude product was recrystallized from ethyl acetate:hexane, yielding **2-6Ba** as clear crystals (38.4 mg, 91%). Our spectroscopic data matches that of the literature.[154] ^{1}H NMR (400 MHz, $CDCl_3$) δ 7.76 (d, J = 7.2 Hz, 2H), 7.52 (t, J = 7.4 Hz, 1H), 7.44 (t, J = 7.4 Hz, 3H), 4.96 (d, J = 6.6 Hz, 1H), 1.16 (s, 9H); ^{13}C NMR (101 MHz, $CDCl_3$) δ 167.31, 132.9 , 131.75, 128.70, 126.81, 55.47, 27.23.

***N′*-acetyl-*N*-phenylpivalohydrazide (2-2Jk).** Synthesized using Method G from *N*'-phenylacetohydrazide (64.8 mg, 0.47 mmol), 5.0 mL of toluene, and pivaloyl chloride (58 µL, 0.47 mmol). After workup, the crude product was recrystallized from ethyl acetate:hexane, yielding **2-2Jk** large, clear crystals (70.9 mg, 70%), mp 90-91 °C. ^{1}H NMR (400 MHz, DMSO-

d_6) δ 10.64 (s, 1H), 7.42 – 7.25 (m, 4H), 7.24 – 7.15 (m, 1H), 1.86 (s, 3H), 1.18 (s, 9H); ^{13}C NMR (101 MHz, DMSO-d_6) δ 177.3 , 169.0 , 143.5 , 128.3 , 126.3 , 125.7 , 27.8 , 20.7. HRMS(ESI) m/z calculated for $C_{13}H_{18}N_2NaO_2$ [M + Na^+], 257.1260, found 257.1245.

***N'*-acetyl-*N*-phenylisobutyrohydrazide (2-2Jl).** Synthesized using Method G from *N*'-phenylacetohydrazide (67.8 mg, 0.45 mmol), 5.0 mL of toluene, and isobutyryl chloride (47 µL, 0.45 mmol). After workup, the crude product was recrystallized from ethyl acetate:hexane, yielding **2-2Jl** as large, clear crystals (69.5 mg, 70%), mp 88-89 °C. This compound exists as a mixture of rotamers at room temperature. ^{1}H NMR (400 MHz, DMSO-d_6) δ 10.85 (s, 0.74*1H), 10.39 (s, 0.26*1H), 7.68 – 6.99 (m, 7H), 2.87 (s, 1H), 2.17 – 1.69 (m, 4H), 1.35 – 0.66 (m, 9H); ^{13}C NMR (101 MHz, DMSO-d_6) δ 177.5 , 168.8 , 146.2 , 142.0 , 128.4 , 125.8 , 124.0 , 30.1 , 20.5 , 19.5 , 19.0. HRMS(ESI) m/z calculated for $C_{12}H_{16}N_2NaO_2$ [M + Na^+], 265.0947, found 265.0944.

***tert*-butyl-2-phenylhydrazine-1-carboxylate (2-2Pa)**. Synthesized using Method E from phenylhydrazine (0.24 mL, 2.4 mmol), di-tert-butyl carbonate (0.6334 g, 2.9 mmol), and PEG-400 (1.0 mL) were combined in a round bottom flask and allowed to stir for 1 hour at room temperature. Water (20 mL) and ethyl acetate (3 x 10 mL) and the crude product was extracted and dried over Na_2SO_4. The solution was concentrated in vacuo and recrystallized from hexane, yielding a yellow, powdery solid (0.3872 g, 76%), mp 91-93 °C. ^{1}H NMR (400 MHz, DMSO-d_6) δ 8.74 (s, 1H), 7.54 (s, 1H), 7.12 (t, J = 7.7 Hz, 2H), 6.70 – 6.59 (m, 3H), 1.41 (s, 9H); ^{13}C NMR

(101 MHz, DMSO-d_6) δ 156.1 , 149.7 , 128.7 , 118.1 , 111.7 , 78.7 , 39.4 , 28.1. HRMS(ESI) m/z calculated for $C_{11}H_{16}N_2NaO_2$ [M + Na^+], 231.1104, found 231.1102.

***tert*-butyl 2-benzoyl-2-phenylhydrazine-1-carboxylate (2-2Pb).** Synthesized using Method G from **3-2Pa** (33.0 mg, 0.16 mmol), 5.0 mL of toluene, solid $NaHCO_3$ (13.0 mg, 0.16 mmol), and benzoyl chloride (20 μL, 0.16 mmol). After workup, the crude product was recrystallized from ethyl acetate:hexane, yielding **2-2Pb** as white crystals (42.6 mg, 85%), mp 138-139 °C. This compound exists as a mixture of rotamers at room temperature. ^{1}H NMR (400 MHz, DMSO-d_6) δ 10.12 (s, 0.78*1H), 9.67 (s, 0.22*1H), 7.66 – 7.27 (m, 9H), 7.22 (t, J = 7.2 Hz, 1H), 1.27 (s, 9H); ^{13}C NMR (101 MHz, DMSO-d_6) δ 170.6 , 154.5 , 142.3 , 135.4 , 130.1 , 128.6 , 127.9 , 127.8 , 127.4 , 126.1 , 124.0 , 80.3 , 80.1 , 27.8 , 27.7. HRMS(ESI) m/z calculated for $C_{18}H_{20}N_2NaO_3$ [M + Na^+] 335.1366, found 335.1376.

tert-butyl 2-(4-fluorobenzoyl)-2-phenylhydrazine-1-carboxylate (2-2Pd). Synthesized using Method G from **2-2Pa** (62.8 mg, 0.30 mmol), 5.0 mL of toluene, solid $NaHCO_3$ (31.4 mg, 0.36 mmol), and 4-fluorobenzoyl chloride (43 μL, 0.36 mmol). After workup, the crude product was recrystallized from hexane, yielding **2-2Pd** as white crystals (57.9 mg, 58%), mp 147-148 °C. This compound exists as a mixture of rotamers at room temperature. ^{1}H NMR (400 MHz, DMSO-d_6) δ 10.54 – 9.22 (m, 1H), 7.92 – 6.76 (m, 9H), 1.63 – 0.95 (m, 9H); ^{13}C NMR (101 MHz, DMSO-d_6) δ 167.4 , 157.9 (d, $^1J_{CF}$ = 247.7 Hz), 154.4 , 141.1 , 131.6 , 128.7 , 126.4 , 124.1 , 123.2 , 115.5 (d, $^2J_{CF}$ = 20.0 Hz), 80.2 , 27.7; ^{19}F NMR (376 MHz, DMSO-d_6) δ -113.92

(0.08*1F) , -114.21 (0.30*1F), -114.75 (0.61*1F). HRMS(ESI) m/z calculated for $C_{18}H_{19}FN_2NaO_3$ [M + Na^+], 353.1272, found 353.1288.

tert-butyl 2-(4-methoxybenzoyl)-2-phenylhydrazine-1-carboxylate (2-2Pe). Synthesized using Method G from **2-2Pa** (60.6 mg, 0.29 mmol), 5.0 mL of toluene, solid $NaHCO_3$ (24.0 mg, 0.29 mmol), and 4-methoxybenzoyl chloride (50.0 mg, 0.29 mmol) dissolved in 0.5 mL of toluene. After workup, the crude product was recrystallized from hexane, yielding **2-2Pe** as a white powder (58.6 mg, 59%), mp 157-158 °C. ^{1}H NMR (400 MHz, Chloroform-*d*) δ 7.44 (d, *J* = 8.8 Hz, 2H), 7.30 – 7.10 (m, 6H), 6.73 (d, *J* = 8.5 Hz, 2H), 3.76 (s, 3H), 1.48 (s, 9H); ^{13}C NMR (101 MHz, Chloroform-*d*) δ 169.8 , 161.6 , 155.7 , 143.6 , 131.2 , 129.0 , 126.7 , 126.3 , 125.7 , 113.4 , 82.1 , 55.4 , 28.3. HRMS(ESI) m/z calculated for $C_{19}H_{22}N_2NaO_4$ [M + Na^+], 365.1472, found 365.1460.

tert-butyl 2-(2-fluorobenzoyl)-2-phenylhydrazine-1-carboxylate (2-2Ph). Synthesized using Method G from **2-2Pa** (62.2 mg, 0.30 mmol), 5.0 mL of toluene, solid $NaHCO_3$ (31.4 mg, 0.36 mmol), and 2-fluorobenzoyl chloride (43 µL, 0.36 mmol). After workup, the crude product was recrystallized from hexane, yielding **2-2Ph** as white crystals (61.3 mg, 62%), mp 108-110 °C. This compound exists as a mixture of rotamers at room temperature. ^{1}H NMR (400 MHz, Chloroform-*d*) δ 8.17 (dd, *J* = 8.7, 5.4 Hz, 1H), 7.48 (dd, *J* = 8.5, 5.5 Hz, 2H), 7.31 – 7.26 (m, 1H), 7.23 – 7.15 (m, 3H), 7.10 (s, 1H), 6.93 (t, *J* = 8.5 Hz, 2H), 1.48 (s, 9H); ^{13}C NMR (101 MHz, Chloroform-*d*) δ 169.3 , 168.2 , 165.6 , 165.3 , 162.8 , 161.4 , 155.5 , 143.1 , 133.5 (d, $^3J_{CF}$ = 9.8 Hz), 131.3 (d, $^3J_{CF}$ = 9.0 Hz), 130.5 , 129.1 , 127.1 , 125.7 , 116.4 (d, $^2J_{CF}$ = 22.1 Hz),

115.3 (d, $^{2}J_{CF}$ = 21.9 Hz), 82.4 , 28.3; ^{19}F NMR (376 MHz, Chloroform-*d*) δ -102.11 (ddd, *J* = 13.6, 8.3, 5.2 Hz, 0.39*1F), -108.43 (s, 0.61*1F). HRMS(ESI) m/z calculated for $C_{18}H_{19}FN_2NaO_3$ [M + Na^+], 353.1272, found 353.1289.

tert-butyl 2-phenyl-2-pivaloylhydrazine-1-carboxylate (2-2Pk). Synthesized using Method G from **2-2Pa** (71.6 mg, 0.34 mmol), 5.0 mL of toluene, solid $NaHCO_3$ (29.3 mg, 0.34 mmol), and pivaloyl chloride (42 μL, 0.34 mmol). After workup, the crude product was recrystallized from hexane, yielding **2-2Pk** as white crystals (74.7 mg, 74%), mp 154-155 °C. This compound exists as a mixture of rotamers at room temperature. ^{1}H NMR (400 MHz, DMSO-d_6) δ 9.96 (s, 0.77*1H), 9.65 – 9.54 (m, 0.23*1H), 7.38 – 7.28 (m, 4H), 7.24 – 7.17 (m, 1H), 1.38 (s, 0.77*9H), 1.27 (s, 0.23*9H), 1.23 (s, 9H); ^{13}C NMR (101 MHz, DMSO-d_6) δ 177.8 , 154.7 , 143.6 , 128.3 , 126.2 , 125.4 , 80.1 , 28.0 , 27.6. HRMS(ESI) m/z calculated for $C_{16}H_{24}N_2NaO_3$ [M + Na^+], 315.1679, found 315.1690.

tert-butyl 2-phenyl-2-(2-phenylacetyl)hydrazine-1-carboxylate (2-2Pm). Synthesized using Method G from **2-2Pa** (63.8 mg, 0.31 mmol), 5.0 mL of toluene, solid $NaHCO_3$ (30.4 mg, 0.31 mmol), and phenylacetyl chloride (41 μL, 0.34 mmol). After workup, the crude product was recrystallized from hexane, yielding **2-2Pm** as a yellow powder (43.9 mg, 44%), mp 130-131 °C. This compound exists as a mixture of rotamers at room temperature. ^{1}H NMR (400 MHz, Chloroform-*d*) δ 7.53 – 7.16 (m, 8H), 7.16 – 6.90 (m, 2H), 3.99 – 3.49 (m, 2H), 1.46 (s, 0.85*9H), 1.33 (s, 0.15*9H);^{13}C NMR (101 MHz, Chloroform-*d*) δ 170.8 , 155.7 , 142.1 , 134.4 ,

129.5 , 129.2 , 128.8 , 128.6 , 128.0 , 127.0 , 124.3 , 123.9 , 82.0 , 41.5 , 40.6 , 28.3. HRMS(ESI) m/z calculated for $C_{19}H_{22}N_2NaO_3$ [M + Na^+], 349.1523, found 349.1504.

tert-butyl 2-phenyl-2-propionylhydrazine-1-carboxylate (2-2Pr). Synthesized using Method G **2-2Pa** (78.7 mg, 0.38 mmol), 5.0 mL of toluene, solid $NaHCO_3$ (34.7 mg, 0.38 mmol), and propionyl chloride (33 μL, 0.38 mmol). After workup, the crude product was recrystallized from hexane, yielding **2-2Pr** as white crystals (58.4 mg, 58%), mp 93-94 °C. This compound exists as a mixture of rotamers at room temperature. ^{1}H NMR (400 MHz, Chloroform-*d*) δ 7.39 (s, 5H), 7.04 (s, 1H), 2.86 – 2.02 (m, 2H), 1.46 (s, 9H), 1.11 (s, 3H); ^{13}C NMR (101 MHz, Chloroform-*d*) δ 173.6 , 155.8 , 142.2 , 129.5 , 128.5 , 127.7 , 124.3 , 81.9 , 28.3 , 27.4 , 9.2. HRMS(ESI) m/z calculated for $C_{14}H_{20}N_2NaO_3$ [M + Na^+], 287.1366, found 287.1371.

tert-butyl 2-(3-methylbutanoyl)-2-phenylhydrazine-1-carboxylate (2-2Ps). Synthesized using Method G from **2-2Pa** (71.2 mg, 0.34 mmol), 5.0 mL of toluene, solid $NaHCO_3$ (29.8 mg, 0.34 mmol), and isovaleryl chloride (42 μL, 0.34 mmol). After workup, the crude product was recrystallized from hexane, yielding **2-2Ps** as white crystals (43.9 mg, 44%), mp 131-132 °C. ^{1}H NMR (400 MHz, Chloroform-*d*) δ 7.38 (s, 4H), 6.96 (s, 1H), 2.71 – 1.91 (m, 3H), 1.47 (s, 9H), 0.98 (d, *J* = 6.6 Hz, 2H), 0.87 (d, *J* = 6.9 Hz, 4H); ^{13}C NMR (101 MHz, Chloroform-*d*) δ 172.3 , 155.8 , 154.4 , 142.4 , 129.5 , 128.5 , 127.8 , 81.9 , 42.5 , 28.3 , 26.0 , 22.6. HRMS(ESI) m/z calculated for $C_{16}H_{24}N_2NaO_3$ [M + Na^+], 315.1679, found 315.1699.

***N′*-(4-fluorophenyl)benzohydrazide (3-3Ba)**. Synthesized using Method E from **3-3Aa·HCl** (142.6 mg, 0.88 mmol), 1.0 M aqueous NaOH (1.5 mL, 1.5 mmol), ethanol (0.3 mL), and

benzoic anhydride (199.1 mg, 0.88 mmol). After workup the crude product was recrystallized from ethyl acetate and hexane, affording, affording **3-3Ba** as a white powder (190.4 mg, 94%), mp 140-142 °C. The ^{1}H, ^{13}C, and ^{19}F NMR data of this compound in CD_3OD match that of the literature.[125] ^{1}H NMR (400 MHz, DMSO-d_6) δ 10.39 (d, J = 2.7 Hz, 1H), 7.93-7.87 (m, 3H), 7.58 (t, J = 7.3 Hz, 1H), 7.50 (t, J = 7.5 Hz, 2H), 7.00 (app t, J = 8.9 Hz, 2H), 6.80 (dd, 8.9, 4.6 Hz, 2H); ^{13}C NMR (101 MHz, DMSO-d_6) δ 166.8, 156.3 (d, $^{1}J_{CF}$ = 233.4 Hz), 146.5 , 133.4 , 132.1 , 128.9 , 127.7 , 115.6 (d, $^{2}J_{CF}$ = 22.3 Hz), 114.0 (d, $^{3}J_{CF}$ = 7.6 Hz); ^{19}F NMR (376 MHz, $CDCl_3$) δ -126.26 (tt, $^{3}J_{HF}$ = 8.6, $^{4}J_{HF}$ = 4.7 Hz). HRMS(ESI) m/z calculated for $C_{13}H_{12}FN_2O$ [M + H^+] 231.0928, found 231.0921.

***N*'-benzoyl-N-(4-fluorophenyl)benzohydrazide (3-3Bb)**. **3-3Aa·HCl** (167.2 mg, 1.0 mmol), benzoyl chloride (0.26 mL, 2.2 mmol), and triethylamine (0.70 mL, 5.0 mmol) were combined with 5.0 mL of dichloromethane in a round bottom flask and stirred at room temperature for 1 hour. Concentration of the reaction mixture in vacuo, aqueous workup, concentration of combined organic extracts in vacuo, and recrystallization (ethyl acetate-hexane) yielded **3-3Bb** as a yellow solid (305.4 mg, 91%), mp 173 °C. ^{1}H NMR (400 MHz, DMSO-d_6) δ 11.54 (s, 1H), 7.65 (br s, 2H), 7.61 – 7.49 (m, 3H), 7.50 – 7.32 (m, 7H), 7.21 (app t, J = 8.1 Hz, 2H).; ^{13}C NMR (101 MHz, DMSO-d6) δ 165.8 , 160.5 (d, $^{1}J_{CF}$ = 242.9 Hz), 135.4 , 132.7 , 132.1 , 130.9 , 129.1 , 128.4 , 128.0 , 127.7 , 116.0 (d, $^{2}J_{CF}$ = 22.7 Hz); ^{19}F NMR (376 MHz, $CDCl_3$) δ -116.82. HRMS(ESI) m/z calculated for $C_{20}H_{16}FN_2O_2$ [M + H^+] 335.1190, found 335.1173.

***N′*-benzoyl-4-fluoro-*N*-(4-fluorophenyl)benzohydrazide (2-3Bd)**. Synthesized using Method G, from **3-3Ba** (65.8 mg, 0.28 mmol), 5.0 mL of toluene, and 4-fluorobenzoyl chloride (33 μL, 0.28 mmol). After workup, the crude product was recrystallized from ethyl acetate:hexane, yielding **2-3Bd** as white crystals (65.7 mg, 65%), mp 151-153 °C. ^{1}H NMR (400 MHz, DMSO-d_6) δ 11.59 (s, 1H), 7.66 (s, 4H), 7.57 (t, J = 7.4 Hz, 1H), 7.47 (t, J = 7.5 Hz, 4H), 7.30 – 7.17 (m, 4H); ^{13}C NMR (101 MHz, DMSO-d_6) δ 165.4 , 163.0 (d, J = 248.2 Hz), 160.1 (d, $^{1}J_{CF}$ = 243.4 Hz), 132.4 , 131.5 , 131.4 , 130.2 , 128.7 , 127.3 , 126.6 , 115.6 (d, $^{2}J_{CF}$ = 22.9 Hz), 115.0 (d, $^{2}J_{CF}$ = 21.9 Hz); ^{19}F NMR (376 MHz, DMSO-d_6) δ -109.48 (s, 1F) , -115.49 (s, 1F). HRMS(ESI) m/z calculated for $C_{20}H_{14}F_2N_2NaO_2$ [M + Na^+], 375.0916 found 375.0943.

***N′*-benzoyl-*N*-(4-fluorophenyl)-4-methoxybenzohydrazide (2-3Be).** Synthesized using Method G from **2-3Ba** (59.8 mg, 0.26 mmol), 5.0 mL of toluene, and 4-methoxybenzoyl chloride (44.4 mg, 0.26 mmol) dissolved in 0.5 mL of toluene. After workup, the crude product was recrystallized from ethyl acetate:hexane, yielding **2-3Be** a white powder (70.3 mg, 74%), mp 152-153 °C. ^{1}H NMR (400 MHz, DMSO-d_6) δ 11.54 (s, 1H), 7.76 (d, J = 7.6 Hz, 2H), 7.57 (t, J = 6.7 Hz, 3H), 7.48 (t, J = 7.6 Hz, 2H), 7.42 (dd, J = 8.7, 4.9 Hz, 2H), 7.22 (t, J = 8.8 Hz, 2H), 6.92 (d, J = 8.8 Hz, 2H), 3.74 (s, 3H); ^{13}C NMR (101 MHz, DMSO-d_6) δ 169.5 , 165.3 , 161.0 , 159.9 (d, 1J_{CF} = 243.4 Hz), 138.8 , 132.3 , 131.7 , 130.0 , 128.7 , 127.4 , 126.7 , 115.5 (d, $^{2}J_{CF}$ = 22.8 Hz), 113.3 , 55.3. HRMS(ESI) m/z calculated for $C_{21}H_{17}FN_2NaO_3$ [M + Na^+], 387.1115, found 387.1130.

***N′*-acetyl-*N′*-(4-fluorophenyl)benzohydrazide (2-3Bj)**. Synthesized using Method G from **3-3Ba** (84.4 mg, 0.37 mmol), 5.0 mL of toluene, and acetyl chloride (31 μL, 0.44 mmol). After workup, the crude product was recrystallized from ethyl acetate:hexane, yielding **3-3Bj** white crystals (70.3 mg, 70%), mp 135-136 °C. This compound exists as a mixture of rotamers at room temperature. ^{1}H NMR (400 MHz, DMSO-d_6) δ 11.08 (s, 0.80*1H), 10.56 (s, 0.20*1H), 7.43 (d, J = 7.6 Hz, 0.80*2H), 7.40 – 7.33 (m, 0.20*2H), 7.15 (d, J = 7.4 Hz, 1H), 7.06 (t, J = 7.6 Hz, 2H), 7.00 (dd, J = 8.8, 5.0 Hz, 2H), 6.80 (d, J = 9.2 Hz, 0.20*2H), 6.73 (t, J = 8.7 Hz, 0.80*2H), 1.66 (s, 0.80*3H), 1.48 (s, 0.20*3H); ^{13}C NMR (101 MHz, DMSO-d_6) δ 171.3 , 165.6 , 159.7 (d, $^{1}J_{CF}$ = 242.7 Hz), 137.8 , 132.5 , 132.0 , 131.6 , 129.5 , 128.7 , 127.5 , 126.1 , 126.0 , 116.2 (d, J_{CF} = 22.4 Hz), 115.2 (d, $^{2}J_{CF}$ = 22.5 Hz), 22.0 , 21.5; ^{19}F NMR (376 MHz, DMSO-d_6) δ -113.91(0.20*1F) , -116.57 (0.80*1F). HRMS(ESI) m/z calculated for $C_{15}H_{13}FN_2NaO_2$ [M + Na^+], 295.0853, found 295.0875.

***N′-tert*-butyl-*N′*-(4-fluorophenyl)benzohydrazide (2-3Bk)**. Synthesized using Method A from **3-3Ba** (73.4 mg, 0.32 mmol), 5.0 mL of tetrahydrofuran, triethylamine (90 μL, 0.64 mmol) and pivaloyl chloride (80 μL, 0.64 mmol). After workup, the crude product was recrystallized from ethyl acetate:hexane, yielding **3-3Bk** white crystals (74.2 mg, 74%), mp 191-192 °C. ^{1}H NMR (400 MHz, Chloroform-d) δ 8.59 (s, 1H), 7.75 (d, J = 7.3 Hz, 2H), 7.58 – 7.45 (m, 3H), 7.39 (t, J = 7.6 Hz, 2H), 7.05 (t, J = 8.5 Hz, 2H), 1.20 (s, 9H); ^{13}C NMR (101 MHz, Chloroform-d) δ 167.0 , 139.3 , 132.6 , 130.8 , 130.7 , 128.9 , 127.5 , 116.2 , 116.0 , 40.2 , 28.8; ^{19}F NMR (376 MHz, Chloroform-d) δ -112.19. HRMS(ESI) m/z calculated for $C_{18}H_{19}FN_2NaO_2$ [M + Na^+], 337.1323, found 337.1334.

***N′*-isobutyryl-*N′*-(4-fluorophenyl)benzohydrazide (2-3Bl)**. Synthesized using Method A from **3-3Ba** (65.8 mg, 0.29 mmol), 5.0 mL of tetrahydrofuran, triethylamine (40 μL, 0.29 mmol) and isobutyryl chloride (60 μL, 0.57 mmol). After workup, the crude product was recrystallized from ethyl acetate:hexane, yielding **3-3Bl** white crystals (42.1 mg, 49%), mp 186-187 °C. This compound exists as a mixture of rotamers at room temperature. ^{1}H NMR (400 MHz, Chloroform-*d*) δ 9.45 (s, 0.86*1H), 9.02 (br s, 0.14*1H), 7.72 (d, *J* = 7.5 Hz, 2H), 7.56 (t, *J* = 6.2 Hz, 2H), 7.47 – 7.28 (m, 3H), 7.09 (d, *J* = 8.5 Hz, 2H), 3.01 (br s, *J* = 15.3 Hz, 0.14*1H), 2.78 – 2.53 (br s, 0.85*1H), 1.16 (d, *J* = 6.7 Hz, 7H); ^{13}C NMR (101 MHz, Chloroform-*d*) δ 177.3 , 166.4 , 137.7 , 132.1 , 131.5 , 129.9 , 128.5 , 127.3 , 116.4 (d, $^{2}J_{CF}$ = 22.9 Hz), 31.2 , 19.4. ^{19}F NMR (376 MHz, Chloroform-*d*) δ -111.75 (s, 0.86*1F), -114.43 (br s, 0.14*1F). HRMS(ESI) m/z calculated for $C_{17}H_{17}FN_2NaO_2$ [M + Na^+], 323.1166, found 323.1176.

***N′*-(4-fluorophenyl)-*N′*-propionylbenzohydrazide (2-3Br)**. Synthesized using Method G, from **3-3Ba** (80.0 mg, 0.35 mmol), 5.0 mL of toluene, and propionyl chloride (31 μL, 0.35 mmol). After workup, the crude product was recrystallized from ethyl acetate:hexane, yielding **2-3Br** white crystals (68.1 mg, 69%), mp 145-146 °C. This compound exists as a mixture of rotamers at room temperature. ^{1}H NMR (400 MHz, DMSO-d_6) δ 11.48 (s, 1H), 11.02 (s, 0H), 7.89 (d, *J* = 7.7 Hz, 2H), 7.61 (d, *J* = 7.4 Hz, 1H), 7.58 – 7.38 (m, 4H), 7.19 (t, *J* = 8.6 Hz, 2H), 2.56 (s, 1H), 2.26 (d, *J* = 61.9 Hz, 1H), 1.02 (t, *J* = 7.5 Hz, 3H); ^{13}C NMR (101 MHz, DMSO-d_6) δ 174.2 , 165.6 , 159.7 (d, $^{1}J_{CF}$ = 243.5 Hz), 138.0 , 132.5 , 131.6 , 129.8 , 128.7 , 127.5 , 126.0 , 115.2 (d, $^{2}J_{CF}$ = 22.7 Hz), 25.8 , 8.8; ^{19}F NMR (376 MHz, DMSO-d_6) δ -113.28 (s, 0.30*1F) , -116.20 (s, 0.70*1F). HRMS(ESI) m/z calculated for $C_{16}H_{15}FN_2NaO_2$ [M + Na^+] 309.1010, found 309.1023.

***N′*-(4-fluorophenyl)-*N′*-(3-methylbutanoyl)benzohydrazide (3-3Bs)**. Synthesized using Method G, 2-**3Ba** (73.5 mg, 0.32 mmol), 5.0 mL of toluene, and isovaleryl chloride (40 μL, 0.32 mmol). After workup, the crude product was recrystallized from ethyl acetate:hexane, yielding **3-3Bs** white crystals (36.7 mg, 37%), mp 119-120 °C. This compound exists as a mixture of rotamers at room temperature. ^{1}H NMR (400 MHz, DMSO-d_6) δ 11.50 (s, 0.74*1H), 11.03 (s, 0.26*1H), 7.91 (d, J = 7.7 Hz, 2H), 7.63 (d, J = 7.4 Hz, 1H), 7.55 (t, J = 7.6 Hz, 2H), 7.47 (dd, J = 8.9, 5.1 Hz, 2H), 7.32 (d, J = 8.6 Hz, 0.29*1H), 7.20 (t, J = 8.6 Hz, 0.71*1H), 2.47 – 2.17 (m, 1H), 2.17 – 1.92 (m, 2H), 0.92 (d, J = 6.5 Hz, 0.75*6H), 0.86 (s, 0.25*6H); ^{13}C NMR (101 MHz, DMSO-d_6) δ 172.9 , 165.6 , 159.7 (d, $^{1}J_{CF}$ = 245.1 Hz), 145.9 , 138.0 , 132.5 , 132.0 , 131.6 , 129.9 , 128.7 , 127.5 , 126.2 , 115.2 (d, $^{2}J_{CF}$ = 22.7 Hz), 41.9 , 41.3 , 25.4 , 24.5 , 22.5. ^{19}F NMR (376 MHz, DMSO-d_6) δ -113.25 , -116.13 (tt, J = 8.9, 4.9 Hz). HRMS(ESI) m/z calculated for $C_{18}H_{19}FN_2NaO_2$ [M + Na^+], 337.1323, found 337.1335.

methyl 2-benzoyl-1-(4-fluorophenyl)hydrazine-1-carboxylate (2-3Bt). Synthesized using Method G from **3-2Aa** (78.3 mg, 0.37 mmol), 5.0 mL of toluene, solid $NaHCO_3$ (31.1 mg, 0.37 mmol), and methyl chloroformate (29 μL, 0.37 mmol). After workup, the crude product was recrystallized from hexane, yielding **2-3Bt** as white crystals (0.0641 mg, 64%), mp 122-123 °C. ^{1}H NMR (400 MHz, DMSO-d_6) δ 11.31 (s, 1H), 7.91 (d, J = 7.2 Hz, 2H), 7.62 (t, J = 7.3 Hz, 1H), 7.53 (t, J = 7.6 Hz, 2H), 7.46 (d, J = 8.0 Hz, 2H), 7.38 (t, J = 7.9 Hz, 2H), 7.21 (t, J = 7.3 Hz, 1H), 3.71 (s, 3H); ^{13}C NMR (101 MHz, DMSO-d_6) δ 165.5 , 159.8 (d, $^{1}J_{CF}$ = 238.9 Hz), 154.6 , 138.2 , 132.4 , 131.7 , 128.7 , 127.5 , 125.7 , 115.4 (d, $^{2}J_{CF}$ = 22.8 Hz), 53.5; ^{19}F NMR

(376 MHz, DMSO-d_6) δ -115.41 (s, 0.38*1F), -116.84 (s, 0.62*1F). HRMS(ESI) m/z calculated for $C_{15}H_{13}FN_2NaO_3$ [M + Na^+], 311.0802 found 311.0822.

***N*'-(4-fluorobenzoyl)-N-(4-fluorophenyl)pivalohydrazide (2-3Dd)**. Synthesized using Method B, from **3-3Aa·HCl** (166.0 mg, 1.0 mmol), 4-fluorobenzoyl chloride (0.26 mL, 2.2 mmol), triethylamine (0.70 mL, 5.0 mmol), and dichloromethane (5.0 mL). After workup, the crude product was recrystallized from ethyl acetate:hexane yielding **3-3Dd** as a white solid (240.0 mg, 65%), mp 145-146 °C. ^{1}H NMR (400 MHz, Chloroform-*d*) δ 10.20 (s, 1H), 7.93 – 7.57 (m, 1H), 7.40 (dd, *J* = 8.5, 5.2 Hz, 2H), 7.19 (dd, *J* = 8.9, 4.7 Hz, 2H), 6.99 – 6.65 (m, 5H); ^{13}C NMR (101 MHz, Chloroform-*d*) δ 171.5 , 169.9 , 166.5 , 165.5 , 165.3 , 164.0 , 162.8 , 162.6 , 160.2 , 138.5 , 131.0 , 130.1 , 130.0 , 129.9 , 128.1 , 127.4 , 127.4 , 116.2 , 116.0 , 115.9 , 115.6 , 115.5 , 115.3; ^{19}F NMR (376 MHz, DMSO-d_6) δ -107.33 (s, 1F), -109.47 (s, 1F), -115.43 (br s, 1F). .HRMS(ESI) m/z calculated for $C_{16}H_{24}FN_2O_2$ [M + H^+] 295.1816, found 295.1825.

***N*'-(4-fluorophenyl)-4-methoxybenzohydrazide (3-3Ea)**. Synthesized using Method F from **3-3Aa·HCl** (61.4 mg, 0.38 mmol), 4-methoxybenzoyl chloride (170.8 mg, 1.0 mmol), and pyridine (3.0 mL). After workup the crude product was recrystallized from ethyl acetate and hexane, affording **3-3Ea** as pink powder (74.2 mg, 75%), mp 163-166 °C. ^{1}H NMR (400 MHz, DMSO-d_6) δ 10.23 (d, *J* = 3.1 Hz, 1H), 7.90 (d, *J* = 8.7 Hz, 2H), 7.81 (d, *J* = 3.1 Hz, 1H), 7.03 (d, *J* = 8.7 Hz, 2H), 6.98 (app t, *J* = 8.9 Hz, 2H), 6.78 (dd, *J* = 9.0, 4.5 Hz, 2H), 3.82 (s, 3H); ^{13}C NMR (101 MHz, DMSO-d_6) δ 166.3 , 162.4 , 156.3 (d, $^1J_{CF}$ = 233.3 Hz), 146.7 , 146.7 , 129.6 , 125.5 , 115.6 (d, $^2J_{CF}$ = 22.3 Hz), 114.1 , 114.0 (d, $^3J_{CF}$ = 7.5 Hz), 55.8; ^{19}F NMR (376 MHz, $CDCl_3$) δ -

126.46 (tt, $^{3}J_{HF}$ = 8.4, $^{4}J_{HF}$ = 4.6 Hz). HRMS(ESI) m/z calculated for $C_{14}H_{14}FN_2O_2$ [M + H^+] 261.1034, found 261.1031.

***N*'-(4-fluorophenyl)pivalohydrazide (3-3Ka)**. Synthesized using Method E from **3-3Aa·HCl** (70.0 mg, 0.43 mmol), 1.0 M aqueous NaOH (1.0 mL, 1.0 mmol), ethanol (0.3 mL) and pivalic anhydride (88 μL, 0.43 mmol). After workup the crude product was recrystallized from ethyl acetate and hexane, affording **3-3Ka** as a yellow powder (90.8 mg, 99%), mp 137-139 °C. ^{1}H NMR (400 MHz, DMSO-d_6) δ 9.48 (d, *J* = 3.4 Hz, 1H), 7.53 (d, *J* = 3.4 Hz, 1H), 6.97 (app t, *J* = 8.8 Hz, 2H), 6.69 (dd, *J* = 8.8, 4.7 Hz, 2H), 1.17 (s, 9H); ^{13}C NMR (101 MHz, DMSO-d_6) δ 177.54 , 156.19 (d, $^{1}J_{CF}$ = 233.0 Hz), 146.84 , 115.49 (d, $^{2}J_{CF}$ = 22.3 Hz), 113.70 (d, *J* = 7.6 Hz), 37.86 , 27.68; ^{19}F NMR (376 MHz, $CDCl_3$) δ -126.60 (tt, $^{3}J_{HF}$ = 8.8, $^{4}J_{HF}$ = 4.7 Hz). HRMS(ESI) m/z calculated for $C_{11}H_{16}FN_2O$ [M + H^+] 211.1241, found 211.1239.

***N*'-pivaloyl-N-(4-fluorophenyl)pivalohydrazide (3-3Kk)**. Synthesized using the same procedure as **3-3Bb**, from **3-3Aa·HCl** (165.0 mg, 1.0 mmol), pivaloyl chloride (0.27 mL, 2.2 mmol), triethylamine (0.70 mL, 5.0 mmol), and dichloromethane (5.0 mL); recrystallization yielded **3-3Kk** as a white solid (134.4 mg, 46%), mp 176-178 °C. ^{1}H NMR (400 MHz, DMSO-d_6) δ 10.35 (s, 1H), 7.36 (dd, *J* = 8.8, 5.2 Hz, 2H), 7.16 (app t, *J* = 8.8 Hz, 2H), 1.19 (s, 9H), 1.10 (s, 9H); ^{13}C NMR (101 MHz, DMSO-d_6) δ 177.9 , 176.8 , 160.3 (d, $^{1}J_{CF}$ = 242.6 Hz), 140.1 , 128.4 (d, $^{3}J_{CF}$ = 8.5 Hz), 115.2 (d, $^{2}J_{CF}$ = 22.6 Hz), 38.0 , 28.2 , 27.0; ^{19}F NMR (376 MHz, $CDCl_3$) δ -115.50. HRMS(ESI) m/z calculated for $C_{20}H_{14}F_3N_2O_2$ [M + H^+] 371.1002, found 371.1006.

***N*'-isobutyryl-N-(4-fluorophenyl)hydrazide (2-3ll)**. Synthesized using the same procedure as **3-3Bb**, from **3-3Aa·HCl** (163.2 mg, 1.0 mmol), isobutyryl chloride (0.23 mL, 2.2 mmol), triethylamine (0.70 mL, 5.0 mmol), and dichloromethane (5.0 mL). After workup, the crude product was recrystallized from ethyl acetate:hexane to yield **3-3ll** as a white solid (215.4 mg, 82%), mp 148-149 °C. ^{1}H NMR (400 MHz, DMSO-d_6) δ 10.88 (s, 1H), 10.30 (s, 0H), 7.55 – 7.26 (m, 2H), 7.19 (t, J = 8.7 Hz, 2H), 3.10 – 2.64 (m, 1H), 2.48 – 2.28 (m, 1H), 1.14 – 0.93 (m, 12H); ^{13}C NMR (101 MHz, DMSO-d_6) δ 177.5 , 175.3 , 138.2 , 126.2 , 115.2 , 115.0 , 32.2 , 30.0 , 19.4 , 18.9; ^{19}F NMR (376 MHz, DMSO-d_6) δ -113.38 , -116.25. HRMS(ESI) m/z calculated for $C_{14}H_{19}FN_2NaO_2$ [M + Na^+] 289.1323, found 289.1335.

***tert*-butyl 2-(4-fluorophenyl)hydrazine-1-carboxylate (2-3Pa).** Synthesized using Method E from **3-3Aa·HCl** (359.5 mg, 2.2 mmol), 1.0 M aqueous NaOH (3.0 mL, 3.0 mmol), ethanol (0.3 mL) and di-*tert*-butyl dicarbonate (523.0 mg, 2.4 mmol). After workup the crude product was recrystallized from hexane, affording **3-3Pa** as yellow crystals (363.5 mg, 73%), mp 115 °C. ^{1}H NMR (400 MHz, Chloroform-*d*) δ 6.93 (t, J = 8.6 Hz, 2H), 6.78 (dd, J = 8.8, 4.5 Hz, 2H), 6.37 (s, 1H), 5.68 (s, 1H), 1.45 (s, 9H); ^{13}C NMR (101 MHz, Chloroform-*d*) δ 157.9 (d, J = 237.8 Hz), 156.4 , 144.7 , 115.9 , 115.7 , 114.5 , 114.4 , 81.6 , 28.4; ^{19}F NMR (376 MHz, Chloroform-*d*) δ -124.23 (tt, J = 8.7, 4.6 Hz). HRMS(ESI) m/z calculated for $C_{11}H_{15}FN_2NaO_2$ [M + Na^+] 249.1010, found 249.1009.

***tert*-butyl 2-benzoyl-2-(4-fluorophenyl)hydrazine-1-carboxylate (2-3Pb).** Synthesized using Method G from **2-3Pa** (67.3 mg, 0.30 mmol), 5.0 mL of toluene, solid $NaHCO_3$ (25.2 mg, 0.30 mmol), and benzoyl chloride (35 μL, 0.30 mmol). After workup the crude product was recrystallized from ethyl acetate:hexane, yielding a white powder (70.7 mg, 72%), mp 155-156 °C. This compound exists as a mixture of rotamers at room temperature. ^{1}H NMR (400 MHz, DMSO-d_6) δ 10.12 (s, 0.76*1H), 9.67 (s, 0.24*1H), 7.78 – 7.26 (m, 7H), 7.22 (t, J = 8.2 Hz, 2H), 1.27 (d, J = 7.1 Hz, 9H); ^{13}C NMR (101 MHz, DMSO-d_6) δ 159.9 (d, $^1J_{CF}$ = 243.6 Hz), 154.4 , 138.7 , 135.2 , 130.2 , 127.8 , 127.4 , 126.4 , 115.4 (d, $^2J_{CF}$ = 22.6 Hz), 80.2 , 27.8 , 27.7; ^{19}F NMR (376 MHz, DMSO-d_6) δ -115.07 – -116.29 (m). HRMS(ESI) m/z calculated for $C_{18}H_{19}FN_2NaO_3$, 353.1272, found 353.1242.

***N'*-(4-methoxyphenyl)benzohydrazide (2-5Ba).** Synthesized using Method E from 4-methoxyphenylhydrazine hydrochloride (71.7 mg, 0.41 mmol), 3.0 mL of PEG-400, and $NaHCO_3$ (103.4 mg, 1.23 mmol), and benzoic anhydride (113.0 mg, 0.50 mmol. After workup, the crude product was recrystallized from ethyl acetate:hexane, yielding **2-5Ba** as an orange solid (63.2 mg, 64%), mp 128-130 °C. ^{1}H NMR (400 MHz, DMSO-d_6) δ 10.32 (d, J = 3.6 Hz, 1H), 7.89 (d, J = 7.1 Hz, 2H), 7.58 – 7.45 (m, 4H), 6.76 (s, 4H), 3.64 (s, 3H); ^{13}C NMR (101 MHz, DMSO-d_6) δ 166.2 , 152.7 , 143.3 , 133.1 , 131.5 , 128.4 , 127.2 , 114.2 , 113.8 , 55.3. HRMS(ESI) m/z calculated for $C_{14}H_{14}N_2NaO_2$ [M + Na^+], 265.0947, found 265.0944.

***N'*-benzoyl-N-(4-methoxyphenyl)benzohydrazide (2-5Bb)**. Synthesized by Method B from **2-5Aa·HCl** (0.0716 mg, 0.41 mmol), 5.0 mL of dichloromethane, benzoyl chloride (mL, 0.41 mmol), and triethylamine (0.70 mL, 5.0 mmol). After workup, the crude product was

recrystallized from ethyl acetate:hexane to yield **2-5Bb** as a brown solid (141.3 mg, 91%), mp 173 °C. ^{1}H NMR (400 MHz, DMSO-d_6) δ 11.45 (s, 1H), 8.11 – 7.18 (m, 12H), 6.93 (s, 2H), 3.74 (s, 3H); ^{13}C NMR (101 MHz, DMSO-d_6) δ 165.2 , 157.6 , 135.3 , 132.1 , 131.9 , 130.2 , 128.5 , 127.8 , 127.2 , 113.9 , 55.3. HRMS(ESI) m/z calculated for $C_{21}H_{18}N_2NaO_3$ [M + Na^+], 369.1210, found 369.1224.

***N′*-benzylidenebenzohydrazide (2-8)**. Benzoyl hydrazine (1.0336 g, 7.6 mmol), hexanes (30 mL), and benzaldehyde (1.16 mL, 11.4 mmol) were combined in a round bottom flask, and allowed to stir at room temperature for 2 hours. Over the course of this time, the crystalline solid starting material became a milky suspension of a fine white powder. *N′*-benzylidenebenzohydrazide was isolated by filtration, yielding **2-8** as a powdery white solid (1.6595 g, 98%), mp 207-208 °C. This compound is known.[30] ^{1}H NMR (500 MHz, DMSO-d_6) δ 11.87 (s, 1H), 8.46 (s, 1H), 7.92 (d, J = 7.5 Hz, 2H), 7.74 (d, J = 8.0 Hz, 2H), 7.60 (t, J = 7.3 Hz, 3H), 7.53 (t, J = 7.5 Hz, 2H), 7.46 (q, J = 7.4, 6.7 Hz, 3H); ^{13}C NMR (101 MHz, DMSO-d_6) δ 163.2 , 147.8 , 134.3 , 133.4 , 131.7 , 130.1 , 128.8 , 128.5 , 127.6 , 127.1. HRMS(ESI) m/z calculated for $C_{14}H_{13}N_2O$ [M + H^+] 225.1022, found 225.1015.

***N*'-(4-fluorophenyl)acetohydrazide (3-3Ja)**. Synthesized using Method E from **3-3Aa·HCl** (97.6 mg, 0.60 mmol), 1.0 M aqueous NaOH (1.0 mL, 1.0 mmol), ethanol (0.3 mL) and acetic anhydride (57 μL, 0.60 mmol). After workup the crude product was recrystallized from ethyl acetate and hexane, affording **3-3Ja** as a white powder (69.6 mg, 69%), mp 147 °C. The melting point and ^{1}H and ^{13}C NMR spectroscopic data of this compound in d_6-DMSO match the literature[93]; we report data in $CDCl_3$ below here since kinetic studies were performed in this

solvent. This compound exists in $CDCl_3$ and DMSO-d_6 as a mixture of conformers. ^{1}H NMR (400 MHz, $CDCl_3$) δ 6.98 (app t, J = 8.7 Hz, 2H*0.25), 6.96 (app. t, J = 8.7 Hz, 2H*0.75), 6.80 (dd, J = 8.9, 4.5 Hz, 2H*0.75), 6.74 (dd, J = 8.8, 4.3 Hz, 2H*0.25), 6.07 (br s, 0.75*1H), 5.77 (s, 0.25*1H), 2.11 (s, 0.25*3H), 2.08 (s, 0.75*3H); ^{13}C NMR (101 MHz, DMSO-d_6) δ 175.5, 169.5, 156.2 (d, $^1J_{CF}$ = 233.3 Hz), 146.4, 146.3, 145.8, 116.0, 115.8, 115.5 (d, $^2J_{CF}$ = 22.6 Hz), 113.7 (d, $^3J_{CF}$ = 7.4 Hz), 113.4, 113.3, 40.6, 40.4, 40.2, 39.9, 39.7, 39.5, 39.3, 21.0, 19.6.; ^{19}F NMR (376 MHz, $CDCl_3$) δ -126.21 (*tt*, $^3J_{HF}$ = 8.5 Hz, $^4J_{HF}$ = 4.4 Hz, 0.25*1F), -126.51 (*tt*, $^3J_{HF}$ = 8.5 Hz, $^4J_{HF}$ = 4.4 Hz, 0.75*1F). HRMS(ESI) m/z calculated for $C_8H_{10}FN_2O$ [M + H^+] 169.0772, found 169.0766.

***N*'-(4-fluorophenyl)-4-chlorobenzohydrazide (3-3Fa).** Synthesized using Method E From **3-3Aa·HCl** (61.4 mg, 0.38 mmol), 1.0 M aqueous NaOH (1.0 mL, 1.0 mmol), ethanol (0.3 mL), and 4-chlorobenzoic anhydride (128.0 mg, 0.38 mmol). After workup the crude product was recrystallized from ethyl acetate and hexane, affording **3-3Fa** as a white powder (92.5 mg, 92%), mp 162-164 °C. ^{1}H NMR (400 MHz, DMSO-d_6) δ 10.47 (s, 1H), 7.93 (d, J = 8.5 Hz, 2H), 7.58 (d, J = 8.5 Hz, 2H), 6.99 (app t, J = 8.8 Hz, 2H), 6.79 (dd, J = 8.9, 4.5 Hz, 2H); ^{13}C NMR (101 MHz, DMSO-d_6) δ 165.8 , 156.4 (d, $^1J_{CF}$ = 233.3 Hz), 146.3 , 137.0 , 132.1 , 129.7 , 129.0 , 115.6 (d, $^2J_{CF}$ = 22.3 Hz), 114.0 (d, $^3J_{CF}$ = 7.7 Hz); ^{19}F NMR (376 MHz, $CDCl_3$) δ -126.02 (tt, $^3J_{HF}$ = 8.7, $^4J_{HF}$ = 4.6 Hz). HRMS(ESI) m/z calculated for $C_{13}H_{11}ClFN_2O$ [M + H^+] 265.0538, found 265.0543.

***N*-(4-fluorophenyl)acetohydrazide hydrochloride (3-3Aj·HCl)**. Synthesized by Method H from *tert*-butyl-2-(4-fluorophenyl)hydrazine-1-carboxylate (90.6 mg, 0.40 mmol), acetyl chloride (28 μL, 0.40 mmol), $NaHCO_3$ (34.0 mg, 0.40 mmol), and toluene (3.0 mL) to afford 107.2 mg (99%) of the intermediate. A portion of this compound (76.2 mg, 0.28 mmol) was dissolved in 4 M HCl in dioxane (0.71 mL, 2.8 mmol). After 1 hr, trituration with diethyl ether afforded **3-3Aj·HCl** as a white solid (55.3 mg, 95%), mp 161-164 °C. This compound exists in $CDCl_3$ and DMSO-d_6 as a mixture of conformers. ^{1}H NMR (400 MHz, DMSO-d_6) δ 7.71 (br s, 0.94*2H), 7.39 (app t, J = 8.7 Hz, 0.85*2H), 7.12 (m, 0.21*2H), 2.26 (br s, 0.14*3H), 1.91 (s, 0.86*3H); ^{13}C NMR (101 MHz, DMSO-d_6) δ 168.5 , 162.8 (d, $^1J_{CF}$ = 240.7 Hz), 134.5 , 131.7 , 117.8 (d, $^2J_{CF}$ = 23.5 Hz), 21.3; ^{19}F NMR (376 MHz, $CDCl_3$) δ -116.36 (tt, $^3J_{HF}$ = 8.4, $^4J_{HF}$ = 4.8 Hz, 0.86*1F), -118.55 (0.14*1F). HRMS(ESI) m/z calculated for $C_8H_{10}FN_2O$ [M + H^+] 169.0772, found 169.0763.

***N*-(4-fluorophenyl)benzohydrazide hydrochloride (3-3Ab·HCl)**. Synthesized by Method H from *tert*-butyl-2-(4-fluorophenyl)hydrazine-1-carboxylate (67.3 mg, 0.30 mmol), benzoyl chloride (35 μL, 0.30 mmol), and solid $NaHCO_3$ (25.4 mg, 0.20 mmol) in toluene (3.0 mL), to afford 70.7 mg (72%) of the intermediate. A portion of this compound (45.4 mg, 0.14 mmol) was dissolved in 4 M HCl in dioxane (0.50 mL, 2.1 mmol), and methanol (1 drop); after reaction was judged complete by TLC, trituration with diethyl ether afforded **3-3Aj·HCl** as a white solid (32.5 mg, 89%), mp 169-172 °C. ^{1}H NMR (400 MHz, DMSO-d_6) δ 10.75-8.04 (br s, 3H), 7.50 (dd, J = 8.8, 4.9 Hz, 2H), 7.44 – 7.35 (m, 3H), 7.36 – 7.27 (m, 2H), 7.21 (app t, J = 8.8 Hz, 2H); ^{13}C NMR (101 MHz, DMSO-d6) δ 168.7 , 161.8 (d, $^1J_{CF}$ = 249.0 Hz), 136.8 , 133.3 , 131.4 , 131.0 , 129.0 , 128.6 , 116.5 (d, $^2J_{CF}$ = 23.0 Hz); ^{19}F NMR (376 MHz, $CDCl_3$) δ -117.83 (tt, $^3J_{HF}$ = 8.4,

$^4J_{HF}$ = 4.9 Hz). HRMS(ESI) m/z calculated for $C_{13}H_{12}FN_2O$ [M + H^+] 231.0928, found 231.0920.

***N*-(4-fluorophenyl)-4-methoxybenzohydrazide hydrochloride (3-3Ae·HCl).** Synthesized using Method H from *tert*-butyl-2-(4-fluorophenyl)hydrazine-1-carboxylate (62.7 mg, 0.28 mmol), 4-methoxybenzoyl chloride (48.6 mg, 0.28 mmol), $NaHCO_3$ (23.8 mg, 0.28 mmol), and toluene (3.0 mL). Recrystallization from hexane yielded 84.2 mg (84%) of the intermediate as a white solid. The intermediate (84.2 mg, 0.234 mmol) was dissolved 4 M HCl in dioxane (1.0 mL, 4.0 mmol), affording **3-3Ae·HCl** as a white solid (64.3 mg, 93%), mp 195-196 °C. ^{1}H NMR (400 MHz, DMSO-d_6) δ 10.55 – 7.83 (br s, 3H), 7.49 (dd, J = 8.9, 4.8 Hz, 2H), 7.39 (d, J = 8.7 Hz, 2H), 7.25 (app t, J = 8.7 Hz, 2H), 6.86 (d, J = 8.8 Hz, 2H), 3.73 (s, 3H).; ^{13}C NMR (101 MHz, DMSO-d_6) δ 168.3 , 161.8 (d, $^1J_{CF}$ = 246.9 Hz), 161.8 , 137.3 , 131.5 , 131.0 (d, $^3J_{CF}$ = 8.1 Hz), 124.7 , 116.7 (d, $^2J_{CF}$ = 23.0 Hz), 114.0 , 55.8; ^{19}F NMR (376 MHz, $CDCl_3$) δ -118.14 (tt, $^3J_{HF}$ = 8.5, $^4J_{HF}$ = 4.8 Hz). HRMS(ESI) m/z calculated for $C_{14}H_{14}FN_2O_2$ [M + H^+] 261.1034, found 261.1036.

***N*-(4-fluorophenyl)-4-chlorobenzohydrazide (3-3Af·HCl).** Synthesized using Method H from *tert*-butyl-2-(4-fluorophenyl)hydrazine-1-carboxylate (66.2 mg, 0.292 mmol), 4-chlorobenzoyl chloride (37 μL, 0.292 mmol), $NaHCO_3$ (24.7 mg, 0.292 mmol), and toluene (3.0 mL). Recrystallization from hexane yielded 100.9 mg (95%) of the intermediate as a white solid. The intermediate (100.9 mg, 0.277 mmol) was dissolved 4 M HCl in dioxane (1.0 mL, 4.0 mmol), affording **3-3Af·HCl** as a white solid (56.9 mg, 68%), mp 195-196 °C. ^{1}H NMR (400 MHz, DMSO-d_6) δ 7.50 (dd, J = 8.7, 5.0 Hz, 2H), 7.46 – 7.38 (m, 4H), 7.23 (t, J = 8.7 Hz, 2H), 7.03 –

6.07 (br s, 3H); ^{13}C NMR (101 MHz, DMSO-d_6) δ 167.2 , 161.4 (d, $^{1}J_{CF}$ = 247.8 Hz), 135.6 , 131.2 , 130.6 , 128.8 , 128.3 , 127.7 , 116.2 (d, $^{2}J_{CF}$ = 22.9 Hz); ^{19}F NMR (376 MHz, $CDCl_3$) δ -117.19 (tt, $^{3}J_{HF}$ = 8.5, $^{4}J_{HF}$ = 4.9 Hz). HRMS(ESI) m/z calculated for $C_{13}H_{11}ClFN_2O$ [M + H^+] 265.0538, found 265.0553.

***N*-(4-fluorophenyl)pivalohydrazide hydrochloride (3-3Ak·HCl)**. Synthesized using Method H from *tert*-butyl-2-(4-fluorophenyl)hydrazine-1-carboxylate (62.7 mg, 0.28 mmol), pivaloyl chloride (31 μL, 0.25 mmol), $NaHCO_3$ (21.3 mg, 0.25 mmol), and toluene (3.0 mL). Recrystallization from hexane yielded 45.7 mg (60%) of the intermediate as a white solid. A portion of this compound (35.9 mg, 0.12 mmol) was dissolved in 4 M HCl in dioxane (1.0 mL, 4.0 mmol) containing methanol (1 drop) were combined. After the reaction was judged complete by TLC, trituration with diethyl ether afforded **3-3Ak·HCl** as a white solid (32.5 mg, 84%), mp 172-175 °C. ^{1}H NMR (400 MHz, DMSO-d_6) 7.64 (dd, *J* = 8.8, 4.9 Hz, 2H), 7.36 (app t, *J* = 8.6 Hz, 2H), 1.06 (s, 9H); ^{13}C NMR (101 MHz, DMSO-d_6) δ 177.0 , 162.6 (d, $^{1}J_{CF}$ = 247.1 Hz), 132.5 , 116.5 (d, $^{2}J_{CF}$ = 22.9 Hz), 28.6; ^{19}F NMR (376 MHz, $CDCl_3$) δ -117.83 (tt, $^{3}J_{HF}$ = 8.4, $^{4}J_{HF}$ = 4.9 Hz). HRMS(ESI) m/z calculated for $C_{11}H_{16}FN_2O$ [M + H^+] 211.1247, found 211.1243.

***N*'-acetyl-N-(4-fluorophenyl)acetohydrazide (3-3Jj)**. This compound was prepared according to a literature method for diacetylphenylhydrazine synthesis.[137] **3-3Aa·HCl** (100.0 mg, 0.62 mmol) and acetic anhydride (1.5 mL, 15.9 mmol) were combined and heated to 100 °C for 1 hour. The reaction was concentrated in vacuo and chromatographed to afford **3-3Jj** as a clear

viscous film (129.9 mg, 99%). This compound exists in $CDCl_3$ as a mixture of conformers. ^{1}H NMR (400 MHz, $CDCl_3$) δ 9.39 (s, 0.40*1H), 8.76 (s, 0.60*1H), 7.45 – 7.35 (m, 0.60*2H), 7.35 – 7.27 (m, 0.40*2H), 7.06 (t, J = 8.4 Hz, 0.60*2H), 6.96 (t, J = 8.4 Hz, 0.40*2H), 2.36 – 1.99 (m, 0.60*3H), 2.00 – 1.91 (m, 0.7*6H); ^{13}C NMR (101 MHz, $CDCl_3$) δ 172.8 , 169.8 , 169.6 , 169.2 , 162.9 (d, $^1J_{CF}$ = 249.4 Hz), 160.5 (d, $^1J_{CF}$ = 246.9 Hz), 138.1 , 137.2 , 129.6 (d, $^3J_{CF}$ = 8.7 Hz), 127.1 (d, $^3J_{CF}$ = 6.3 Hz), 116.5 (d, $^2J_{CF}$ = 22.8 Hz), 115.7 (d, $^2J_{CF}$ = 22.7 Hz), 22.1 , 21.3 , 20.7 , 19.7; ^{19}F NMR (376 MHz, $CDCl_3$) δ -117.26 (m, 0.39*1F), -117.72 (0.05*1F), -114.72 (tt, $^3J_{HF}$ = 9.0, $^4J_{HF}$ = 4.9 Hz, 0.56*1F). HRMS(ESI) m/z calculated for $C_{10}H_{12}FN_2O_2$ [M + H^+] 211.0877, found 211.0885.

***N*'-(4-methoxybenzoyl)-N-(4-methoxy)-(4-fluorophenyl)benzohydrazide (3-3Ee)**.

Synthesized using the same procedure for **3-3Bb**, from **3-3Aa·HCl** (28.8 mg, 0.18 mmol), 4-methoxybenozyl chloride (61.8 mg, 0.35 mmol), triethylamine (0.13 mL, 0.9 mmol), and dichloromethane (2.0 mL); recrystallization yielded **3-3Ee** as a white powder (40.1 mg, 57%), mp 122-124 °C. ^{1}H NMR (400 MHz, $CDCl_3$) δ 9.35 (s, 1H), 7.79 (d, J = 8.7 Hz, 2H), 7.43 (d, J = 8.7 Hz, 2H), 7.26 – 7.20 (m, 2H), 6.91 (app t, J = 8.6 Hz, 2H), 6.79 (d, J = 8.8 Hz, 2H), 6.72 (d, J = 8.7 Hz, 2H), 3.81 (s, 3H), 3.77 (s, 3H).; ^{13}C NMR (101 MHz, $CDCl_3$) δ 170.0 , 166.4 , 162.8 , 161.6 , 161.1 (d, $^1J_{CF}$ = 247.7 Hz), 139.5 , 131.1 , 129.4 , 128.1 (d, $^3J_{CF}$ = 8.7 Hz), 125.6 , 123.7 , 115.8 (d, $^2J_{CF}$ = 23.0 Hz), 113.8 , 113.3 , 55.3; ^{19}F NMR (376 MHz, $CDCl_3$) δ -117.32 (tt, $^3J_{HF}$ = 8.3 Hz, $^4J_{HF}$ = 4.6 Hz). HRMS(ESI) m/z calculated for $C_{22}H_{20}FN_2O_4$ [M + H^+] 395.1402, found 395.1399.

***N*'-(4-chlorobenzoyl)-N-(4-chloro)-(4-fluorophenyl)benzohydrazide (3-3Ff).** Synthesized using the same procedure for **3-3Bb**, from **3-3Aa·HCl** (40.6 mg, 0.25 mmol), 4-chlorobenzoyl chloride (71 μL, 0.55 mmol), triethylamine (0.173 mL, 1.24 mmol) and dichloromethane (2.0 mL); recrystallization yielded **3-3Ff** as a yellow solid (57.3 mg, 57%), mp 183-184 °C. ^{1}H NMR (400 MHz, $CDCl_3$) δ 9.45 (s, 1H), 7.71 (d, J = 8.2 Hz, 2H), 7.38 (d, J = 8.2 Hz, 2H), 7.31 (d, J = 8.5 Hz, 2H), 7.28 – 7.10 (m, 4H), 6.94 (app t, J = 8.5 Hz, 2H); ^{13}C NMR (101 MHz, $CDCl_3$) δ 169.3 , 165.7 , 161.5 (d, $^{1}J_{CF}$ = 248.9 Hz), 139.0 , 138.4 , 137.4 , 131.9 , 130.2 , 129.5 , 129.0 , 128.8 , 128.5 , 128.3 (d, $^{3}J_{CF}$ = 7.9 Hz), 116.22 (d, $^{2}J_{CF}$ = 22.8 Hz); ^{19}F NMR (376 MHz, $CDCl_3$) δ -115.73. HRMS(ESI) m/z calculated for $C_{20}H_{14}Cl_2FN_2O_2$ [M + H^+] 403.0411, found 403.0378.

One-Step Synthesis

Preparative reactions for the synthesis of proximal aroyl arylhydazines were prepared using Method **I**. Method I: hydrazine hydrochlorides **3-3Aa**, **3-2Aa**, **3-4Aa**, or **3-5Aa** (0.47 mmol), and triethylamine (1.03 mmol) were combined in 5.0 mL of dichloromethane at room temperature and allowed to stir for 5 minutes in open air. After the solution appeared to be homogeneous, a 0.25 M solution of **3-10b**, **3-10c**, or **3-10d** was added slowly (~1.88. mL, 0.47 mmol) at a rate of 0.10 mL/5 minutes and was monitored by TLC for full conversion of the starting material. After the last of the solution was added, the reaction was allowed to continue stirring for another 5 minutes. After stirring, the reaction solution was directly chromatographed by silica column with 20:80 ethyl acetate and hexane, with a solvent gradient of increasing ethyl acetate. Concentration in vacuo after chromatography yielded the desired product.

***N*-(4-fluorophenyl)benzohydrazide (3-3Ab)**. Synthesized using Method I from **3-3Aa·HCl** (76.5 mg, 0.47 mmol), 0.25 M benzoyl chloride in dichloromethane (1.88 mL, 0.47 mmol), triethylamine (0.14 mL, 1.03 mmol) and dichloromethane (5.0 mL); chromatography afforded **3-3Ab** as an orange solid (63.4 mg, 59%), mp 110-113 °C. ^{1}H NMR (400 MHz, Chloroform-*d*) δ 7.31 (t, *J* = 7.5 Hz, 3H), 7.24 (d, *J* = 7.2 Hz, 2H), 7.10 (dd, *J* = 8.8, 4.8 Hz, 2H), 6.91 (t, *J* = 8.5 Hz, 2H), 4.95 (s, 2H); ^{13}C NMR (101 MHz, Chloroform-*d*) δ 169.6 , 161.0 (d, $^{1}J_{CF}$ = 247.4 Hz), 139.7 , 134.6 , 130.5 , 128.8 , 128.2 , 128.0 (d, $^{3}J_{CF}$ = 8.5 Hz), 115.9 (d, $^{2}J_{CF}$ = 22.9 Hz); ^{19}F NMR (376 MHz, Chloroform-*d*) δ -117.85 (tt, *J* = 8.3, 4.8 Hz). HRMS(ESI) m/z calculated for $C_{13}H_{12}FN_2O$ [M + H^+] 231.0928, found 231.0931.

***N*-(4-fluorophenyl)-4-methoxybenzohydrazide (3-3Ae)**. Synthesized using Method I from **3-3Aa·HCl** (76.2 mg, 0.47 mmol), 0.25 M 4-methoxybenzoyl chloride in dichloromethane (1.88 mL, 0.47 mmol), triethylamine (0.14 mL, 1.03 mmol) and dichloromethane (5.0 mL); chromatography afforded **3-3Ae** as an orange solid (73.2 mg, 60%), mp 114-116 °C. ^{1}H NMR (400 MHz, Chloroform-*d*) δ 7.30 (d, *J* = 8.8 Hz, 2H), 7.15 – 7.03 (m, 2H), 6.93 (t, *J* = 8.5 Hz, 2H), 6.72 (d, *J* = 8.8 Hz, 2H), 4.95 (s, 2H), 3.77 (s, 3H); ^{13}C NMR (101 MHz, Chloroform-*d*) δ 169.4 , 161.3 , 160.9 (d, $^{1}J_{CF}$ = 247.1 Hz), 140.3 , 131.0 , 128.0 (d, $^{3}J_{CF}$ = 8.5 Hz), 126.4 , 115.9 (d, $^{2}J_{CF}$ = 22.9 Hz), 113.4 , 55.4; ^{19}F NMR (376 MHz, Chloroform-*d*) δ -118.2 (tt, *J* = 8.3, 4.8 Hz). HRMS(ESI) m/z calculated for $C_{14}H_{14}FN_2O_2$ [M + H^+] 261.1034, found 261.1043.

4-chloro-*N*-(4-fluorophenyl)benzohydrazide (3-3Af). Synthesized using Method I from **3-3Aa·HCl** (76.2 mg, 0.47 mmol), 0.25 M 4-chlorobenzoyl chloride in dichloromethane (1.88 mL,

0.47 mmol), triethylamine (0.14 mL, 1.03 mmol) and dichloromethane (5.0 mL); chromatography afforded **3-3Af** as a yellow solid (80.0 mg, 64%), mp 209-211 °C. ^{1}H NMR (400 MHz, $CDCl_3$) δ 7.27 (d, J = 8.4 Hz, 2H), 7.21 (d, J = 8.4 Hz, 2H), 7.10 (dd, J = 8.8, 4.9 Hz, 2H), 6.94 (app t, J = 8.5 Hz, 2H), 4.95 (s, 2H); ^{13}C NMR (101 MHz, $CDCl_3$) δ 168.3 , 161.0 (d, $^{1}J_{CF}$ = 248.0 Hz), 139.2 , 136.5 , 132.8 , 130.2 , 128.3 , 127.9 (d, $^{3}J_{CF}$ = 8.6 Hz), 116.0 (d, $^{2}J_{CF}$ = 22.9 Hz); ^{19}F NMR (376 MHz, $CDCl_3$) δ -117.22 (tt, $^{3}J_{HF}$ = 8.4, $^{4}J_{HF}$ = 4.9 Hz). HRMS(ESI) m/z calculated for $C_{13}H_{11}FClN_2O$ [M + H^+] 265.0538, found 265.0539.

***N*-phenylbenzohydrazide (3-2Ab)**. Synthesized using Method I from **3-2Aa·HCl** (68.1 mg, 0.47 mmol), 0.25 M benzoyl chloride in dichloromethane (1.88 mL, 0.47 mmol), triethylamine (0.14 mL, 1.03 mmol) and dichloromethane (5.0 mL); chromatography afforded **3-2Ab** as an orange solid (51.2 mg, 51%). The ^{1}H and ^{13}C NMR spectroscopic data of this compound match the literature.[155-156] ^{1}H NMR (400 MHz, Chloroform-*d*) δ 7.37 – 7.27 (m, 3H), 7.21 (q, J = 7.1 Hz, 4H), 7.14 (t, J = 8.8 Hz, 3H), 4.98 (s, 2H); ^{13}C NMR (101 MHz, Chloroform-*d*) δ 169.5 , 143.5 , 134.8 , 130.3 , 128.9 , 128.9 , 128.0 , 126.8 , 126.3. HRMS(ESI) m/z calculated for $C_{13}H_{13}N_2O$ [M + H^+] 213.1022, found 213.1023.

4-methoxy-*N*-phenylbenzohydrazide (3-2Ae). Synthesized using Method I from **3-2Aa·HCl** (68.3 mg, 0.47 mmol), 0.25 M 4-methoxybenzoyl chloride in dichloromethane (1.88 mL, 0.47 mmol), triethylamine (0.14 mL, 1.03 mmol) and dichloromethane (5.0 mL); chromatography afforded **3-2Ae** as a sticky yellow film (61.7 mg, 54%). ^{1}H NMR (400 MHz, Chloroform-*d*) δ 7.3 (d, J = 8.76 Hz, 2H), 7.3 – 7.2 (m, 2H), 7.1 (t, J = 8.80 Hz, 3H), 6.7 (d, J = 8.77 Hz, 2H), 4.9

(s, 2H), 3.8 (s, 3H); ^{13}C NMR (101 MHz, Chloroform-*d*) δ 169.4 , 161.2 , 144.1 , 131.1 , 129.0 , 126.6 , 126.3 , 113.3 , 55.4. HRMS(ESI) m/z calculated for $C_{14}H_{15}N_2O_2$ [M + H^+] 243.1128, found 243.1136.

4-chloro-*N*-phenylbenzohydrazide (3-2Af). Synthesized using Method I from **3-2Aa·HCl** (68.3 mg, 0.47 mmol), 0.25 M 4-chlorobenzoyl chloride in dichloromethane (1.88 mL, 0.47 mmol), triethylamine (0.14 mL, 1.03 mmol) and dichloromethane (5.0 mL); chromatography afforded **3-2Af** as an orange solid (59.6 mg, 51%), mp 102-104 °C. ^{1}H NMR (400 MHz, Chloroform-*d*) δ 7.3 – 7.2 (m, 4H), 7.2 (d, *J* = 8.42 Hz, 3H), 7.1 (d, *J* = 7.55 Hz, 2H), 5.0 (s, 2H); ^{13}C NMR (101 MHz, Chloroform-*d*) δ 168.4 , 143.3 , 136.5 , 133.2 , 130.4 , 129.2 , 128.4 , 127.1 , 126.3. HRMS(ESI) m/z calculated for $C_{13}H_{15}ClN_3O$ [M + NH_4^+] 264.0898 , found 264.0919.

***N*-(4-methoxyphenyl)benzohydrazide (3-4Ab)**. Synthesized using Method I from **3-4Aa·HCl** (82.4 mg, 0.47 mmol), 0.25 M benzoyl chloride in dichloromethane (1.88 mL, 0.47 mmol), triethylamine (0.14 mL, 1.03 mmol) and dichloromethane (5.0 mL); chromatography afforded **3-4Ab** as an orange solid (60.2 mg, 53%), mp 69-72 °C. ^{1}H NMR (400 MHz, Chloroform-*d*) δ 7.34 (d, *J* = 7.3 Hz, 2H), 7.31 – 7.27 (m, 1H), 7.21 (t, *J* = 7.4 Hz, 2H), 7.05 (d, *J* = 8.8 Hz, 2H), 6.74 (d, *J* = 8.9 Hz, 2H), 5.07 (s, 2H), 3.75 (s, 3H); ^{13}C NMR (101 MHz, Chloroform-*d*) δ 169.3 , 158.3 , 136.5 , 134.9 , 130.1 , 128.9 , 128.0 , 127.8 , 114.2 , 55.5. HRMS(ESI) m/z calculated for $C_{14}H_{14}N_2NaO_2$ [M + Na^+] 265.0947, found 265.0953.

4-methoxy-*N*-(4-methoxyphenyl)benzohydrazide (3-4Ae). Synthesized using Method I from **3-4Aa·HCl** (82.6 mg, 0.47 mmol), 0.25 M 4-methoxybenzoyl chloride in dichloromethane (1.88

mL, 0.47 mmol), triethylamine (0.14 mL, 1.03 mmol) and dichloromethane (5.0 mL); chromatography afforded **3-4Ae** as an orange solid (80.7 mg, 63%), mp 97-100 °C. ^{1}H NMR (400 MHz, Chloroform-*d*) δ 7.31 (d, *J* = 8.7 Hz, 2H), 7.05 (d, *J* = 8.9 Hz, 2H), 6.76 (d, *J* = 8.9 Hz, 2H), 6.71 (d, *J* = 8.8 Hz, 2H), 4.94 (s, 2H), 3.76 (s, 6H); ^{13}C NMR (101 MHz, Chloroform-*d*) δ 169.1 , 161.0 , 158.2 , 137.1 , 131.0 , 127.7 , 126.8 , 114.3 , 113.3 , 55.5 , 55.4. HRMS(ESI) m/z calculated for $C_{15}H_{16}N_2NaO_3$ [M + Na^+] 295.1053, found 295.1062.

4-chloro-*N*-(4-methoxyphenyl)benzohydrazide (3-4Af). Synthesized using Method I from **3-4Aa·HCl** (82.7 mg, 0.47 mmol), 0.25 M 4-chlorobenzoyl chloride in dichloromethane (1.88 mL, 0.47 mmol), triethylamine (0.14 mL, 1.03 mmol) and dichloromethane (5.0 mL); chromatography afforded **3-4Af** as an orange solid (92.0 mg, 70%), mp 131-132 °C. ^{1}H NMR (400 MHz, Chloroform-*d*) δ 7.28 (d, *J* = 8.2 Hz, 2H), 7.18 (d, *J* = 8.5 Hz, 2H), 7.04 (d, *J* = 8.8 Hz, 2H), 6.76 (d, *J* = 8.8 Hz, 2H), 4.97 (s, 2H), 3.76 (s, 3H); ^{13}C NMR (101 MHz, Chloroform-*d*) δ 168.1 , 158.5 , 136.2 , 136.1 , 133.3 , 130.3 , 128.3 , 127.7 , 114.4 , 55.5. HRMS(ESI) m/z calculated for $C_{14}H_{13}ClN_2NaO_2$ [M + Na^+] 299.0558, found 299.0570.

***N*-(4-bromophenyl)benzohydrazide (3-5Ab)**. Synthesized using Method I from **3-5Aa·HCl** (105.2 mg, 0.47 mmol), 0.25 M benzoyl chloride in dichloromethane (1.88 mL, 0.47 mmol), triethylamine (0.14 mL, 1.03 mmol) and dichloromethane (5.0 mL); chromatography afforded **3-5Ab** as an orange solid (64.2 mg, 47%), mp 86-88 °C. ^{1}H NMR (400 MHz, Chloroform-*d*) δ 7.39 – 7.30 (m, 4H), 7.29 – 7.22 (m, 2H), 7.00 (d, *J* = 8.7 Hz, 2H), 4.92 (s, 2H); ^{13}C NMR (101

MHz, Chloroform-*d*) δ 169.7 , 142.7 , 134.5 , 132.0 , 130.7 , 128.8 , 128.3 , 127.6 , 120.0. HRMS(ESI) m/z calculated for $C_{13}H_{12}BrN_2O$ [M + H^+] 291.0128, found 291.0139.

***N*-(4-bromophenyl)-4-methoxybenzohydrazide (3-5Ae)**. Synthesized using Method I from **3-5Aa·HCl** (105.4 mg, 0.47 mmol), 0.25 M 4-methoxybenzoyl chloride in dichloromethane (1.88 mL, 0.47 mmol), triethylamine (0.14 mL, 1.03 mmol) and dichloromethane (5.0 mL); chromatography afforded **3-5Ae** as an orange solid (61.2 mg, 40%), mp 123-126 °C. ^{1}H NMR (400 MHz, Chloroform-*d*) δ 7.33 (dd, *J* = 13.0, 8.7 Hz, 4H), 7.00 (d, *J* = 8.7 Hz, 2H), 6.74 (d, *J* = 8.8 Hz, 2H), 4.88 (s, 2H), 3.79 (s, 3H); ^{13}C NMR (101 MHz, Chloroform-*d*) δ 169.5 , 161.5 , 143.3 , 132.0 , 131.0 , 127.6 , 119.8 , 113.6 , 55.4. HRMS(ESI) m/z calculated for $C_{14}H_{14}BrN_2O_2$ [M + H^+] 321.0233, found 321.0240.

***N*-(4-bromophenyl)-4-chlorobenzohydrazide (3-5Af)**. Synthesized using Method I from **3-5Aa·HCl** (105.4 mg, 0.47 mmol), 0.25 M 4-chlorobenzoyl chloride in dichloromethane (1.88 mL, 0.47 mmol), triethylamine (0.14 mL, 1.03 mmol) and dichloromethane (5.0 mL); chromatography afforded **3-5Af** as an orange solid (65.4 mg, 43%), mp 105-107 °C. ^{1}H NMR (400 MHz, Chloroform-*d*) δ 7.36 (d, *J* = 8.7 Hz, 2H), 7.28 (d, *J* = 8.5 Hz, 2H), 7.23 (d, *J* = 8.5 Hz, 2H), 6.99 (d, *J* = 8.6 Hz, 2H), 4.91 (s, 2H); ^{13}C NMR (101 MHz, Chloroform-*d*) δ 168.5 , 167.3 , 142.4 , 136.9 , 132.8 , 132.2 , 130.4 , 128.6 , 127.6 , 120.4. HRMS(ESI) m/z calculated for $C_{13}H_{11}BrClN_2O$ [M + H^+] 324.9738, found 324.9743.

Regioselectivity Experiments

All regioselectivity experiments were run under inert atmosphere using standard techniques due to the sensitivity of 4-fluorophenylhydrazine and distal monoacylhydrazines to air oxidation. By adding only 0.2 equiv of the acylating agent. Under these conditions no diacylation products were observed.

Triethylamine as base: **3-3Aa·HCl** (14.5 mg, 0.089 mmol), 1 drop of C_6F_6, and 2.0 mL of $CDCl_3$ were combined into an oven-dried round bottom flask equipped with magnetic stirrer. The flask was capped with a septum, purged with N_2, triethylamine (0.45 mmol) was added, and the solution was allowed to stir for 10 minutes. Next, a dilute solution (0.25 M) of acylating reagent in chloroform was added (70 μL, 0.0178 mmol) and allowed to stir for 1 hour for acid chlorides, and 2 hours for anhydrides. A standard NMR tube was then purged with nitrogen for 10 min, and at the end of the reaction time, 0.65 mL of the reaction solution was added to this NMR tube under the purge, and then quickly capped, wrapped with parafilm, and subjected to ^{19}F NMR immediately. Using the standards as references, peaks in the reaction mixture could be identified and their relative concentrations determined by integration.

Pyridine as base: **3-3Aa·HCl** (14.5 mg, 0.089 mmol), 1 drop of C_6F_6, and 2.0 mL of $CDCl_3$ were combined into an oven-dried round bottom flask and magnetic stirrer. The flask was capped with a septum, purged with N_2, pyridine (0.45 mmol) was added, and the solution was allowed to stir. Next, a dilute solution (0.25 M) of acid chloride in chloroform was added (70 μL, 0.0178 mmol) and allowed to stir for 1 hour. Note that at this point unreacted **5** (HCl salt) remained undissolved. To dissolve the residual **5** (and thus allow determination of % conversion by ^{19}F

NMR), triethylamine (31 μL, 0.222 mmol) was added and the mixture was allowed to stir for 1 hour. This mixture was then analyzed as described above.

Sodium Hydroxide as base: **3-3Aa·HCl** (14.5 mg, 0.089 mmol), 1 drop of C_6F_6, and 2.0 mL of $CDCl_3$ were combined into an oven-dried round bottom flask and magnetic stirrer. The flask was capped with a septum, purged with N_2, 1.0 M NaOH (108 μL, 0.108 mmol) was added, and the solution was allowed to stir for 20 minutes. Then, a saturated solution of NaCl (0.35 mL) was added and allowed to stir for 20 minutes. Next, a dilute solution (0.25 M) of acid chloride in chloroform was added (70 μL, 0.0178 mmol) and allowed to stir for 1 hour for acid chlorides. A standard NMR tube was then purged with nitrogen for 10 min, and at the end of the reaction time, 0.65 mL of organic phase was removed and subjected to NMR analysis as described above.

5.2 XYZ coordinates of computed equilibrium geometries and transition states

B3LYP/6-31G(d) Equilibrium geometry of (*Z*,*Z*)-(*P*)-**4-1**

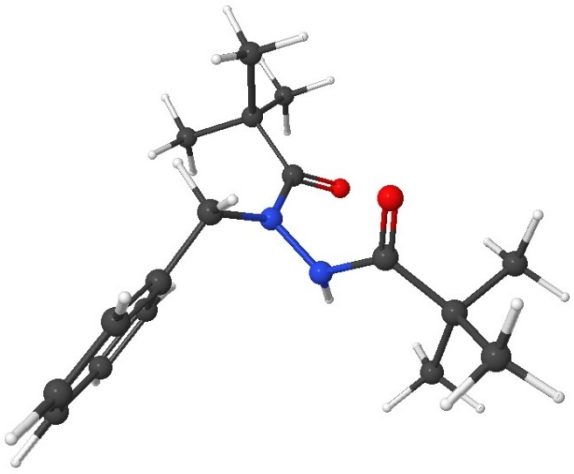

```
C    0.00000000  0.00000000  0.00000000
C   -1.07387100 -0.92110100 -0.55300100
C   -1.58162600 -1.94899600  0.24832000
C   -2.60883500 -2.77382300 -0.21387300
C   -3.13612600 -2.58412900 -1.49164800
C   -2.63002400 -1.56520100 -2.30197400
C   -1.60765100 -0.73930000 -1.83481300
H   -1.21197700  0.04685200 -2.47237500
H   -3.03222000 -1.41326600 -3.30034900
H   -3.93207900 -3.22791500 -1.85624200
H   -2.99005500 -3.56879700  0.42171000
H   -1.16700600 -2.10720900  1.24150000
N    1.04592600  0.32041400 -0.97190600
N    1.80143000 -0.79872400 -1.34108300
C    2.88895400 -1.12881100 -0.54088100
C    3.92949600 -2.09559000 -1.14233300
C    5.26200100 -1.31272400 -1.17715900
H    5.53212600 -0.97417000 -0.17322600
H    6.06459100 -1.95314400 -1.56160100
H    5.18099100 -0.43155100 -1.82352300
C    4.05083700 -3.29726400 -0.18221300
H    4.24867300 -2.95356300  0.83632600
H    3.12899600 -3.89131900 -0.17055500
H    4.87107500 -3.95173600 -0.49956000
C    3.58604200 -2.59481400 -2.55808100
H    3.58189900 -1.77986100 -3.29328400
H    4.34683500 -3.31194500 -2.88616500
H    2.61683700 -3.10557500 -2.59078400
O    2.98631700 -0.70551100  0.60087200
H    1.92515100 -0.86946800 -2.34212900
C    1.61726700  1.54225400 -1.32953300
O    2.61896900  1.52622700 -2.03640400
C    0.98095800  2.89038000 -0.89528100
C    1.11673900  3.09192000  0.63365300
H    2.15693300  2.95836400  0.94944300
H    0.81387000  4.11343400  0.89160100
H    0.50203700  2.40915300  1.22552400
C    1.78968300  4.00773700 -1.58805900
H    2.84063400  3.97951800 -1.29079000
H    1.75342200  3.90909800 -2.67639500
H    1.37138200  4.98228200 -1.31082000
C   -0.48824600  3.02001500 -1.36067600
H   -1.16804000  2.29303200 -0.90927800
H   -0.86112800  4.01817500 -1.10301600
H   -0.55960200  2.91214400 -2.44924200
H   -0.45077600  0.93371600  0.33066800
H    0.47499700 -0.45256700  0.87734400
```

B3LYP/6-31G(d) Equilibrium geometry of (*E*,*Z*)-(*P*)-**4-1**

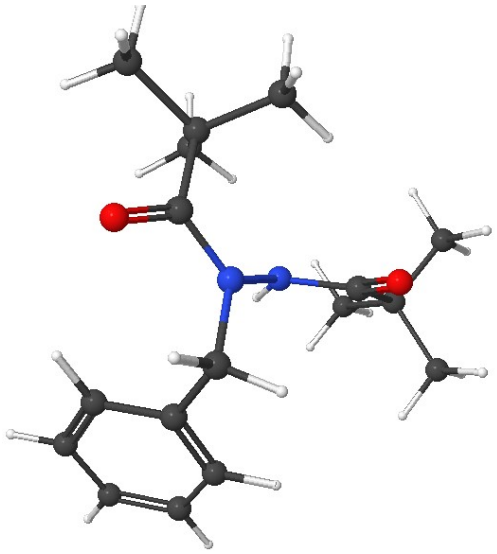

C	0.00000000	0.00000000	0.00000000
C	-1.23467700	0.14281900	0.86509600
C	-2.28528400	0.98103000	0.47704800
C	-3.43315300	1.09977000	1.26464400
C	-3.53887400	0.38560800	2.45798000
C	-2.49253900	-0.45020300	2.85857200
C	-1.35103600	-0.57087500	2.06736800
H	-0.54010100	-1.22525300	2.37859100
H	-2.56964100	-1.01304900	3.78527300
H	-4.42987700	0.47792000	3.07323300
H	-4.24072300	1.75380800	0.94646900
H	-2.20492500	1.54266500	-0.45094600
N	1.22405900	0.34558800	0.74352200
N	1.30954500	1.65706200	1.19819800
C	1.56542100	2.68519400	0.29870700
C	1.48052300	4.06734000	0.87113100
C	1.63343600	4.34514900	2.23735900
C	1.54465600	5.65814700	2.69956400
C	1.30245700	6.70068900	1.80323400
C	1.16332700	6.43030400	0.43920900
C	1.25885400	5.12133800	-0.02570700
H	1.16752700	4.89112100	-1.08218600
H	0.98431700	7.24133100	-0.26126800
H	1.23173300	7.72277900	2.16543800
H	1.67448100	5.86743700	3.75774900
H	1.86278100	3.54651800	2.93712000
O	1.85722000	2.46225400	-0.86652200
H	0.76038200	1.85107000	2.02586700
C	2.40528600	-0.34264600	0.45572800
O	2.40429000	-1.28574200	-0.32226300

C	3.65438600	0.06621200	1.18042300
C	3.67596700	0.39595200	2.54224400
C	4.88554100	0.67030400	3.17898900
C	6.08104500	0.63247200	2.45772900
C	6.06543900	0.29779000	1.10203600
C	4.85946200	0.00089600	0.46982900
H	4.83394000	-0.28491800	-0.57665000
H	6.99394000	0.25994700	0.53897300
H	7.02226000	0.85572400	2.95314000
H	4.89572900	0.91100500	4.23876700
H	2.75036500	0.41331100	3.10919100
H	0.14125700	-1.03005100	-0.33405000
H	-0.07073600	0.63117900	-0.89300800

B3LYP/6-31G(d) Equilibrium geometry of (*Z*,*E*)-(*P*)-**4-1**

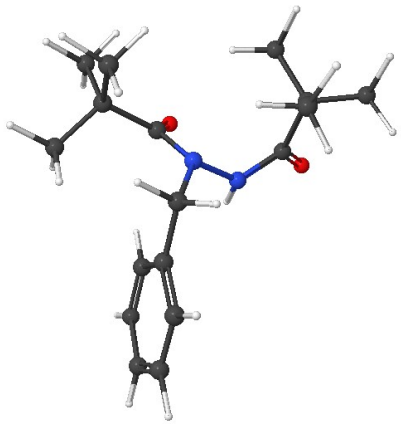

C	0.00000000	0.00000000	0.00000000
C	-1.31320000	-0.49493000	-0.59285300
C	-2.12519000	-1.33991500	0.17383100
C	-3.35972100	-1.77552700	-0.30697700
C	-3.79573700	-1.38139000	-1.57328800
C	-2.98910200	-0.54977500	-2.35049800
C	-1.75785900	-0.10709500	-1.86272700
H	-1.14118800	0.53708400	-2.48424000
H	-3.31486600	-0.24471600	-3.34129100
H	-4.75317100	-1.72595000	-1.95414100
H	-3.97560500	-2.43095400	0.30302900
H	-1.78618000	-1.66193100	1.15635500
N	1.06391500	0.26707800	-0.97680000
N	1.39176800	-0.88222500	-1.70969100
C	2.67374300	-1.41948100	-1.86641800
C	3.78545100	-1.20359400	-0.81367500
C	3.26122500	-1.20589400	0.63602200
H	2.66958600	-2.10512200	0.84469500

H	4.11113000	-1.20266700	1.32864900
H	2.65102000	-0.32793300	0.85740400
C	4.79111900	-2.36166500	-0.97691400
H	4.32204200	-3.32740200	-0.76075800
H	5.18069600	-2.40547500	-1.99588700
H	5.62663700	-2.22111000	-0.28136600
C	4.51165200	0.12678600	-1.12180000
H	3.86373800	0.99554000	-0.98262000
H	5.37403400	0.23455400	-0.45300000
H	4.87519100	0.14196700	-2.15435100
O	2.85025400	-2.12835800	-2.84454300
H	0.87005400	-0.98243900	-2.57803000
C	1.27785700	1.48640500	-1.65330800
O	1.76492100	1.45600300	-2.77273900
C	1.00208500	2.84727300	-0.94796000
C	1.60799700	2.90041900	0.47334600
H	2.67690600	2.66137600	0.45266200
H	1.50380000	3.91686500	0.87005700
H	1.12940000	2.22486400	1.18730500
C	1.70018800	3.93193800	-1.79737800
H	2.78002900	3.76470900	-1.84850800
H	1.32042900	3.93983400	-2.82123200
H	1.52207700	4.91498600	-1.34667600
C	-0.51017900	3.17777500	-0.92364100
H	-1.10704000	2.48305900	-0.32733200
H	-0.65117100	4.17975400	-0.50205200
H	-0.92161900	3.18518900	-1.93891400
H	-0.17265600	0.90920200	0.57590800
H	0.38189800	-0.74795700	0.70099500

B3LYP/6-31G(d) Equilibrium geometry of (*E*,*E*)-(*P*)-**4-1**

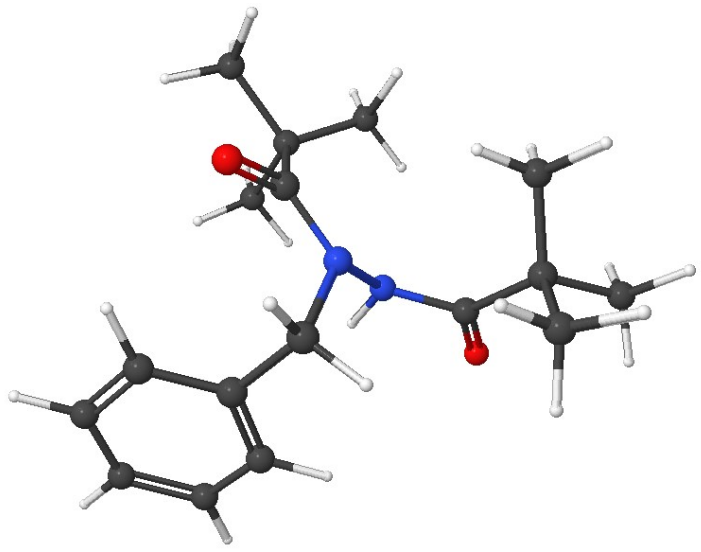

```
C    0.00000000  0.00000000  0.00000000
C   -1.32760700 -0.29811100 -0.66703800
C   -1.44731100 -1.36977200 -1.56338100
C   -2.65834200 -1.62744700 -2.20984100
C   -3.76737800 -0.81805600 -1.96189000
C   -3.66050400  0.24896700 -1.06620400
C   -2.44993900  0.50930300 -0.42402700
H   -2.36515300  1.34052100  0.26957400
H   -4.52395400  0.87710100 -0.86316300
H   -4.71229100 -1.02041500 -2.45906700
H   -2.73478800 -2.46339800 -2.89997400
H   -0.59025600 -2.01387600 -1.74970500
N    0.83504000  0.95906000 -0.78234600
N    1.34507500  0.45638300 -1.97875400
C    2.46200000 -0.38601800 -2.09675400
C    3.63759000 -0.37682500 -1.08542300
C    3.25724800 -1.18121900  0.18099200
H    2.83187300 -2.15881700 -0.07413000
H    4.16155800 -1.35868600  0.77436100
H    2.55104900 -0.64094100  0.81619200
C    4.82085500 -1.08679200 -1.77551600
H    4.56841700 -2.11504100 -2.04460700
H    5.11375300 -0.56855400 -2.69366200
H    5.68072500 -1.10051800 -1.09612400
C    4.08024300  1.03980200 -0.67218900
H    3.28926800  1.58644400 -0.15486900
H    4.93434100  0.95993800  0.01068200
H    4.40295100  1.62666600 -1.53763800
O    2.48213000 -1.10655200 -3.08450100
H    0.63928000  0.17919000 -2.66088700
C    0.49879700  2.31995000 -0.65377700
O   -0.06778300  2.66551800  0.37463700
C    0.73628600  3.35145300 -1.79350700
C   -0.23918700  3.02031600 -2.95085600
H   -1.26617400  2.90401100 -2.58708200
H   -0.23090000  3.84480800 -3.67310900
H    0.04275300  2.11247000 -3.49096600
C    0.36389400  4.73698500 -1.22521800
H   -0.67229100  4.76577400 -0.88072200
H    1.00052300  5.00248900 -0.37585100
H    0.49620000  5.49392000 -2.00663300
C    2.18056000  3.42632900 -2.32744200
H    2.49674600  2.50147600 -2.81029100
H    2.23930800  4.23250500 -3.06847100
H    2.88834700  3.66431400 -1.52662400
H   -0.14001700  0.44254100  0.98513100
H    0.58227700 -0.91618400  0.10510500
```

B3LYP/6-31G(d) Equilibrium geometry of (*Z*,*Z*)-(*P*)-**4-2**

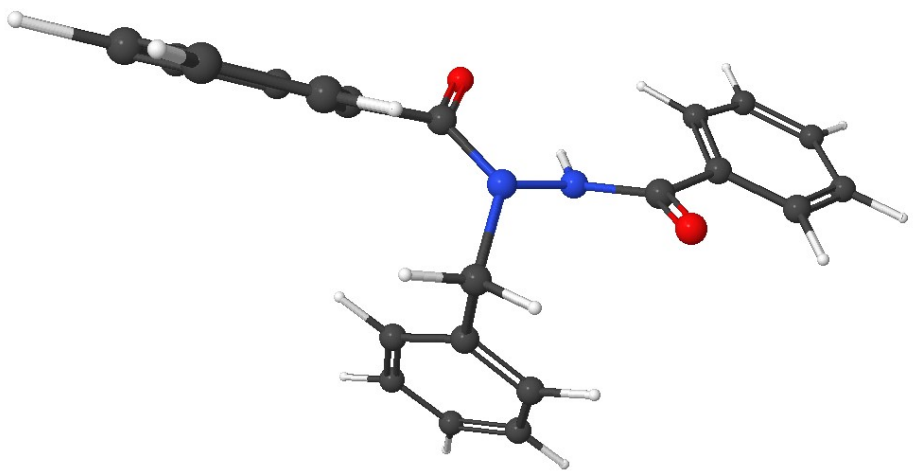

C	0.00000000	0.00000000	0.00000000
C	-0.20649000	1.33216500	-0.69137000
C	-1.33744300	2.10578000	-0.40644300
C	-1.53808500	3.33177000	-1.04287300
C	-0.60706300	3.79714300	-1.97264900
C	0.52578300	3.03285800	-2.26254000
C	0.72367700	1.80833200	-1.62480500
H	1.60999700	1.21867600	-1.85013400
H	1.25738800	3.39327900	-2.98096700
H	-0.76063700	4.75261500	-2.46729800
H	-2.42035300	3.92291500	-0.81187900
H	-2.06061700	1.74110400	0.31883400
N	-0.44022700	-1.16501600	-0.81203200
N	-1.77723800	-1.11679400	-1.22278200
C	-2.79728600	-1.33551800	-0.32931500
C	-4.13370400	-1.61274800	-0.95489200
C	-4.28099400	-2.23697700	-2.20224000
C	-5.55401900	-2.49448200	-2.71084100
C	-6.68686100	-2.13005900	-1.98100300
C	-6.54503000	-1.52010900	-0.73173800
C	-5.27510300	-1.27004500	-0.21798200
H	-5.14214300	-0.81312300	0.75725400
H	-7.42516700	-1.24368900	-0.15753200
H	-7.67772700	-2.32927800	-2.38040700
H	-5.65977100	-2.98728700	-3.67330900
H	-3.41021000	-2.56294700	-2.76568700
O	-2.64538700	-1.23792100	0.88502900
H	-1.87205500	-1.33637400	-2.20806900
C	0.36355200	-1.83974900	-1.72005200
O	-0.11405700	-2.30096600	-2.75757600
C	1.80699600	-2.03657700	-1.37678500
C	2.23405000	-2.36772800	-0.08269100

C	3.58246800	-2.62529900	0.16443600
C	4.51215300	-2.54901500	-0.87459100
C	4.08872100	-2.23363500	-2.16829200
C	2.74020600	-1.99212600	-2.42185800
H	2.39174600	-1.77494900	-3.42662900
H	4.80856500	-2.18498800	-2.98064100
H	5.56292600	-2.74498100	-0.67888900
H	3.90515300	-2.89218700	1.16693200
H	1.50719000	-2.44937300	0.72026000
H	1.05439800	-0.15691500	0.22486000
H	-0.56575700	-0.04514500	0.93173700

B3LYP/6-31G(d) Equilibrium geometry of (*E*,*Z*)-(*P*)-**4**-**2**

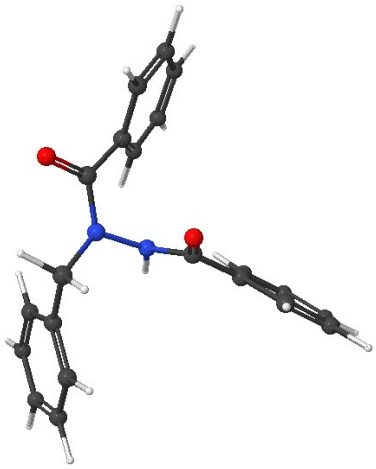

C	0.00000000	0.00000000	0.00000000
C	-1.23467700	0.14281900	0.86509600
C	-2.28528400	0.98103000	0.47704800
C	-3.43315300	1.09977000	1.26464400
C	-3.53887400	0.38560800	2.45798000
C	-2.49253900	-0.45020300	2.85857200
C	-1.35103600	-0.57087500	2.06736800
H	-0.54010100	-1.22525300	2.37859100
H	-2.56964100	-1.01304900	3.78527300
H	-4.42987700	0.47792000	3.07323300
H	-4.24072300	1.75380800	0.94646900
H	-2.20492500	1.54266500	-0.45094600
N	1.22405900	0.34558800	0.74352200
N	1.30954500	1.65706200	1.19819800
C	1.56542100	2.68519400	0.29870700
C	1.48052300	4.06734000	0.87113100
C	1.63343600	4.34514900	2.23735900
C	1.54465600	5.65814700	2.69956400

C	1.30245700	6.70068900	1.80323400
C	1.16332700	6.43030400	0.43920900
C	1.25885400	5.12133800	-0.02570700
H	1.16752700	4.89112100	-1.08218600
H	0.98431700	7.24133100	-0.26126800
H	1.23173300	7.72277900	2.16543800
H	1.67448100	5.86743700	3.75774900
H	1.86278100	3.54651800	2.93712000
O	1.85722000	2.46225400	-0.86652200
H	0.76038200	1.85107000	2.02586700
C	2.40528600	-0.34264600	0.45572800
O	2.40429000	-1.28574200	-0.32226300
C	3.65438600	0.06621200	1.18042300
C	3.67596700	0.39595200	2.54224400
C	4.88554100	0.67030400	3.17898900
C	6.08104500	0.63247200	2.45772900
C	6.06543900	0.29779000	1.10203600
C	4.85946200	0.00089600	0.46982900
H	4.83394000	-0.28491800	-0.57665000
H	6.99394000	0.25994700	0.53897300
H	7.02226000	0.85572400	2.95314000
H	4.89572900	0.91100500	4.23876700
H	2.75036500	0.41331100	3.10919100
H	0.14125700	-1.03005100	-0.33405000
H	-0.07073600	0.63117900	-0.89300800

B3LYP/6-31G(d) Equilibrium geometry of (*Z*,*E*)-(*P*)-**4**-**2**

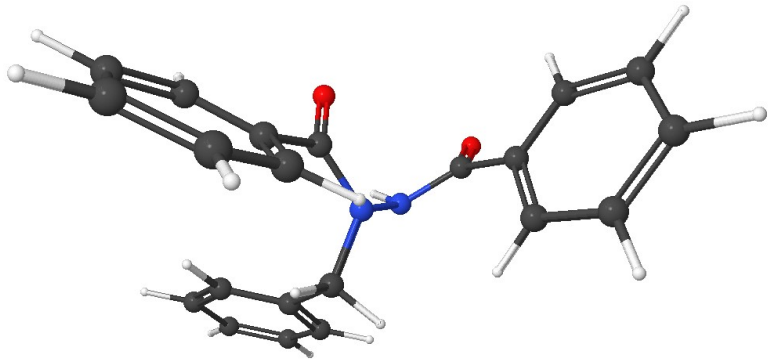

C	0.00000000	0.00000000	0.00000000
C	1.34651600	-0.61533000	0.33526800
C	1.56291500	-1.99015600	0.17921200
C	2.79422500	-2.55839500	0.51044800
C	3.82496700	-1.75572100	1.00137400
C	3.62019800	-0.38310700	1.15877800
C	2.38907400	0.18237900	0.82732500
H	2.23554900	1.25228800	0.94957000

```
H    4.42076100  0.24781100  1.53562600
H    4.78456700 -2.19649700  1.25770400
H    2.94771500 -3.62665800  0.38357200
H    0.76044700 -2.61703600 -0.20116900
N   -0.92253300  0.07716100  1.15620400
N   -1.23815700 -1.18270900  1.68510600
C   -2.55115000 -1.48866000  2.06701600
C   -3.68997700 -0.86884100  1.31736300
C   -3.64181200 -0.55307700 -0.04736700
C   -4.76894600 -0.04077900 -0.68962700
C   -5.94816100  0.17248400  0.02771900
C   -6.00396800 -0.14770700  1.38612200
C   -4.88495800 -0.67816400  2.02419600
H   -4.91654400 -0.95195400  3.07364000
H   -6.92176900  0.00904400  1.94610800
H   -6.82294100  0.57925100 -0.47276800
H   -4.72852100  0.18632700 -1.75170500
H   -2.73620700 -0.73583400 -0.61557400
O   -2.73152300 -2.29925300  2.96113000
H   -0.58848300 -1.50054700  2.40372300
C   -0.86286000  1.11651400  2.10074000
O   -1.04279500  0.90024100  3.28896500
C   -0.65420900  2.50817800  1.58186900
C   -1.28493400  2.97805700  0.42101100
C   -1.12784000  4.30751000  0.02886400
C   -0.33386100  5.17200600  0.78530900
C    0.28671400  4.71067200  1.94915100
C    0.11539600  3.38863700  2.35465400
H    0.56479600  3.02436300  3.27323000
H    0.89495400  5.38458100  2.54613200
H   -0.20732900  6.20557800  0.47462300
H   -1.63082500  4.66968700 -0.86355400
H   -1.92207400  2.31113100 -0.15273300
H    0.13237600  1.01219800 -0.38252300
H   -0.50304800 -0.58909200 -0.77259100
```

B3LYP/6-31G(d) Equilibrium geometry of (*E*,*E*)-(*P*)-**4-2**

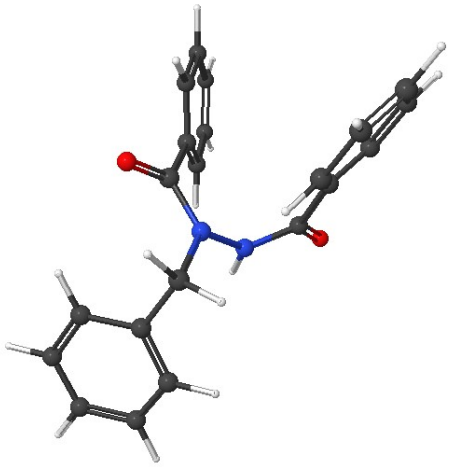

C	0.00000000	0.00000000	0.00000000
C	1.37510800	0.37669900	0.51516200
C	1.98635800	-0.36287300	1.53451200
C	3.24016000	0.00639000	2.02762800
C	3.89435700	1.12188800	1.50429200
C	3.29150900	1.86615700	0.48633800
C	2.04038400	1.49674000	-0.00552300
H	1.56948900	2.07362000	-0.79730700
H	3.79968400	2.73290800	0.07202200
H	4.87109100	1.40914300	1.88439900
H	3.70431100	-0.57872200	2.81713300
H	1.48058100	-1.23653200	1.94008200
N	-1.06993100	0.82605000	0.59199900
N	-1.38481800	0.54740400	1.90958500
C	-2.59916100	0.10788600	2.42230200
C	-3.66855600	-0.42464600	1.51728500
C	-3.44299100	-1.04225200	0.27858300
C	-4.51220800	-1.56002400	-0.45258800
C	-5.81489700	-1.45903500	0.03762900
C	-6.04635200	-0.85126000	1.27394300
C	-4.97956600	-0.34741800	2.01244600
H	-5.13754600	0.10958100	2.98329200
H	-7.05744600	-0.77544200	1.66443200
H	-6.64566400	-1.85711100	-0.53898300
H	-4.32446300	-2.04358800	-1.40726800
H	-2.43951500	-1.13883000	-0.11641300
O	-2.75616800	0.17362200	3.63497200
H	-0.75904000	0.91242500	2.62194500
C	-1.55380700	1.93213700	-0.10165500
O	-1.23945000	2.09624600	-1.27600100
C	-2.50065800	2.88464300	0.57381200
C	-2.31685500	3.40247800	1.86319000

C	-3.19382800	4.36370800	2.36628700
C	-4.26893800	4.80608000	1.59471000
C	-4.45237200	4.30159900	0.30506900
C	-3.56453000	3.35982800	-0.20787100
H	-3.67822600	2.98313200	-1.21898500
H	-5.28181300	4.64954100	-0.30446100
H	-4.95719400	5.54620900	1.99403000
H	-3.03579000	4.76331800	3.36399000
H	-1.48269800	3.07808600	2.47504800
H	-0.06808100	0.13999600	-1.07944000
H	-0.22441800	-1.04347100	0.24131800

B3LYP/6-31G(d) Equilibrium geometry of (*Z*,*Z*)-(*M*)-**4**-**6**

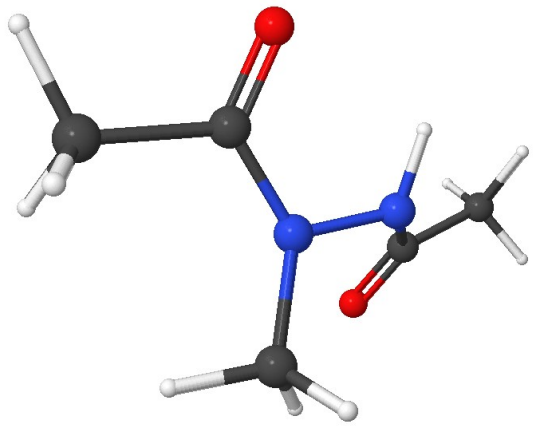

C	0.00000000	0.00000000	0.00000000
N	0.15290800	-1.39497500	0.39946700
C	-0.86679700	-2.29020100	0.63516400
O	-0.65084300	-3.50044300	0.61258600
C	-2.24361500	-1.71910900	0.91973200
H	-2.22309800	-0.97934100	1.72654400
H	-2.88590200	-2.55110000	1.21049400
H	-2.66996500	-1.24000100	0.03080100
N	1.36436800	-1.99197200	0.01861800
C	2.51932500	-1.66752200	0.71143000
C	3.69778400	-2.57315800	0.39454200
H	3.44656800	-3.40324400	-0.27215100
H	4.09099300	-2.97225300	1.33440100
H	4.49071700	-1.97619400	-0.06669700
O	2.60481100	-0.69621100	1.44507900
H	1.20553500	-2.96572800	-0.22972600
H	-0.92438900	0.39586300	0.41984300
H	0.84008900	0.56726000	0.40295100
H	-0.02349400	0.09863100	-1.09339600

B3LYP/6-31G(d) N-N Bond Rotation Transition Structure (*Z*,*Z*)-(*M*)-**4-6*** θ = -20.8°

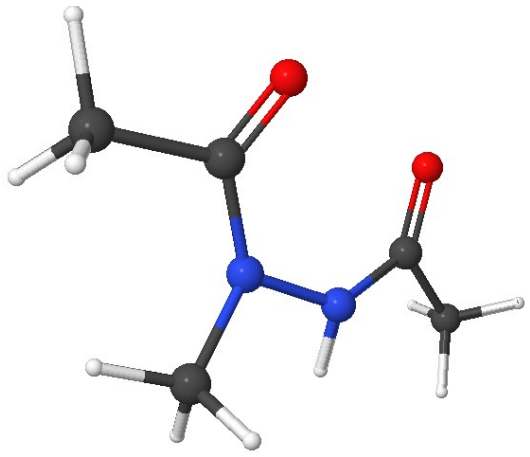

C	0.00000000	0.00000000	0.00000000
N	0.57206300	-1.31301200	0.28750800
C	-0.16822200	-2.49023400	0.17449600
O	0.31640200	-3.59373800	0.03958400
C	-1.68455600	-2.31396600	0.28918500
H	-2.11148700	-1.85126000	-0.60827200
H	-2.09850300	-3.31804100	0.38721100
H	-1.98274600	-1.71895400	1.15882800
N	1.98945500	-1.23057800	0.10118800
C	3.03698500	-2.15811900	0.14609100
C	4.37940300	-1.42059000	0.24516300
H	4.34113800	-0.35616700	-0.00939600
H	4.76713200	-1.52587700	1.26475400
H	5.08062700	-1.91862000	-0.42806600
O	2.99079900	-3.36400400	0.08537100
H	2.27825900	-0.32296000	0.44069700
H	0.18067800	0.29878900	-1.04156700
H	0.44810800	0.75309700	0.66227300
H	-1.06922700	-0.00426400	0.19266700

B3LYP/6-31G(d) N-N Bond Rotation Transition Structure (*Z*,*Z*)-**4-6*** θ = -180°

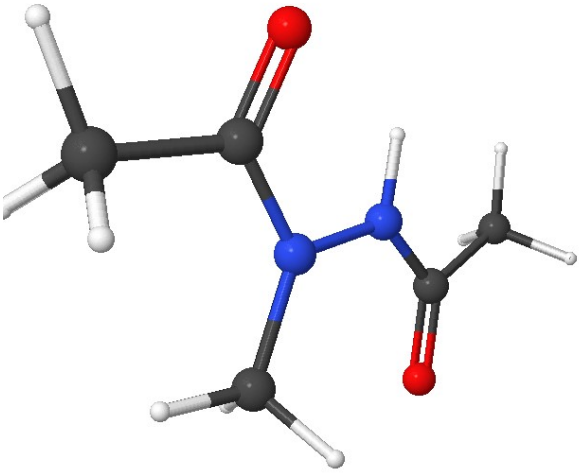

C	0.00000000	0.00000000	0.00000000
N	-0.03464200	-1.45816600	0.00014200
C	-1.14484700	-2.26367700	0.00000000
O	-1.01865300	-3.49158900	-0.00012400
C	-2.50945100	-1.59969200	0.00005600
H	-2.66346100	-0.97485100	-0.88642900
H	-3.25035900	-2.39975500	-0.00010200
H	-2.66340100	-0.97521500	0.88681800
N	1.16278300	-2.19047500	0.00009600
C	2.43948000	-1.71258700	-0.00003700
C	3.48114700	-2.82411000	0.00009500
H	3.06052900	-3.83407700	-0.00034400
H	4.11765600	-2.70276100	-0.88173500
H	4.11681900	-2.70326000	0.88260800
O	2.75461300	-0.52771400	-0.00012100
H	0.93636400	-3.18050000	-0.00029400
H	0.51662100	0.37699800	-0.88435700
H	0.51679100	0.37711300	0.88422200
H	-1.02924600	0.35561600	0.00013600

B3LYP/6-31G(d) Equilibrium geometry of (*E*,*Z*)-(*M*)-**4**-**6**

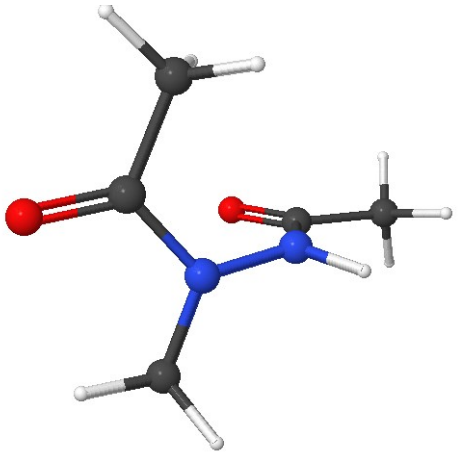

C	0.00000000	0.00000000	0.00000000
N	0.17657800	-1.40770200	-0.34793100
C	-0.76999300	-2.35317700	0.04165500
O	-1.85161800	-2.00407000	0.48493200
C	-0.38699300	-3.81024600	-0.13705600
H	0.02505000	-4.01414600	-1.12981200
H	-1.28464100	-4.40892300	0.02257500
H	0.36831000	-4.09029300	0.60525100
N	1.46255500	-1.81398400	-0.66376000
C	2.42169400	-2.00219900	0.31752300
C	3.82622200	-2.23217100	-0.21514300
H	3.86565000	-2.39466000	-1.29682400
H	4.25541900	-3.09904900	0.29371300
H	4.44590800	-1.36387800	0.03335600
O	2.14577900	-2.00025200	1.50377700
H	1.74364800	-1.68312800	-1.62831300
H	-1.05627300	0.15203100	0.21816400
H	0.59748800	0.25541200	0.88215200
H	0.29911500	0.63118000	-0.84387800

B3LYP/6-31G(d) N-N Bond Rotation Transition Structure (*E*,*Z*)-(*M*)-**4**-**6*** θ = -16.3°

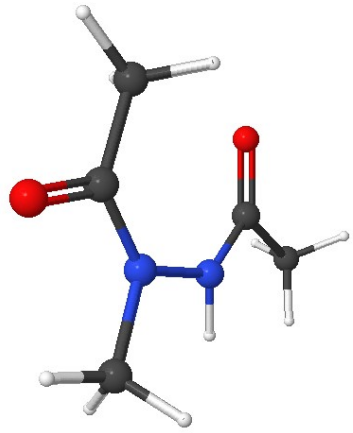

C	0.00000000	0.00000000	0.00000000
N	0.56111600	-1.34429400	-0.10667300
C	-0.31838700	-2.42946800	-0.02950400
O	-1.52081600	-2.18692100	0.00452700
C	0.16920600	-3.85866100	-0.03307300
H	0.77365700	-4.08441300	0.84659700
H	-0.72790000	-4.47942000	-0.04189000
H	0.79214800	-4.07899100	-0.90043600
N	1.97834200	-1.27148100	0.02491600
C	3.00521500	-2.18612600	-0.00972600
C	4.37093200	-1.49953700	-0.02826800
H	4.34533900	-0.41116100	0.08656300
H	4.97304600	-1.92421200	0.77951300
H	4.86885700	-1.74367000	-0.97228900
O	2.91471600	-3.40202300	0.00138700
H	2.26082900	-0.31744600	-0.13974100
H	-1.07861600	-0.08911100	-0.09488600
H	0.38758300	0.63566400	-0.80731300
H	0.24748400	0.45257000	0.96950000

B3LYP/6-31G(d) N-N Bond Rotation Transition Structure (*E*,*Z*)-(*M*)-**4**-**6*** θ = -177.6°

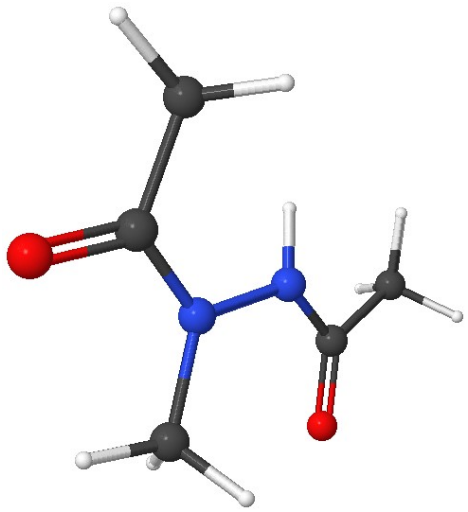

C	0.00000000	0.00000000	0.00000000
N	0.11526000	1.45472900	-0.11722600
C	1.35807300	2.05504700	-0.05893500
O	2.38762700	1.39128400	-0.07536300
C	1.40138400	3.57773900	-0.00745600
H	0.89622800	3.97421900	0.88170800
H	2.45220900	3.86510300	0.02874200
H	0.95219500	4.03851000	-0.89758900
N	-1.03896600	2.25764600	0.03629000
C	-2.34888300	1.83680100	-0.04032800
C	-3.33423500	3.00031500	-0.05788300
H	-2.87643100	3.98675600	0.06798500
H	-3.88220700	2.98056400	-1.00555100
H	-4.06112900	2.84494500	0.74420900
O	-2.72279300	0.67489300	-0.05272100
H	-0.86363900	3.22154800	-0.19979900
H	1.02169800	-0.37236200	-0.05293400
H	-0.60273300	-0.40800700	-0.81008500
H	-0.45578900	-0.27850800	0.95341200

B3LYP/6-31G(d) Equilibrium geometry of (*Z*,*E*)-(*M*)-**4**-**6**

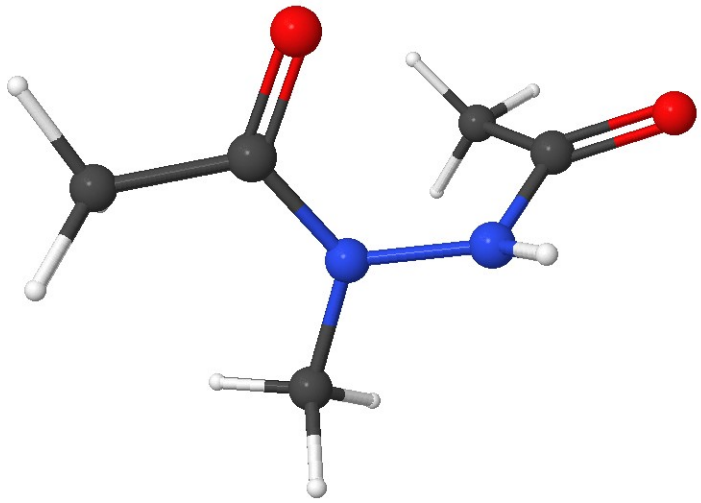

C	0.00000000	0.00000000	0.00000000
N	0.57496600	-1.33727200	-0.10746400
C	-0.14090000	-2.53080800	-0.07556500
O	0.38912000	-3.58596900	-0.38423400
C	-1.58582000	-2.45407800	0.39201300
H	-1.66596400	-2.02389800	1.39648200
H	-1.97741700	-3.47170600	0.40823700
H	-2.19926400	-1.84671400	-0.28307800
N	1.84980800	-1.37327500	-0.67093600
C	2.94048000	-1.89879300	0.02897900
C	2.80244200	-1.99507800	1.53398700
H	2.34281700	-1.10157400	1.96740600
H	3.79689200	-2.14585000	1.95620300
H	2.17351000	-2.85597200	1.78625000
O	3.94444200	-2.21144500	-0.58204900
H	1.87476000	-1.61893200	-1.65864100
H	-0.90012900	-0.02414200	0.61512800
H	0.72963500	0.66004400	0.47533700
H	-0.25382900	0.41625400	-0.98480800

B3LYP/6-31G(d) Equilibrium geometry of (*E*,*E*)-(*M*)-**4**-**6**

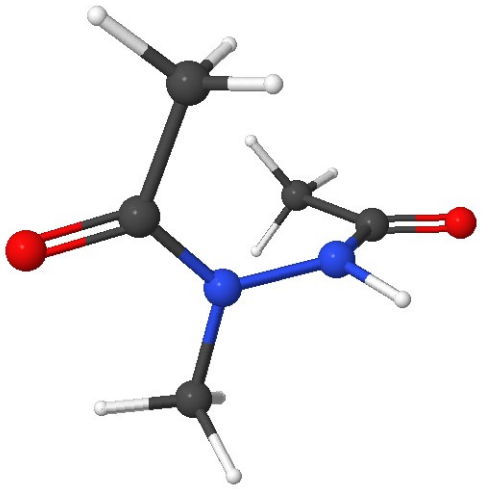

C	0.00000000	0.00000000	0.00000000
N	0.17783200	-1.44967600	0.02095700
C	-0.91170800	-2.29061500	0.24483900
O	-1.98867400	-1.83619400	0.59555900
C	-0.67184900	-3.77727800	0.04897700
H	-0.41792000	-4.00540000	-0.99149200
H	-1.59246600	-4.29542300	0.31997400
H	0.15242500	-4.14512600	0.66759900
N	1.33926400	-1.95961400	-0.53762200
C	2.53833900	-2.08246800	0.15634700
C	2.45854400	-1.98605400	1.66766100
H	1.73690800	-2.69904700	2.07891900
H	2.14339700	-0.98651900	1.98605700
H	3.45092500	-2.19479500	2.06875900
O	3.56879400	-2.29333400	-0.45842200
H	1.44249000	-1.88777200	-1.54794500
H	-0.95278100	0.22389300	0.47837100
H	0.81543600	0.48731800	0.54321100
H	-0.01386800	0.37898700	-1.03069900

B3LYP/6-31G(d) Equilibrium geometry of (*Z*,*Z*)-(*M*)-**4**-**7**

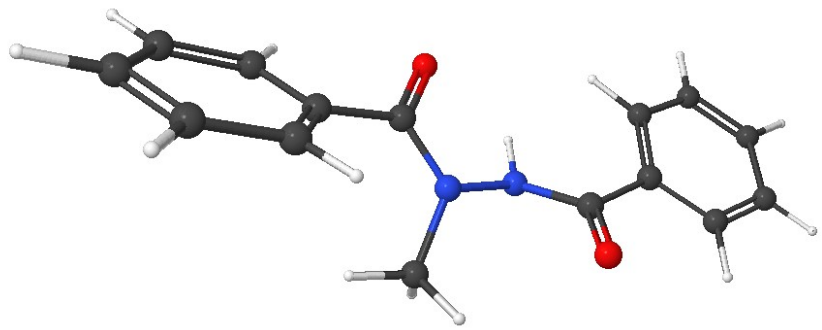

C	0.00000000	0.00000000	0.00000000
N	-0.39877600	1.15633700	-0.81066300
N	-1.74667900	1.51323500	-0.65794500
C	-2.71620000	0.78395000	-1.32030700
C	-4.05517000	1.45528300	-1.41763700
C	-4.21261900	2.84731100	-1.48741600
C	-5.48610200	3.40301100	-1.61028700
C	-6.60961700	2.57602300	-1.66064100
C	-6.45686300	1.18813300	-1.60422700
C	-5.18580400	0.63069300	-1.49191400
H	-5.04338100	-0.44468600	-1.46357900
H	-7.32893200	0.54167500	-1.65211600
H	-7.60098200	3.01154900	-1.75290100
H	-5.59887300	4.48168900	-1.67447600
H	-3.34733900	3.50566100	-1.48993200
O	-2.51832700	-0.35540200	-1.72352300
H	-1.83891200	2.51950900	-0.55833200
C	0.41167500	2.23655000	-1.11709100
O	-0.06791500	3.36744200	-1.22068500
C	1.86499400	1.98154500	-1.36265800
C	2.32390700	0.85502800	-2.06061900
C	3.68379000	0.70789400	-2.33404300
C	4.59250500	1.67909800	-1.90919300
C	4.13745400	2.80993000	-1.22588700
C	2.77829600	2.96752500	-0.96505900
H	2.40608600	3.85248200	-0.45888600
H	4.84168900	3.57203700	-0.90385500
H	5.65212700	1.56040100	-2.11901700
H	4.03182500	-0.16127800	-2.88523300
H	1.61374500	0.11210900	-2.41178400
H	1.08118400	-0.11878400	-0.04260900
H	-0.49129800	-0.89147800	-0.39257100
H	-0.30817400	0.15678100	1.04089100

B3LYP/6-31G(d) N-N Bond Rotation Transition Structure (*Z*,*Z*)-(*M*)-**4**-**7*** θ = -14.7°

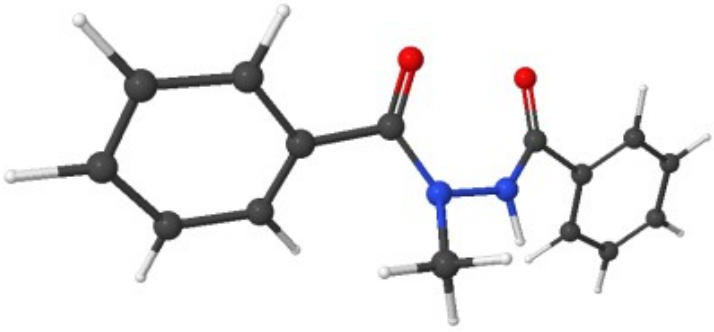

C	0.00000000	0.00000000	0.00000000
N	0.34167200	0.86621200	-1.13643100
N	1.75842200	1.03758700	-1.14822400
C	2.63622200	1.94817800	-1.73095400
O	2.40844400	3.07690100	-2.11424200
C	4.04615100	1.38966000	-1.75838700
C	4.35828500	0.05238500	-2.04079500
C	5.68836800	-0.36994200	-2.08673800
C	6.71863700	0.53965700	-1.84851400
C	6.41526700	1.87803300	-1.58295200
C	5.08942400	2.30211300	-1.54956800
H	4.83766500	3.34197100	-1.36864300
H	7.21491600	2.59257200	-1.40741100
H	7.75381700	0.21074800	-1.88100400
H	5.91718900	-1.40637500	-2.31974900
H	3.57131200	-0.66267500	-2.27183300
H	2.17566200	0.13185800	-0.98549900
C	-0.56298700	1.85849900	-1.55017700
O	-0.26557600	3.00073700	-1.83490200
C	-1.98727000	1.38149600	-1.69128300
C	-2.32574700	0.11456300	-2.18747000
C	-3.66324500	-0.22717500	-2.38985800
C	-4.67262900	0.69005900	-2.09151300
C	-4.34041800	1.95790100	-1.60672500
C	-3.00473400	2.30641100	-1.41982400
H	-2.72931500	3.29729300	-1.07304100
H	-5.12302700	2.67760300	-1.38270000
H	-5.71437600	0.42159400	-2.24542500
H	-3.91604100	-1.20642500	-2.78747500
H	-1.53957700	-0.59255100	-2.43603000
H	0.38786900	0.42369100	0.93514400
H	0.43352500	-0.99848000	-0.14390800
H	-1.07971600	-0.10503000	0.07087500

B3LYP/6-31G(d) N-N Bond Rotation Transition Structure (*Z,Z*)-(*M*)-**4-7*** θ = -177.6°

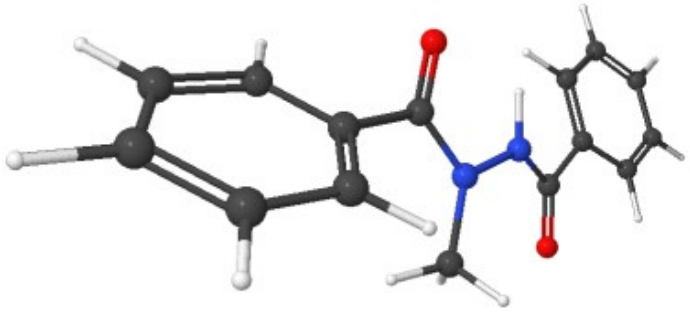

C	0.00000000	0.00000000	0.00000000
N	-0.35984300	-1.34793000	0.43600300
C	0.46446400	-2.43797000	0.58327200
O	-0.02281800	-3.56096000	0.76817100
C	1.94988200	-2.24663400	0.55399400
C	2.70558400	-3.17444100	-0.17639100
C	4.09656500	-3.10121400	-0.17929600
C	4.74853100	-2.11945200	0.57125300
C	4.00324800	-1.21316400	1.32700300
C	2.60928200	-1.27302300	1.31757000
H	2.03612200	-0.57773800	1.92421500
H	4.50564100	-0.46195300	1.93013200
H	5.83389500	-2.06783900	0.57501500
H	4.67323500	-3.81630400	-0.75941500
H	2.18961800	-3.95191400	-0.73072300
N	-1.70905600	-1.68089500	0.62209700
C	-2.81614600	-0.97185700	0.24693900
O	-2.80780800	0.19240600	-0.14621100
C	-4.09998700	-1.73937700	0.42367100
C	-4.18610900	-3.13862600	0.37706300
C	-5.42006800	-3.77091200	0.52988300
C	-6.57600800	-3.01432300	0.72981200
C	-6.49737000	-1.61979800	0.76310500
C	-5.26759800	-0.98601500	0.60369000
H	-5.18659400	0.09589100	0.61082300
H	-7.39591400	-1.02675400	0.91039800
H	-7.53580000	-3.50950400	0.85050700
H	-5.47788500	-4.85489600	0.48439800
H	-3.30407700	-3.74509900	0.18688400
H	-1.76179800	-2.65626000	0.89860100
H	-0.55662600	0.26699800	-0.89678700
H	-0.22792500	0.73483800	0.77727200
H	1.06694900	0.00200900	-0.21152600

B3LYP/6-31G(d) Equilibrium geometry of (*E*,*Z*)-(*M*)-**4**-**7**

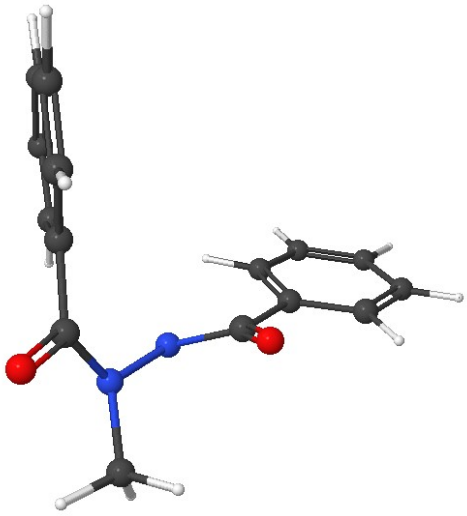

C	0.00000000	0.00000000	0.00000000
N	0.20216400	-1.45163000	0.03301300
N	-0.95343300	-2.22406200	0.02915000
C	-1.76380600	-2.29518700	1.15233000
C	-3.03193900	-3.07389300	0.97139800
C	-3.17567700	-4.09898400	0.02509200
C	-4.38457400	-4.78631500	-0.08530400
C	-5.45645900	-4.45468200	0.74527500
C	-5.31301500	-3.44391800	1.69965400
C	-4.10454900	-2.76218500	1.81777700
H	-3.96777100	-1.98446000	2.56210400
H	-6.14256800	-3.19114100	2.35415600
H	-6.39813400	-4.98960700	0.65629500
H	-4.48525900	-5.58741600	-0.81233900
H	-2.33456400	-4.39470300	-0.59595800
O	-1.45076800	-1.76499700	2.20745400
H	-1.33458000	-2.43864300	-0.88268100
C	1.32318600	-1.94136300	0.71021200
O	2.16484500	-1.17425200	1.15241400
C	1.49111800	-3.42946600	0.80723200
C	1.21182700	-4.30012300	-0.25478600
C	1.47857700	-5.66335400	-0.13442000
C	2.01278200	-6.16985700	1.05264400
C	2.29994900	-5.30524900	2.11107300
C	2.05437300	-3.93929600	1.98357100
H	2.29453600	-3.25181700	2.78810200
H	2.72294700	-5.69408400	3.03327100
H	2.21228500	-7.23386400	1.14857000
H	1.27401800	-6.32995200	-0.96810400
H	0.81326100	-3.90708400	-1.18531300
H	0.97254400	0.47603700	-0.11767400

```
H   -0.46539200  0.35203800  0.92632700
H   -0.63901100  0.24295300 -0.85413000
```

B3LYP/6-31G(d) N-N Bond Rotation Transition Structure (*E,Z*)-(*M*)-**4**-**7*** θ = -35.5°

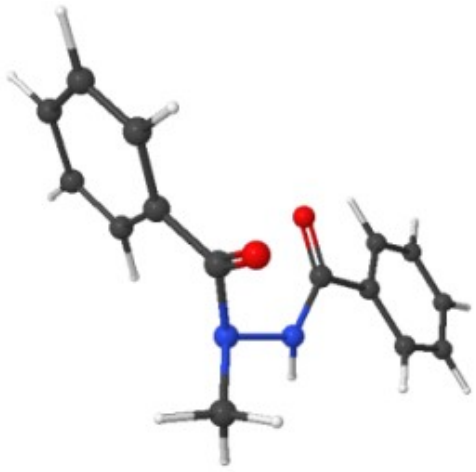

```
C    0.00000000  0.00000000  0.00000000
N    0.07114100 -1.47185400 -0.05389200
C   -0.80483200 -1.95395500 -1.16073500
O   -0.82857300 -1.37279000 -2.22350800
C   -1.77382700 -3.01285300 -0.77809100
C   -2.68213100 -3.45523900 -1.75242800
C   -3.62441900 -4.42965200 -1.43984000
C   -3.67206700 -4.96803000 -0.15001200
C   -2.77394700 -4.52799200  0.82450300
C   -1.82701500 -3.55325800  0.51384300
H   -1.12738500 -3.19857800  1.26177800
H   -2.81208300 -4.94407500  1.82767900
H   -4.40928400 -5.72859800  0.09414800
H   -4.32276000 -4.77158100 -2.19888300
H   -2.62707900 -3.02521600 -2.74697600
N    1.45386500 -1.82023900 -0.25530100
C    1.81591300 -3.00586300 -0.84223600
O    1.00869100 -3.72712500 -1.42300300
C    3.27517200 -3.33964300 -0.74783800
C    4.27353800 -2.37599200 -0.54308400
C    5.61231400 -2.75869700 -0.46511800
C    5.96427200 -4.10378800 -0.59396900
C    4.97452400 -5.06521200 -0.81367600
C    3.63710300 -4.68511100 -0.89657600
H    2.85442300 -5.41428000 -1.07841500
H    5.24664700 -6.11138000 -0.92356800
H    7.00790500 -4.40056900 -0.53354500
```

H	6.38093900	-2.00523900	-0.31641000
H	4.01170300	-1.32316900	-0.48330200
H	2.00720200	-1.52836600	0.54200400
H	0.35669400	0.47430200	-0.92139100
H	0.59305100	0.34814100	0.85300400
H	-1.04139800	0.28100400	0.17685600

B3LYP/6-31G(d) N-N Bond Rotation Transition Structure (*E,Z*)-(*M*)-**4**-**7*** θ = -165.0°

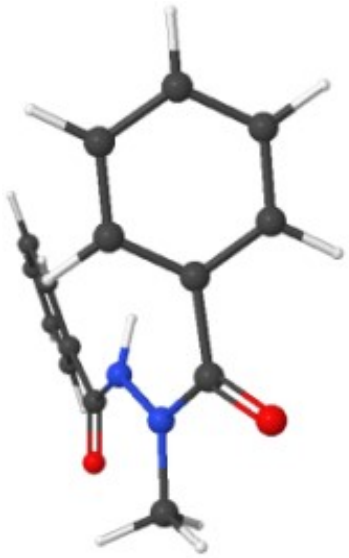

C	0.00000000	0.00000000	0.00000000
N	0.19592700	-1.44490700	-0.12752600
C	1.45793400	-1.95047900	-0.35681800
O	2.41330000	-1.20930200	-0.57330700
C	1.65618600	-3.44524900	-0.32469600
C	2.41487000	-4.02283600	-1.35242100
C	2.71121500	-5.38389300	-1.32842000
C	2.27956200	-6.17741700	-0.26220700
C	1.55056300	-5.60415100	0.78087800
C	1.23424800	-4.24443900	0.74963200
H	0.68043500	-3.79837000	1.57139800
H	1.23480600	-6.21136800	1.62485800
H	2.51987000	-7.23684000	-0.23987200
H	3.28903300	-5.82458000	-2.13606800
H	2.77545900	-3.39002500	-2.15722100
N	-0.91277700	-2.31772100	-0.10023200
C	-2.24029800	-1.96013500	-0.17360600
O	-2.66263100	-0.81014100	-0.14486400
C	-3.16828200	-3.14337700	-0.27212000
C	-4.45405100	-2.88929600	-0.76866200

C	-5.37807600	-3.92346200	-0.89614600
C	-5.03237800	-5.22299400	-0.51772400
C	-3.75983400	-5.48113500	-0.00534900
C	-2.83138800	-4.44766300	0.11958600
H	-1.85853200	-4.66447700	0.55266100
H	-3.49114900	-6.48622200	0.30800600
H	-5.75401900	-6.02971300	-0.61381600
H	-6.36977500	-3.71587600	-1.28860100
H	-4.70692900	-1.87115900	-1.04480300
H	-0.66333400	-3.24347200	-0.41834900
H	1.00092900	0.42345700	0.06552100
H	-0.52425200	0.40945700	-0.86495900
H	-0.57618900	0.22321000	0.89826500

B3LYP/6-31G(d) Equilibrium geometry of (*Z*,*E*)-(*M*)-**4-7**

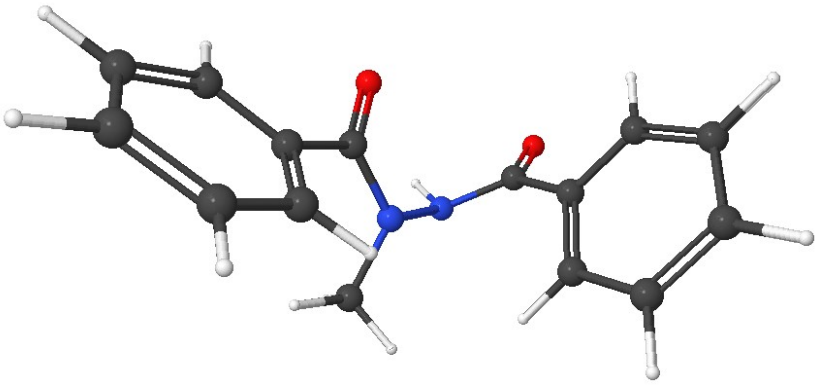

C	0.00000000	0.00000000	0.00000000
N	0.50697500	0.02278600	-1.37386900
N	1.65036000	-0.77248700	-1.54047600
C	2.74400000	-0.30579600	-2.28559600
C	3.05432400	1.15878400	-2.28025200
C	2.81876200	1.99835800	-1.18305800
C	3.19524600	3.34034500	-1.23283500
C	3.79722300	3.85717400	-2.38221800
C	4.04149900	3.02284000	-3.47547600
C	3.68422800	1.67755000	-3.41962700
H	3.88436000	1.01041500	-4.25160200
H	4.51709200	3.41915100	-4.36835400
H	4.08265700	4.90507700	-2.42204100
H	3.02440200	3.98129100	-0.37193200
H	2.37313800	1.59816400	-0.27896900
O	3.44584000	-1.11463900	-2.86997400
H	1.43785200	-1.72929700	-1.82472000
C	-0.33401200	0.09803200	-2.49585900

O	-0.07808300	-0.52720600	-3.51395400
C	-1.50519600	1.02978300	-2.41821400
C	-1.43103900	2.27797900	-1.78331000
C	-2.52453100	3.14341400	-1.81247700
C	-3.69908000	2.76593600	-2.46647000
C	-3.77252000	1.52823700	-3.11107400
C	-2.67588000	0.66941200	-3.09934400
H	-2.70715400	-0.28274900	-3.61949300
H	-4.68144500	1.23741000	-3.63038400
H	-4.55202600	3.43906300	-2.48301000
H	-2.45663600	4.11513800	-1.33108900
H	-0.50813000	2.58137000	-1.29756400
H	-0.96053800	0.51089400	0.04813400
H	0.70633200	0.49949600	0.66933200
H	-0.13087700	-1.03416900	0.34495900

B3LYP/6-31G(d) Equilibrium geometry of (*E*,*E*)-(*M*)-**4**-**7**

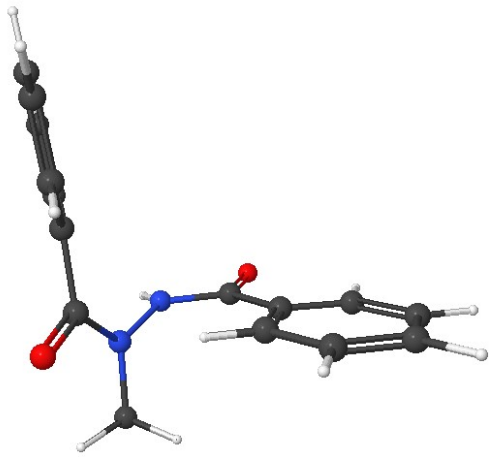

C	0.00000000	0.00000000	0.00000000
N	-0.78606600	-0.96279300	0.77042000
N	-0.45397000	-1.14348700	2.10297600
C	0.69416600	-1.74126700	2.62713500
C	1.56080200	-2.67684700	1.83140500
C	1.30715100	-3.17057800	0.54046100
C	2.20558500	-4.05158000	-0.06366700
C	3.36392500	-4.45148400	0.60180700
C	3.62437900	-3.96679200	1.88567500
C	2.73076900	-3.09109300	2.49279600
H	2.91236600	-2.71096200	3.49162200
H	4.52317200	-4.27270600	2.41402200
H	4.05900100	-5.13668600	0.12380200

```
H    1.99222200 -4.42520900 -1.06127200
H    0.42357000 -2.88659700 -0.01283400
O    0.94698100 -1.48687100  3.79908700
H   -0.81970400 -0.44978500  2.74991900
C   -1.71918800 -1.77648900  0.13592900
O   -1.78172400 -1.79127400 -1.08900200
C   -2.63143200 -2.63243900  0.96509800
C   -3.23378300 -2.21012900  2.15812100
C   -4.14657400 -3.03425200  2.81472200
C   -4.45660900 -4.29228400  2.29471700
C   -3.86903700 -4.71513400  1.10044800
C   -2.97435900 -3.88313300  0.43172400
H   -2.53470100 -4.18532900 -0.51318300
H   -4.11523300 -5.68857000  0.68543600
H   -5.16016300 -4.93709300  2.81445600
H   -4.61538800 -2.69292000  3.73344100
H   -3.01350600 -1.23011900  2.56669900
H   -0.49079000  0.14834100 -0.96101200
H    1.01946300 -0.36504900 -0.17069700
H    0.04638600  0.94545000  0.55043600
```

5.3 NMR spectra for regioselectivity experiments

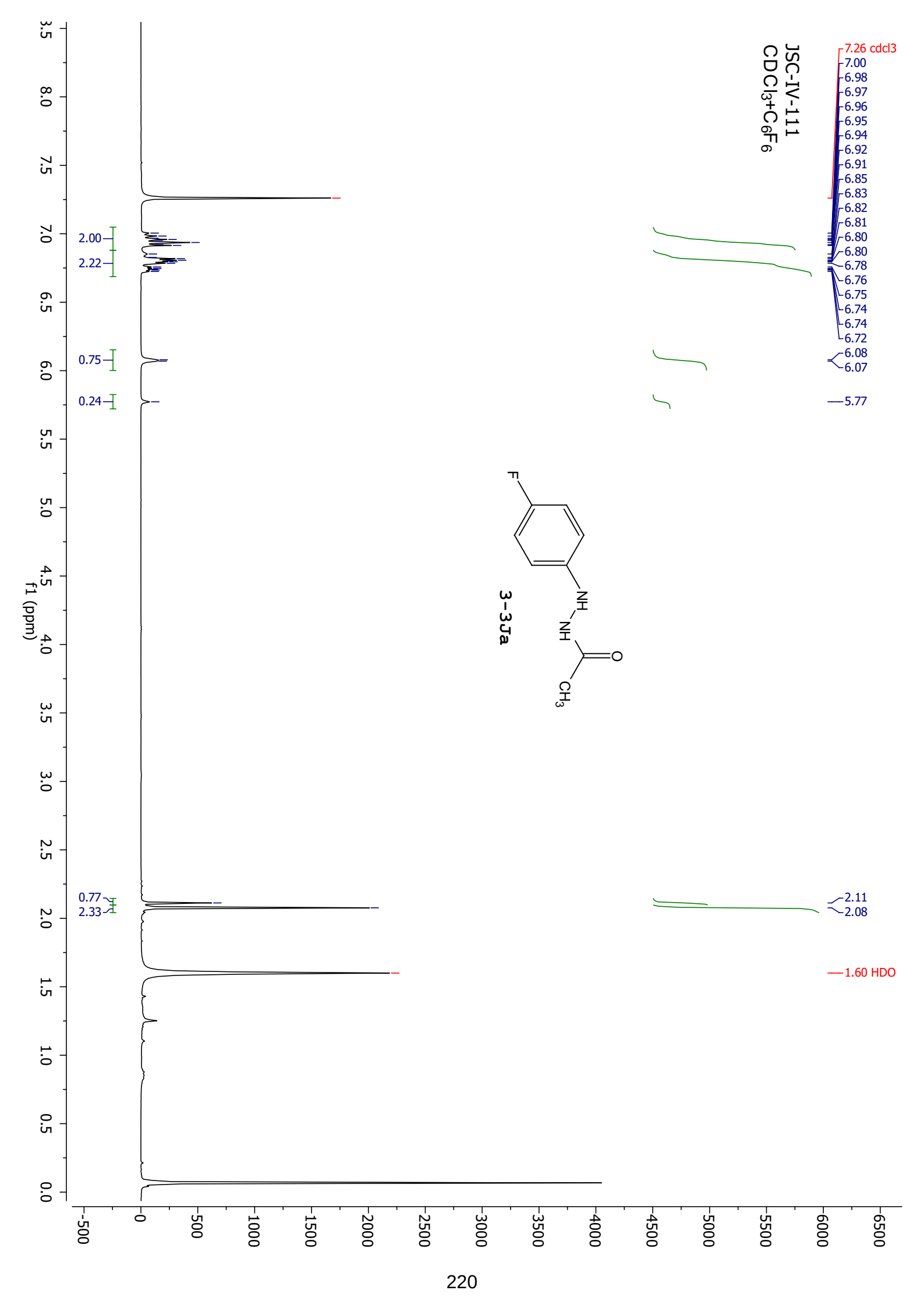
JSC-IV-111
CDCl3+C6F6
7.26 cdcl3
7.00
6.98
6.97
6.96
6.95
6.94
6.92
6.91
6.85
6.83
6.82
6.81
6.80
6.80
6.78
6.76
6.75
6.74
6.74
6.72
6.08
6.07
5.77
2.11
2.08
1.60 HDO
2.00
2.22
0.75
0.24
0.77
2.33
F
NH
NH
O
CH3
3-3Ja
f1 (ppm)

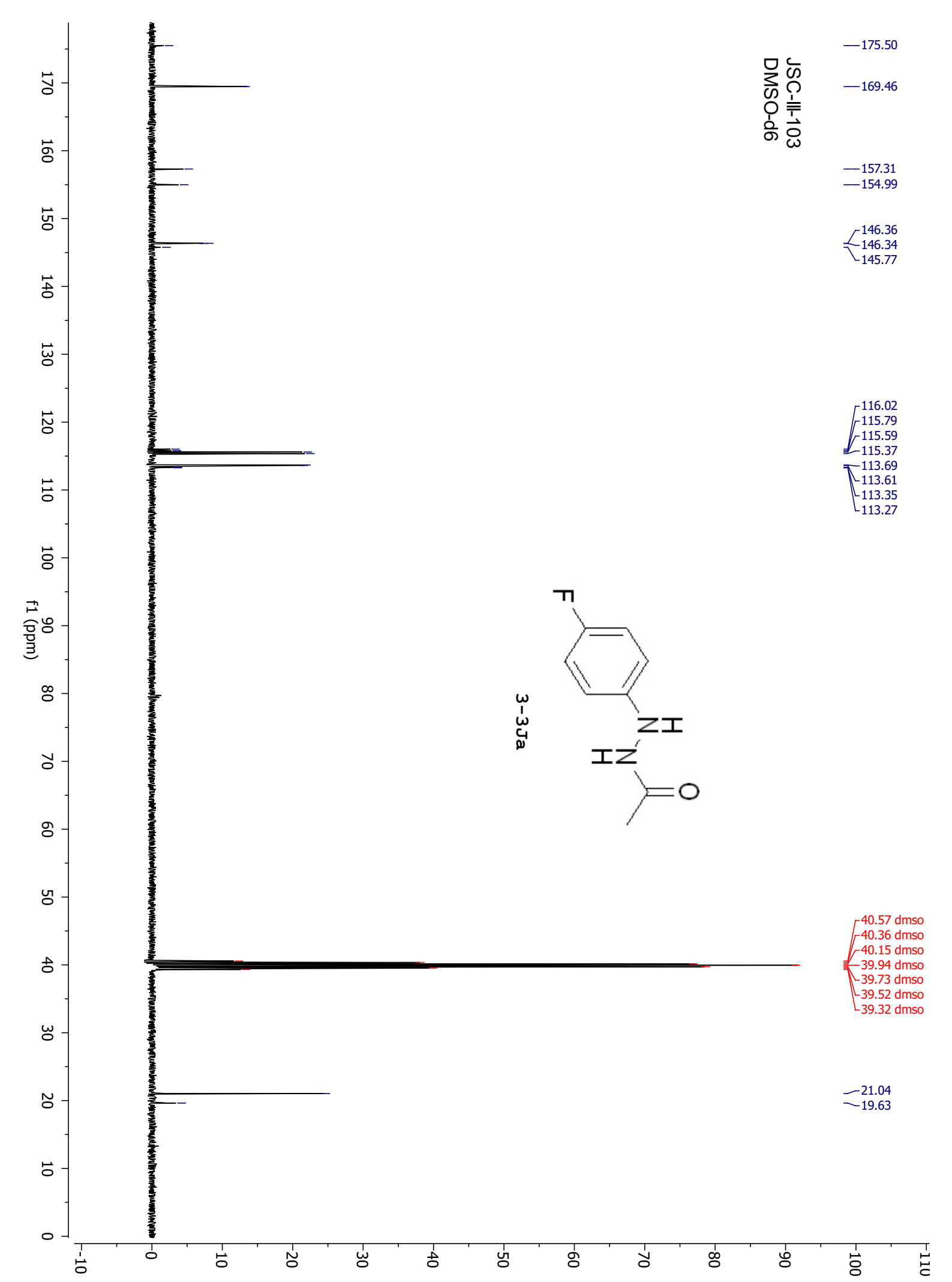
JSC-III-103
DMSO-d6
175.50
169.46
157.31
154.99
146.36
146.34
145.77
116.02
115.79
115.59
115.37
113.69
113.61
113.35
113.27
40.57 dmso
40.36 dmso
40.15 dmso
39.94 dmso
39.73 dmso
39.52 dmso
39.32 dmso
21.04
19.63
3-3Ja
F
NH
HN
O
f1 (ppm)

$CDCl_3+C_6F_6$

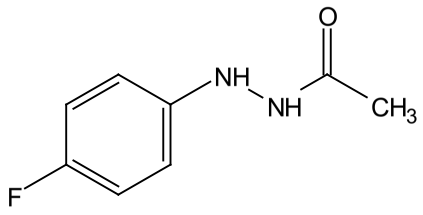

3-3Ja

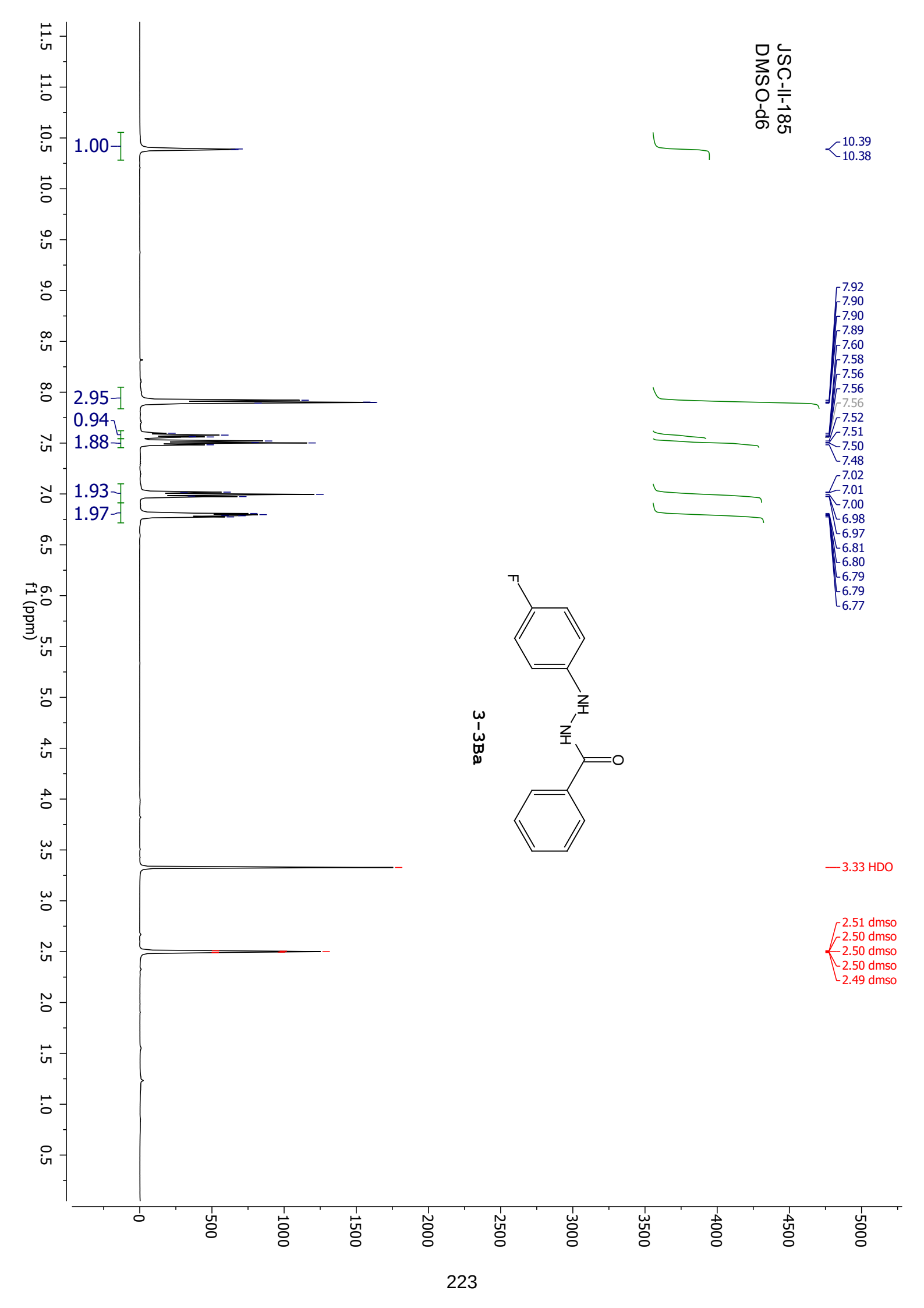
JSC-II-185
DMSO-d6
1.00
2.95
0.94
1.88
1.93
1.97
10.39
10.38
7.92
7.90
7.90
7.89
7.60
7.58
7.56
7.56
7.56
7.52
7.51
7.50
7.48
7.02
7.01
7.00
6.98
6.97
6.81
6.80
6.79
6.79
6.77
3.33 HDO
2.51 dmso
2.50 dmso
2.50 dmso
2.50 dmso
2.49 dmso
F
NH
NH
O
3-3Ba
f1 (ppm)

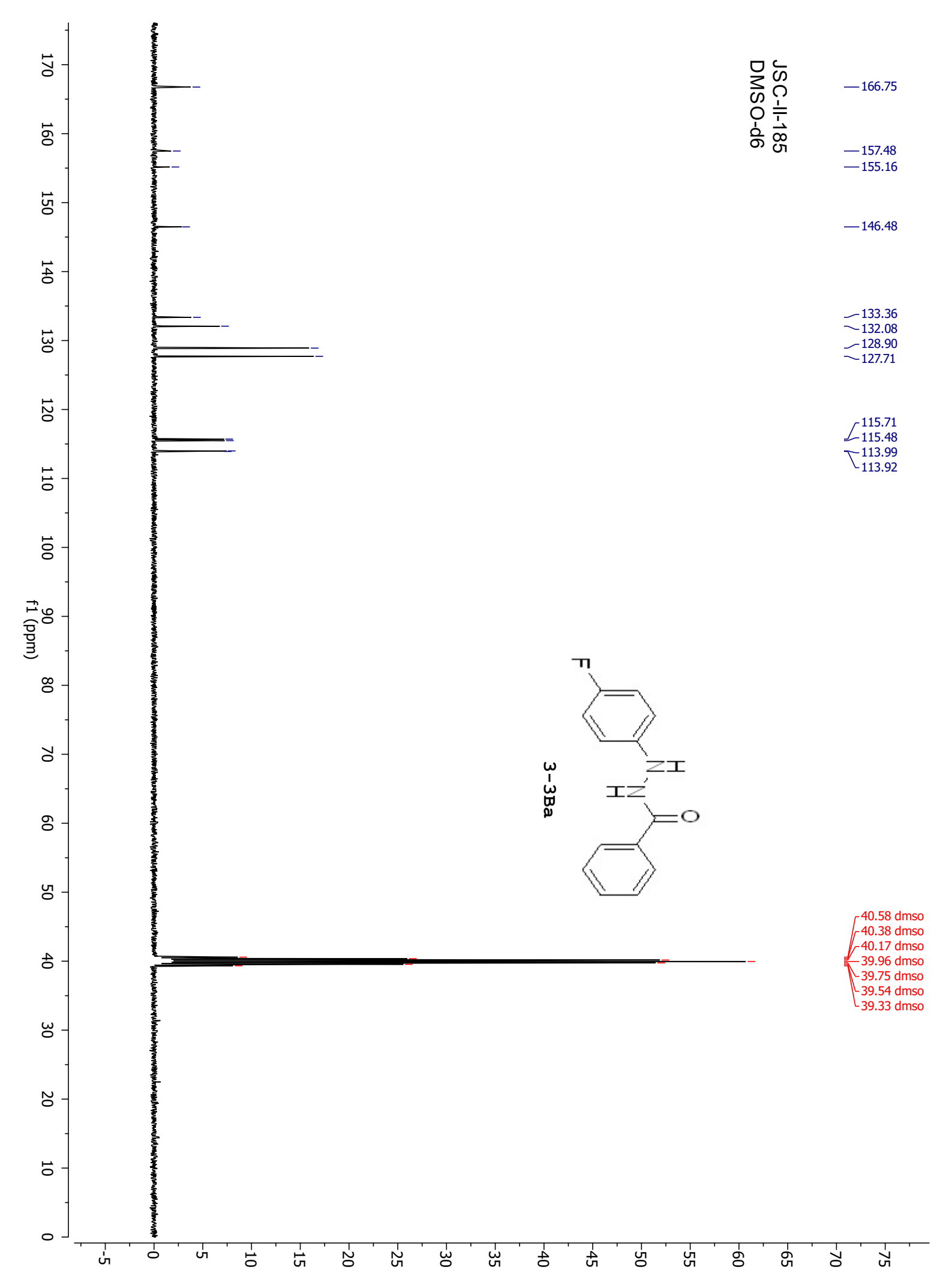
JSC-II-185
DMSO-d6
166.75
157.48
155.16
146.48
133.36
132.08
128.90
127.71
115.71
115.48
113.99
113.92
40.58 dmso
40.38 dmso
40.17 dmso
39.96 dmso
39.75 dmso
39.54 dmso
39.33 dmso
F
NH
HN
O
3-3Ba
f1 (ppm)

JSC-II-185

$CDCl_3 + C_6F_6$

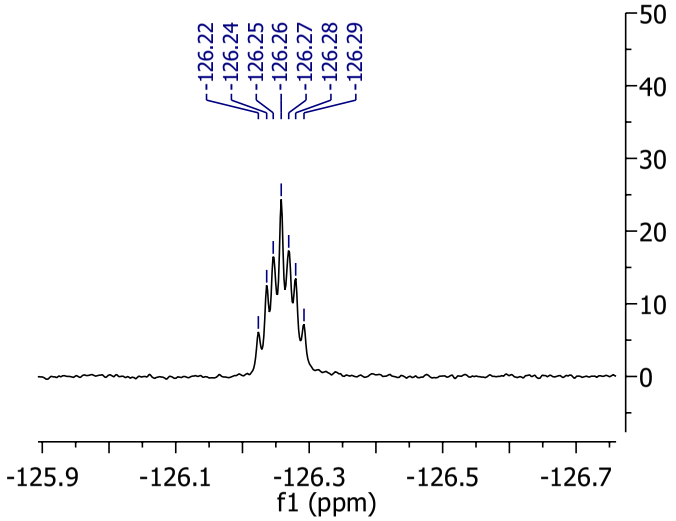

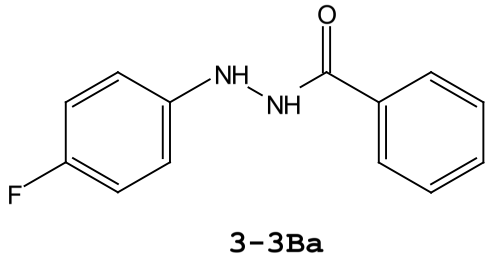

3-3Ba

225

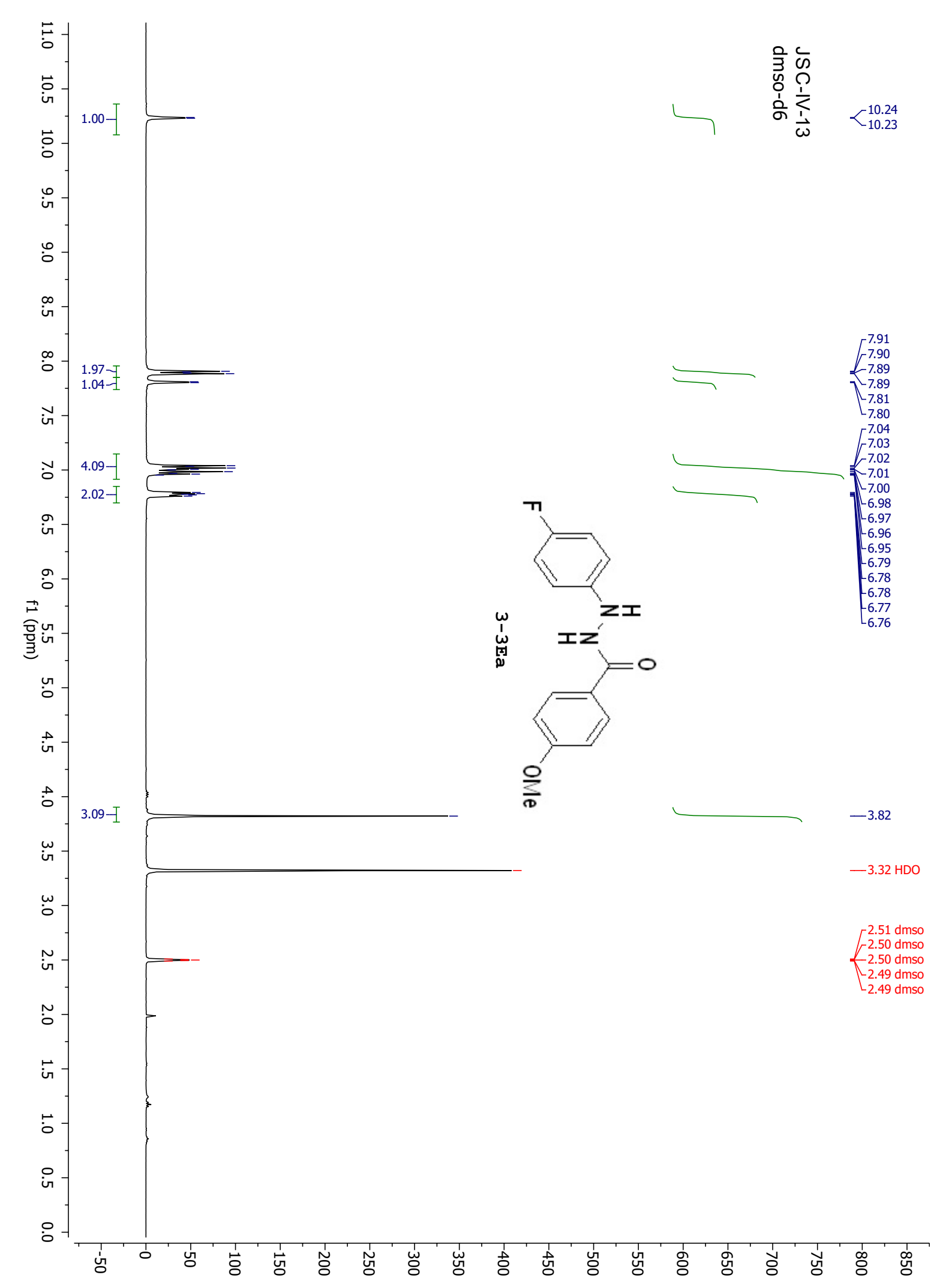
JSC-IV-13
dmso-d6
3-3Ea
F
N
H
N
H
O
OMe
1.00
1.97
1.04
4.09
2.02
3.09
10.24
10.23
7.91
7.90
7.89
7.89
7.81
7.80
7.04
7.03
7.02
7.01
7.00
6.98
6.97
6.96
6.95
6.79
6.78
6.78
6.77
6.76
3.82
3.32 HDO
2.51 dmso
2.50 dmso
2.50 dmso
2.49 dmso
2.49 dmso
f1 (ppm)

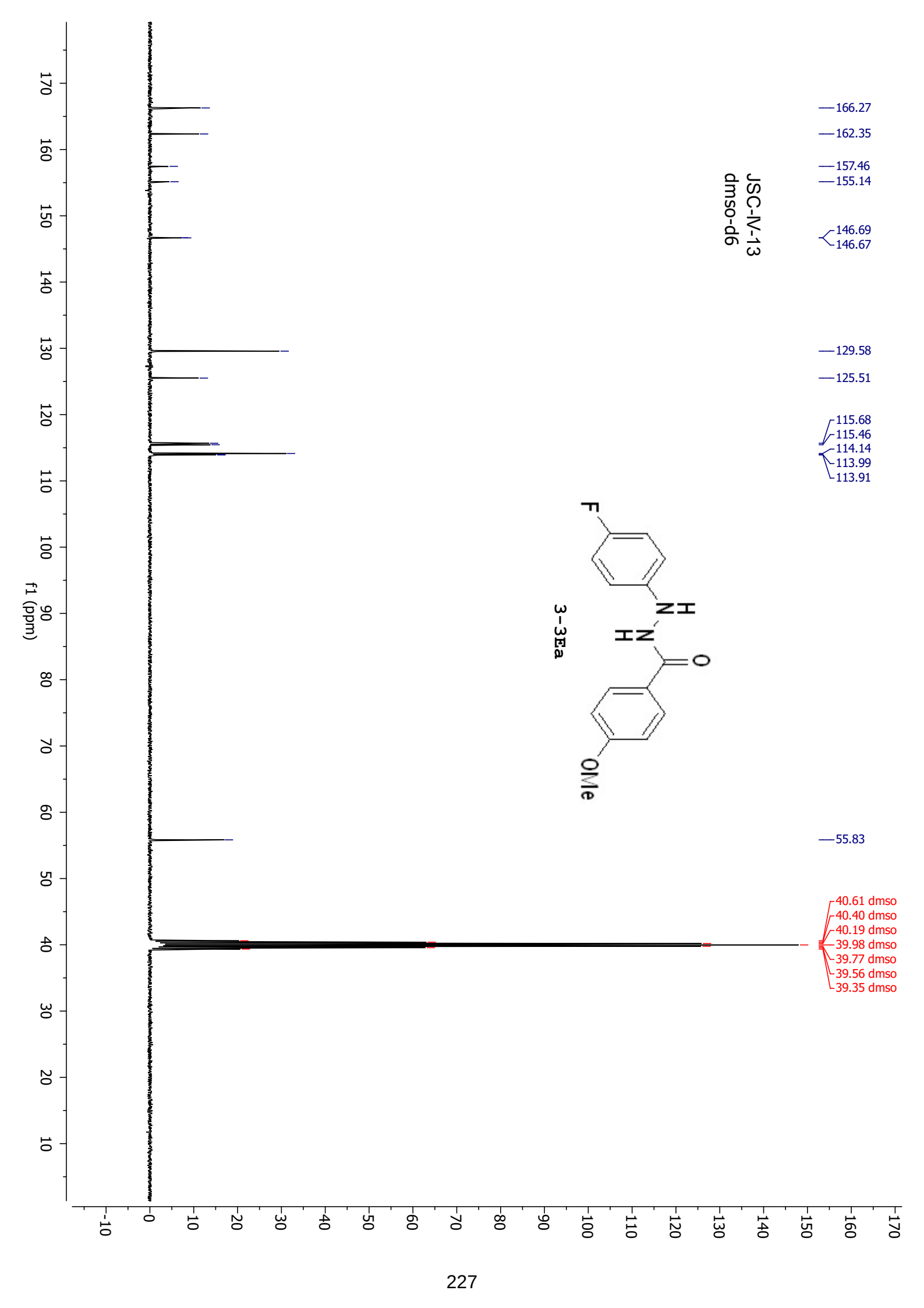
JSC-IV-13
dmso-d6
3-3Ea
166.27
162.35
157.46
155.14
146.69
146.67
129.58
125.51
115.68
115.46
114.14
113.99
113.91
55.83
40.61 dmso
40.40 dmso
40.19 dmso
39.98 dmso
39.77 dmso
39.56 dmso
39.35 dmso
f1 (ppm)

JSC-IV-13
chloroform-d

-126.43
-126.44
-126.45
-126.46
-126.48
-126.49
-126.50

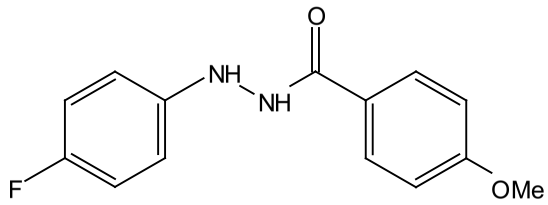

3-3Ea

228

f1 (ppm)

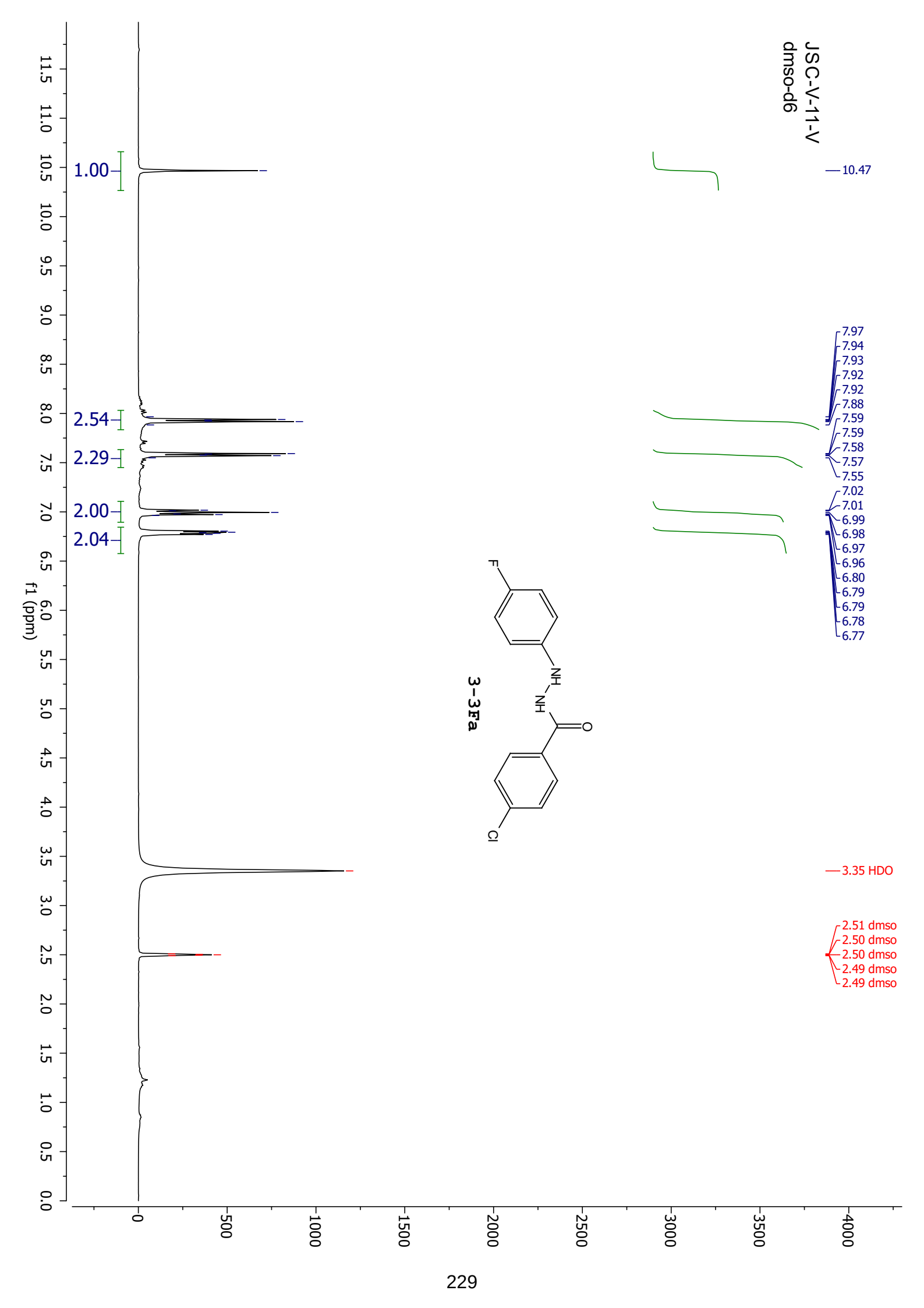
JSC-V-11-V
dmso-d6
10.47
7.97
7.94
7.93
7.92
7.92
7.88
7.59
7.59
7.58
7.57
7.55
7.02
7.01
6.99
6.98
6.97
6.96
6.80
6.79
6.79
6.78
6.77
3.35 HDO
2.51 dmso
2.50 dmso
2.50 dmso
2.49 dmso
2.49 dmso
1.00
2.54
2.29
2.00
2.04
3-3Fa
F
NH
NH
O
Cl
f1 (ppm)

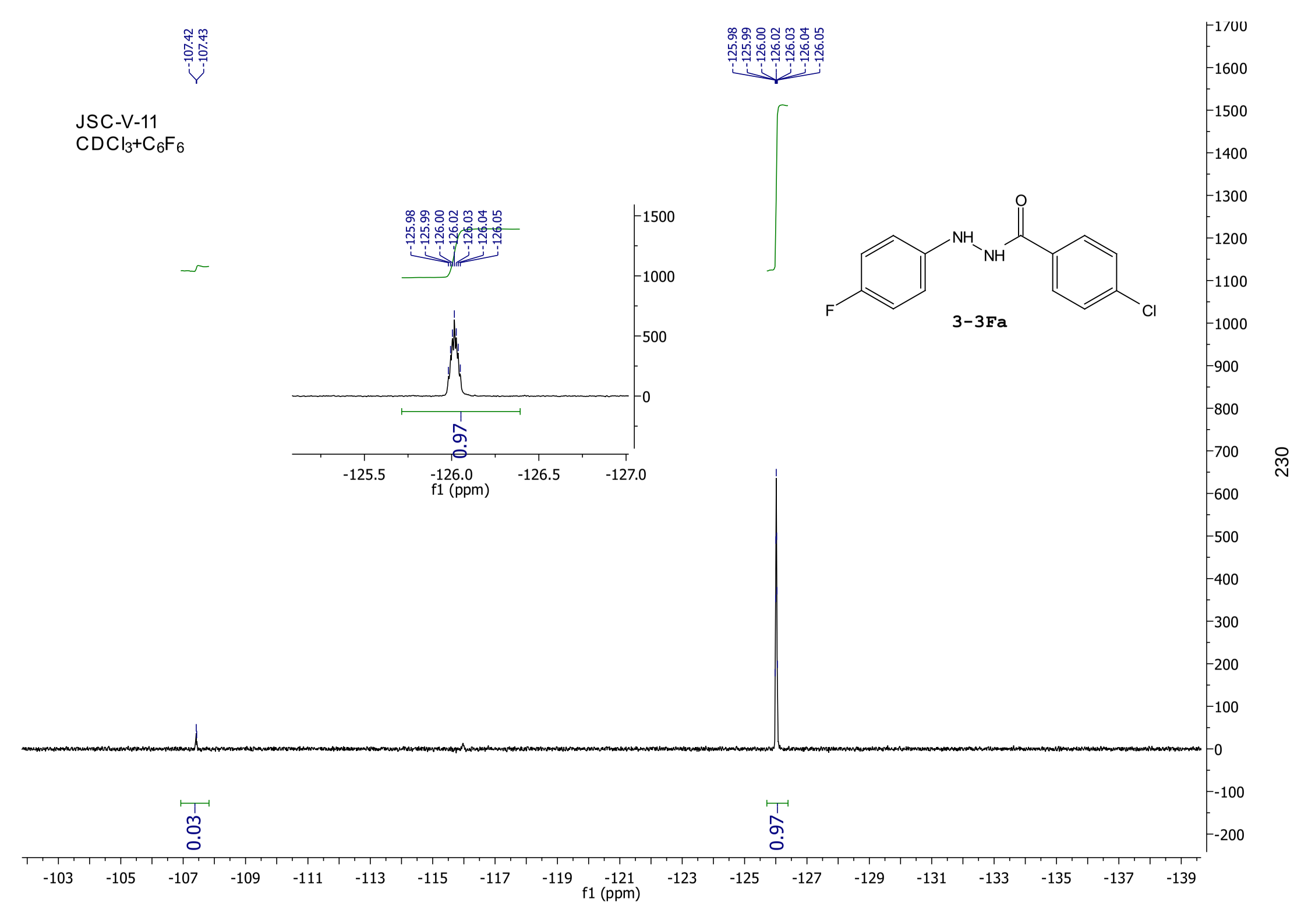
JSC-V-11
CDCl3+C6F6
-107.42
-107.43
-125.98
-125.99
-126.00
-126.02
-126.03
-126.04
-126.05
NH
NH
O
F
Cl
3-3Fa
0.03
0.97
0.97
f1 (ppm)
f1 (ppm)
230

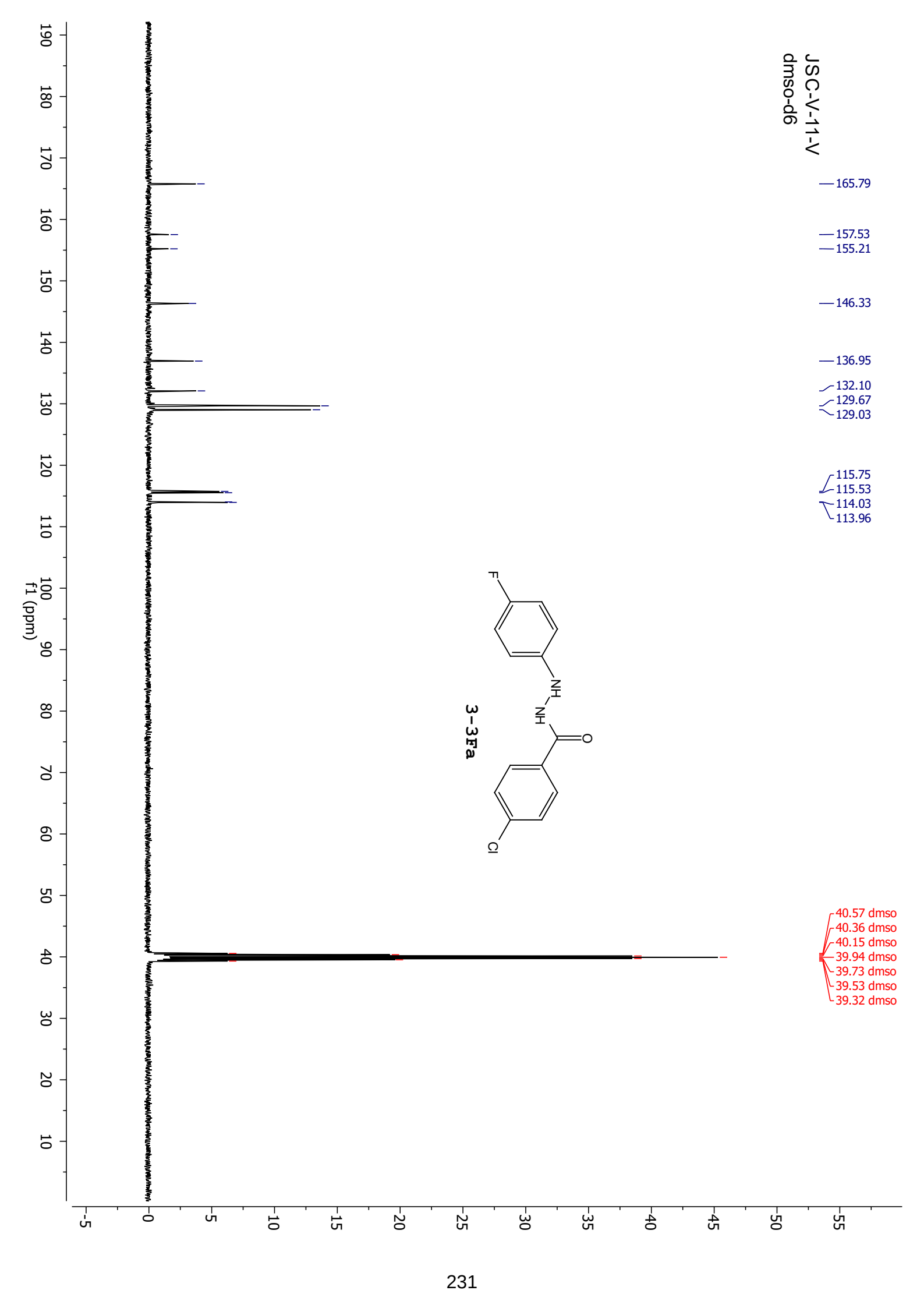
JSC-V-11-V
dmso-d6
165.79
157.53
155.21
146.33
136.95
132.10
129.67
129.03
115.75
115.53
114.03
113.96
40.57 dmso
40.36 dmso
40.15 dmso
39.94 dmso
39.73 dmso
39.53 dmso
39.32 dmso
F
NH
NH
O
Cl
3-3Fa
f1 (ppm)

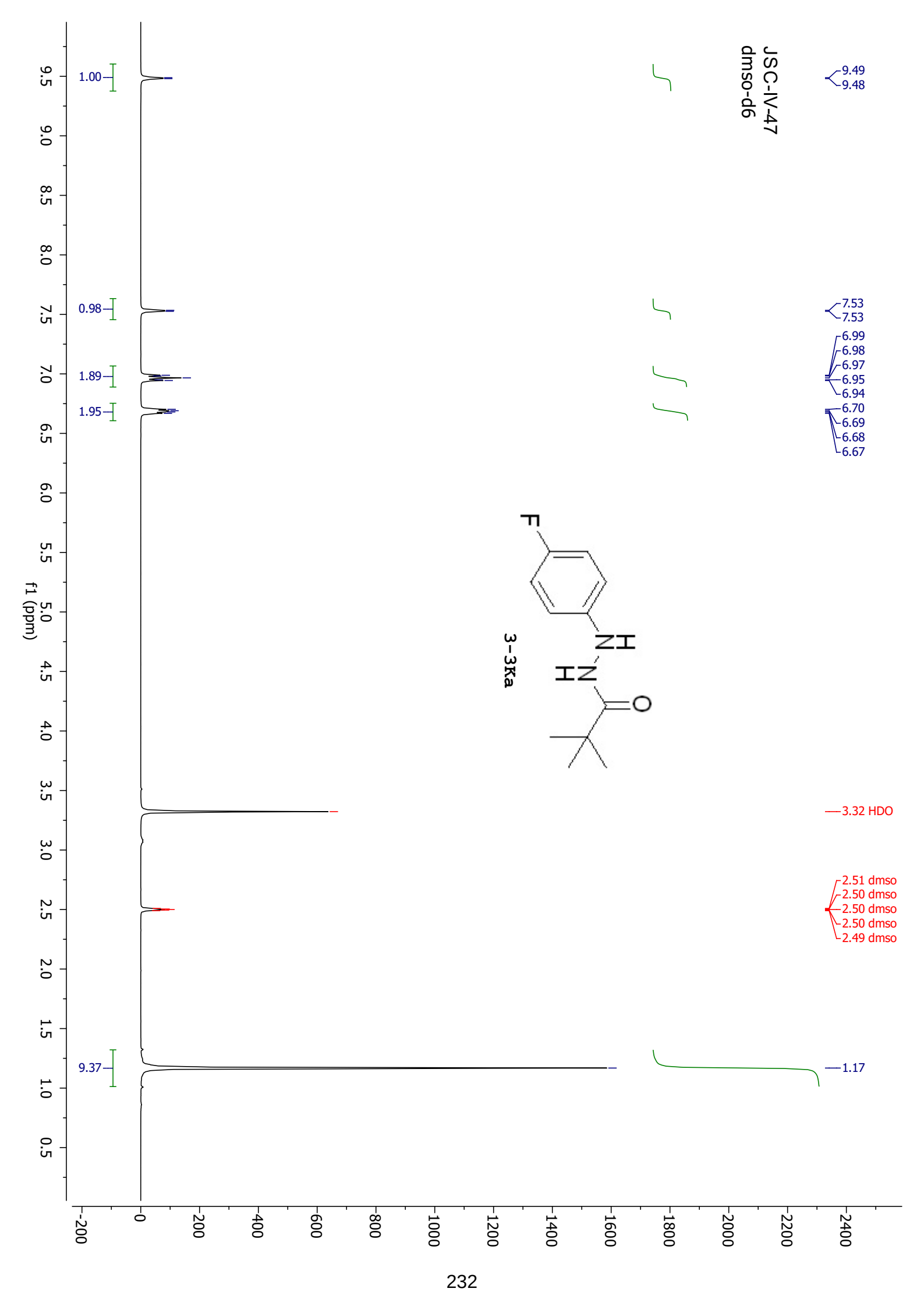
JSC-IV-47
dmso-d6
3-3Ka
F
NH
HN
O
9.49
9.48
7.53
7.53
6.99
6.98
6.97
6.95
6.94
6.70
6.69
6.68
6.67
3.32 HDO
2.51 dmso
2.50 dmso
2.50 dmso
2.50 dmso
2.49 dmso
1.17
1.00
0.98
1.89
1.95
9.37
f1 (ppm)

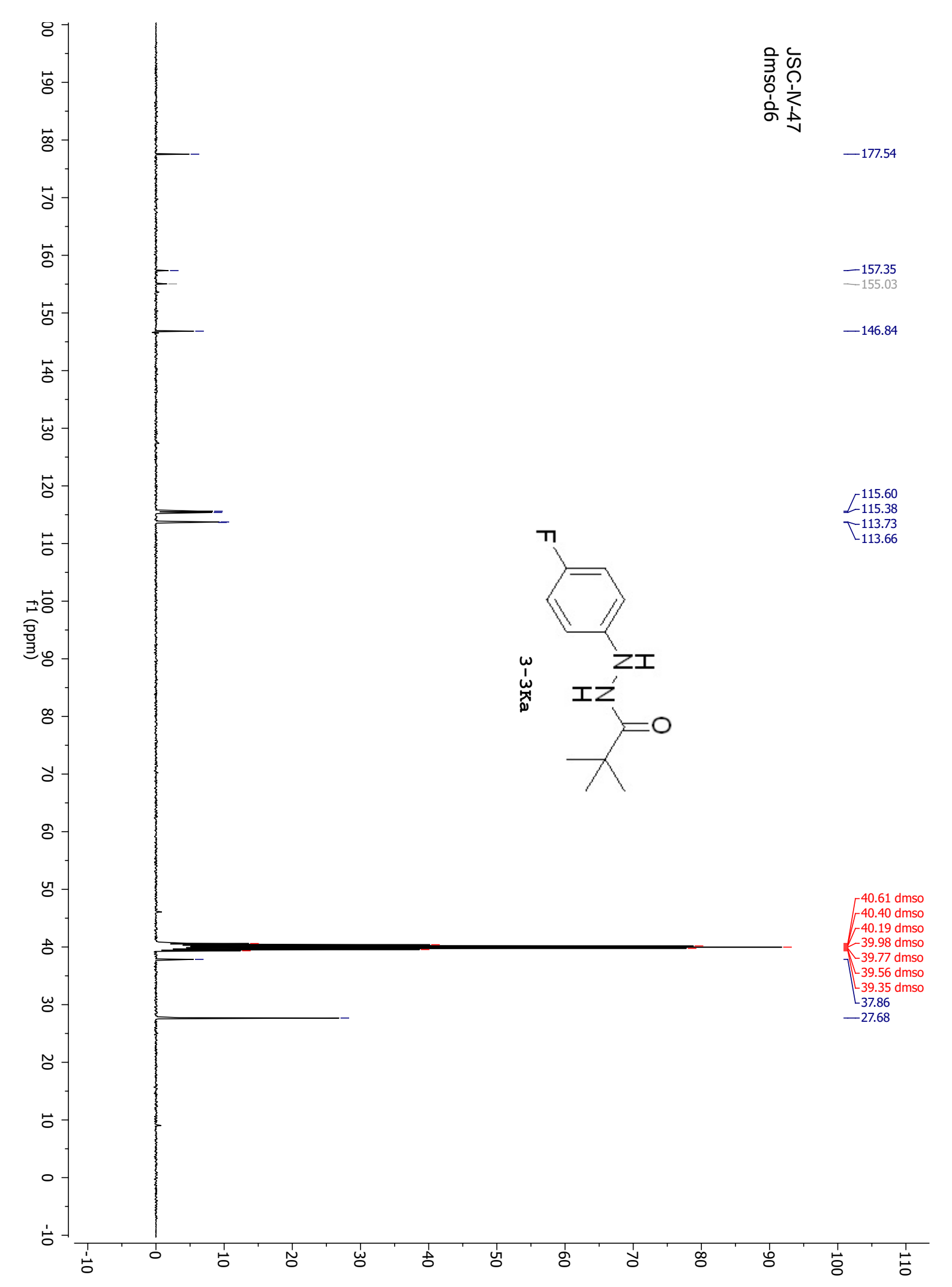
JSC-IV-47
dmso-d6
177.54
157.35
155.03
146.84
115.60
115.38
113.73
113.66
40.61 dmso
40.40 dmso
40.19 dmso
39.98 dmso
39.77 dmso
39.56 dmso
39.35 dmso
37.86
27.68
F
NH
HN
O
3-3Ka
f1 (ppm)

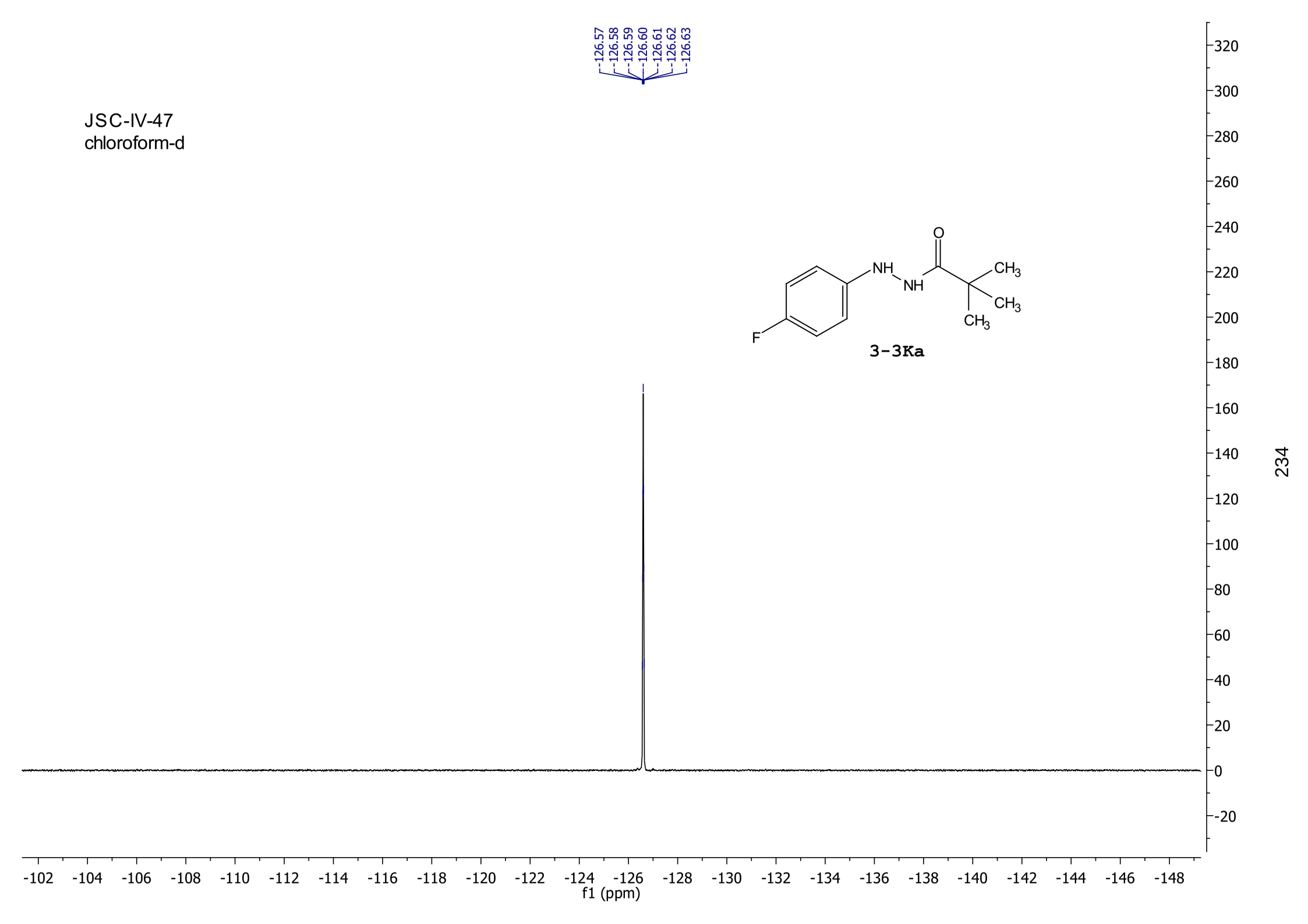
126.57
126.58
126.59
126.60
126.61
126.62
126.63
JSC-IV-47
chloroform-d
O
NH
NH
CH3
CH3
CH3
F
3-3Ka
320
300
280
260
240
220
200
180
160
140
120
100
80
60
40
20
0
-20
234
-102 -104 -106 -108 -110 -112 -114 -116 -118 -120 -122 -124 -126 -128 -130 -132 -134 -136 -138 -140 -142 -144 -146 -148
f1 (ppm)

JSC-IV-153-III
dmso-d6

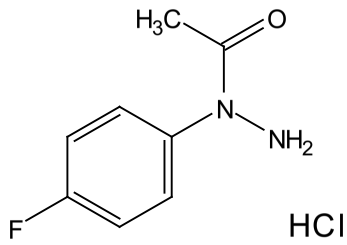

HCl

3-3Aj

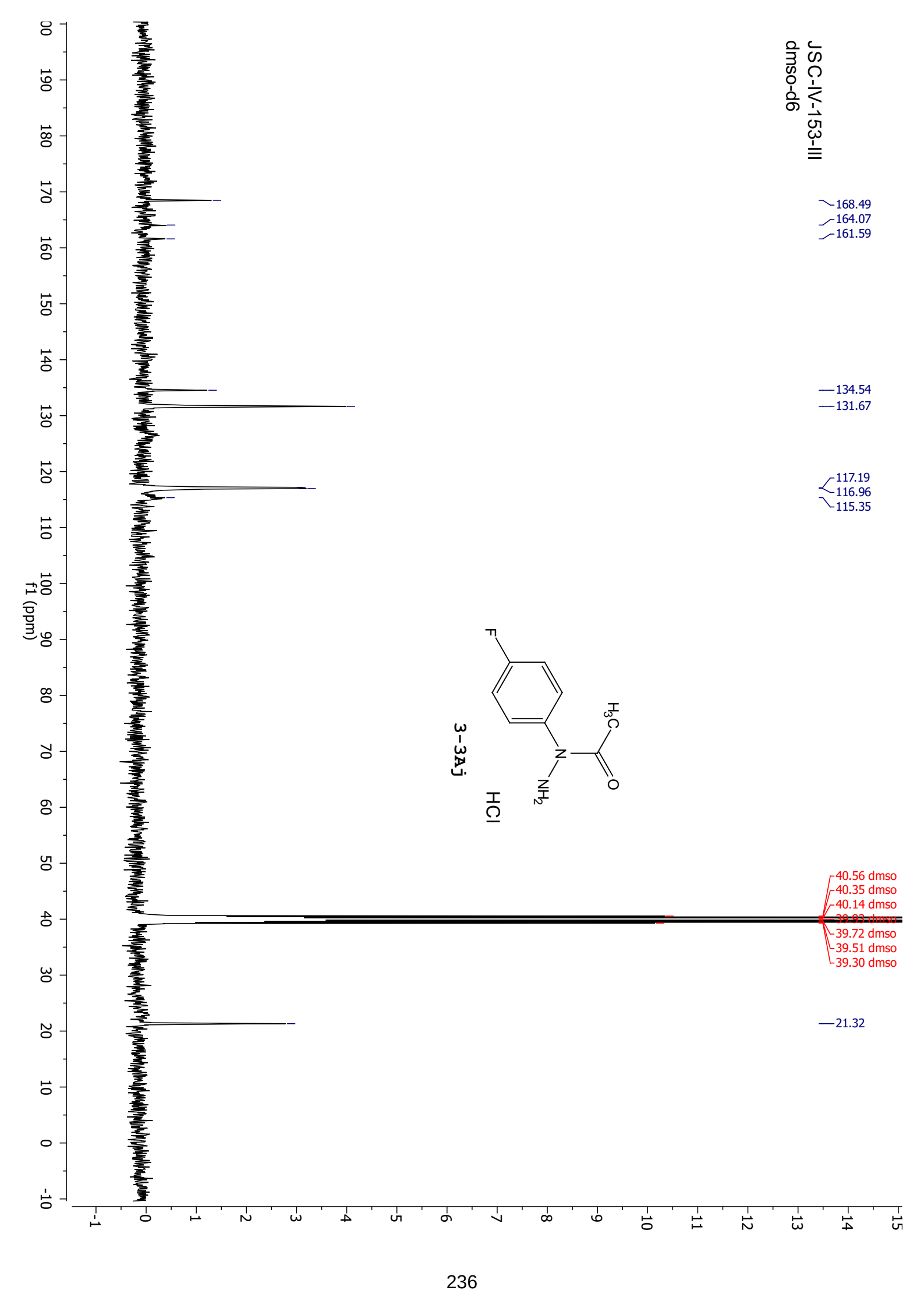
JSC-IV-153-III
dmso-d6
168.49
164.07
161.59
134.54
131.67
117.19
116.96
115.35
40.56 dmso
40.35 dmso
40.14 dmso
39.72 dmso
39.51 dmso
39.30 dmso
21.32
3-3Aj
HCl
F
N
NH2
H3C
O
f1 (ppm)


JSC-IV-153-III
chloroform-d
-116.28
-116.29
-116.30
-116.32
-116.33
-116.34
-116.35
-118.66
H3C
O
N
NH2
F
3-3Aj
0.89
0.11
5000
4500
4000
3500
3000
2500
2000
1500
1000
500
0
-500
237
-105 -106 -107 -108 -109 -110 -111 -112 -113 -114 -115 -116 -117 -118 -119 -120 -121 -122 -123 -124 -125 -126 -127 -128 -129
f1 (ppm)

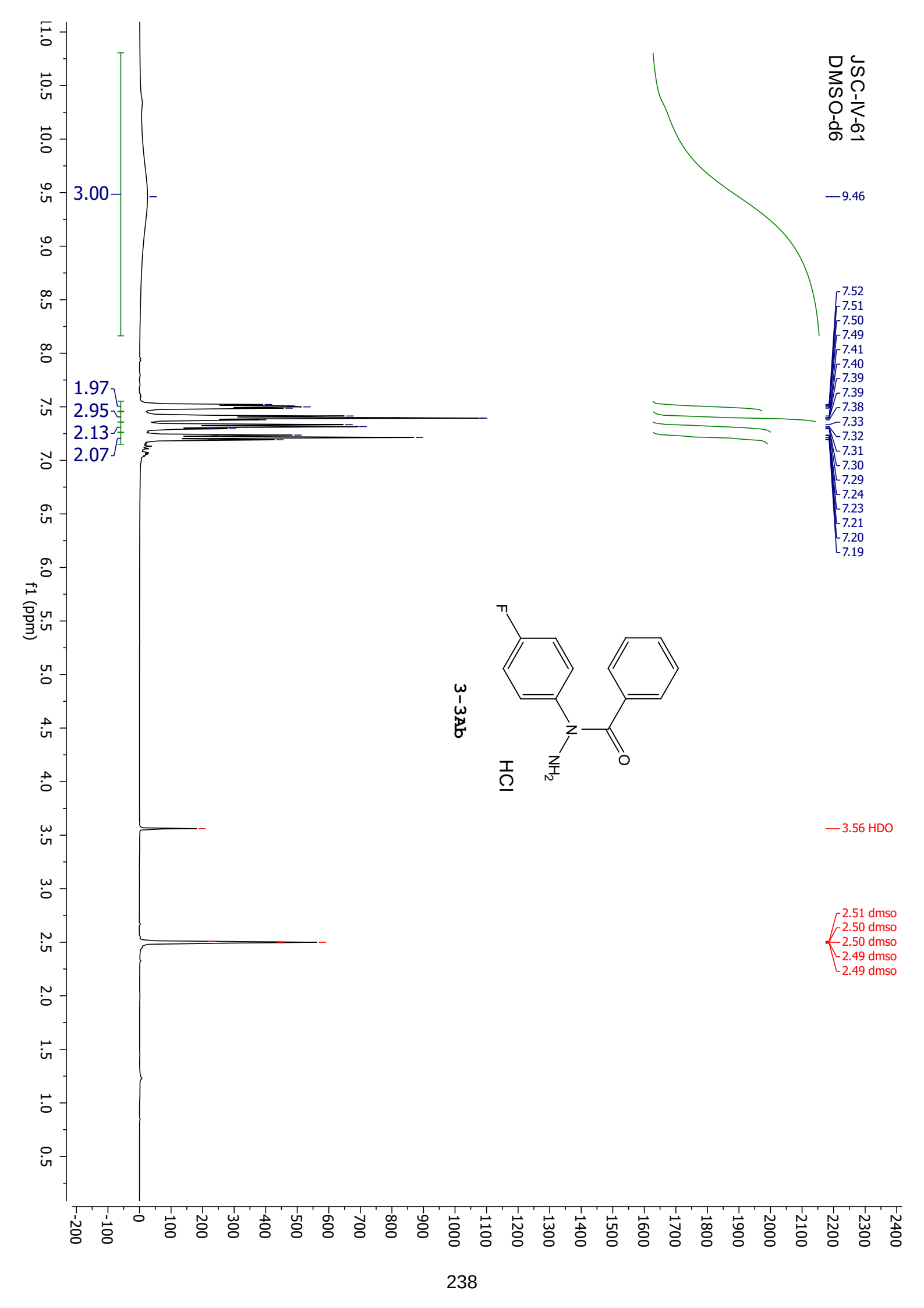
JSC-IV-61
DMSO-d6
3.00
1.97
2.95
2.13
2.07
9.46
7.52
7.51
7.50
7.49
7.41
7.40
7.39
7.39
7.38
7.33
7.32
7.31
7.30
7.29
7.24
7.23
7.21
7.20
7.19
3.56 HDO
2.51 dmso
2.50 dmso
2.50 dmso
2.49 dmso
2.49 dmso
F
N
NH2
O
HCl
3-3Ab
f1 (ppm)

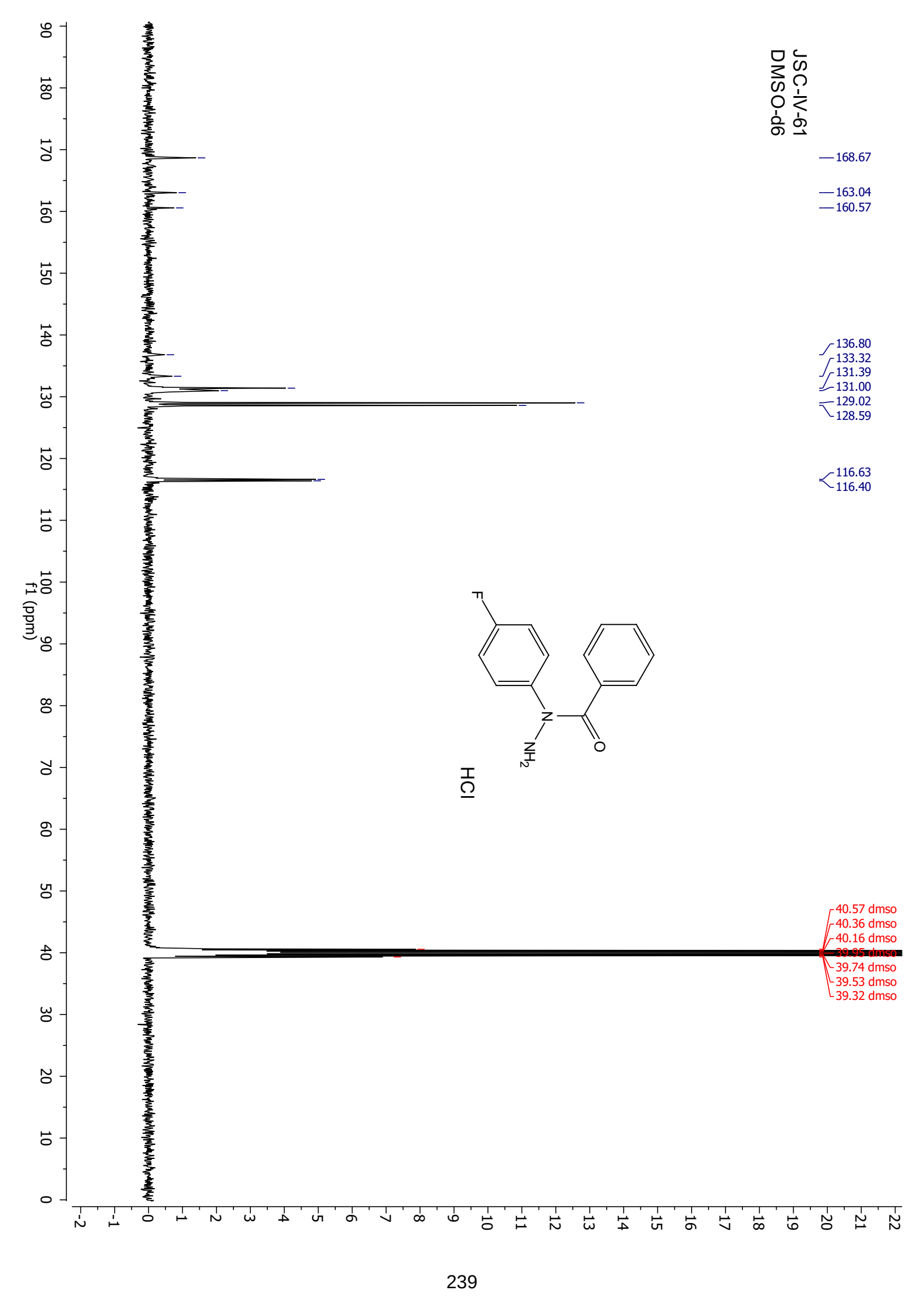
JSC-IV-61
DMSO-d6
168.67
163.04
160.57
136.80
133.32
131.39
131.00
129.02
128.59
116.63
116.40
40.57 dmso
40.36 dmso
40.16 dmso
39.95 dmso
39.74 dmso
39.53 dmso
39.32 dmso
F
N
NH2
O
HCl
f1 (ppm)

JSC-IV-61

$CDCl_3 + C_6F_6 + TEA$

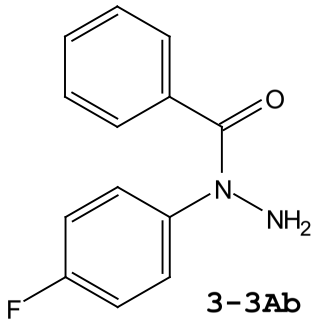

3-3Ab

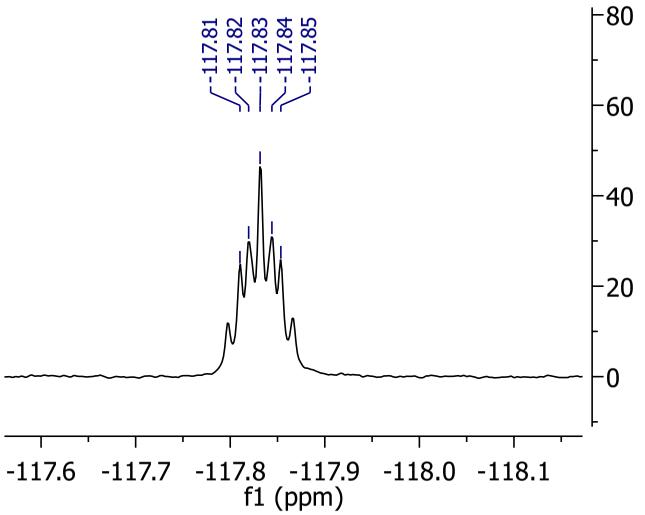

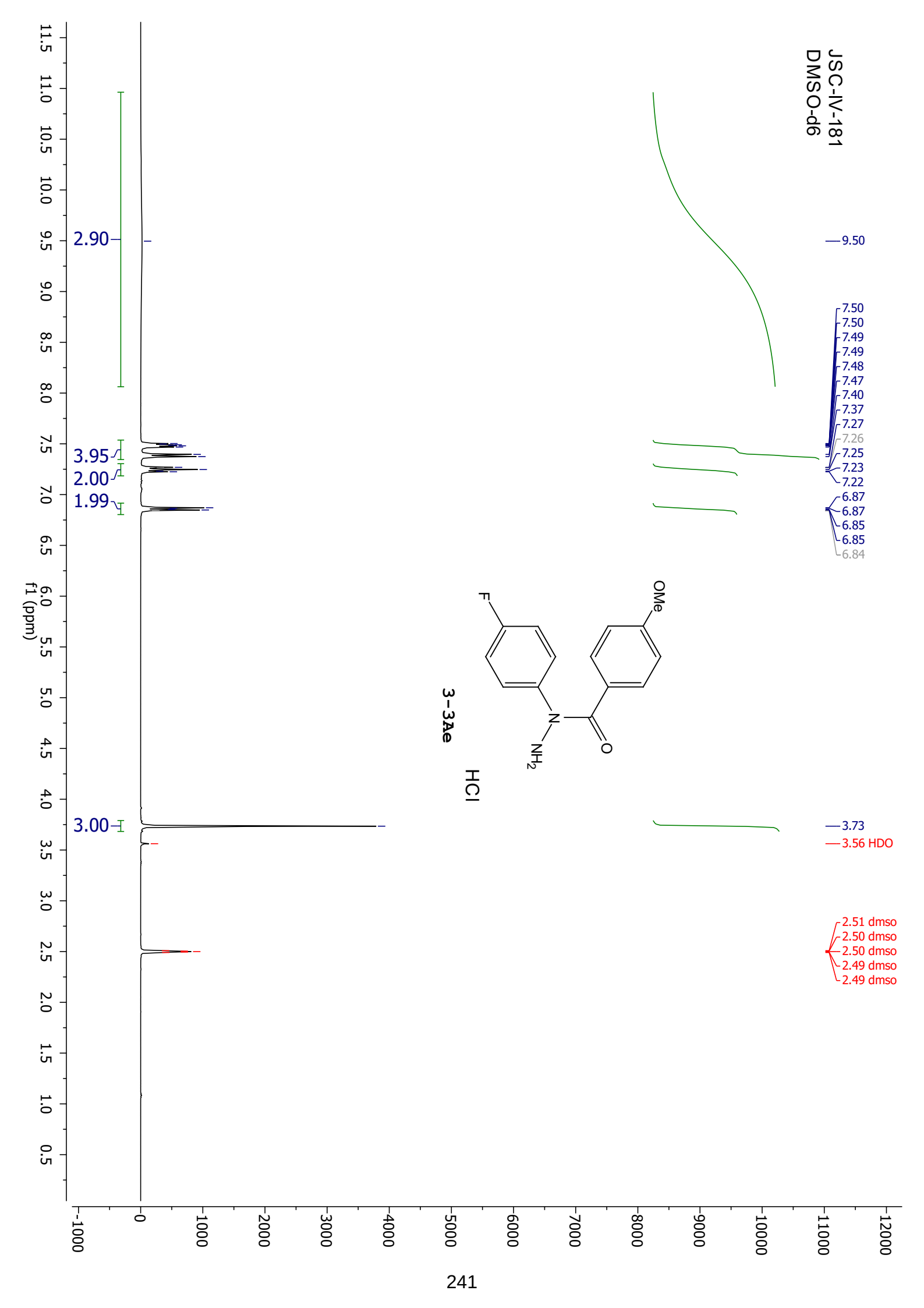
JSC-IV-181
DMSO-d6
3-3Ae
HCl
F
OMe
N
NH2
O
2.90
3.95
2.00
1.99
3.00
9.50
7.50
7.50
7.49
7.49
7.48
7.47
7.40
7.37
7.27
7.26
7.25
7.23
7.22
6.87
6.87
6.85
6.85
6.84
3.73
3.56 HDO
2.51 dmso
2.50 dmso
2.50 dmso
2.49 dmso
2.49 dmso
f1 (ppm)

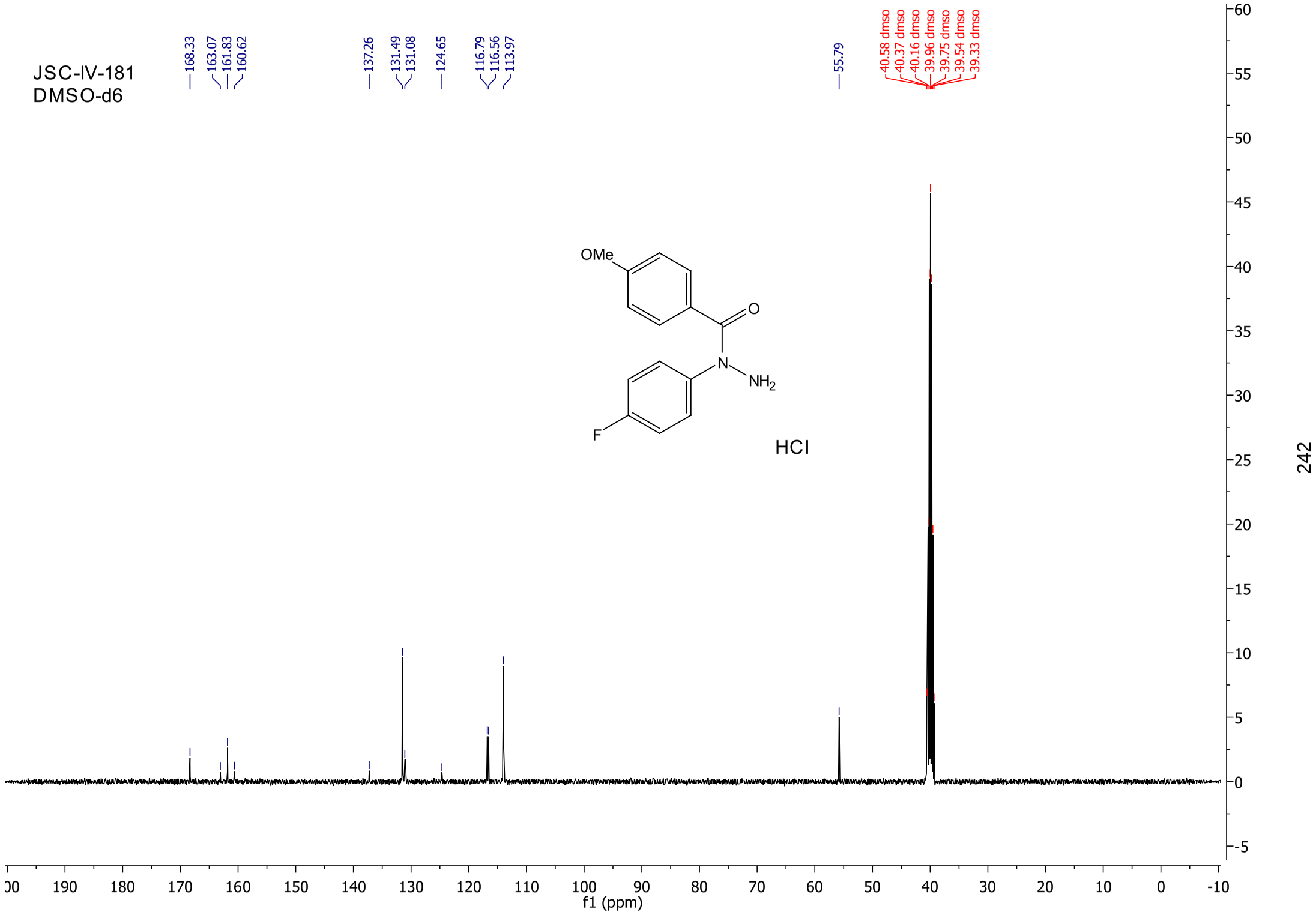
JSC-IV-181
DMSO-d6
168.33
163.07
161.83
160.62
137.26
131.49
131.08
124.65
116.79
116.56
113.97
55.79
40.58 dmso
40.37 dmso
40.16 dmso
39.96 dmso
39.75 dmso
39.54 dmso
39.33 dmso
OMe
O
N
NH2
F
HCl
242
f1 (ppm)

JSC-IV-181
chloroform-d+TEA

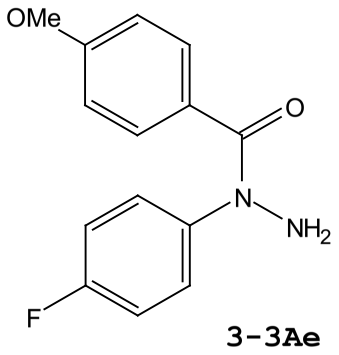

3-3Ae

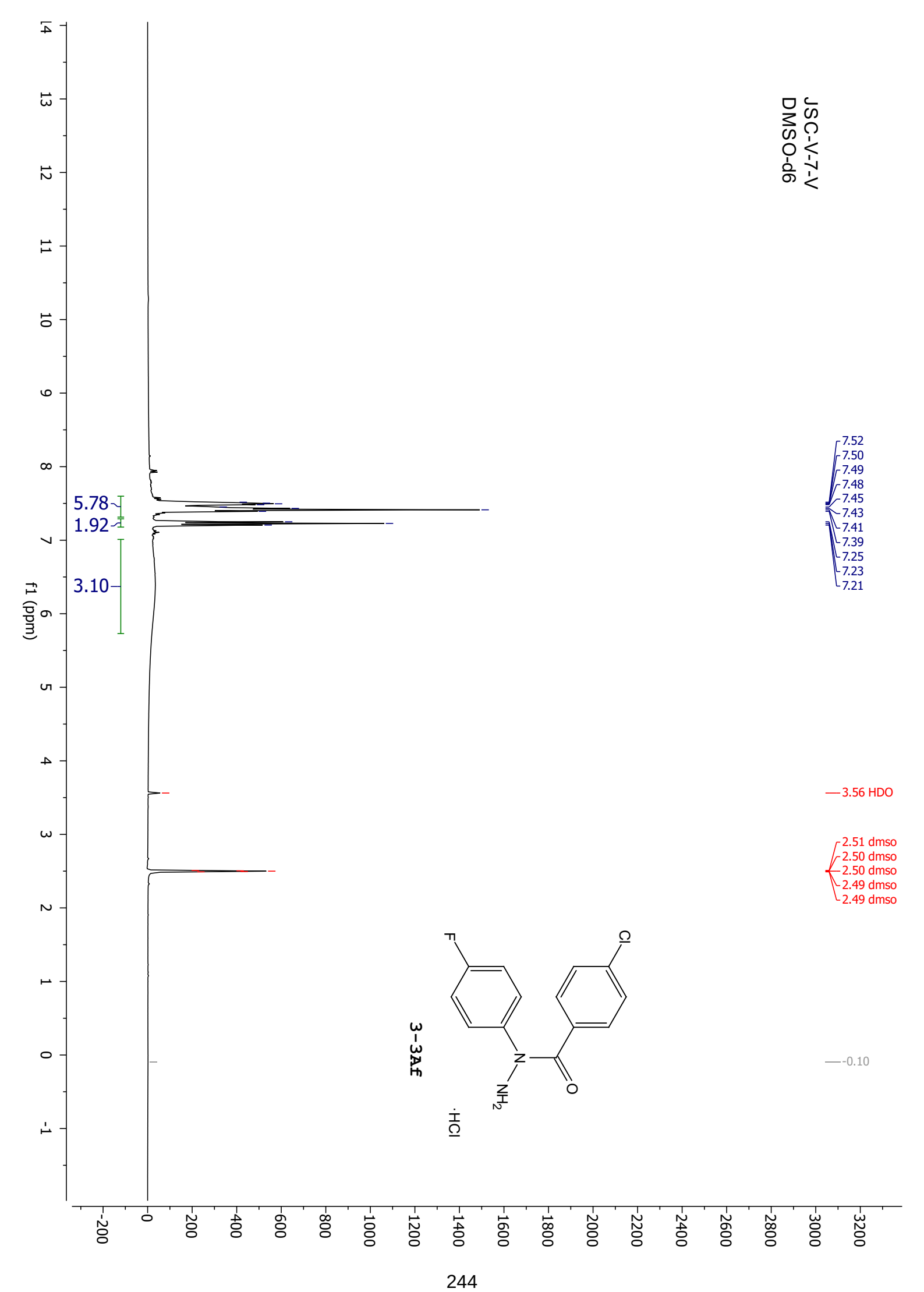
JSC-V-7-V
DMSO-d6
7.52
7.50
7.49
7.48
7.45
7.43
7.41
7.39
7.25
7.23
7.21
5.78
1.92
3.10
3.56 HDO
2.51 dmso
2.50 dmso
2.50 dmso
2.49 dmso
2.49 dmso
-0.10
f1 (ppm)
3-3Af
F
Cl
N
NH2
O
·HCl

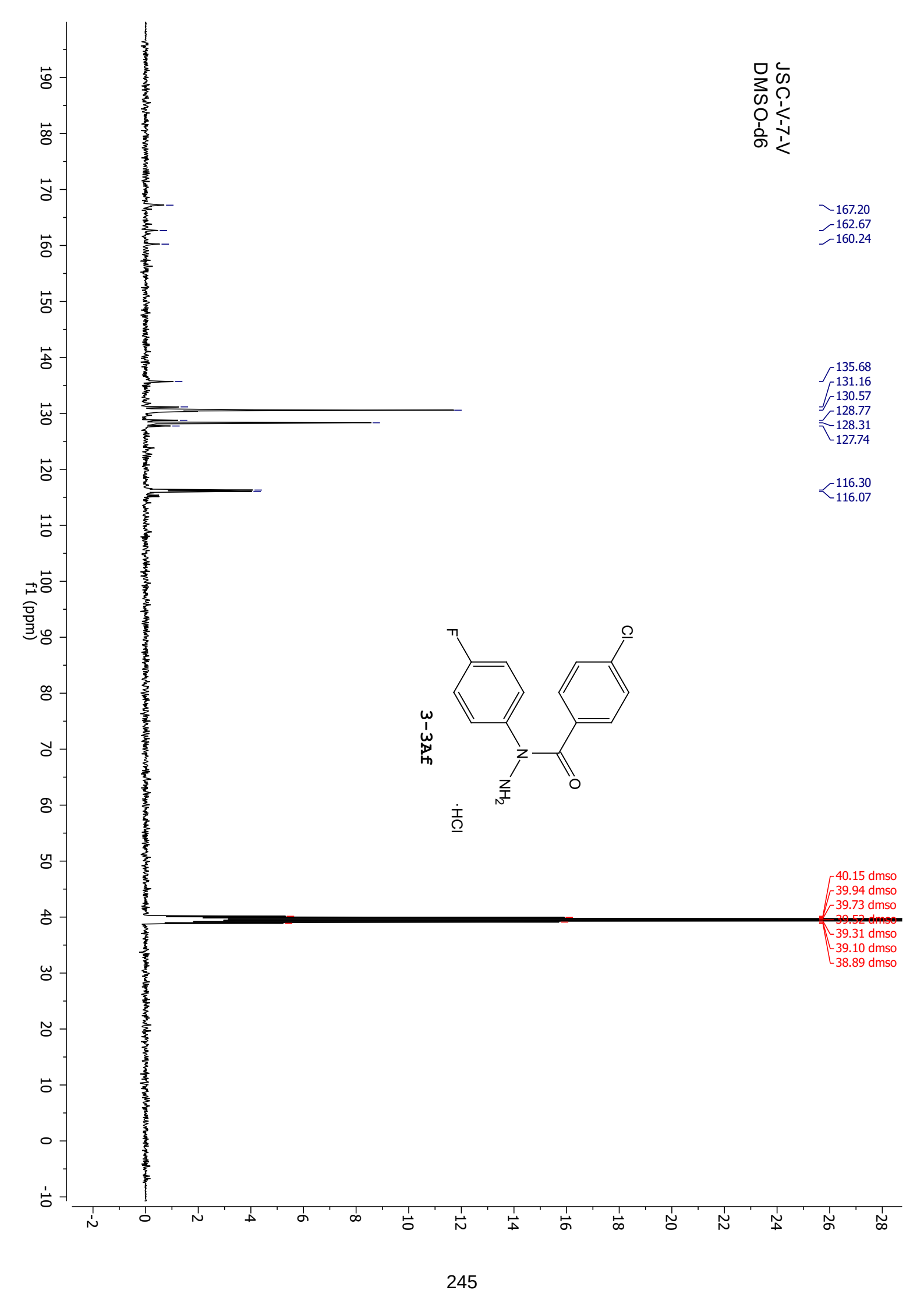
JSC-V-7-V
DMSO-d6
167.20
162.67
160.24
135.68
131.16
130.57
128.77
128.31
127.74
116.30
116.07
40.15 dmso
39.94 dmso
39.73 dmso
39.52 dmso
39.31 dmso
39.10 dmso
38.89 dmso
F
Cl
N
NH2
O
·HCl
3-3Af
f1 (ppm)

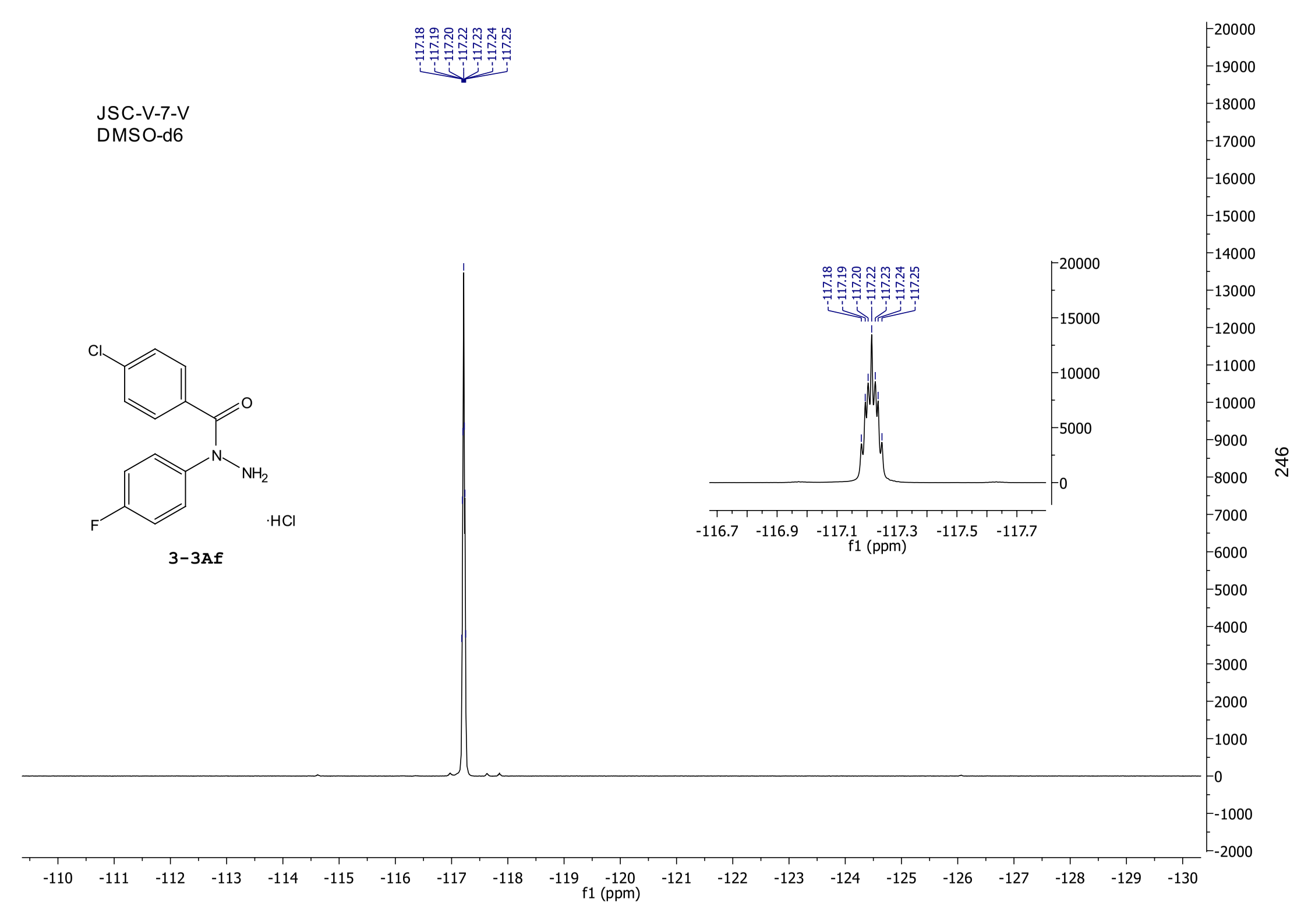
JSC-V-7-V
DMSO-d6
-117.18
-117.19
-117.20
-117.22
-117.23
-117.24
-117.25
Cl
O
N
NH2
F
·HCl
3-3Af
f1 (ppm)
246

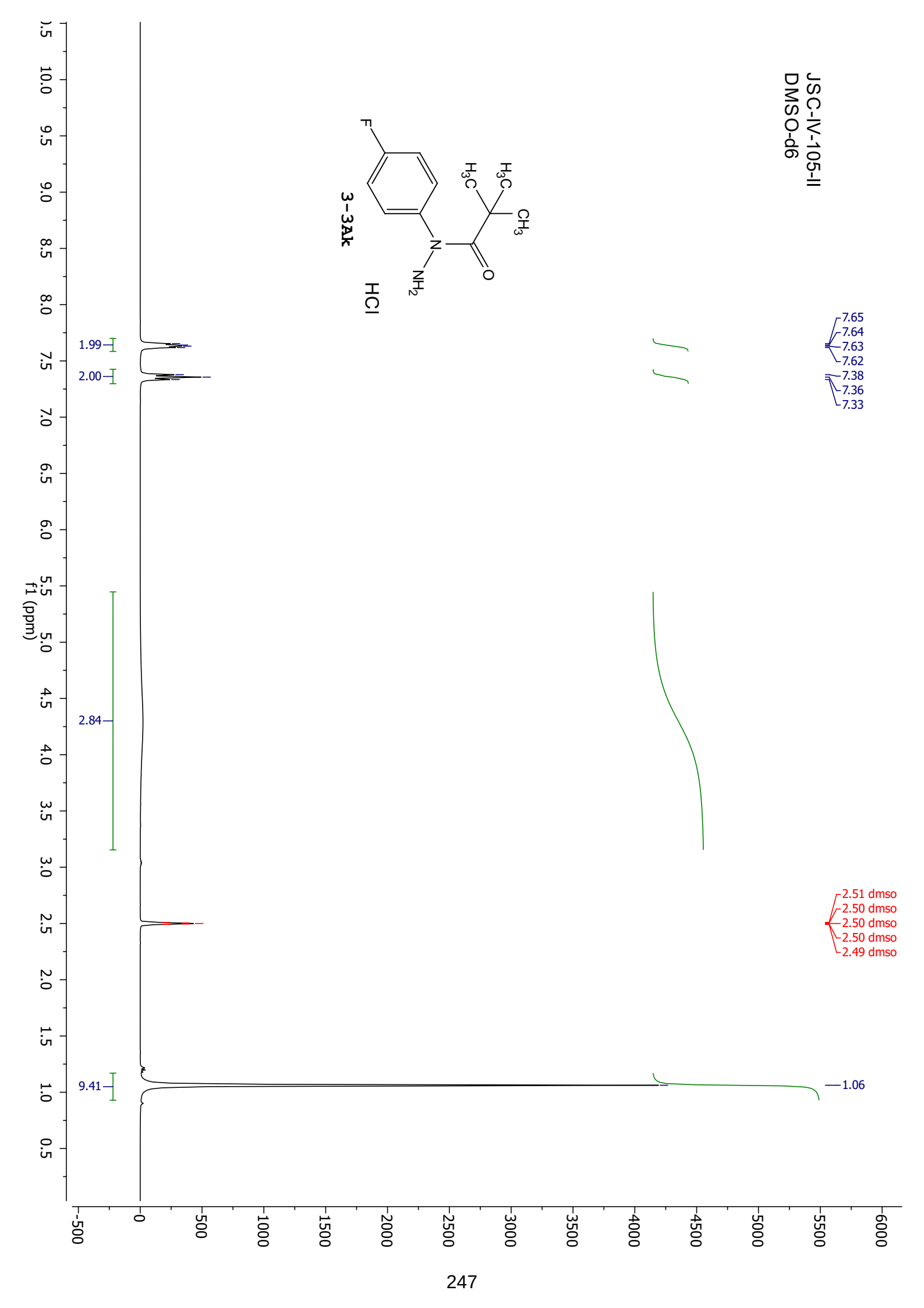
JSC-IV-105-II
DMSO-d6
3-3Ak
HCl
F
N
NH2
O
H3C
H3C
CH3
7.65
7.64
7.63
7.62
7.38
7.36
7.33
2.51 dmso
2.50 dmso
2.50 dmso
2.50 dmso
2.49 dmso
1.99
2.00
2.84
9.41
1.06
f1 (ppm)

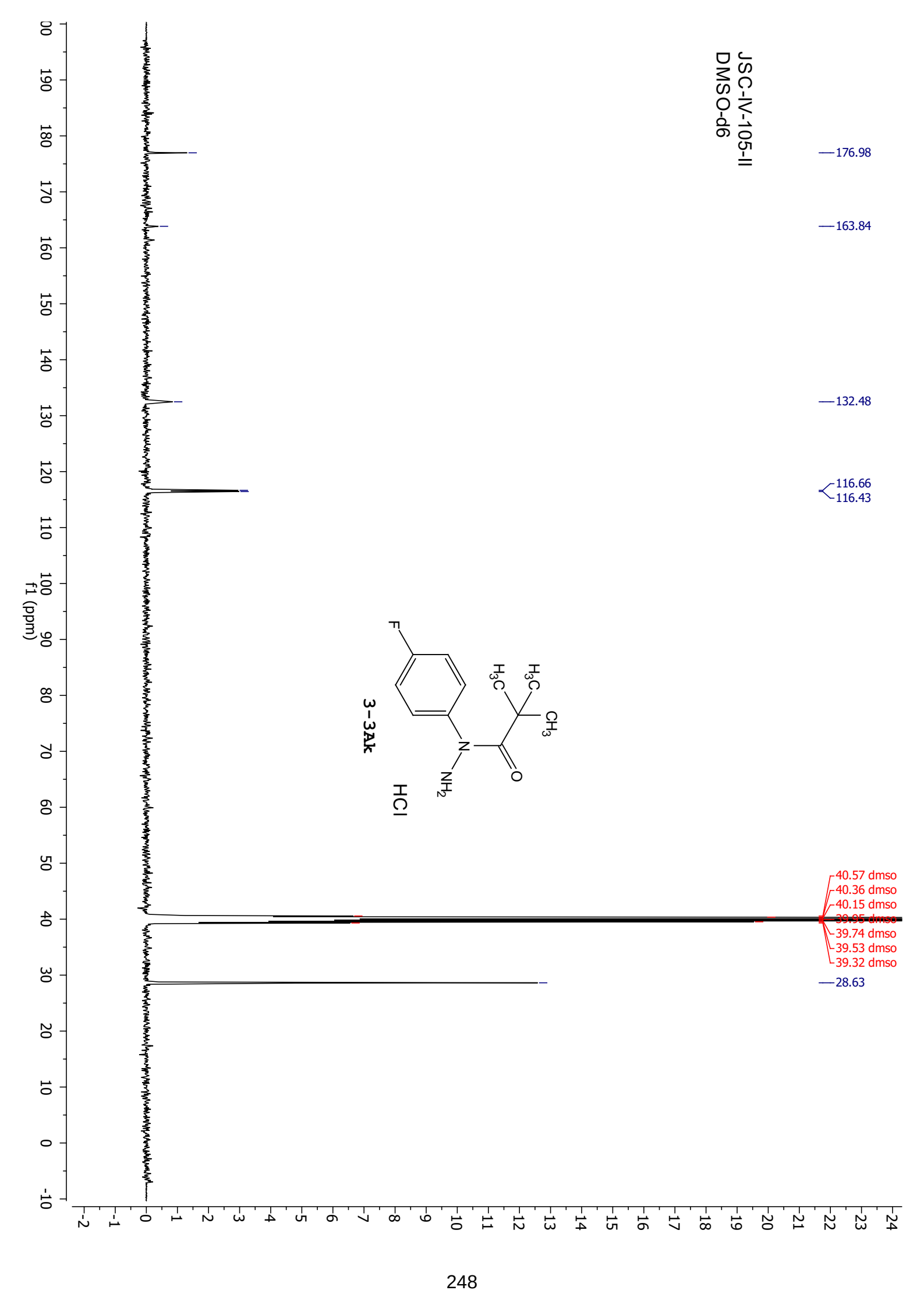
JSC-IV-105-II
DMSO-d6
176.98
163.84
132.48
116.66
116.43
40.57 dmso
40.36 dmso
40.15 dmso
39.74 dmso
39.53 dmso
39.32 dmso
28.63
F
H3C
H3C
CH3
N
NH2
O
HCl
3-3Ak
f1 (ppm)

JSC-IV-105

$CDCl_3$ + TEA

-116.80

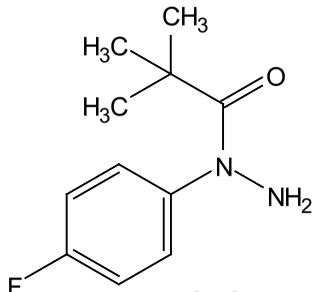

3-3Ak

249

f1 (ppm)

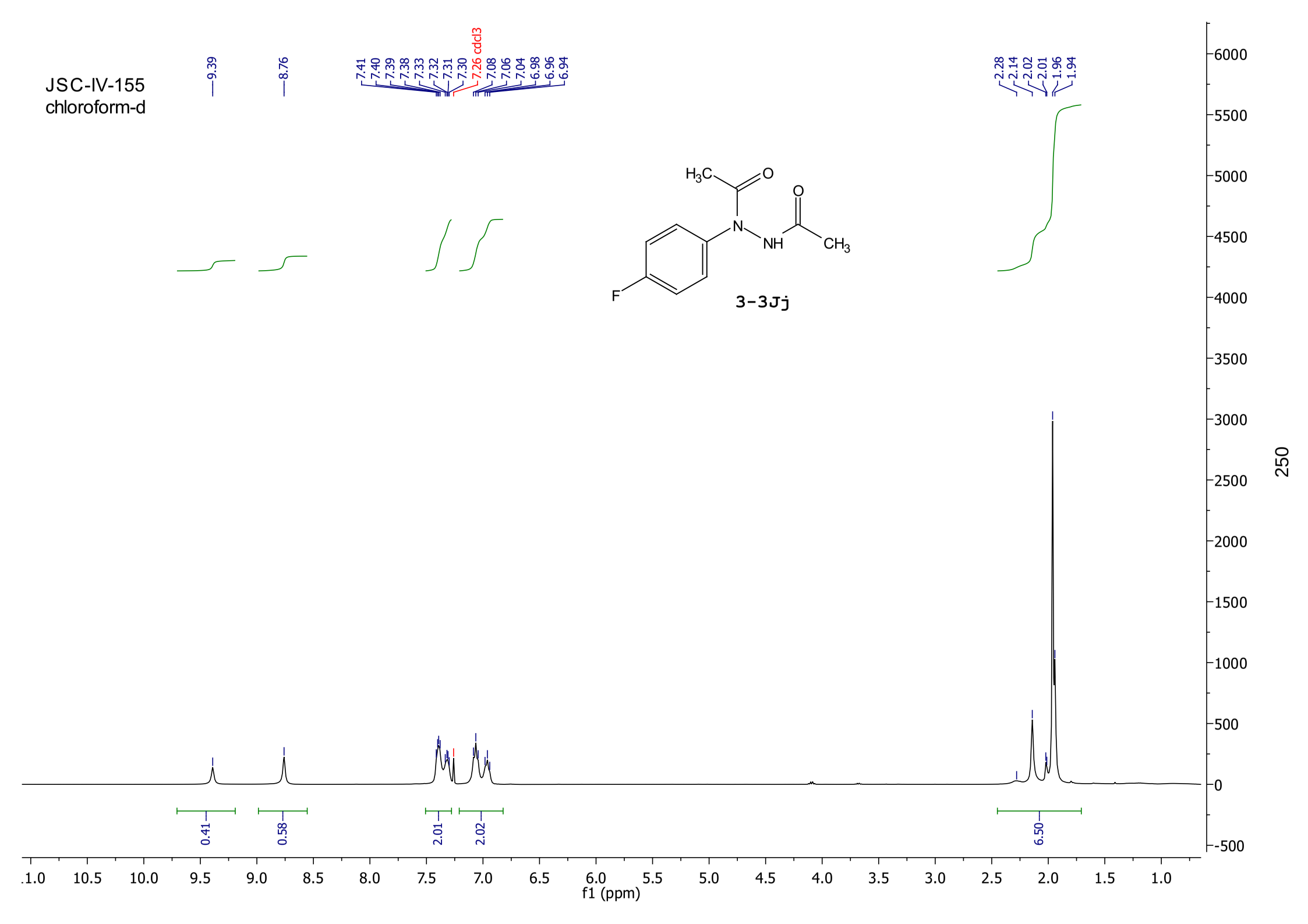
JSC-IV-155
chloroform-d
9.39
8.76
7.41
7.40
7.39
7.38
7.33
7.32
7.31
7.30
7.26 cdcl3
7.08
7.06
7.04
6.98
6.96
6.94
2.28
2.14
2.02
2.01
1.96
1.94
H3C
O
O
N
NH
CH3
F
3-3Jj
0.41
0.58
2.01
2.02
6.50
f1 (ppm)
250

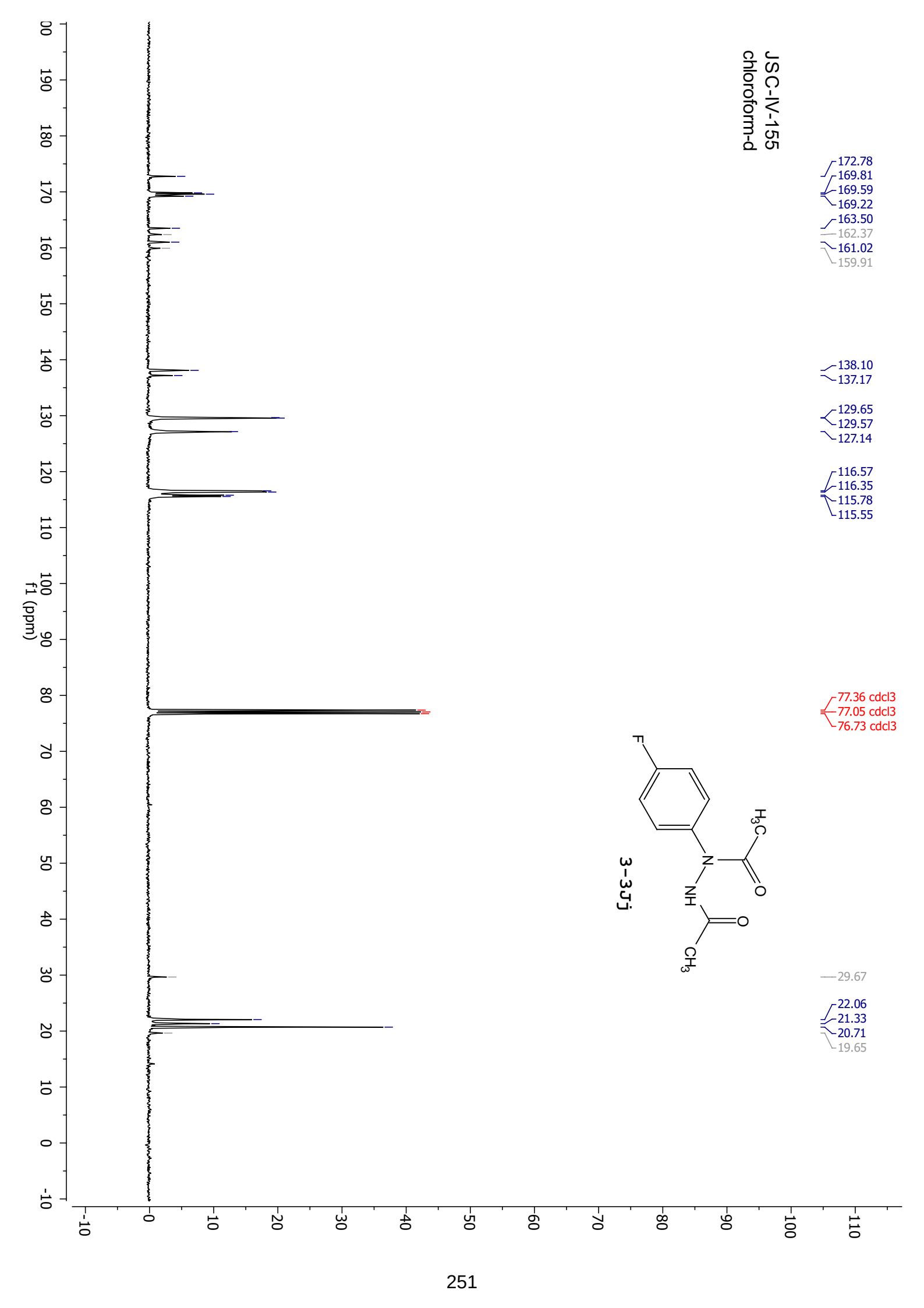
JSC-IV-155
chloroform-d
172.78
169.81
169.59
169.22
163.50
162.37
161.02
159.91
138.10
137.17
129.65
129.57
127.14
116.57
116.35
115.78
115.55
77.36 cdcl3
77.05 cdcl3
76.73 cdcl3
29.67
22.06
21.33
20.71
19.65
3-3Jj
F
N
NH
O
O
H3C
CH3
f1 (ppm)

JSC-IV-155
chloroform-d

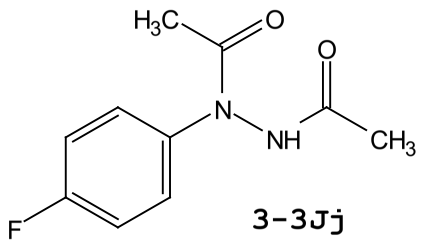

3-3Jj

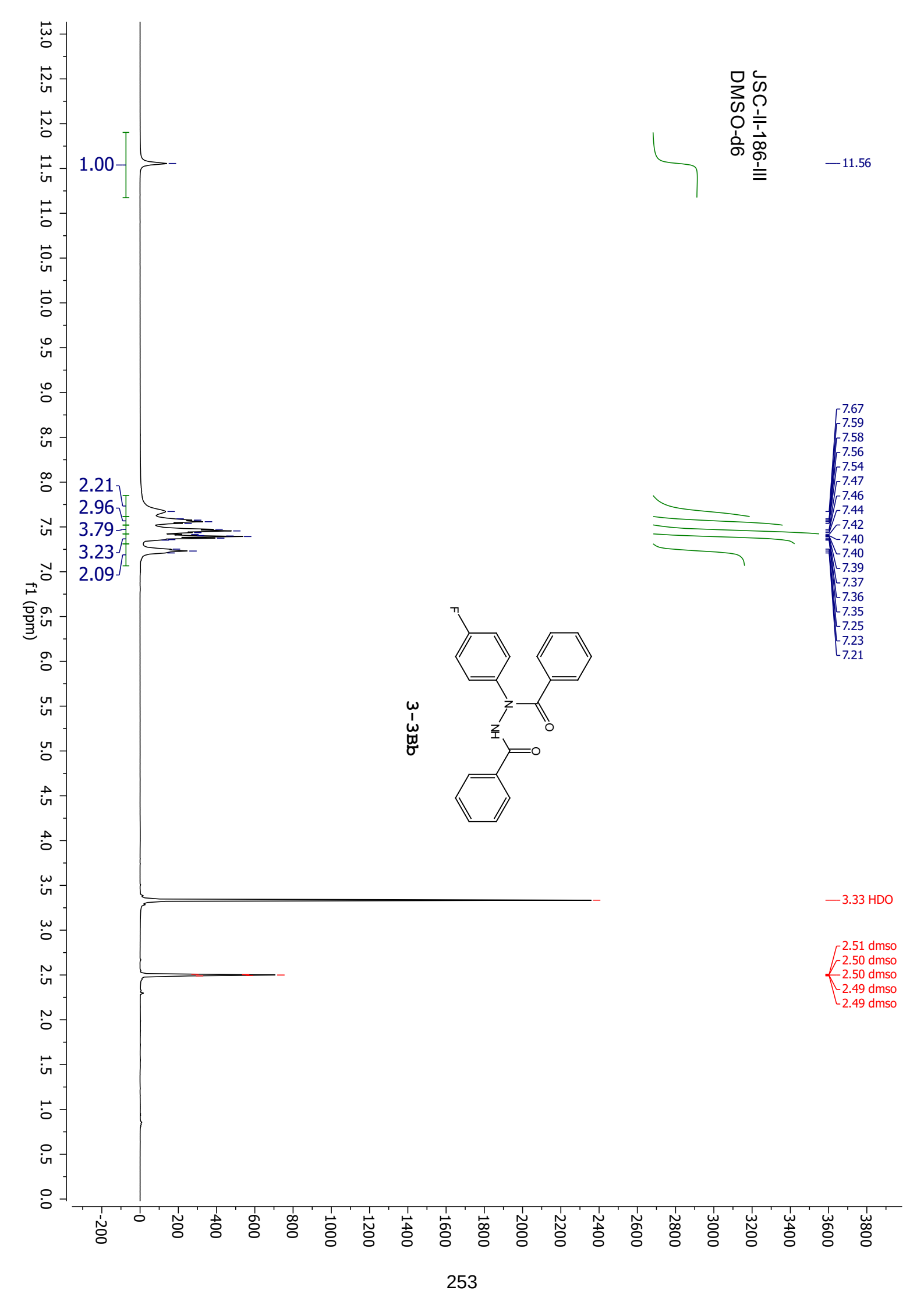
JSC-II-186-III
DMSO-d6
3-3Bb
1.00
2.21
2.96
3.79
3.23
2.09
11.56
7.67
7.59
7.58
7.56
7.54
7.47
7.46
7.44
7.42
7.40
7.40
7.39
7.37
7.36
7.35
7.25
7.23
7.21
3.33 HDO
2.51 dmso
2.50 dmso
2.50 dmso
2.49 dmso
2.49 dmso
f1 (ppm)

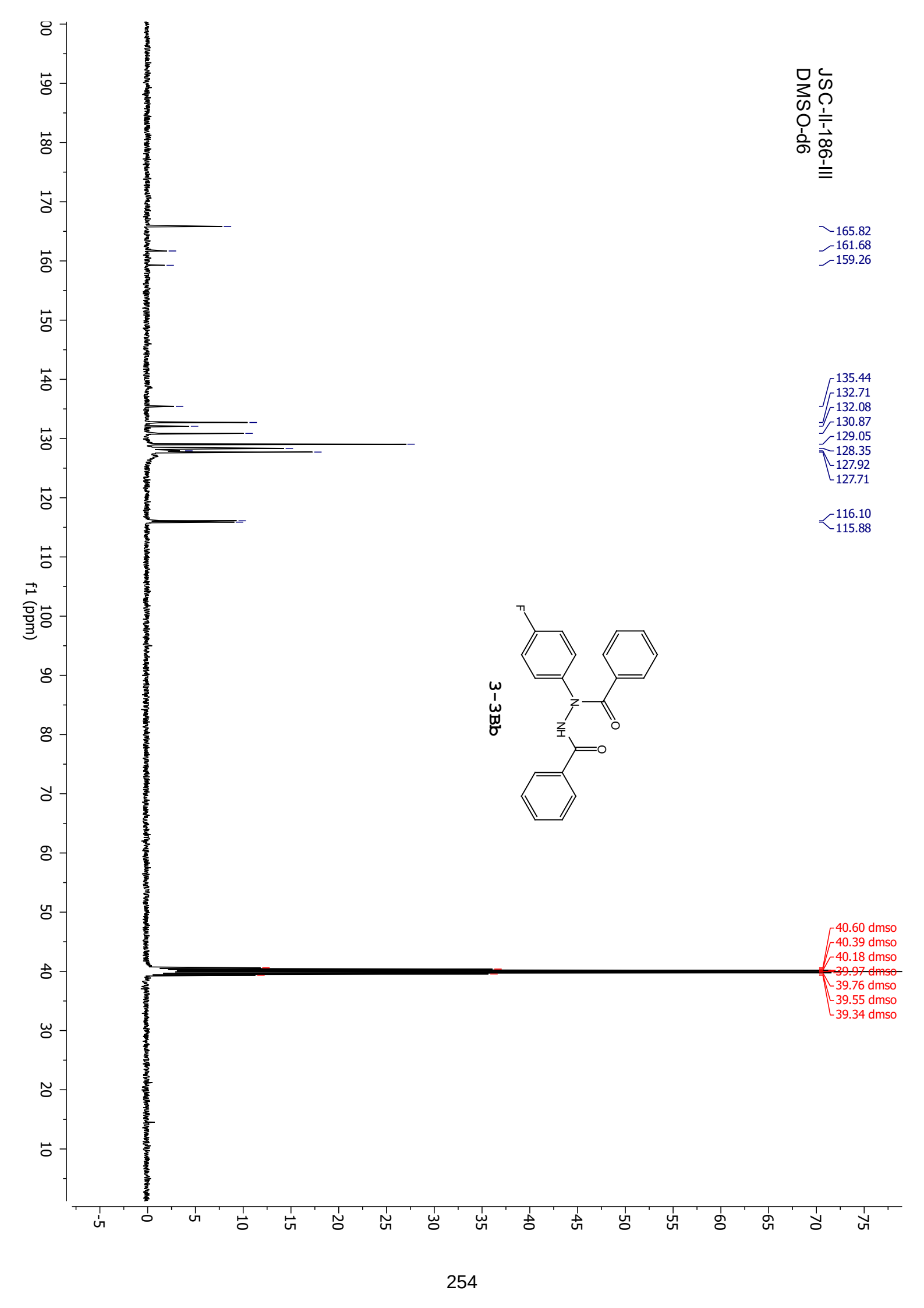
JSC-II-186-III
DMSO-d6
165.82
161.68
159.26
135.44
132.71
132.08
130.87
129.05
128.35
127.92
127.71
116.10
115.88
40.60 dmso
40.39 dmso
40.18 dmso
39.97 dmso
39.76 dmso
39.55 dmso
39.34 dmso
3-3Bb
F
N
NH
O
O
f1 (ppm)

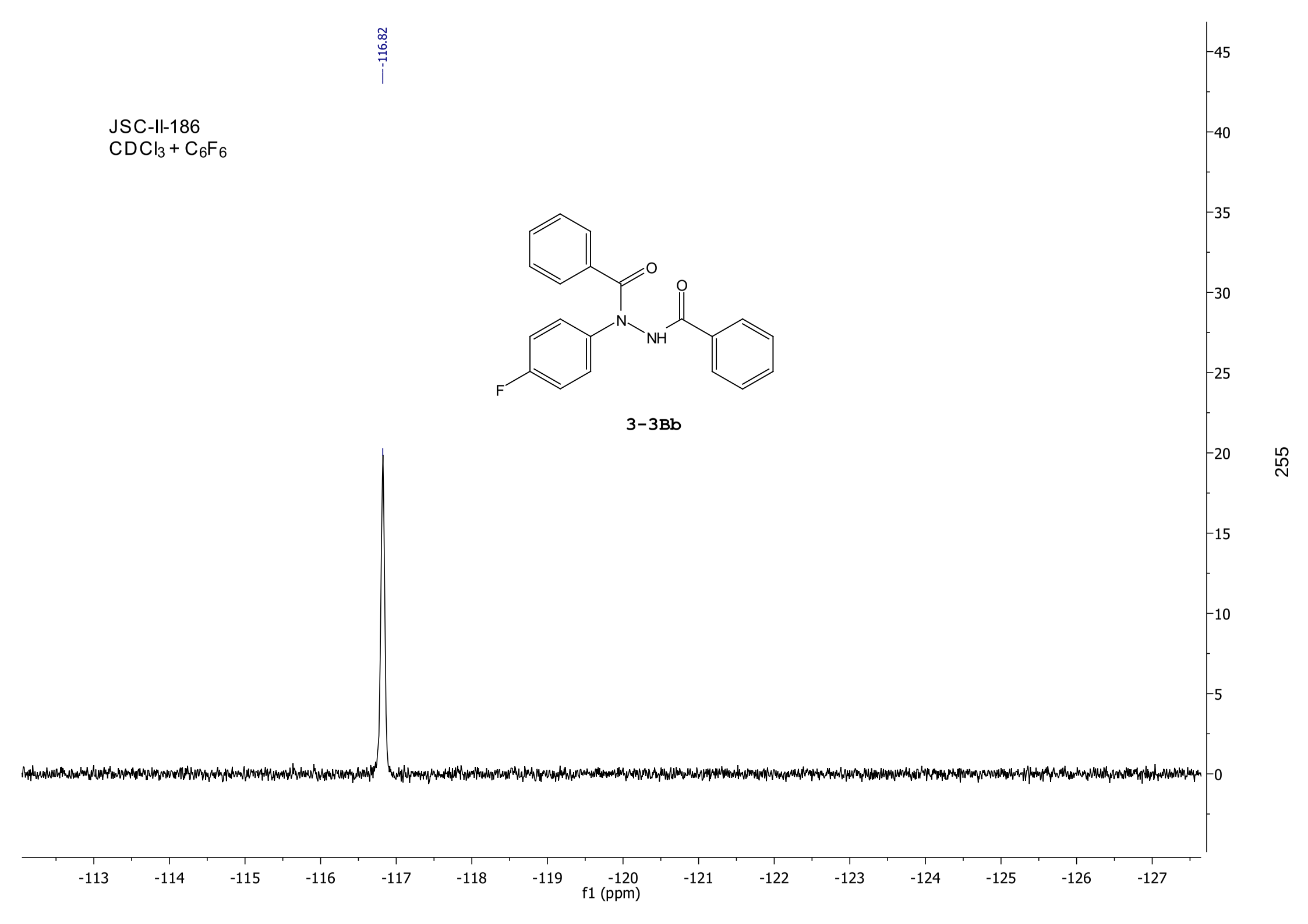
-116.82
JSC-II-186
CDCl3 + C6F6
O
O
N
NH
F
3-3Bb
255
45
40
35
30
25
20
15
10
5
0
-113
-114
-115
-116
-117
-118
-119
-120
-121
-122
-123
-124
-125
-126
-127
f1 (ppm)

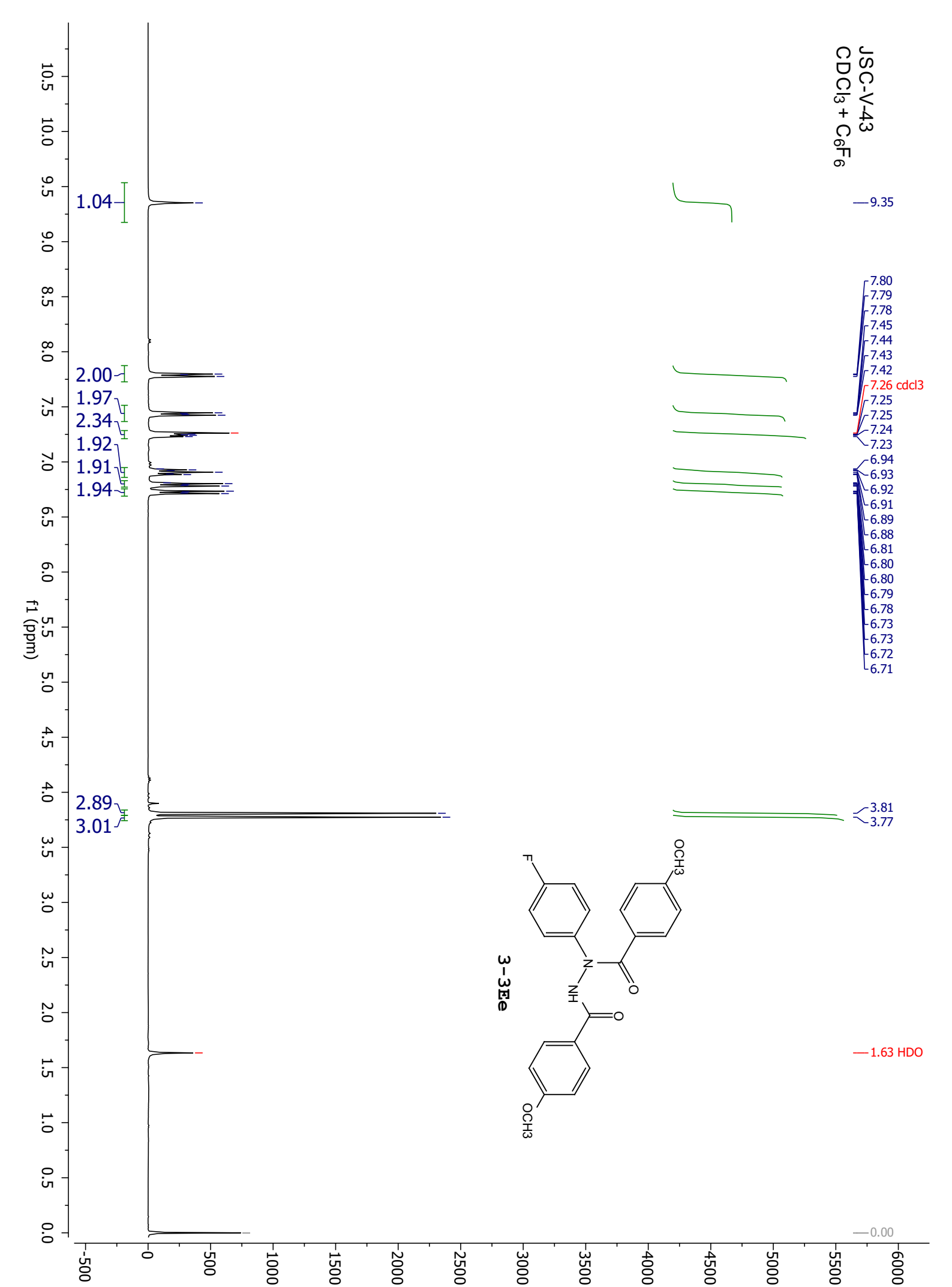
JSC-V-43
CDCl3 + C6F6
1.04
2.00
1.97
2.34
1.92
1.91
1.94
2.89
3.01
9.35
7.80
7.79
7.78
7.45
7.44
7.43
7.42
7.26 cdcl3
7.25
7.25
7.24
7.23
6.94
6.93
6.92
6.91
6.89
6.88
6.81
6.80
6.80
6.79
6.78
6.73
6.73
6.72
6.71
3.81
3.77
1.63 HDO
0.00
f1 (ppm)
3-3Ee
F
OCH3
N
NH
O
O
OCH3

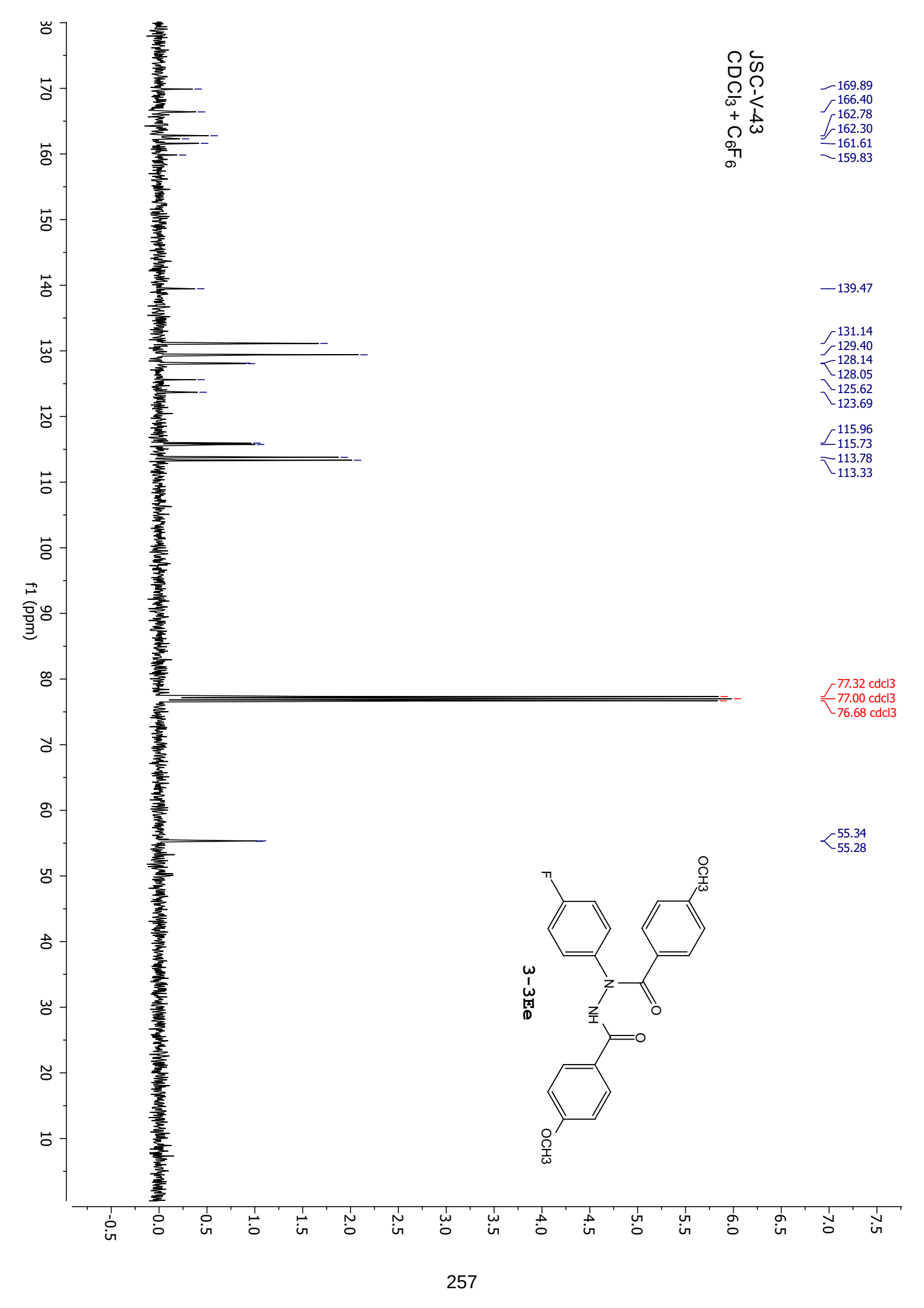
JSC-V-43
CDCl3 + C6F6
169.89
166.40
162.78
162.30
161.61
159.83
139.47
131.14
129.40
128.14
128.05
125.62
123.69
115.96
115.73
113.78
113.33
77.32 cdcl3
77.00 cdcl3
76.68 cdcl3
55.34
55.28
F
OCH3
N
NH
O
O
OCH3
3-3Ee
f1 (ppm)


-117.29
-117.30
-117.31
-117.32
-117.33
-117.34
-117.36
JSC-V-43
CDCl3 + C6F6
OCH3
O
O
N
NH
F
OCH3
3-3Ee
600
550
500
450
400
350
300
250
200
150
100
50
0
-50
-100
258
-109 -110 -111 -112 -113 -114 -115 -116 -117 -118 -119 -120 -121 -122 -123 -124 -125 -126 -127 -128 -129 -130 -131 -132 -133
f1 (ppm)

JSC-V-19-III

$CDCl_3 + C_6F_6$

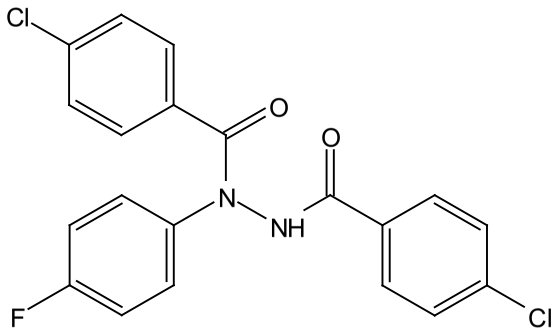

3-3Ff

0.00 TMS

1.00 2.01 8.12 1.91

f1 (ppm)

259

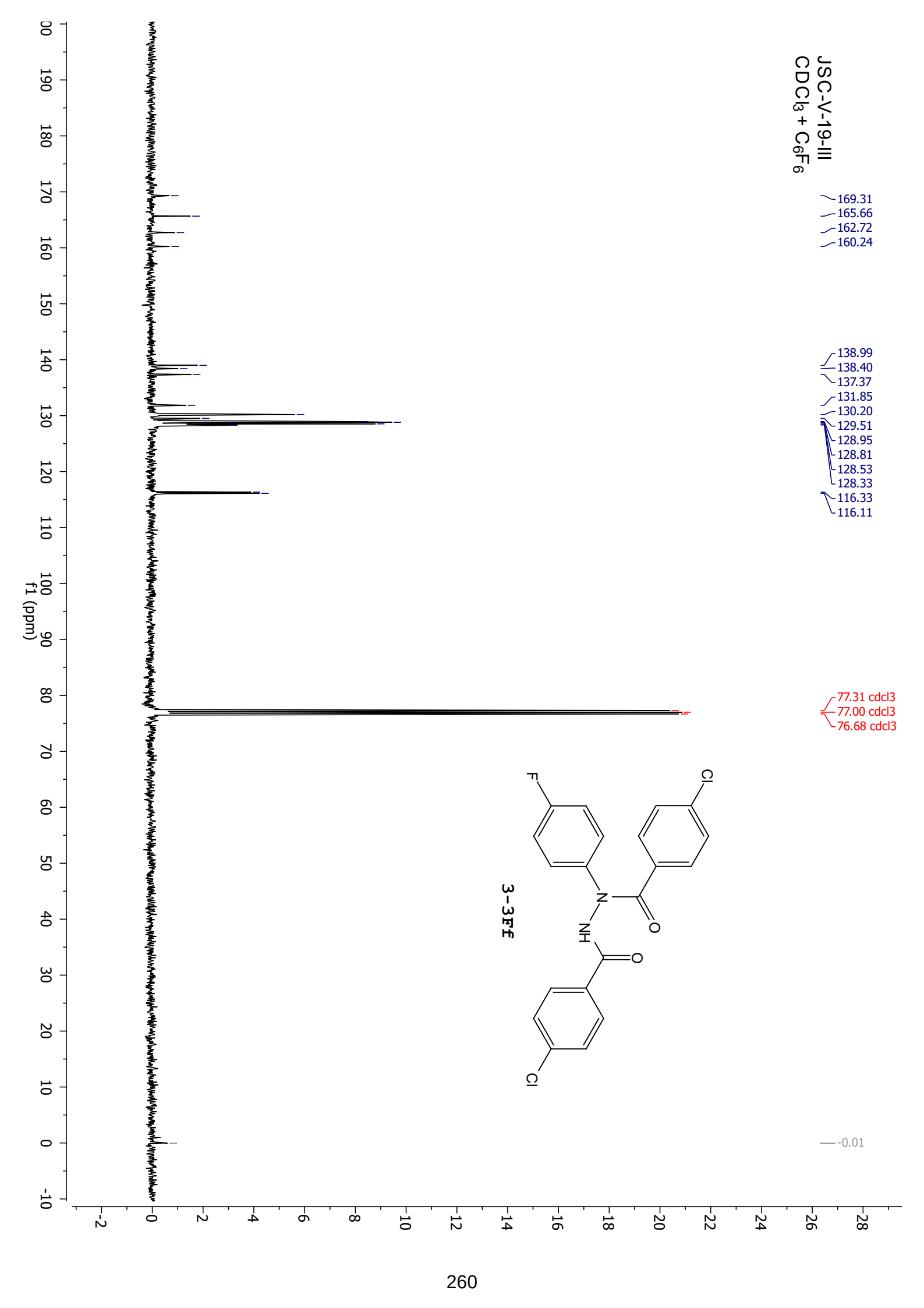
JSC-V-19-III
CDCl3 + C6F6
169.31
165.66
162.72
160.24
138.99
138.40
137.37
131.85
130.20
129.51
128.95
128.81
128.53
128.33
116.33
116.11
77.31 cdcl3
77.00 cdcl3
76.68 cdcl3
-0.01
f1 (ppm)
3-3ff
F
Cl
N
NH
O
O
Cl

JSC-V-19-III

$CDCl_3 + C_6F_6$

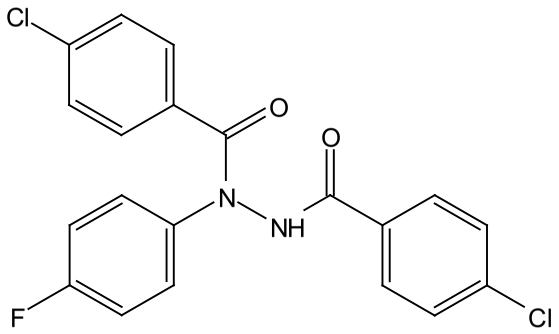

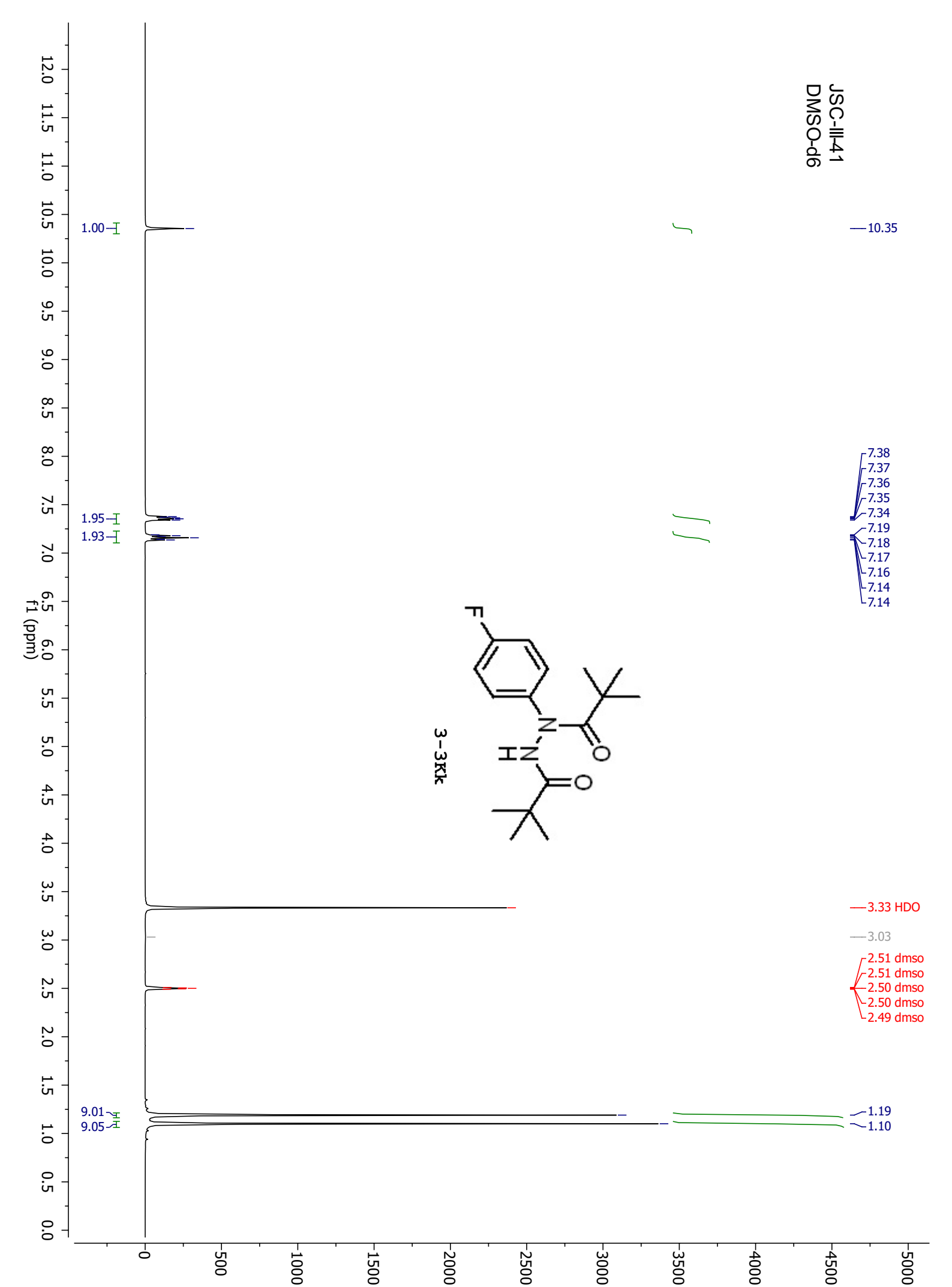
JSC-III-41
DMSO-d6
3-3Kk
1.00
1.95
1.93
9.01
9.05
10.35
7.38
7.37
7.36
7.35
7.34
7.19
7.18
7.17
7.16
7.14
7.14
3.33 HDO
3.03
2.51 dmso
2.51 dmso
2.50 dmso
2.50 dmso
2.49 dmso
1.19
1.10
f1 (ppm)

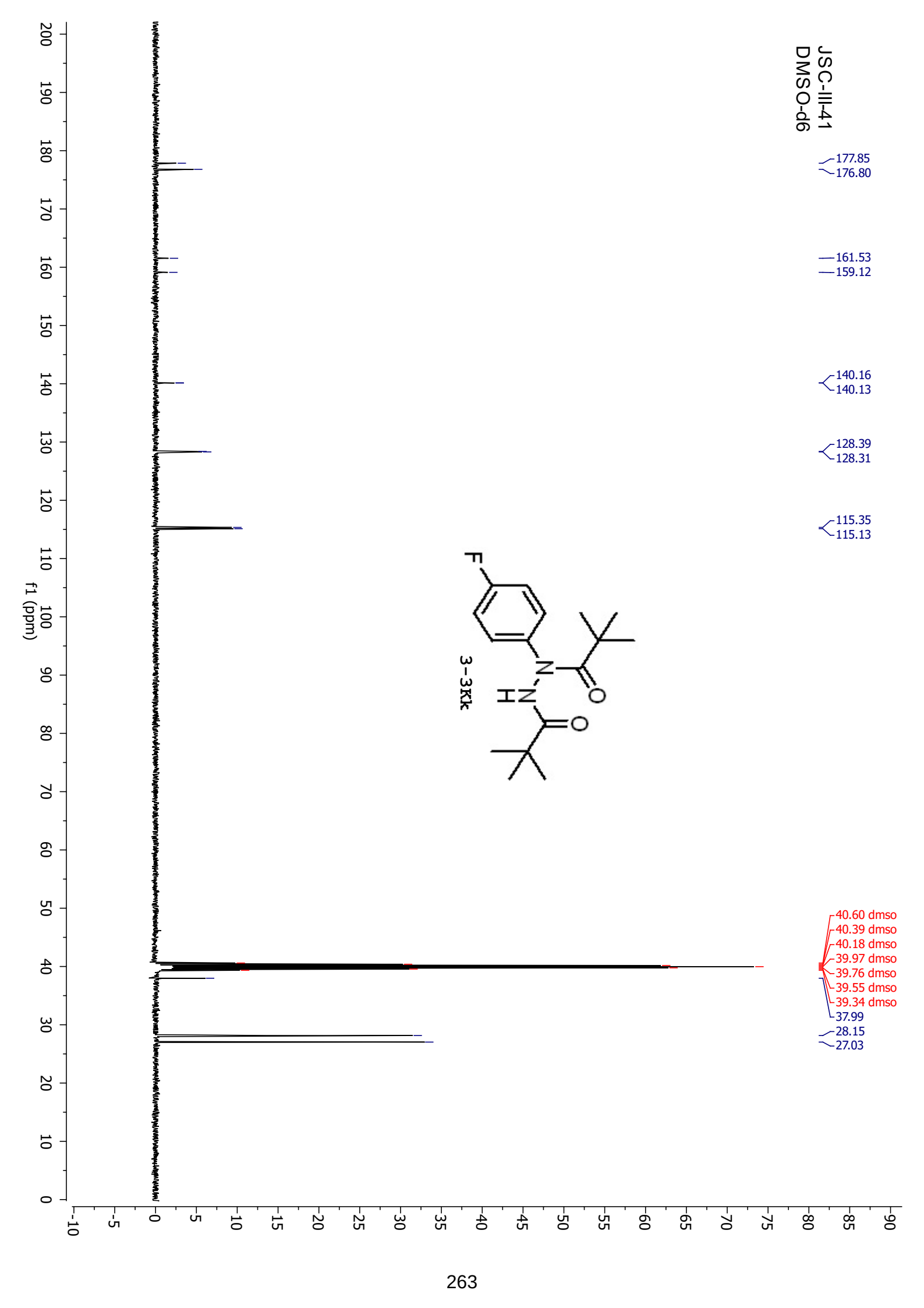
JSC-III-41
DMSO-d6
177.85
176.80
161.53
159.12
140.16
140.13
128.39
128.31
115.35
115.13
40.60 dmso
40.39 dmso
40.18 dmso
39.97 dmso
39.76 dmso
39.55 dmso
39.34 dmso
37.99
28.15
27.03
3-3Kk
F
N
H
N
O
O
f1 (ppm)

JSC-III-41
$CDCl_3 + C_6F_6$

-115.50

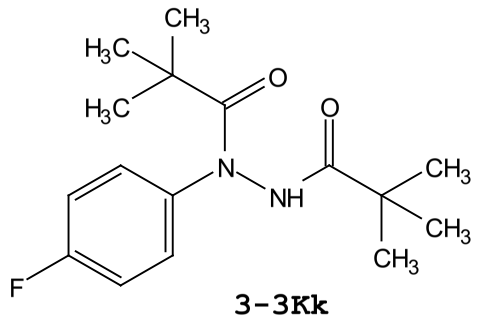

3-3Kk

264

f1 (ppm)

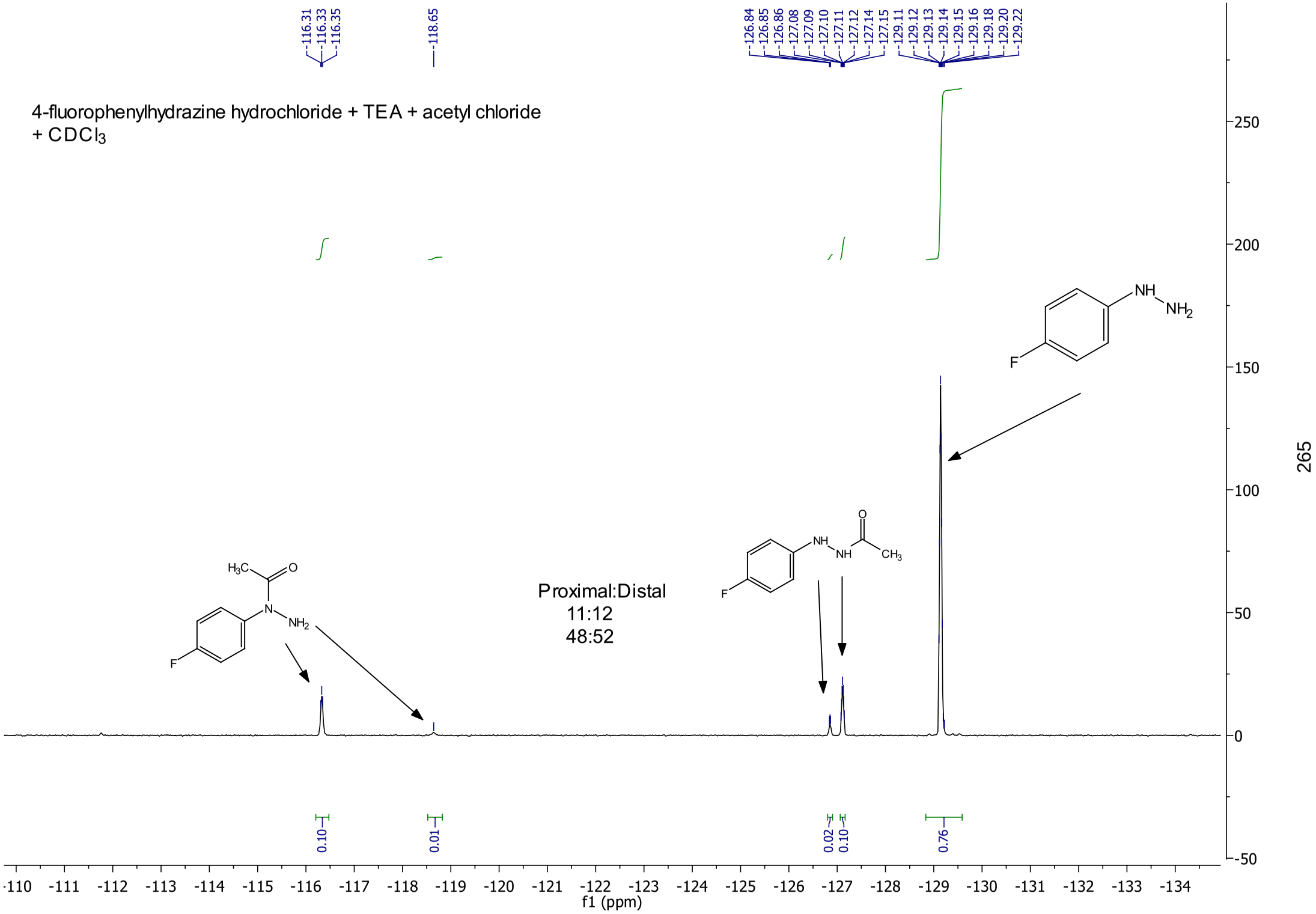
4-fluorophenylhydrazine hydrochloride + TEA + acetyl chloride
+ CDCl3
Proximal:Distal
11:12
48:52
f1 (ppm)

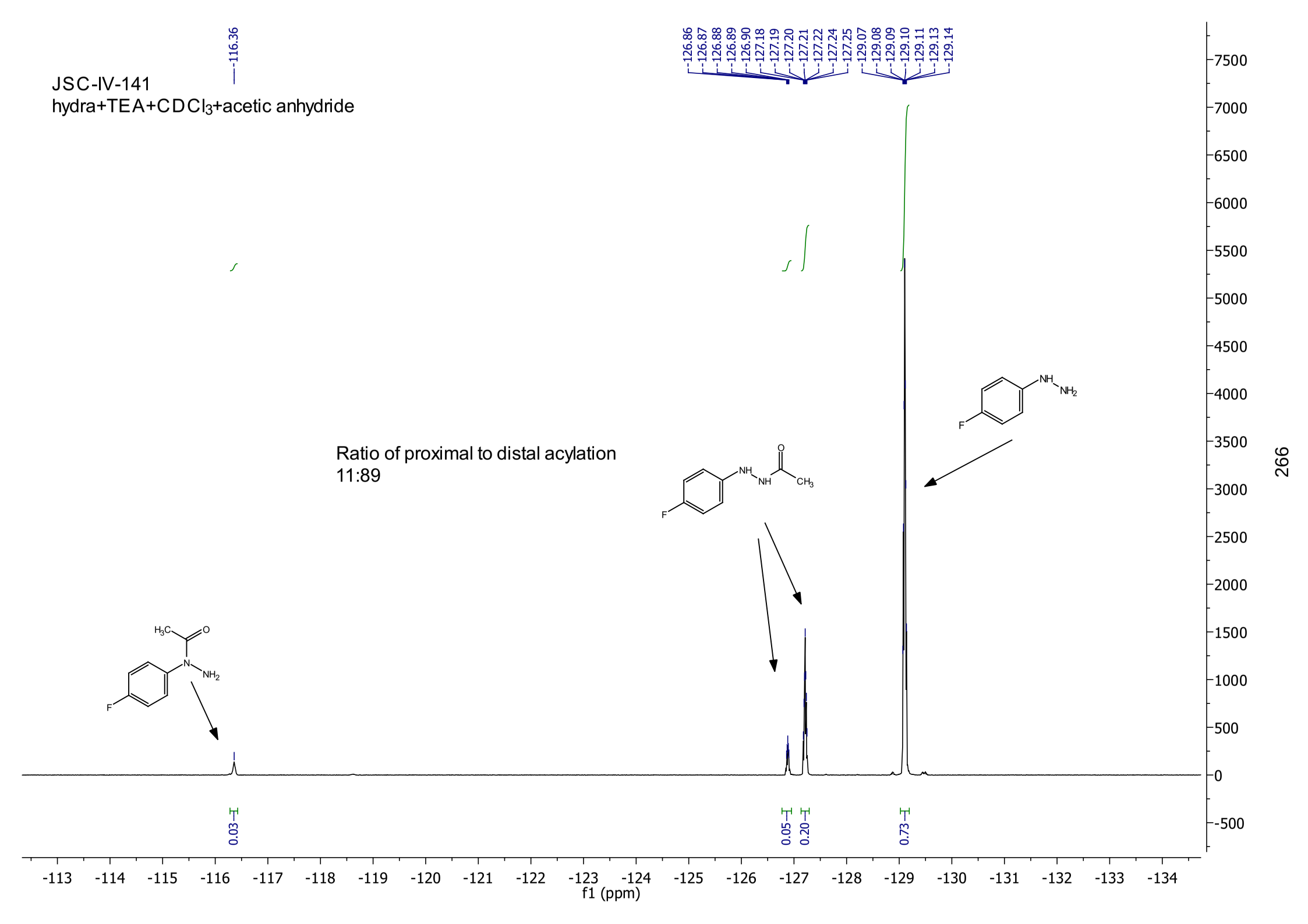
JSC-IV-141
hydra+TEA+CDCl3+acetic anhydride
Ratio of proximal to distal acylation
11:89
-116.36
-126.86
-126.87
-126.88
-126.89
-126.90
-127.18
-127.19
-127.20
-127.21
-127.22
-127.24
-127.25
-129.07
-129.08
-129.09
-129.10
-129.11
-129.13
-129.14
0.03
0.05
0.20
0.73
f1 (ppm)
266

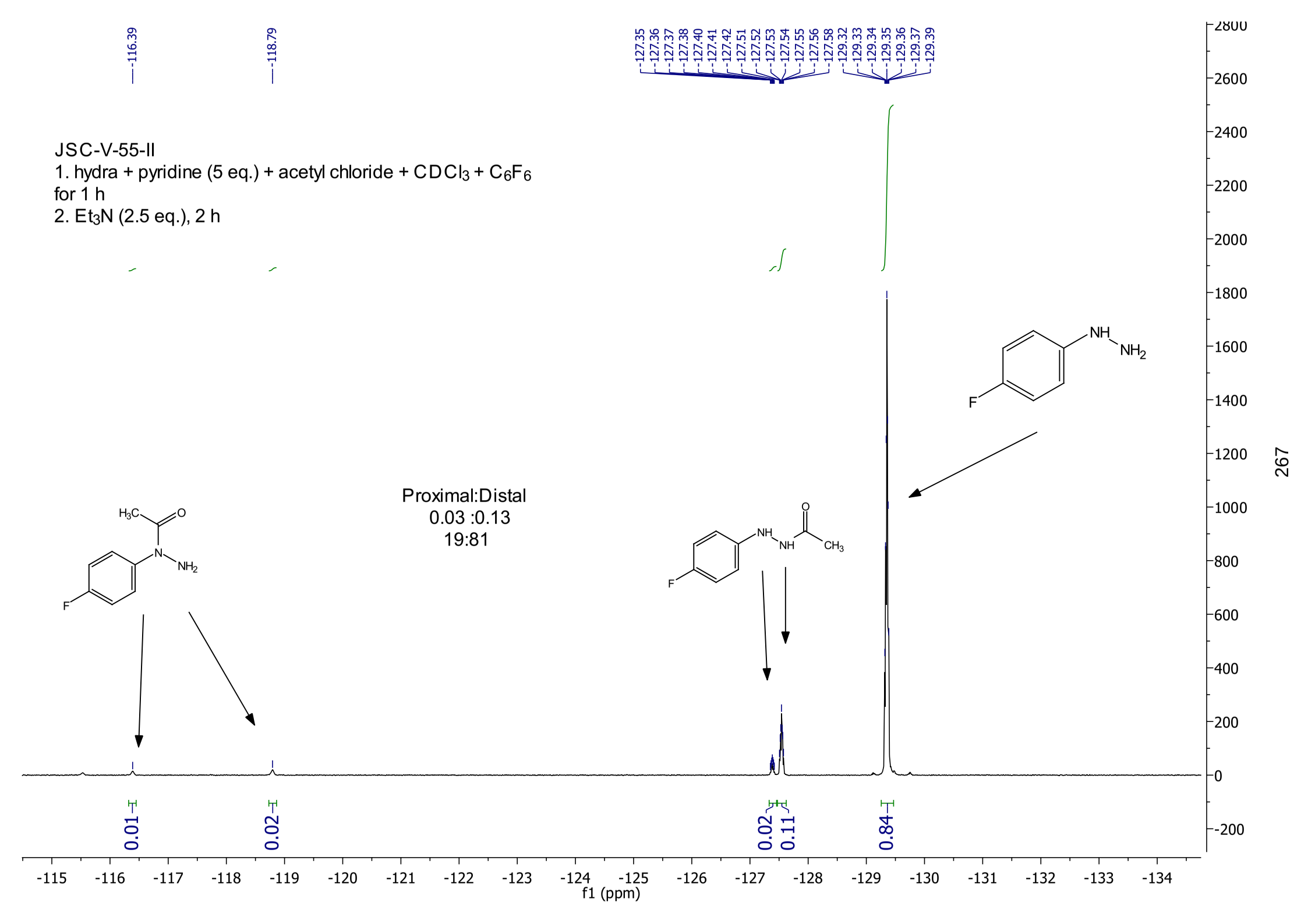
JSC-V-55-II
1. hydra + pyridine (5 eq.) + acetyl chloride + $CDCl_3$ + C_6F_6
for 1 h
2. Et_3N (2.5 eq.), 2 h
Proximal:Distal
0.03 :0.13
19:81
-116.39
-118.79
-127.35
-127.36
-127.37
-127.38
-127.40
-127.41
-127.42
-127.51
-127.52
-127.53
-127.54
-127.55
-127.56
-127.58
-129.32
-129.33
-129.34
-129.35
-129.36
-129.37
-129.39
0.01
0.02
0.02
0.11
0.84
f1 (ppm)
267

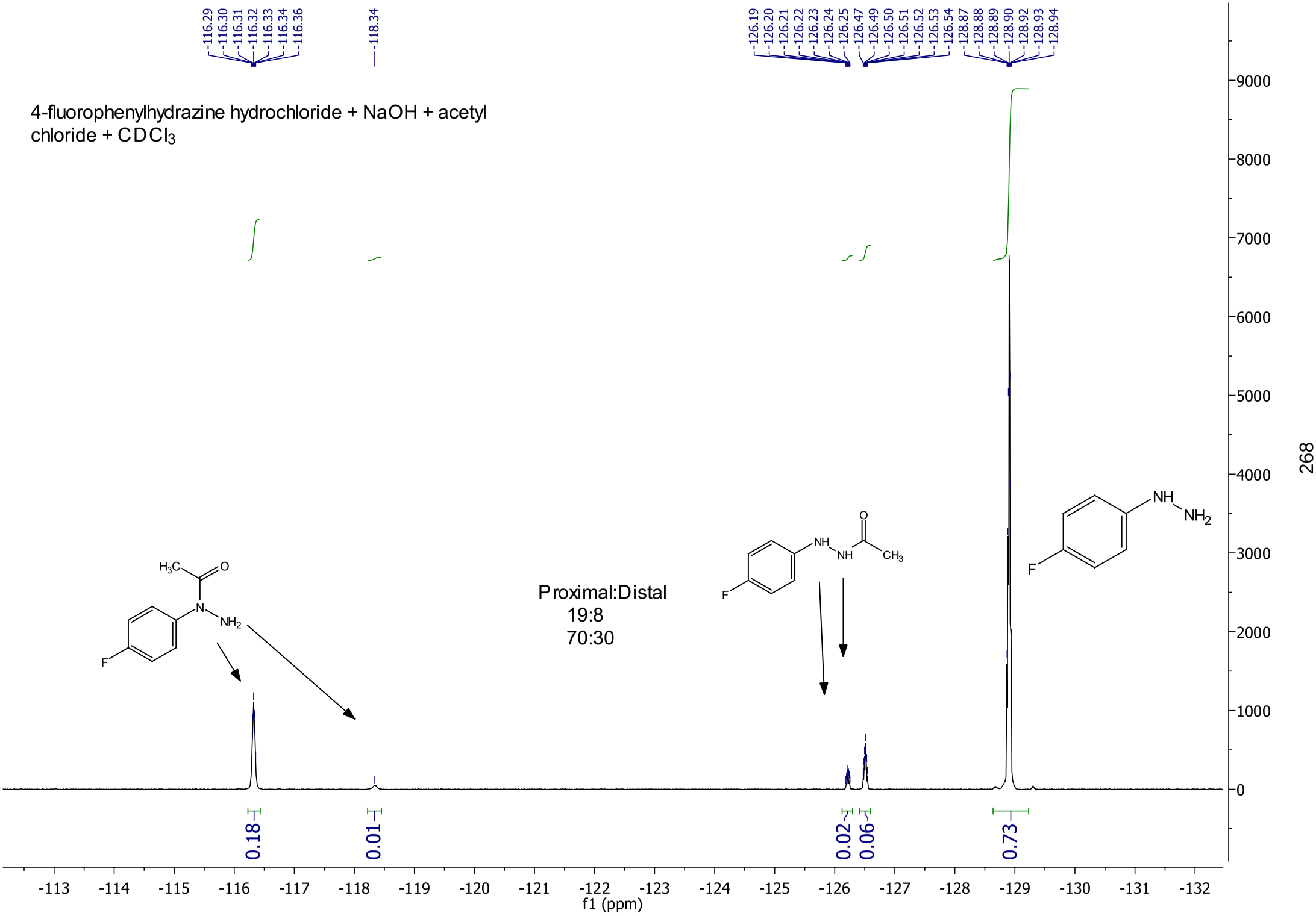
4-fluorophenylhydrazine hydrochloride + NaOH + acetyl chloride + CDCl3
-116.29
-116.30
-116.31
-116.32
-116.33
-116.34
-116.36
-118.34
-126.19
-126.20
-126.21
-126.22
-126.23
-126.24
-126.25
-126.47
-126.49
-126.50
-126.51
-126.52
-126.53
-126.54
-128.87
-128.88
-128.89
-128.90
-128.92
-128.93
-128.94
Proximal:Distal
19:8
70:30
0.18
0.01
0.02
0.06
0.73
f1 (ppm)
268

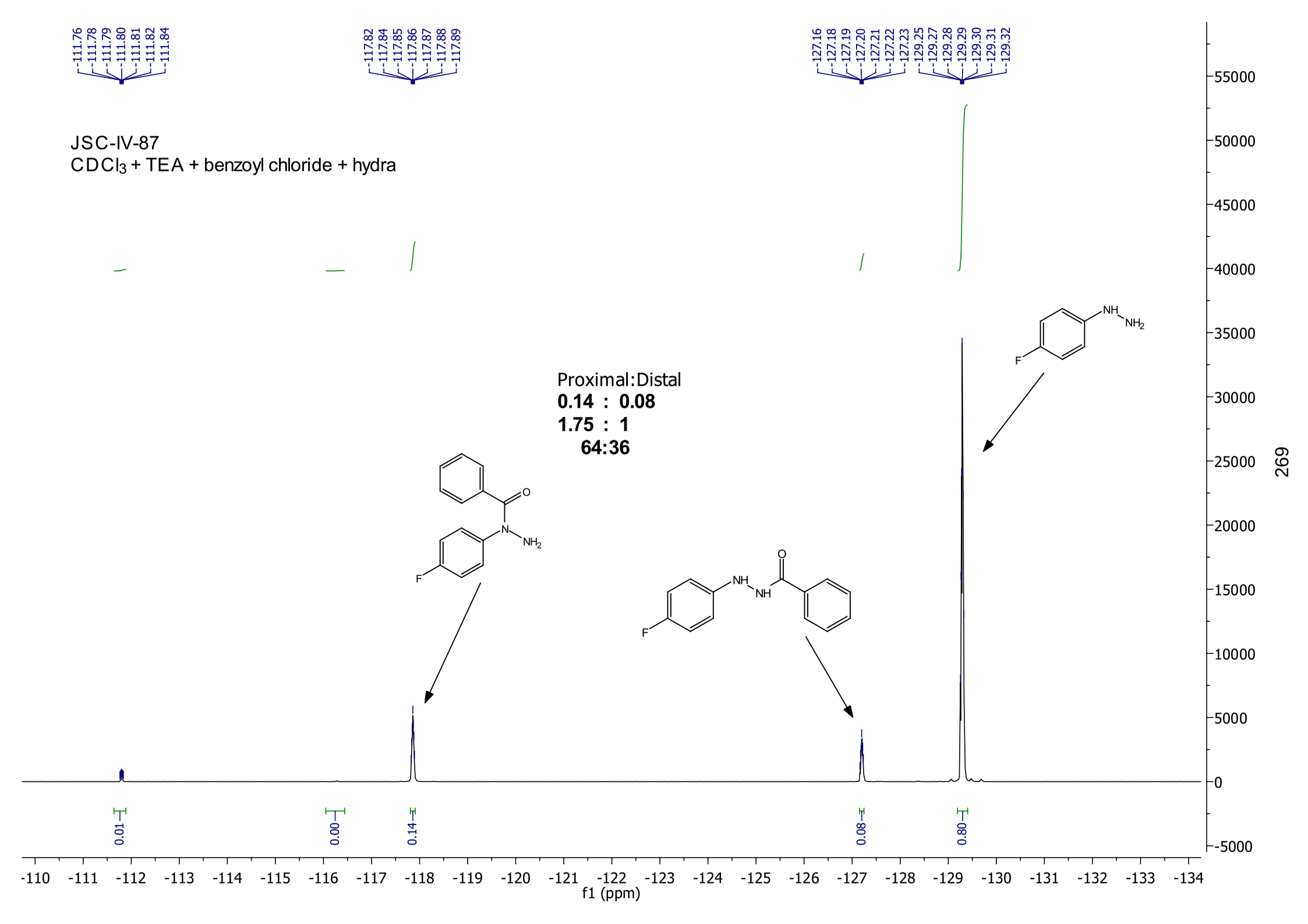
JSC-IV-87
CDCl3 + TEA + benzoyl chloride + hydra
Proximal:Distal
0.14 : 0.08
1.75 : 1
64:36
f1 (ppm)
269

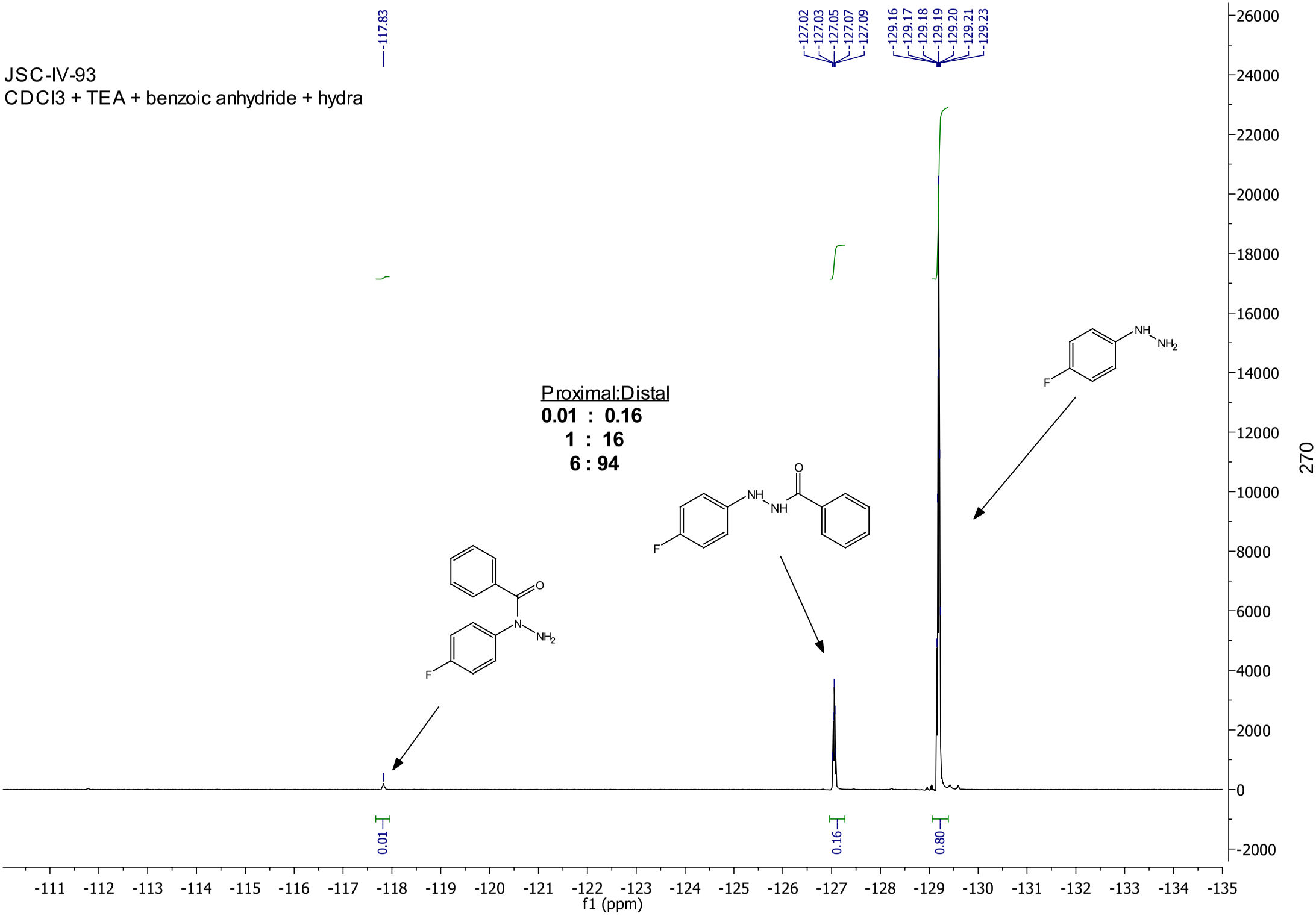
JSC-IV-93
CDCl3 + TEA + benzoic anhydride + hydra
-117.83
-127.02
-127.03
-127.05
-127.07
-127.09
-129.16
-129.17
-129.18
-129.19
-129.20
-129.21
-129.23
Proximal:Distal
0.01 : 0.16
1 : 16
6 : 94
0.01
0.16
0.80
f1 (ppm)
270

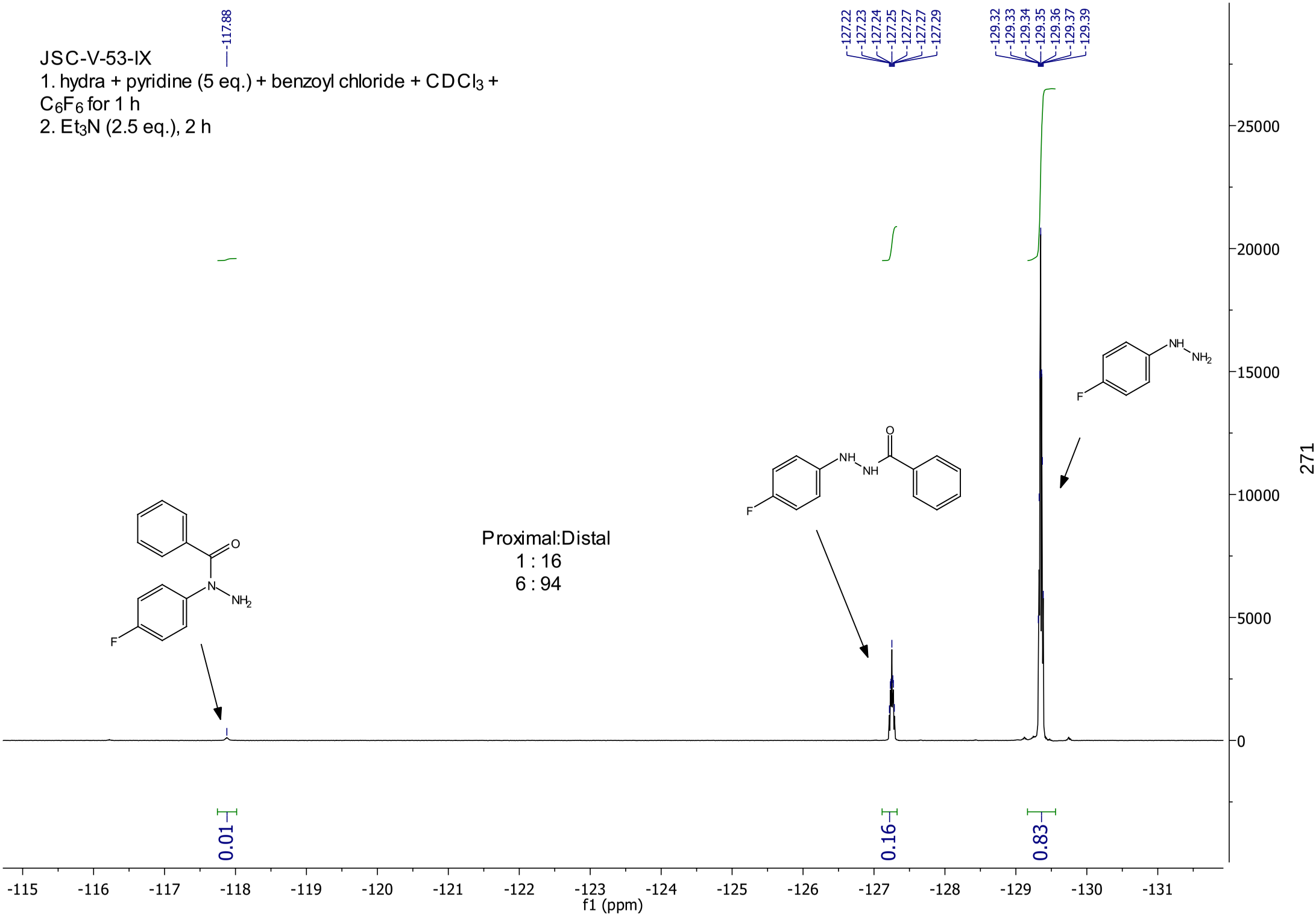
JSC-V-53-IX
1. hydra + pyridine (5 eq.) + benzoyl chloride + $CDCl_3$ +
C_6F_6 for 1 h
2. Et_3N (2.5 eq.), 2 h
-117.88
-127.22
-127.23
-127.24
-127.25
-127.27
-127.27
-127.29
-129.32
-129.33
-129.34
-129.35
-129.36
-129.37
-129.39
Proximal:Distal
1 : 16
6 : 94
0.01
0.16
0.83
f1 (ppm)
271

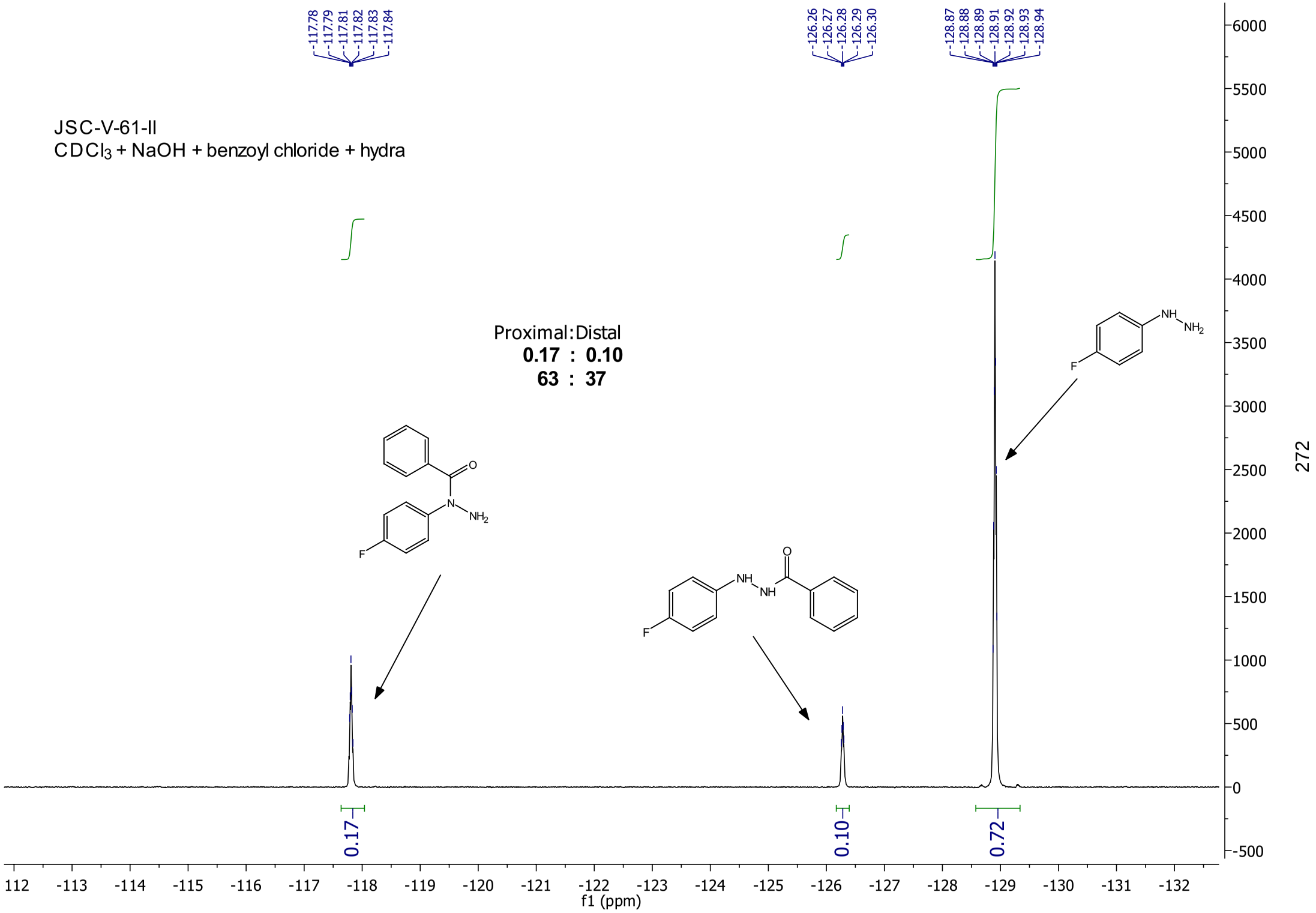
JSC-V-61-II
CDCl3 + NaOH + benzoyl chloride + hydra
Proximal:Distal
0.17 : 0.10
63 : 37
0.17
0.10
0.72
f1 (ppm)

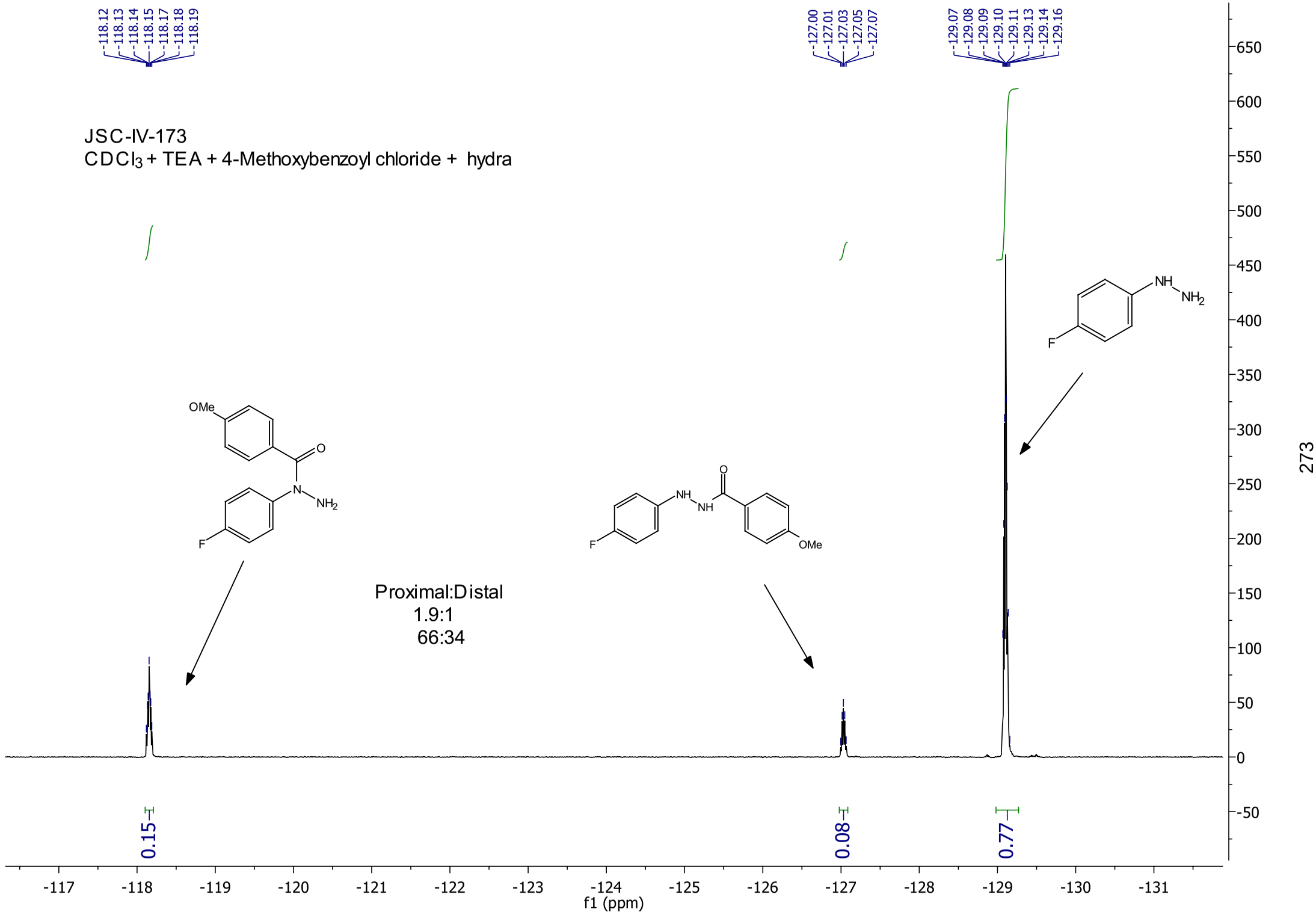
JSC-IV-173
CDCl3 + TEA + 4-Methoxybenzoyl chloride + hydra
Proximal:Distal
1.9:1
66:34
0.15
0.08
0.77
f1 (ppm)
273

JSC-IV-175

$CDCl_3$+TEA+hydra+4-methoxybenzoic anhydride

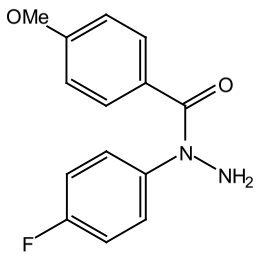

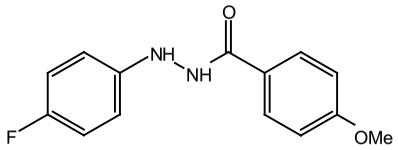

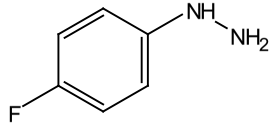

Proximal:Distal
1:8.5
10:90

0.02 0.17 0.81

f1 (ppm)

274

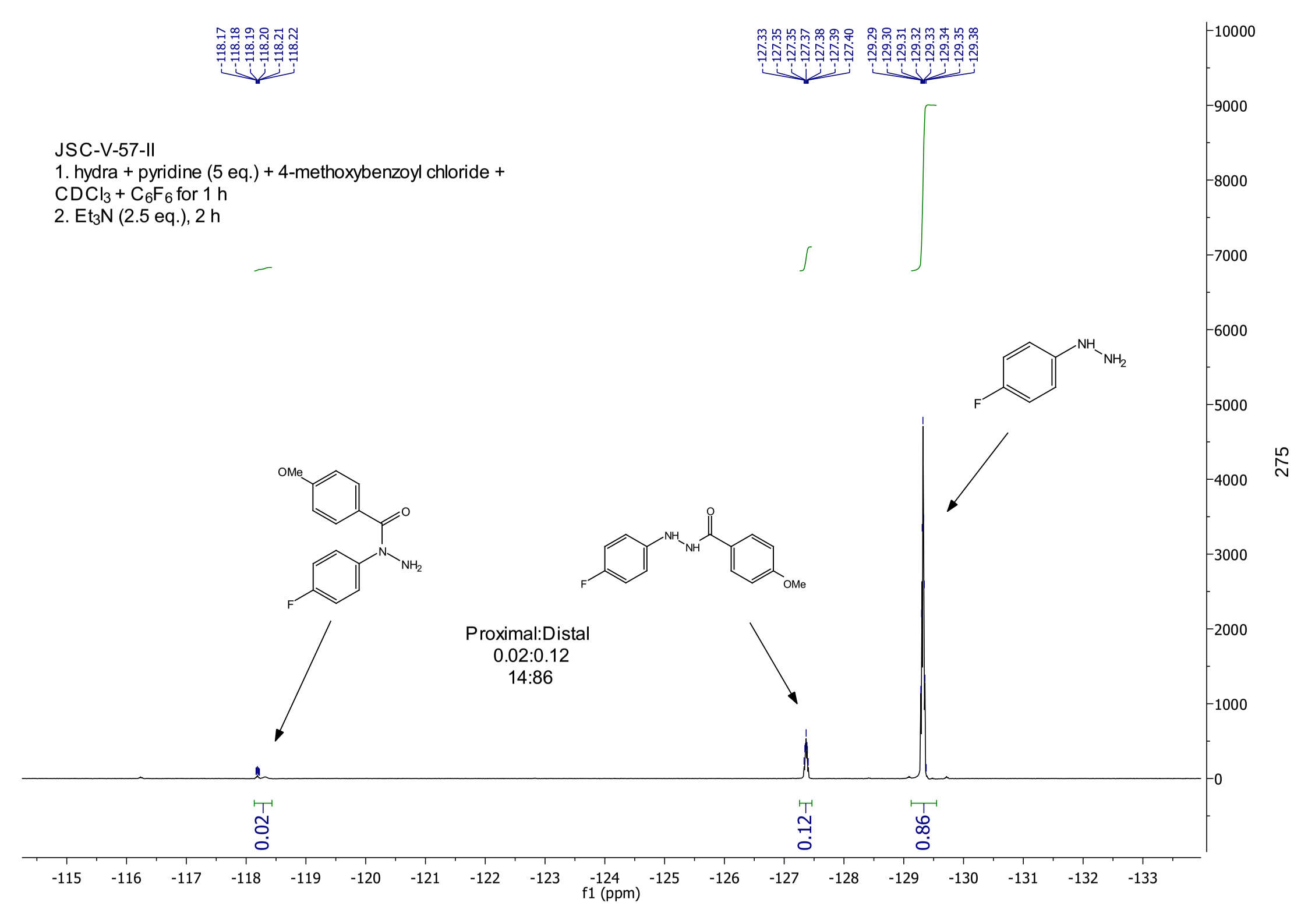
JSC-V-57-II
1. hydra + pyridine (5 eq.) + 4-methoxybenzoyl chloride +
CDCl3 + C6F6 for 1 h
2. Et3N (2.5 eq.), 2 h
Proximal:Distal
0.02:0.12
14:86
0.02
0.12
0.86
f1 (ppm)
275

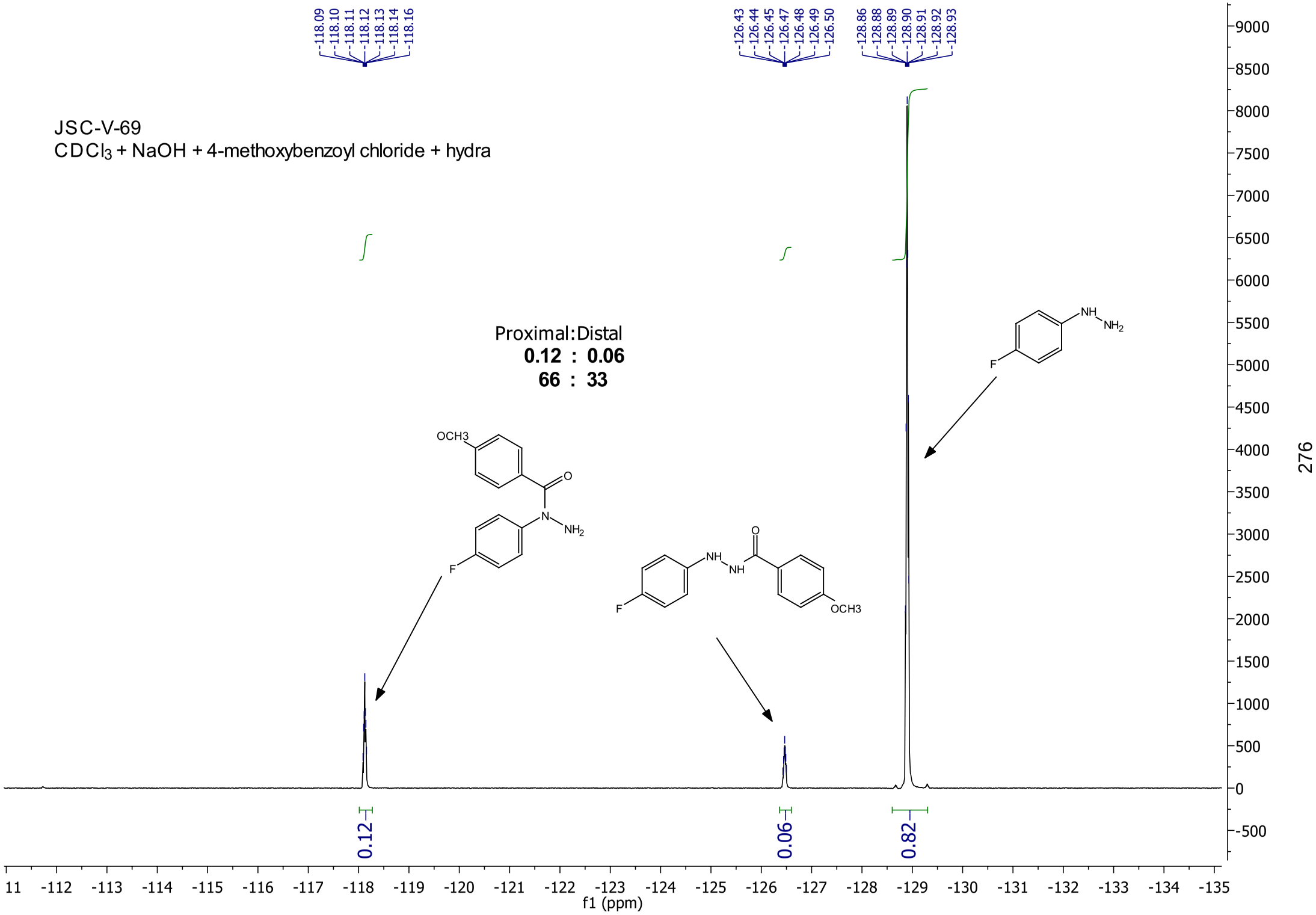
JSC-V-69
CDCl3 + NaOH + 4-methoxybenzoyl chloride + hydra
Proximal:Distal
0.12 : 0.06
66 : 33
0.12
0.06
0.82
f1 (ppm)
276

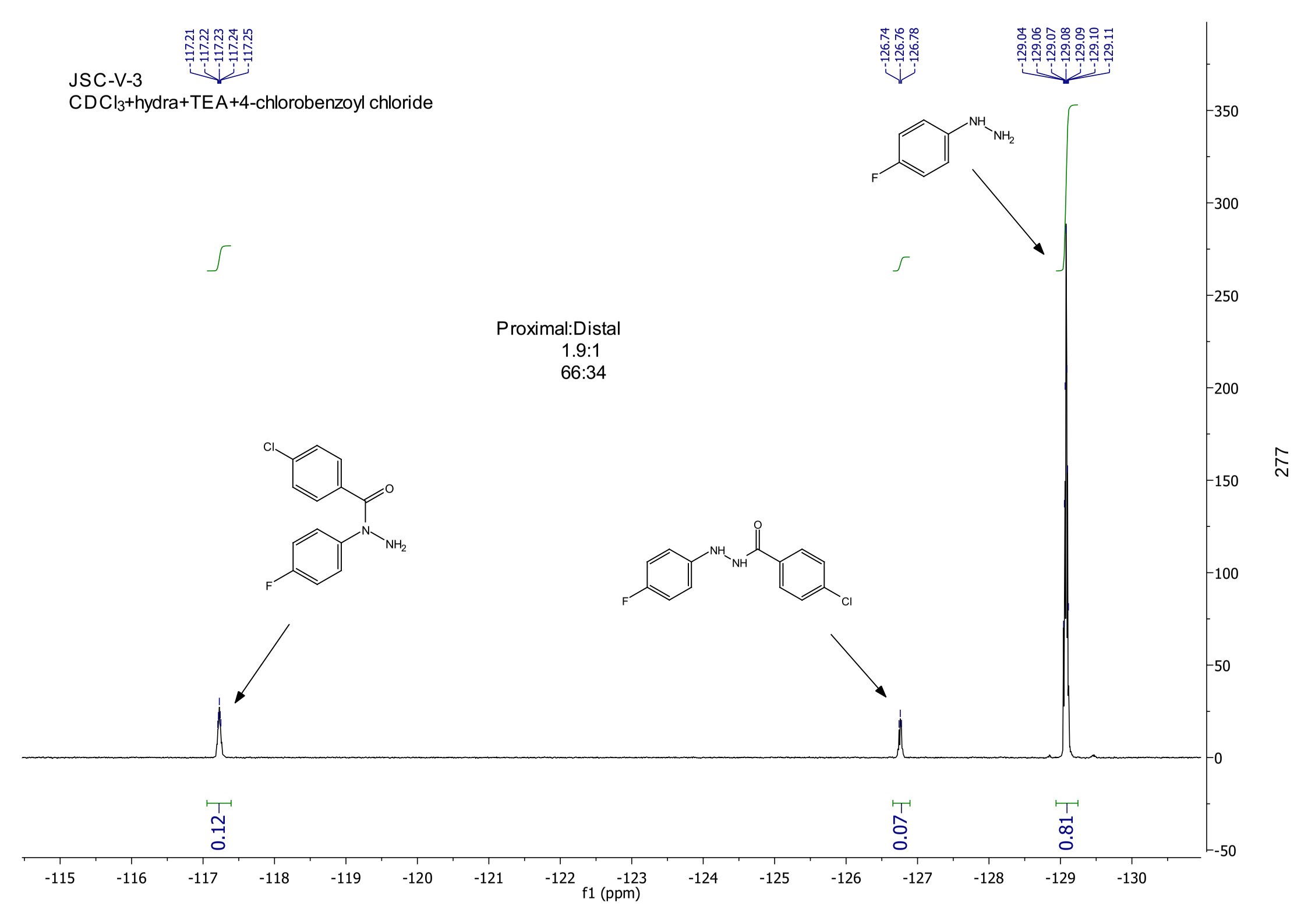
JSC-V-3
CDCl3+hydra+TEA+4-chlorobenzoyl chloride
-117.21
-117.22
-117.23
-117.24
-117.25
-126.74
-126.76
-126.78
-129.04
-129.06
-129.07
-129.08
-129.09
-129.10
-129.11
Proximal:Distal
1.9:1
66:34
Cl
O
N
NH2
F
NH
NH
O
F
Cl
NH
NH2
F
0.12
0.07
0.81
f1 (ppm)
277

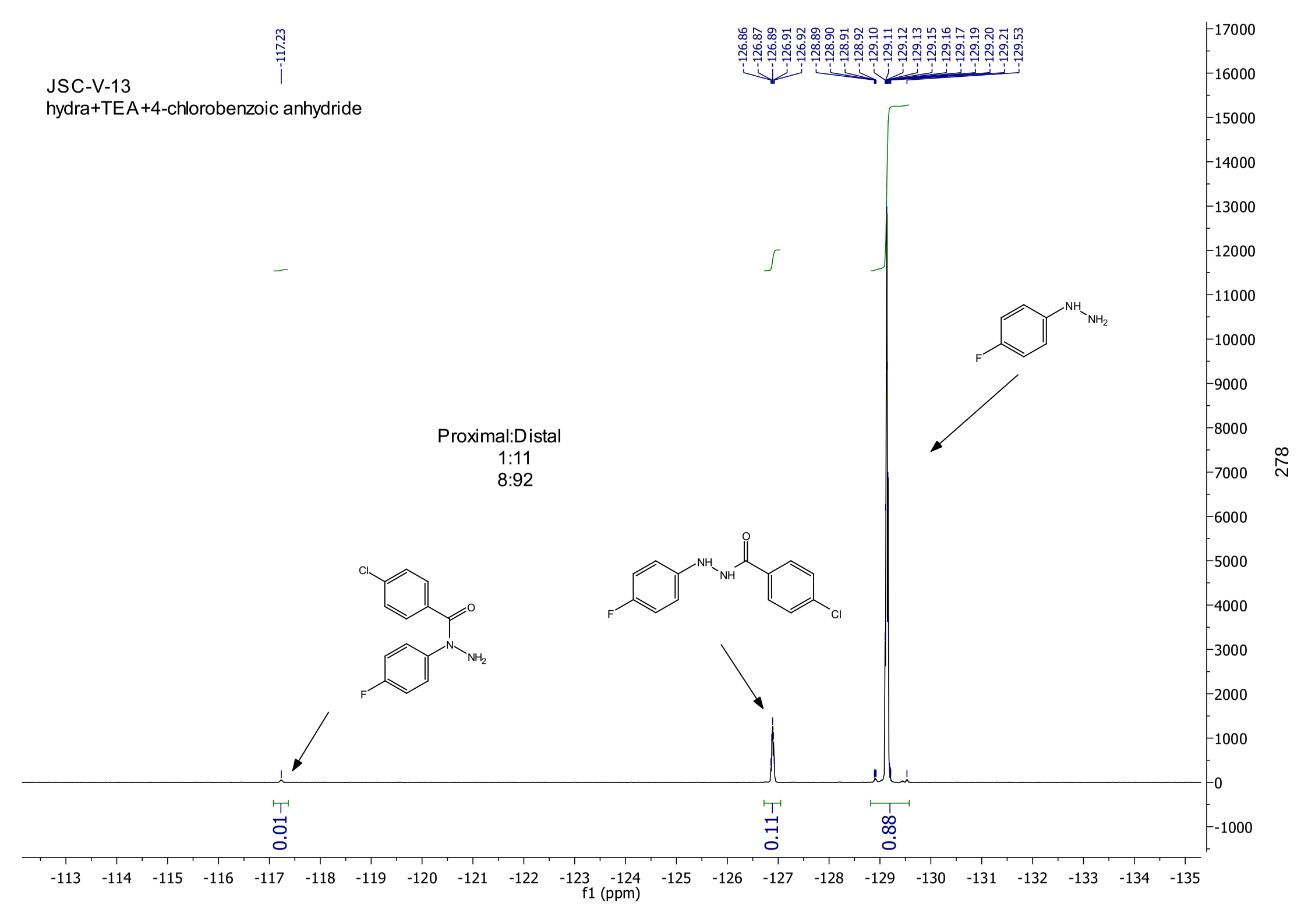
JSC-V-13
hydra+TEA+4-chlorobenzoic anhydride
Proximal:Distal
1:11
8:92
-117.23
126.86
126.87
126.89
126.91
126.92
128.89
128.90
128.91
128.92
129.10
129.11
129.12
129.13
129.15
129.16
129.17
129.19
129.20
129.21
129.53
0.01
0.11
0.88
f1 (ppm)
278

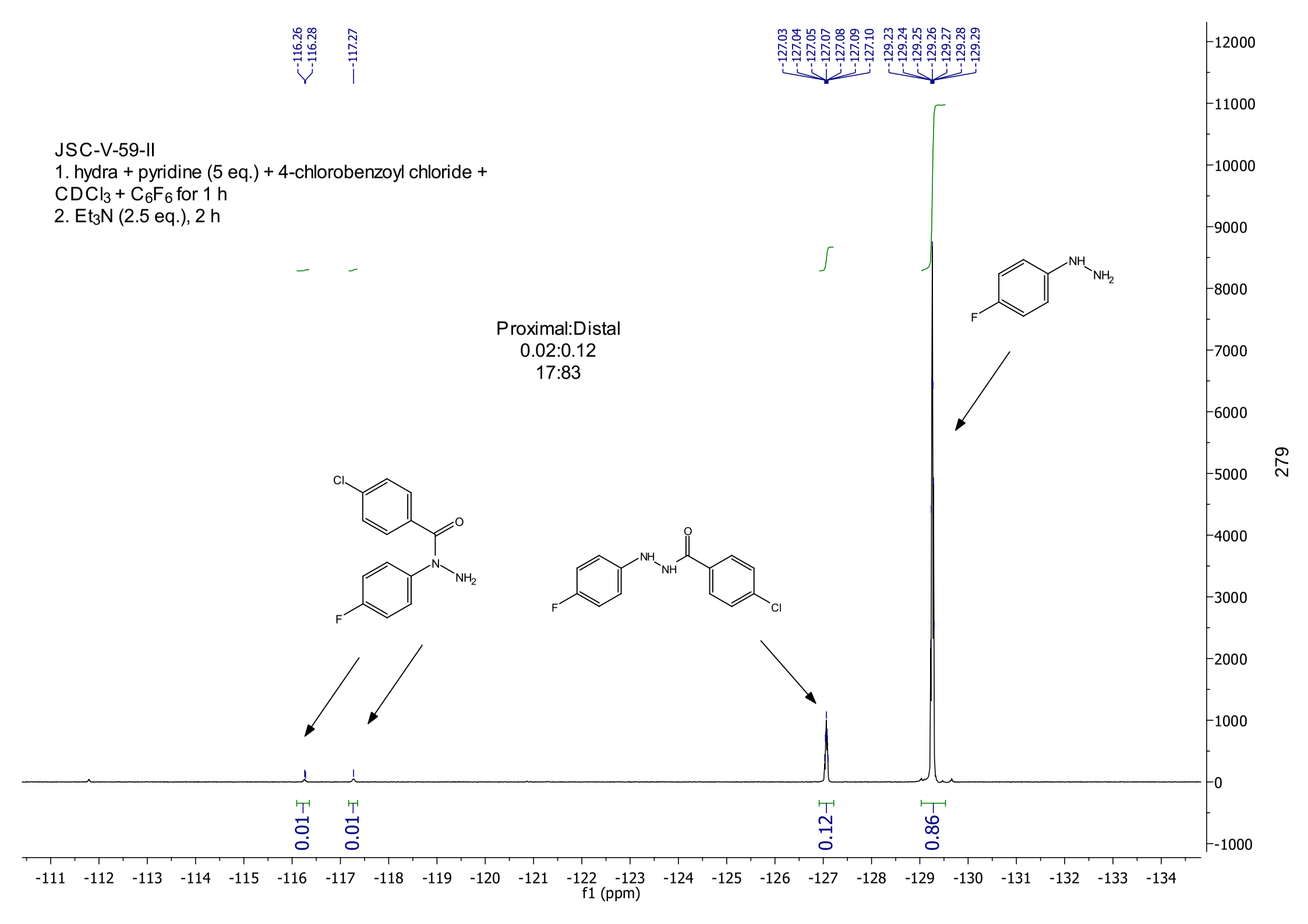
JSC-V-59-II
1. hydra + pyridine (5 eq.) + 4-chlorobenzoyl chloride +
CDCl3 + C6F6 for 1 h
2. Et3N (2.5 eq.), 2 h
Proximal:Distal
0.02:0.12
17:83
-116.26
-116.28
-117.27
-127.03
-127.04
-127.05
-127.07
-127.08
-127.09
-127.10
-129.23
-129.24
-129.25
-129.26
-129.27
-129.28
-129.29
0.01
0.01
0.12
0.86
f1 (ppm)
279

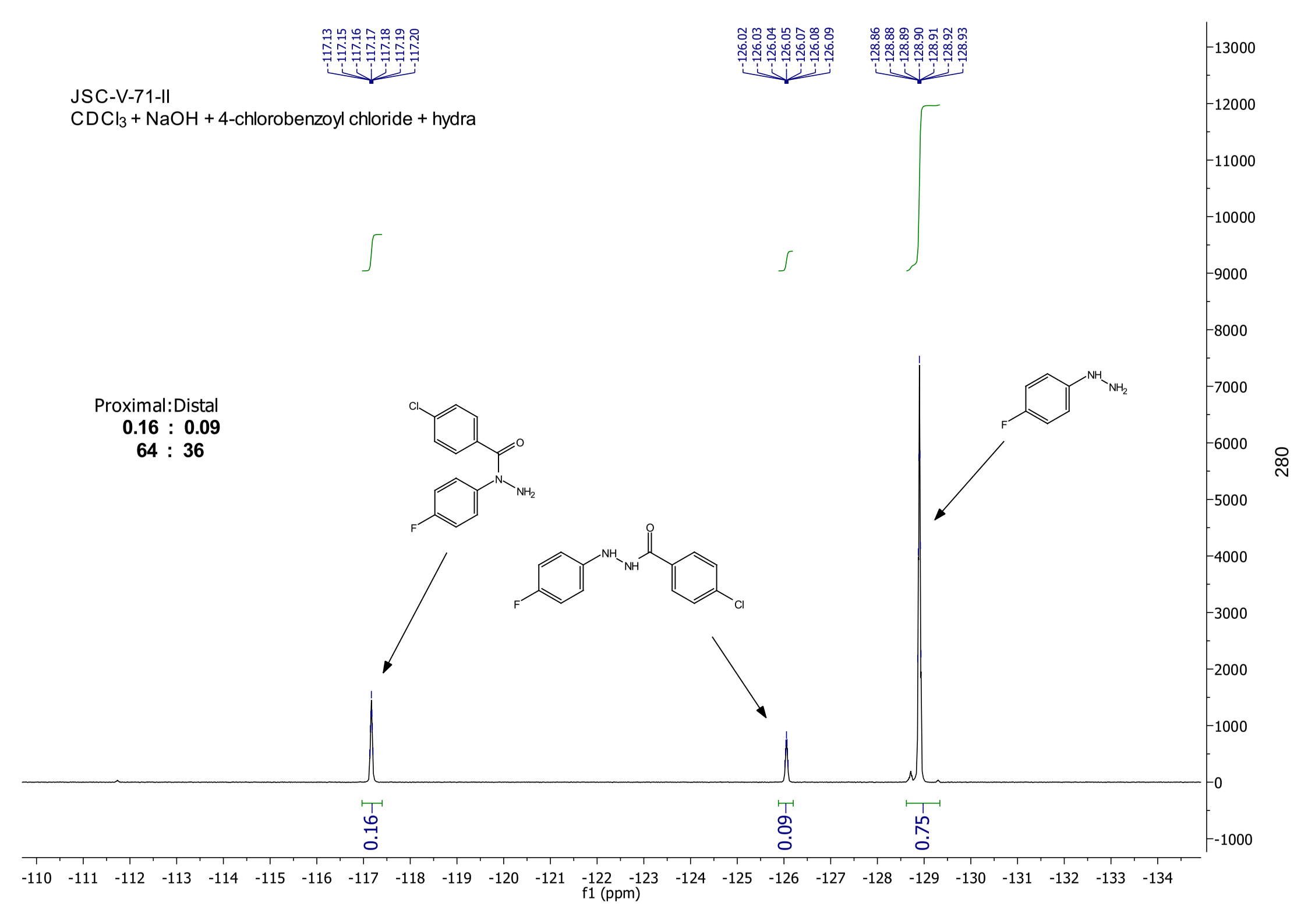
JSC-V-71-II
CDCl3 + NaOH + 4-chlorobenzoyl chloride + hydra
Proximal:Distal
0.16 : 0.09
64 : 36
0.16
0.09
0.75
f1 (ppm)
280

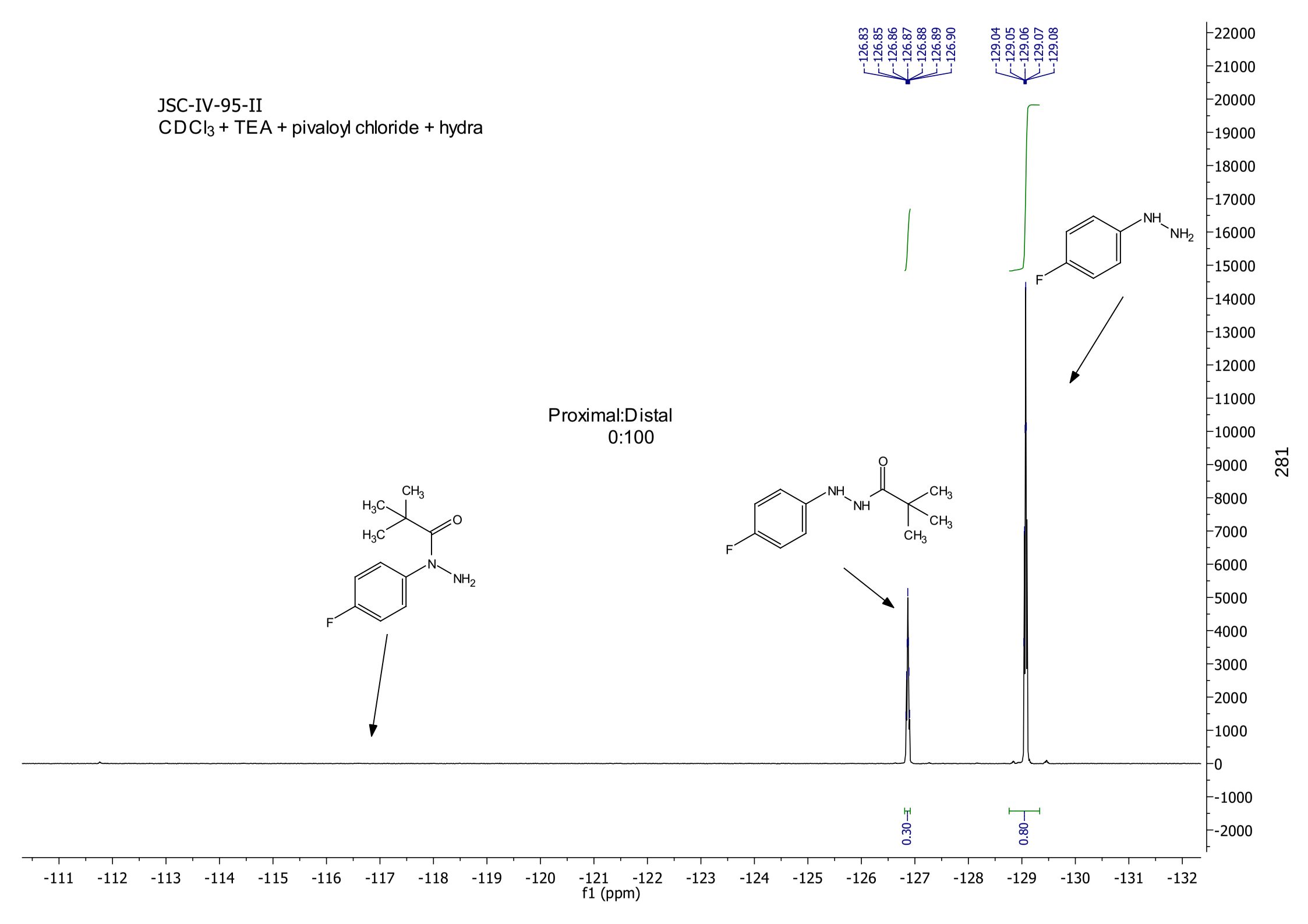
JSC-IV-95-II
CDCl3 + TEA + pivaloyl chloride + hydra
Proximal:Distal
0:100
126.83
126.85
126.86
126.87
126.88
126.89
126.90
129.04
129.05
129.06
129.07
129.08
0.30
0.80
f1 (ppm)
281

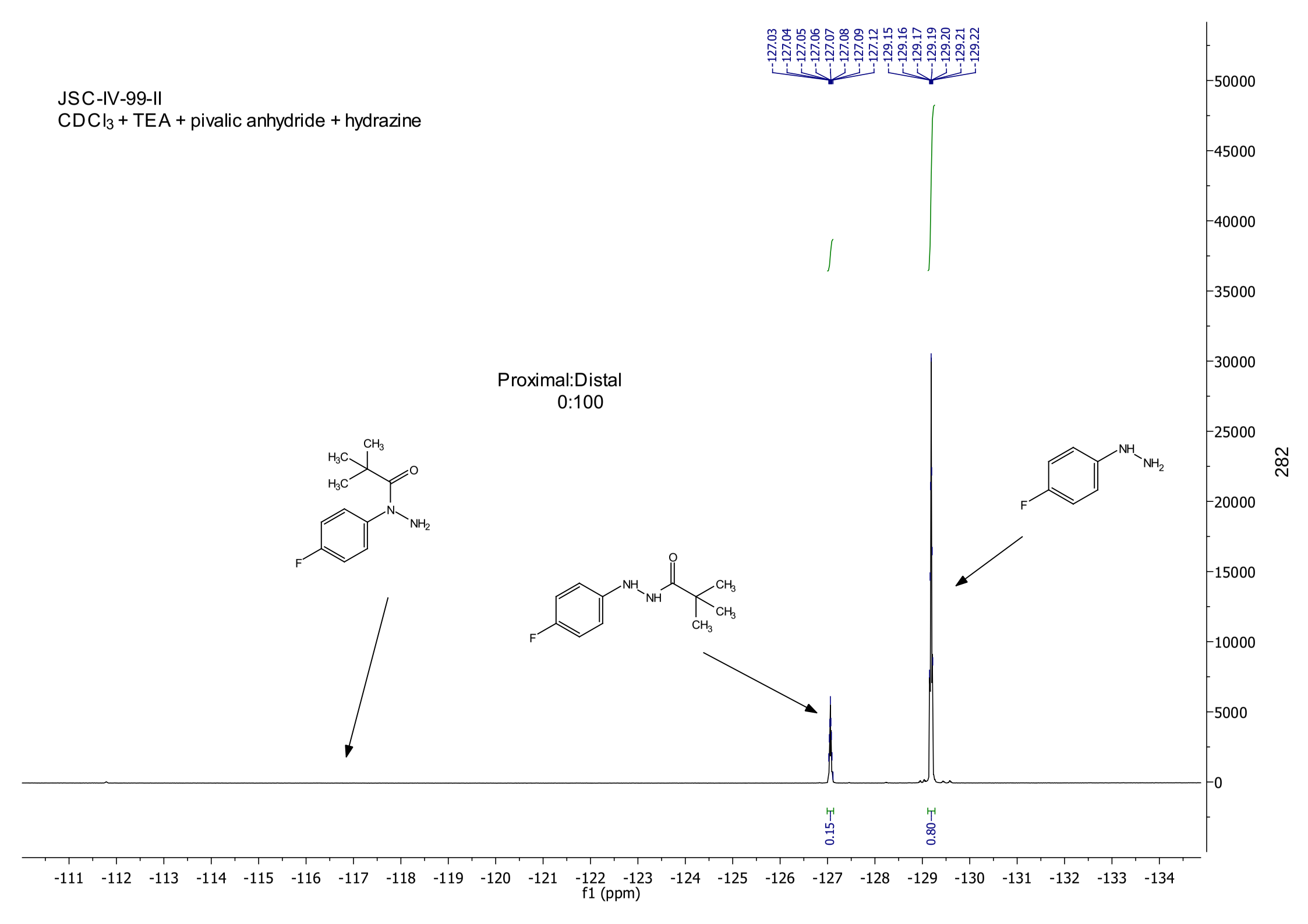
JSC-IV-99-II
CDCl3 + TEA + pivalic anhydride + hydrazine
Proximal:Distal
0:100
-127.03
-127.04
-127.05
-127.06
-127.07
-127.08
-127.09
-127.12
-129.15
-129.16
-129.17
-129.19
-129.20
-129.21
-129.22
0.15
0.80
f1 (ppm)
282

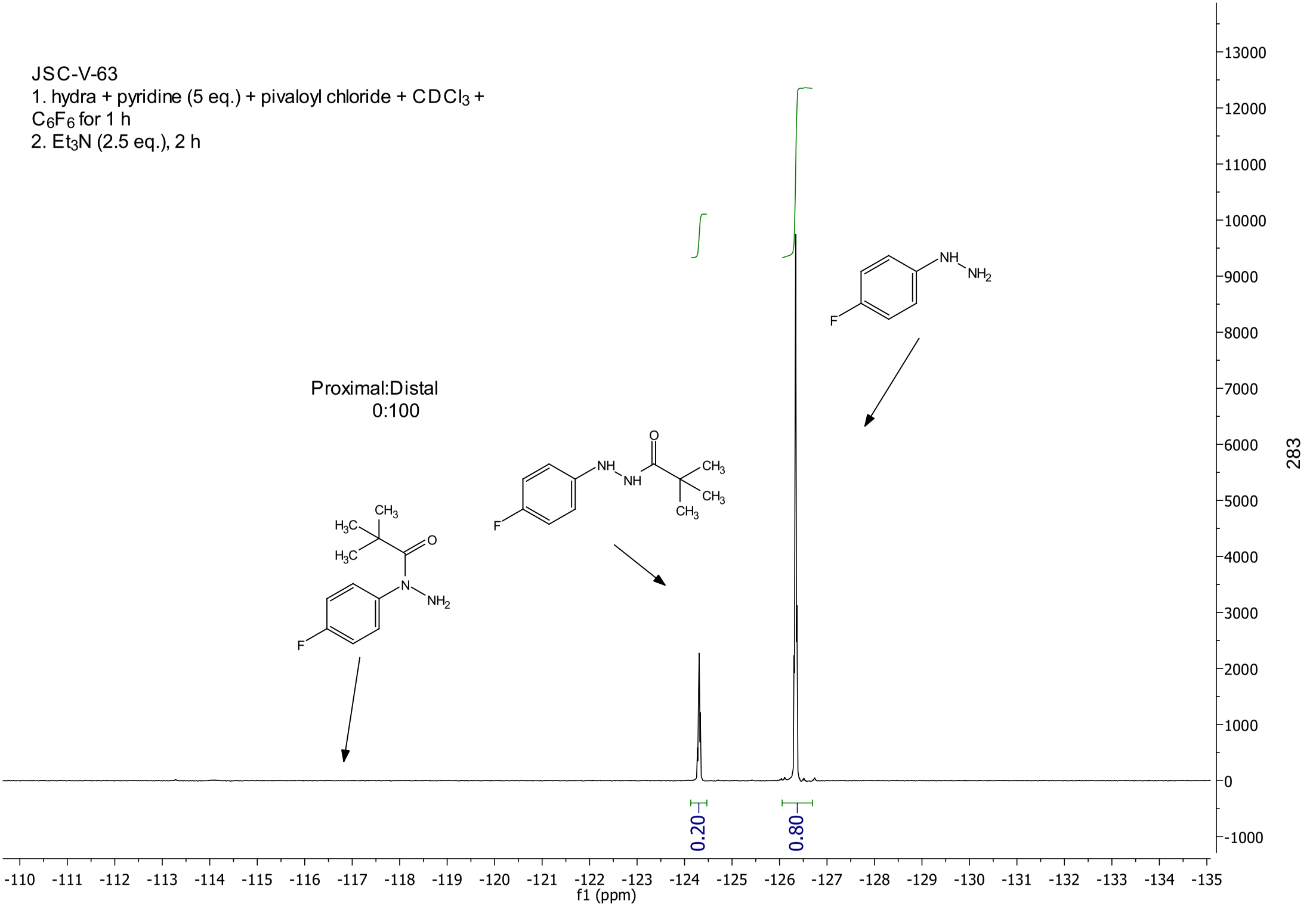
JSC-V-63
1. hydra + pyridine (5 eq.) + pivaloyl chloride + CDCl3 +
C6F6 for 1 h
2. Et3N (2.5 eq.), 2 h
Proximal:Distal
0:100
0.20
0.80
f1 (ppm)
283

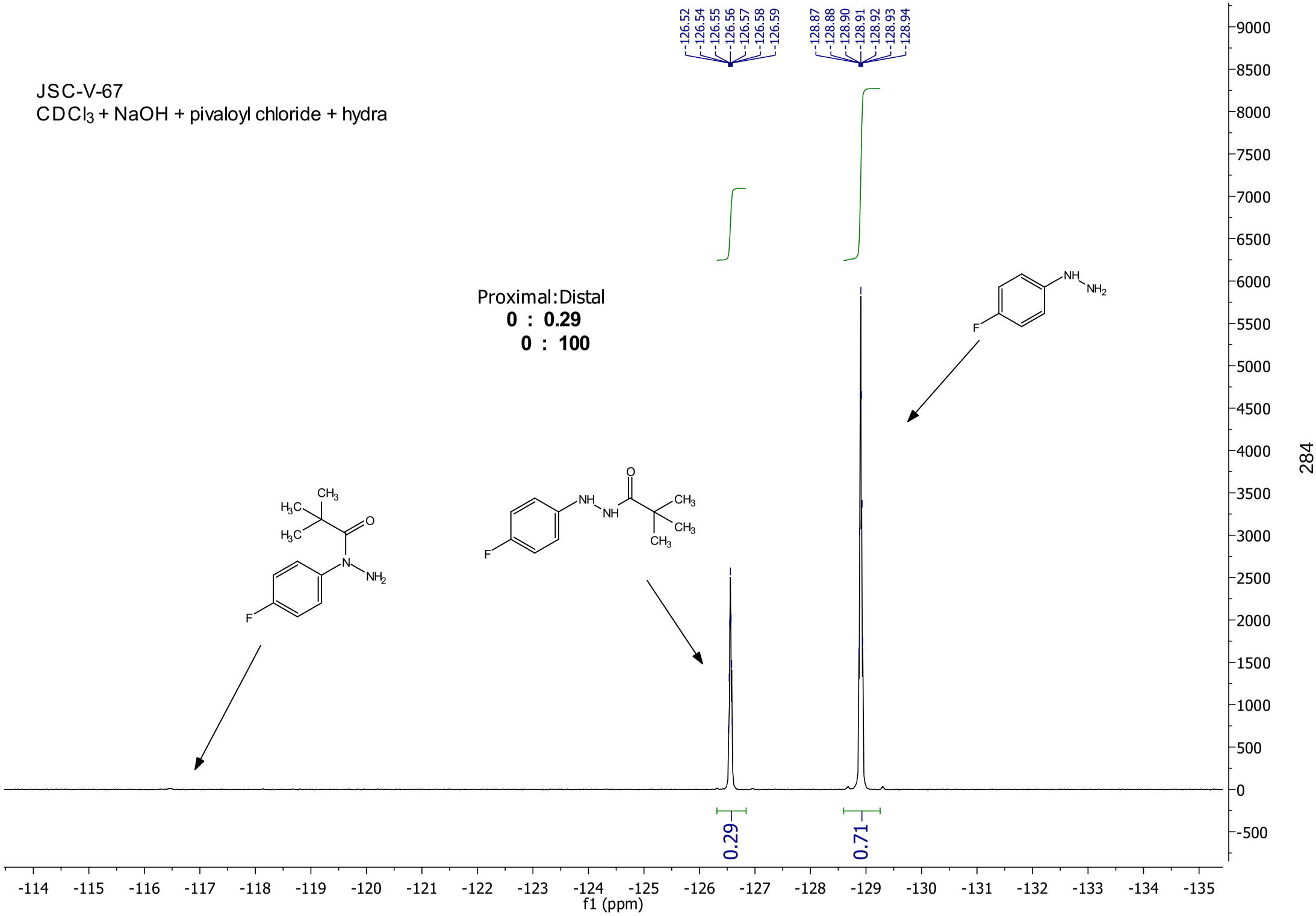
JSC-V-67
CDCl3 + NaOH + pivaloyl chloride + hydra
Proximal:Distal
0 : 0.29
0 : 100
126.52
126.54
126.55
126.56
126.57
126.58
126.59
128.87
128.88
128.90
128.91
128.92
128.93
128.94
0.29
0.71
f1 (ppm)
284

References

1. Jain, S. R., Self-igniting fuel-oxidizer systems and hybrid rockets. *J. Sci. Ind. Res.* **2003,** *62*, 293-310.
2. Schirmann, J.-P.; Bourdauducq, P., Hydrazine. In *Ullmann's Encyclopedia of Industrial Chemistry*, Wiley-VCH Verlag GmbH & Co. KGaA: 2000.
3. Barton, D. H. R.; Ives, D. A. J.; Thomas, B. R., A Wolff-Kishner Reduction Procedure for Sterically Hindered Carbonyl Groups. *J. Chem. Soc.* **1955**, 2056-2056.
4. Robinson, B., The Fischer Indole Synthesis. *Chem. Rev.* **1963,** *63*, 373-401.
5. Mohamed Ahmed, M. S.; Kobayashi, K.; Mori, A., One-pot construction of pyrazoles and isoxazoles with palladium-catalyzed four-component coupling. *Org. Lett.* **2005,** *7*, 4487-9.
6. Patel, N. B.; Khan, I. H.; Rajani, S. D., Pharmacological evaluation and characterizations of newly synthesized 1,2,4-triazoles. *Eur. J. Med. Chem.* **2010,** *45*, 4293-9.
7. Wong, B.; Stumpf, A.; Carrera, D.; Gu, C. A.; Zhang, H. M., A Safe Synthesis of 1,5-Disubstituted 3-Amino-1*H*-1,2,4-triazoles from 1,3,4-Oxadiazolium Hexafluorophosphates. *Synthesis* **2013,** *45*, 1083-1093.
8. Andersen, T. L.; Caneschi, W.; Ayoub, A.; Lindhardt, A. T.; Couri, M. R. C.; Skrydstrup, T., 1,2,4-and 1,3,4-Oxadiazole Synthesis by Palladium-Catalyzed Carbonylative Assembly of Aryl Bromides with Amidoximes or Hydrazides. *Adv. Synth. Catal.* **2014,** *356*, 3074-3082.
9. Buscemi, S.; Pace, A.; Piccionello, A. P.; Pibiri, I.; Vivona, N.; Giorgi, G.; Mazzanti, A.; Spinelli, D., Five-to-six membered ring-rearrangements in the reaction of 5-perfluoroalkyl-1,2,4-oxadiazoles with hydrazine and methylhydrazine. *J. Org. Chem.* **2006,** *71*, 8106-13.
10. Han, H.; Janda, K. D., Azatides: Solution and liquid phase syntheses of a new peptidomimetic. *J. Am. Chem. Soc.* **1996,** *118*, 2539-2544.
11. Thormann, M.; Hofmann, H.-J., Conformational properties of azapeptides. *J. Mol. Struc-Theochem* **1999,** *469*, 63-76.
12. Evans, D. A.; Manley, K. A.; Mc, K. V., Genetic control of isoniazid metabolism in man. *Brit. Med. J.* **1960,** *2*, 485-91.
13. Rickman, K. A.; Swancutt, K. L.; Mezyk, S. P.; Kiddle, J. J., Isoniazid: Radical-induced oxidation and reduction chemistry. *Bioorg. Med. Chem. Lett.* **2013,** *23*, 3096-3100.
14. Zhang, Y.; Malamakal, R. M.; Chenoweth, D. M., Aza-Glycine Induces Collagen Hyperstability. *J. Am. Chem. Soc.* **2015,** *137*, 12422-5.
15. Hsu, A. C. T.; Fujimoto, T. T.; Dhadialla, T. S., Structure-Activity Study and Conformational Analysis of RH-5992, the First Commercialized Nonsteroidal Ecdysone Agonist. In *Phytochemicals for Pest Control*, American Chemical Society: 1997; Vol. 658, pp 206-219.
16. Bloomquist, J. R.; Mutunga, J. M.; Islam, R. M.; Verma, A.; Ma, M.; Totrov, M.; Carlier, P. R., Voltage-Sensitive Potassium Kv2 Channels as New Targets for Insecticides. In *Biopesticides: State of the Art and Future Opportunities*, American Chemical Society: 2014; Vol. 1172, pp 71-81.
17. Harper, K.; Armelagos, G., The Changing Disease-Scape in the Third Epidemiological Transition. *Int. J. Environ. Res. Public Health* **2010,** *7*, 675.
18. Paul, R., From Shakespeare to Defoe: Malaria in England in the Little Ice Age. *Emerging Infect. Dis.* **2000,** *6*, 1.

19. Chan, M. *World Malaria Report 2015*; World Health Organization: Geneva, Switzerland, 2015.
20. Bonner, M. R.; Coble, J.; Blair, A.; Beane Freeman, L. E.; Hoppin, J. A.; Sandler, D. P.; Alavanja, M. C. R., Malathion Exposure and the Incidence of Cancer in the Agricultural Health Study. *Am. J. Epidemiol.* **2007,** *166*, 1023-1034.
21. Soderlund, D. M.; Clark, J. M.; Sheets, L. P.; Mullin, L. S.; Piccirillo, V. J.; Sargent, D.; Stevens, J. T.; Weiner, M. L., Mechanisms of pyrethroid neurotoxicity: implications for cumulative risk assessment. *Toxicology* **2002,** *171*, 3-59.
22. Retnakaran, A.; Krell, P.; Feng, Q.; Arif, B., Ecdysone agonists: mechanism and importance in controlling insect pests of agriculture and forestry. *Arch. Insect Biochem. Physiol.* **2003,** *54*, 187-99.
23. Salgado, V. L., Block of Voltage-Dependent K^+ Channels in Insect Muscle by the Diacylhydrazine Insecticide Rh-5849, 4-Aminopyridine, and Quinidine. *Arch. Insect Biochem. Physiol.* **1992,** *21*, 239-252.
24. Salgado, V. L., Block of neuronal voltage-dependent K^+ channels by diacylhydrazine insecticides. *Neurotoxicology* **1998,** *19*, 245-252.
25. Monthéan, C.; Potter, D. A., Effects of RH-5849, a Novel Insect Growth-Regulator, on Japanese-Beetle (Coleoptera, Scarabaeidae) and Fall Armyworm (Lepidoptera, Noctuidae) in Turfgrass. *J. Econ. Entomol.* **1992,** *85*, 507-513.
26. Raphemot, R.; Rouhier, M. F.; Hopkins, C. R.; Gogliotti, R. D.; Lovell, K. M.; Hine, R. M.; Ghosalkar, D.; Longo, A.; Beyenbach, K. W.; Denton, J. S.; Piermarini, P. M., Eliciting Renal Failure In Mosquitoes With A Small-Molecule Inhibitor Of Inward-Rectifying Potassium Channels. *PLoS One* **2013,** *8*, e64905.
27. Smith, P. A. S.; DeWall, G. L., Hydrazines as ambident nucleophiles: the site of benzylation of N-benzyl-N-phenylhydrazines. *J. Am. Chem. Soc.* **1977,** *99*, 5751-5760.
28. Hinman, R. L., Base Strengths of Some Alkylhydrazines. *J. Org. Chem.* **1958,** *23*, 1587-1588.
29. Aue, D. H.; Bowers, M. T.; Webb, H. M., Quantitative Relative Gas-Phase Basicities of Alkylamines - Correlation with Solution Basicity. *J. Am. Chem. Soc.* **1972,** *94*, 4726-&.
30. Wu, P.-L.; Peng, S.-Y.; Magrath, J., 1-Acyl-2-alkylhydrazines by the Reduction of Acylhydrazones. *Synthesis* **1995,** *1995*, 435-438.
31. Licandro, E.; Perdicchia, D., N-acylhydrazines: Future perspectives offered by new syntheses and chemistry. *Eur. J. Org. Chem.* **2004,** *2004*, 665-675.
32. Peet, N. P.; Sunder, S.; Cregge, R. J., Preparation and Utility of 1-Acetyl-1-Methylhydrazine. *J. Org. Chem.* **1976,** *41*, 2733-2736.
33. Hinman, R. L.; Fulton, D., The Reactions of Methylhydrazine and Unsym-Dimethylhydrazine with Esters and Anhydrides of Carboxylic Acids - the Application of Paper Chromatography to Problems in Synthetic Organic Chemistry. *J. Am. Chem. Soc.* **1958,** *80*, 1895-1900.
34. Condon, F. E., Selective Acetylation Of Methylhydrazine. 1-Acetyl-1-Methyl- And 1-Acetyl-2-Methylhydrazine. *J. Org. Chem.* **1972,** *37*, 3608-3615.
35. Liu, S., Origin and nature of bond rotation barriers: a unified view. *J. Phys. Chem. A.* **2013,** *117*, 962-5.
36. Song, L.; Liu, M.; Wu, W.; Zhang, Q.; Mo, Y., Origins of Rotational Barriers in Hydrogen Peroxide and Hydrazine. *J. Chem. Theory Comput.* **2005,** *1*, 394-402.

37. Lee, H. J.; Lee, M. H.; Choi, Y. S.; Park, H. M.; Lee, K. B., NBO approach to evaluate origin of rotational barrier of diformylhydrazine. *J. Mol. Struc-Theochem* **2003,** *631*, 101-110.
38. Dewar, M. J. S.; Jennings, W. B., Conformational Interchange in Acyclic Hydrazines. *J. Am. Chem. Soc.* **1973,** *95*, 1562-1569.
39. Bishop, G. J.; Price, B. J.; Sutherland, I. O., Torsional barriers in *N*,*N*′-diacylhydrazines. *Chem. Commun.* **1967,** *0*, 672-674.
40. Reynolds, C. H.; Hormann, R. E., Theoretical study of the structure and rotational flexibility of diacylhydrazines: Implications for the structure of nonsteroidal ecdysone agonists and azapeptides. *J. Am. Chem. Soc.* **1996,** *118*, 9395-9401.
41. Toya, T.; Yamaguchi, K.; Endo, Y., Cyclic dibenzoylhydrazines reproducing the conformation of ecdysone agonists, RH-5849. *Bioorg. Med. Chem.* **2002,** *10*, 953-61.
42. Hsu, A. C.-T., 1,2-Diacyl-1-alkylhydrazines. In *Synthesis and Chemistry of Agrochemicals II*, American Chemical Society: 1991; Vol. 443, pp 478-490.
43. Wing, K. D., RH 5849, a Nonsteroidal Ecdysone Agonist: Effects on a Drosophila Cell Line. *Science* **1988,** *241*, 467-469.
44. Beckage, N. E.; Marion, K. M.; Walton, W. E.; Wirth, M. C.; Tan, F. F., Comparative larvicidal toxicities of three ecdysone agonists on the mosquitoes Aedes aegypti, Culex quinquefasciatus, and Anopheles gambiae. *Arch. Insect Biochem. Physiol.* **2004,** *57*, 111-122.
45. Aller, H. E.; Ramsay, J. R. In *RH-5849 - A Novel Insect Growth-Regulator with a New Mode of Action*, British Crop Protection Council: 1988; pp 511-518.
46. Salgado, V. L., The neurotoxic insecticidal mechanism of the nonsteroidal ecdysone agonist RH-5849: K^+ channel block in nerve and muscle. *Pestic. Biochem. Physiol.* **1992,** *43*, 1-13.
47. Jiang, Y.; Lee, A.; Chen, J.; Ruta, V.; Cadene, M.; Chait, B. T.; MacKinnon, R., X-ray structure of a voltage-dependent K+ channel. *Nature* **2003,** *423*, 33-41.
48. Gutman, G. A.; Chandy, K. G.; Grissmer, S.; Lazdunski, M.; Mckinnon, D.; Pardo, L. A.; Robertson, G. A.; Rudy, B.; Sanguinetti, M. C.; Stühmer, W.; Wang, X., International Union of Pharmacology. LIII. Nomenclature and Molecular Relationships of Voltage-Gated Potassium Channels. *Pharmacol. Rev.* **2005,** *57*, 473-508.
49. Morales-Reyes, I.; Seseña-Rubfiaro, A.; Acosta-García, M. C.; Batina, N.; Godínez-Fernández, R., Simultaneous recording of the action potential and its whole-cell associated ion current on NG108-15 cells cultured over a MWCNT electrode. *Meas. Sci. Technol.* **2016,** *27*, 085701.
50. Cadogan, B. L.; Scharbach, R. D.; Krause, R. E.; Knowles, K. R., Evaluation of Tebufenozide Carry-Over and Residual Effects on Spruce Budworm (Lepidoptera: Tortricidae). *J. Econ. Entomol.* **2002,** *95*, 578-586.
51. Edwards, J. O.; Pearson, R. G., The Factors Determining Nucleophilic Reactivities. *J. Am. Chem. Soc.* **1962,** *84*, 16-24.
52. Fina, N. J.; Edwards, J. O., The Alpha Effect. A Review. *Int. J. Chem. Kinet.* **1973,** *5*, 1-26.
53. Jencks, W. P.; Carriuolo, J., Reactivity of Nucleophilic Reagents toward Esters. *J. Am. Chem. Soc.* **1960,** *82*, 1778-1786.
54. Kirby, A. J.; Younas, M., The reactivity of phosphate esters. Reactions of diesters with nucleophiles. *J. Chem. Soc. B* **1970**, 1165-1172.

55. Milan, J.; Milica, P., Pyridinium Oximes as Cholinesterase Reactivators. Structure-Activity Relationship and Efficacy in the Treatment of Poisoning with Organophosphorus Compounds. *Curr. Med. Chem.* **2009,** *16*, 2177-2188.
56. Hoz, S., The α effect: on the origin of transition-state stabilization. *J. Org. Chem.* **1982,** *47*, 3545-3547.
57. Ashby, E. C.; Bowers, J. S., Nature of alkyl transfer in reactions of Grignard reagents with ketones. *J. Am. Chem. Soc.* **1977,** *99*, 8504-8505.
58. Johnson, R. W.; Widlanski, T.; Breslow, R., Evidence for an electron transfer mechanism in the coupling of cyclopropenyl cations with cyclopropenyl anions. *Tetrahedron Lett.* **1976,** *17*, 4685-4686.
59. Walling, C., Reality of electron transfer in slow organic reactions. *J. Am. Chem. Soc.* **1980,** *102*, 6854-6855.
60. Esteves, P. M.; de M. Carneiro, J. W.; Cardoso, S. P.; Barbosa, A. G. H.; Laali, K. K.; Rasul, G.; Prakash, G. K. S.; Olah, G. A., Unified Mechanistic Concept of Electrophilic Aromatic Nitration: Convergence of Computational Results and Experimental Data. *J. Am. Chem. Soc.* **2003,** *125*, 4836-4849.
61. Gregory, M. J.; Bruice, T. C., The α Effect. II. Displacements on sp^3 carbon. *J. Am. Chem. Soc.* **1967,** *89*, 4400-4402.
62. Fountain, K. R., The size of the alpha-effects in methyl transfers correlate with Koopmans' theorem ionization potentials. *J. Phys. Org. Chem.* **2005,** *18*, 481-485.
63. Afzal, D.; Fountain, K. R., Exploration of the α-effect by substitution on hydroxylamine anions. I. Effects of alkyl- and fluoroalkylation. *Canadian Journal of Chemistry* **2014,** *92*, 346-353.
64. Ren, Y.; Yamataka, H., The α-Effect in Gas-Phase SN2 Reactions Revisited. *Org. Lett.* **2006,** *8*, 119-121.
65. Garver, J. M.; Gronert, S.; Bierbaum, V. M., Experimental validation of the alpha-effect in the gas phase. *J Am Chem Soc* **2011,** *133*, 13894-7.
66. Buncel, E.; Um, I.-H., The α-effect and its modulation by solvent. *Tetrahedron* **2004,** *60*, 7801-7825.
67. Buncel, E.; Um, I.-H., The solvent effect on the α-effect. *J. Chem. Soc., Chem. Commun.* **1986**, 595-595.
68. Ritchie, C. D., Cation-anion combination reactions. 24. Ionization potentials, solvation energies, and reactivities of nucleophiles in water. *J. Am. Chem. Soc.* **1983,** *105*, 7313-7318.
69. Licandro, E.; Maiorana, S.; Manzotti, R.; Papagni, A.; Perdicchia, D.; Licandro, E.; Pryce, M.; Tiripicchio, A.; Lanfranchi, M., New synthesis of Fischer-type hydrazino(alkyl) complexes. First X-ray characterisation of a chelate hydrazino derivative. *Chem. Commun.* **1998**, 383-384.
70. Hsu, A. C. T.; Aller, H. E.; Le, D. P.; Hamp, D. E.; Weinstein, B.; Murphy, R. A. Insecticidal N'-substituted-N,N'-disubstitutedhydrazines. U.S. Patent 6,013,836, January 11, 2000, 1995.
71. Sawada, Y.; Yanai, T.; Nakagawa, H.; Tsukamoto, Y.; Yokoi, S.; Yanagi, M.; Toya, T.; Sugizaki, H.; Kato, Y.; Shirakura, H.; Watanabe, T.; Yajima, Y.; Kodama, S.; Masui, A., Synthesis and insecticidal activity of benzoheterocyclic analogues of N '-benzoyl-N-(tert-butyl)benzohydrazide: Part 1. Design of benzoheterocyclic analogues. *Pest Manag. Sci.* **2003,** *59*, 25-35.

72. Wang, Q. M.; Huang, R. Q., Alkylgermasesquioxide derivatives of tert-butyl-diacylhydrazines. *Heteroat. Chem* **2003,** *14*, 293-297.
73. Smith, R. F.; Bates, A. C.; Battisti, A. J.; Byrnes, P. G.; Mroz, C. T.; Smearing, T. J.; Albrecht, F. X., Reactions of Hydrazines with Esters and Carboxylic Acids. *J. Org. Chem.* **1968,** *33*, 851-5.
74. Baumgarten, H. E.; Chen, P. Y. N.; Taylor, H. W.; Hwang, D. R., Reactions of Amines. 20. Syntheses of Racemic and Optically-Active Alkylhydrazines and N-Acyl-N-Alkylhydrazines and N-Acyl-N-Arylhydrazines. *J. Org. Chem.* **1976,** *41*, 3805-3811.
75. Siddaiah, V.; Basha, G. M.; Rao, G. P.; Prasad, U. V.; Rao, R. S., PEG-mediated Facile Protocol for N-Boc Protection of Amines. *Chem. Lett.* **2010,** *39*, 1127-1129.
76. Moore, R. F.; Plant, S. G. P., Oxindoles formerly regarded as ψ-indoxyls. *J. Chem. Soc.* **1951**, 3475-3478.
77. Hearn, M. J.; Grimwade, J. E., A Convenient Method for the Preparation of 1-Acyl-2-Phenylhydrazines. *Org. Prep. Proced. Int.* **1980,** *12*, 249-251.
78. Hearn, M. J.; Magee, D. J.; Alhart, R.; Gleva, M.; Goldstein, S.; Levy, F.; Muenzen, C.; Neuringer, I.; Racin, M.; Rosenberg, J.; Silva, H.; Williams, P., Acylation Reactions of Phenylhydrazines - Preparation and Properties of New Diacylphenylhydrazines. *J. Chem. Eng. Data.* **1985,** *30*, 129-131.
79. Zhao, D.; Shi, Z.; Glorius, F., Indole Synthesis By Rhodium(III)-Catalyzed Hydrazine-Directed C-H Activation: Redox-Neutral And Traceless By N-N Bond Cleavage. *Angew. Chem. Int. Edit.* **2013,** *52*, 12426-12429.
80. Paulsen, H.; Stoye, D., The chemistry of hydrazides. In *Chemistry of Amides*, Zabicky, J., Ed. John Wiley & Sons, Ltd.: 1970; pp 515-589.
81. Cohen, S. G.; Nicholson, J., Formation of Phenyldiimide and Phenyl Radical by Heterolysis of N-Phenyl-N'-benzoyldiimide. *J. Org. Chem.* **1965,** *30*, 1162-1168.
82. Zhang, C. Y.; Liu, X. H.; Wang, B. L.; Wang, S. H.; Li, Z. M., Synthesis and antifungal activities of new pyrazole derivatives via 1,3-dipolar cycloaddition reaction. *Chem. Biol. Drug Des.* **2010,** *75*, 489-93.
83. Catarzi, D.; Varano, F.; Poli, D.; Squarcialupi, L.; Betti, M.; Trincavelli, L.; Martini, C.; Dal Ben, D.; Thomas, A.; Volpini, R.; Colotta, V., 1,2,4-Triazolo[1,5-a]quinoxaline derivatives and their simplified analogues as adenosine A3 receptor antagonists. Synthesis, structure–affinity relationships and molecular modeling studies. *Bioorg. Med. Chem.* **2015,** *23*, 9-21.
84. McCarthy, A. R.; Ollis, W. D.; Barnes, A. N. M.; Sutton, L. E.; Ainsworth, C., Cyclic meso-ionic compounds. Part VI. Synthesis, spectroscopic properties, and dipole moments of the isosydnones. *J. Chem. Soc. B* **1969**, 1185.
85. Beltrami, R. T.; Bissell, E. R., Some Methylhydrazonium Salts; An Improved Synthesis of Tetramethylhydrazine1. *J. Am. Chem. Soc.* **1956,** *78*, 2467-2468.
86. Jones, T. O.; Halter, R. E.; Myers, W. L., The Reaction of Esters with Phenylhydrazine in the Presence of Phosphoric Acid. *J. Am. Chem. Soc.* **1953,** *75*, 6055-6056.
87. Benderly, A.; Stavchansky, S., A new synthesis of carboxylic acid hydrazides organoaluminum reagents. *Tetrahedron Lett.* **1988,** *29*, 739-740.
88. Contó, M. B.; de Carvalho, J. G. B.; Benedito, M. A. C., Behavioral differences between subgroups of rats with high and low threshold to clonic convulsions induced by DMCM, a benzodiazepine inverse agonist. *Pharmacol. Biochem. Behav.* **2005,** *82*, 417-426.
89. Rosamilia, A. E.; Arico, F.; Tundo, P., Reaction of the ambident electrophile dimethyl carbonate with the ambident nucleophile phenylhydrazine. *J. Org. Chem.* **2008,** *73*, 1559-62.

90. Rosamilia, A. E.; Aricò, F.; Tundo, P., Insight into the Hard−Soft Acid−Base Properties of Differently Substituted Phenylhydrazines in Reactions with Dimethyl Carbonate. *J. Phys. Chem. B.* **2008,** *112*, 14525-14529.
91. Verardo, G.; Toniutti, N.; Giumanini, A. G., Preparation, properties, and reductive alkylation of arylhydrazides. *Can. J. Chem.* **1998,** *76*, 1180-1187.
92. Hojo, K.; Maeda, M.; Smith, T. J.; Kawasaki, K., Acylation of hydrazides with acetic acid and formic acid. *Chem Pharm Bull (Tokyo)* **2002,** *50*, 140-2.
93. Zhan, F.; Liang, G., Formation of Enehydrazine Intermediates through Coupling of Phenylhydrazines with Vinyl Halides: Entry into the Fischer Indole Synthesis. *Angew. Chem. Int. Edit.* **2013,** *52*, 1266-1269.
94. Zhang, X.; Breslav, M.; Grimm, J.; Guan, K.; Huang, A.; Liu, F.; Maryanoff, C. A.; Palmer, D.; Patel, M.; Qian, Y.; Shaw, C.; Sorgi, K.; Stefanick, S.; Xu, D., A new procedure for preparation of carboxylic acid hydrazides. *J. Org. Chem.* **2002,** *67*, 9471-4.
95. Katritzky, A. R.; Rao, M. S. C., Preparation of 1, 1-disubstituted hydrazines and their 2-acyl derivatives. *J. Chem. Soc., Perkin Trans. 1* **1989**, 2297-2303.
96. Poesen, N.; de Moor, A.; Busschots, A.; Dooms-Goossens, A., Contact allergy to dicyclohexyl carbodiimide and diisopropyl carbodiimide. *Contact Dermatitis* **1995,** *32*, 368-369.
97. Giger, W.; Schaffner, C.; Kohler, H.-P. E., Benzotriazole and Tolyltriazole as Aquatic Contaminants. 1. Input and Occurrence in Rivers and Lakes. *Environ. Sci. Technol.* **2006,** *40*, 7186-7192.
98. Ottersen, T., The Structure of Diformylhydrazine at 19 degrees C and -165 degrees C. *Acta Chem. Scand.* **1974,** *28a*, 1145-1149.
99. Ottersen, T., The Crystal and Molecular Structure of 1,2-Dimethyl-1,2-diformylhydrazine at 110 K. *Acta Chem. Scand.* **1978,** *32a*, 127-131.
100. Caira, M. R.; Watson, W. H.; Vogtle, F.; Muller, W., A 1:2 host-guest complex between 1,4,7,10,13,16-hexaoxacyclooctadecane (18-crown-6) and *N*,*N*'-diformohydrazide, $C_{12}H_{24}O_6$*$2C_2H_4N_2O_2$. *Acta Crystallographica Section C* **1984,** *40*, 136-138.
101. Dewar, M. J. S.; Jennings, W. B., Barrier to pyramidal inversion of nitrogen in dibenzylmethylamine. *J. Am. Chem. Soc.* **1971,** *93*, 401-403.
102. Kölmel, C.; Ochsenfeld, C.; Ahlrichs, R., An ab initio investigation of structure and inversion barrier of triisopropylamine and related amines and phosphines. *Theoretica chimica acta* **1992,** *82*, 271-284.
103. Majumdar, P.; Pati, A.; Patra, M.; Behera, R. K.; Behera, A. K., Acid Hydrazides, Potent Reagents for Synthesis of Oxygen-, Nitrogen-, and/or Sulfur-Containing Heterocyclic Rings. *Chem. Rev.* **2014,** *114*, 2942-2977.
104. Dains, F. B., On the action of acid chlorides on mixtures of amines. *J. Am. Chem. Soc.* **1906,** *28*, 1183-1188.
105. Kim, Y. J.; Lee, D., Use of N-N bond stereodynamics in ring-closing metathesis to form medium-sized rings and macrocycles. *Org. Lett.* **2004,** *6*, 4351-3.
106. Bailly, S.; Pocidalo, J. J.; Fay, M.; Gougerot-Pocidalo, M. A., Differential modulation of cytokine production by macrolides: interleukin-6 production is increased by spiramycin and erythromycin. *Antimicrob. Agents Chemother.* **1991,** *35*, 2016-2019.
107. Enders, D.; Grobner, R.; Raabe, G.; Runsink, J., Enantioselective synthesis of 2-substituted 5-, 6- and 7-membered lactams via alpha-alkylation of their chiral N-dialkylamino derivatives. *Synthesis* **1996**, 941-&.

108. Huang, Y.-C.; Fang, G.-M.; Liu, L., Chemical synthesis of proteins using hydrazide intermediates. *Natl. Sci. Rev.* **2016,** *3*, 107-116.
109. Dawson, P. E.; Muir, T. W.; Clark-Lewis, I.; Stephen, B. H. K., Synthesis of Proteins by Native Chemical Ligation. *Science* **1994,** *266*, 776-779.
110. Ottersbach, P. A.; Schnakenburg, G.; Gutschow, M., Induction of chirality: experimental evidence of atropisomerism in azapeptides. *Chem. Commun.* **2012,** *48*, 5772-4.
111. Le Goff, G.; Ouazzani, J., Natural hydrazine-containing compounds: Biosynthesis, isolation, biological activities and synthesis. *Bioorg. Med. Chem.* **2014,** *22*, 6529-6544.
112. Ito, M. S., N.; Ito, K.; Mizobe, F.; Hanada, K.; Mizoue, K.; Bhandari, R.;; Eguchi, T. K., K., A novel fungal metabolite NG-061 enhances and mimics neurotrophic effect of NGF on neurite outgrowth on PC12 cells. *J. Antibiot.* **1999,** *52*, 224-230.
113. Klosterman, H. J.; Lamoureux, G. L.; Parsons, J. L., Isolation, Characterization, and Synthesis of Linatine. A Vitamin B6 Antagonist from Flaxseed (Linum usitatissimum)*. *Biochemistry* **1967,** *6*, 170-177.
114. Ferrucci, V.; Boffa, I.; De Masi, G.; Zollo, M., Natural compounds for pediatric cancer treatment. *Naunyn Schmiedebergs Arch. Pharmacol.* **2016,** *389*, 131-149.
115. Mutunga, J. M.; Anderson, T. D.; Craft, D. T.; Gross, A. D.; Swale, D. R.; Tong, F.; Wong, D. M.; Carlier, P. R.; Bloomquist, J. R., Carbamate and pyrethroid resistance in the akron strain of Anopheles gambiae. *Pestic. Biochem. Physiol.* **2015,** *121*, 116-121.
116. Wing, K. D. Anthelmintic N-alkyl-N,N'-diacylhydrazines: Nonsteroidal Ecdysone Agonists. U.S. Patent 5,424,333, June 13, 1995, 1995.
117. Calabretta, R.; Gallina, C.; Giordano, C., Sodium Cyanoborohydride Reduction of (Benzyloxycarbonyl)- and (tert-Butoxycarbonyl)hydrazones. *Synthesis* **1991,** *1991*, 536-539.
118. Korzekwa, K.; Trager, W.; Gouterman, M.; Spangler, D.; Loew, G., Cytochrome P450 mediated aromatic oxidation: a theoretical study. *J. Am. Chem. Soc.* **1985,** *107*, 4273-4279.
119. Wolter, M.; Klapars, A.; Buchwald, S. L., Synthesis of N-aryl hydrazides by copper-catalyzed coupling of hydrazides with aryl iodides. *Org. Lett.* **2001,** *3*, 3803-5.
120. Huang, P.-Q.; Zheng, X.; Deng, X.-M., DIBAL–H–H2NR and DIBAL–H–HNR1R2·HCl complexes for efficient conversion of lactones and esters to amides. *Tetrahedron Lett.* **2001,** *42*, 9039-9041.
121. Larson, N. R.; Carlier, P. R.; Gross, A. D.; Islam, R. M.; Ma, M.; Sun, B.; Totrov, M. M.; Yadav, R.; Bloomquist, J. R., Toxicology of potassium channel-directed compounds in mosquitoes. *NeuroToxicology*.
122. Brown, N. A.; Kemp, J. A.; Seabrook, G. R., Block of human voltage-sensitive Na^+ currents in differentiated SH-SY5Y cells by lifarizine. *British Journal of Pharmacology* **1994,** *113*, 600-606.
123. Pridgeon, J. W.; Becnel, J. J.; Clark, G. C.; Linthicum, K. J., A High-Throughput Screening Method to Identify Potential Pesticides for Mosquito Control. *J. Med. Entomol.* **2009,** *46*, 335-341.
124. Bloomquist, J. R.; Mutunga, J. M.; Islam, R. M.; Verma, A.; Ma, M.; Totrov, M. M.; Carlier, P. R., Voltage-Sensitive Potassium Kv2 Channels as New Targets for Insecticides. In *Biopesticides: State of the Art and Future Opportunities*, American Chemical Society: 2014; Vol. 1172, pp 71-81.
125. Bonini, B. F.; Franchini, M. C.; Gentili, D.; Locatelli, E.; Ricci, A., 1,3-Dipolar Cycloaddition of Nitrile Imines with Functionalized Acetylenes: Regiocontrolled $Sc(OTf)_3$-Catalyzed Synthesis of 4- and 5-Substituted Pyrazoles. *Synlett* **2009,** *2009*, 2328-2332.

126. Avan, I.; Hall, C. D.; Katritzky, A. R., Peptidomimetics via modifications of amino acids and peptide bonds. *Chem. Soc. Rev.* **2014,** *43*, 3575-94.
127. Beveridge, R. E.; Batey, R. A., Total Synthesis of the Cytotoxic Enehydrazide Natural Products Hydrazidomycins A and B by a Carbazate Addition/Peterson Olefination Approach. *Org. Lett.* **2013,** *15*, 3086-3089.
128. Le Goff, G.; Roulland, E.; Ouazzani, J., Total synthesis of geralcin A, a representative of a new family of hydrazine-containing natural products. *Tetrahedron Lett.* **2013,** *54*, 5299-5301.
129. Wheelock, C. E.; Nakagawa, Y.; Harada, T.; Oikawa, N.; Akamatsu, M.; Smagghe, G.; Stefanou, D.; Iatrou, K.; Swevers, L., High-throughput screening of ecdysone agonists using a reporter gene assay followed by 3-D QSAR analysis of the molting hormonal activity. *Bioorg. Med. Chem.* **2006,** *14*, 1143-1159.
130. Huang, Z.; Liu, Y.; Li, Y.; Xiong, L.; Cui, Z.; Song, H.; Liu, H.; Zhao, Q.; Wang, Q., Synthesis, Crystal Structures, Insecticidal Activities, and Structure−Activity Relationships of Novel *N*′-tert-Butyl-*N*′-substituted-benzoyl-*N*-[di(octa)hydro]benzofuran{(2,3-dihydro)benzo[1,3]([1,4])dioxine}carbohydrazide Derivatives. *J. Agric. Food Chem.* **2011,** *59*, 635-644.
131. Mhashilkar, A. S.; Vankayala, S. L.; Liu, C.; Kearns, F.; Mehrotra, P.; Tzertzinis, G.; Palli, S. R.; Woodcock, H. L.; Unnasch, T. R., Identification of Ecdysone Hormone Receptor Agonists as a Therapeutic Approach for Treating Filarial Infections. *PLoS Negl. Trop. Dis.* **2016,** *10*, 1-19.
132. Morou, E.; Lirakis, M.; Pavlidi, N.; Zotti, M.; Nakagawa, Y.; Smagghe, G.; Vontas, J.; Swevers, L., A New Dibenzoylhydrazine With Insecticidal Activity Against Anopheles Mosquito Larvae. *Pest Manag. Sci.* **2013,** *69*, 827-833.
133. Song, G. P.; Hu, D. K.; Tian, H.; Li, Y. S.; Cao, Y. S.; Jin, H. W.; Cui, Z. N., Synthesis and Larvicidal Activity of Novel Thenoylhydrazide Derivatives. *Sci Rep* **2016,** *6*, 22977.
134. O'Toole, S. E.; Connon, S. J., The Enantioselective Benzoin Condensation Promoted By Chiral Triazolium Precatalysts: Stereochemical Control Via Hydrogen Bonding. *Org. Biomol. Chem.* **2009,** *7*, 3584-93.
135. Barton, D. H. R.; Ollis, W. D., Comprehensive Organic Chemistry: The Synthesis and Reactions of Organic Compounds. Pergamon Press: 1978; pp 228-229.
136. Zarchi, M. A. K.; Bahadoran, A., Convenient Synthesis of Benzamides Mediated by Poly(4-vinylpyridine)-Supported Benzoyl Chloride. *J. Appl. Polym. Sci.* **2011,** *119*, 2345-2349.
137. Behrend, R.; Reinsberg, W., Über die Phenylhydrazone der Glucose. *Liebigs Ann.* **1910,** *377*, 189-220.
138. Hearn, M. J.; Defurio, L.; Hurst, W.; Koss, C.; Licthman, M.; Lucas, L.; Mabrouk, P.; Teng, S.; Waud, C., Anhydride Acylation Reactions Of 2,4-Dinitrophenylhydrazine. *Org. Prep. Proced. Int.* **1982,** *14*, 406-409.
139. Paukstelis, J. V.; Kim, M.-G., *N*-Acyl-*N*,*N*,*N*-Trialkylammonium Fluoroborates. Synthesis And Reactions. *J. Org. Chem.* **1974,** *39*, 1503-1507.
140. Held, I.; Villinger, A.; Zipse, H., The stability of acylpyridinium cations and their relation to the catalytic activity of pyridine bases. *Synthesis* **2005**, 1425-1430.
141. Maguire, A. R.; Plunkett, S. J.; Papot, S.; Clynes, M.; O'Connor, R.; Touhey, S., Synthesis of indomethacin analogues for evaluation as modulators of MRP activity. *Bioorg. Med. Chem.* **2001,** *9*, 745-762.
142. Yamamoto, H., 1-Acylindoles. III. Novel Synthesis Of 9-Acyltetrahydrocarbazole And 5-Acyl-γ-Carboline Derivatives. *The Journal of Organic Chemistry* **1967,** *32*, 3693-3695.

143. Hormann, R. E.; Dinan, L.; Whiting, P., Superimposition evaluation of ecdysteroid agonist chemotypes through multidimensional QSAR. *J. Comput. Aided Mol. Des.* **2003,** *17*, 135-153.
144. Heidberg, J.; Weil, J. A.; Janusonis, G. A.; Anderson, J. K., Conformation and Internal Rotation of Nitroaromatic Amines in Solution as Detected by Proton Magnetic Resonance. *J. Chem. Phys.* **1964,** *41*, 1033-1044.
145. Kessler, H., Detection of intramolecular mobility by nmr spectroscopy. *Angew. Chem. Int. Edit.* **1970,** *9*, 219-235.
146. Bilton, C.; Allen, F. H.; Shields, G. P.; Howard, J. A. K., Intramolecular hydrogen bonds: common motifs, probabilities of formation and implications for supramolecular organization. *Acta Crystallogr.* **2000,** *56*, 849-856.
147. Rydberg, E. H.; Brumshtein, B.; Greenblatt, H. M.; Wong, D. M.; Shaya, D.; Williams, L. D.; Carlier, P. R.; Pang, Y.-P.; Silman, I.; Sussman, J. L., Complexes of Alkylene-Linked Tacrine Dimers with Torpedo californica Acetylcholinesterase: Binding of Bis(5)-tacrine Produces a Dramatic Rearrangement in the Active-Site Gorge. *J. Med. Chem.* **2006,** *49*, 5491-5500.
148. Carlier, P. R.; Sun, Y. S.; Hsu, D. C.; Chen, Q. H., Axial-Selective H/D Exchange of Glycine-Derived 1H-Benzo e 1,4 diazepin-2(3H)-ones: Kinetic and Computational Studies of Enantiomerization. *J. Org. Chem.* **2010,** *75*, 6588-6594.
149. Dinan, L.; Nakagawa, Y.; Hormann, R. E., Structure-Activity Relationships of Ecdysteroids and Non-Steroidal Ecdysone Agonists. In *Advances in Insect Physiology, Vol 43: Insect Growth Disruptors*, Dhadialla, T. S., Ed. Academic Press Ltd-Elsevier Science Ltd: London, 2012; Vol. 43, pp 251-298.
150. Sui, Z. H.; Guan, J. H.; Ferro, M. P.; McCoy, K.; Wachter, M. P.; Murray, W. V.; Singer, M.; Steber, M.; Ritchie, D. M.; Argentieri, D. C., 1,3-Diarylcycloalkanopyrazoles And Diphenyl Hydrazides As Selective Inhibitors Of Cyclooxygenase-2. *Bioorg. Med. Chem. Lett.* **2000,** *10*, 601-604.
151. Okawara, T.; Kanazawa, Y.; Yamasaki, T.; Furukawa, M., Convenient Syntheses of 1-Acyl-2-alkylhydrazines. *Synthesis* **1987,** *1987*, 183-184.
152. Sandstrom, J., The Reaction Between Thiohydrazides And Ethylbenzylchloroacetate. Ii.*. Formation Of Ethoxycarbonylmethyl Thiolcarboxylate Benzoylhydrazones. *Acta Chem. Scand.* **1963,** *17*, 95-102.
153. Wang, X.; Yu, H.; Xu, P.; Zheng, R., A facile synthesis of acylhydrazines from acylbenzotriazoles. *Journal of Chemical Research* **2005,** *2005*, 595-597.
154. Zhao, P.-L.; Li, J.; Yang, G.-F., Synthesis and insecticidal activity of chromanone and chromone analogues of diacylhydrazines. *Bioorg. Med. Chem.* **2007,** *15*, 1888-1895.
155. Yamasaki, R.; Tanatani, A.; Azumaya, I.; Masu, H.; Yamaguchi, K.; Kagechika, H., Solvent-Dependent Conformational Switching of N-Phenylhydroxamic Acid and Its Application in Crystal Engineering. *Cryst. Growth Des.* **2006,** *6*, 2007-2010.
156. Zhu, M.; Zheng, N., Photoinduced Cleavage of N-N Bonds of Aromatic Hydrazines and Hydrazides by Visible Light. *Synthesis* **2011,** *2011*, 2223-2236.